UNIVERSITY OF BIRMINGHAM

BREAST CANCER PREDISPOSITION GENE BRCA1, PATHOGENIC C61G MUTATION IN MICE: SYNTHETIC VIABILITY IN DNA REPAIR AND TUMOUR DEVELOPMENT

by

KIRSTY JOSEPHINE LAWRENCE

A thesis submitted to the University of Birmingham for the degree of

DOCTOR OF PHILOSOPHY

School of Cancer Sciences
College of Medical and Dental Studies
University of Birmingham
2016

Abstract

The N-terminal *BRCA1* C61G mutation is clinically important in the development of breast cancer but the aetiology of this pathogenic *BRCA1* mutation is not clear. *Brca1* C61G homozygote mice are embryonic lethal and tissue-specific *Brca1* C61G leads to tumourigenesis.

This thesis shows the removal of *53bp1* rescues the mouse embryonic lethality of *Brca1* C61G homozygote mutation. *53bp1*$^{-/-}$*Brca1*$^{C61G/C61G}$ mice have an increased rate of tumour development compared to *53bp1*-null mice and show male-specific sterility. The *Brca1* C61G mutation causes a reduced level of Brca1 protein suggesting this missense mutation causes protein-wide affects. This mutation causes defects in DSB and DNA crosslink repair foci and defects in the response of *53bp1*$^{-/-}$*Brca1*$^{C61G/C61G}$ cells to chemotherapy agents, particularly IR and Cisplatin. Brca1 C61G appears to cause deficient DSB repair despite displaying normal Rad51 foci levels, which is an indication of functional homologous recombination, and a previously undescribed increase in FANCD2 foci upon induction of DNA crosslinks. *53bp1*-null cells that are heterozygote for the *Brca1* C61G mutation display phenotypes that are suggestive of haploinsufficiency caused by Brca1 C61G protein.

Overall, the *Brca1* C61G missense mutation can cause cells that affect DNA repair and increase genome stability that leads to tumour development.

Dedication

I would like to dedicate this thesis to those who have supported me in this long and difficult journey.
To my parents and family, for their undying support.
To my best friend Emily Sanctuary, who is my rock. Without who I simply would not have survived. I owe you more than I can ever say.
To Jo Strachan, who made me believe in myself as a scientist and inserted laughter into the dark times.
Special thanks to Laura Al-Bandar, Clare Elliot, Mike Ridley, and Emma Murdoch for enriching my life and providing support. To my Birmingham and Leicester University friends, who provided sanity and insanity into my life in beautiful ways. Especially to the MRes'ers, thanks for sharing the love of science and the baptism by fire, which is the PhD, particularly Kabir Khan, Bonita Apta and Emily Halford.

Acknowledgements

I would like to thank my supervisor, Jo Morris, and the lab group (Ruth Densham, Alex Garvin, Jo Strachan, Sarah Blair-Reid, Helen Stone, Manolo Daza Martin and James Beesley). I also would like to thank the students/doctors that have passed through the lab, specifically Balraj, Jia and Ravindhi. Other members of the DNA damage and genome stability groups have also contributed to my ability to gain my PhD, namely Anastasia Zlatanou, Panagiotis Kotsantis, Becky Jones, Clare Davies, Kelly Chiang, Tom Clarke, Eva Petermann, Rob Hollingworth, Tracey Perry, Paul Murray and, my second supervisor, Tatjana Stankovic.

Gratitude is also due to the many services provided to the department from the BMSU and its' staff, the administration and I.T. staff that support the department, the technology hub, and Alan the autoclave guy, often the unsung hero.

Personally, my work would not be possible without the scientific guidance of the postdocs that have supported my development and those postdocs that provided invaluable techniques (especially Jo S, Natasha, Sarah and Panos).

Table of Contents

Table of Figures

Chapter 4

Chapter 5

Table of Tables

Chapter 6

Abbreviations

Δ11: Deletion of exon 11
53BP1 (TP53BP1): Tumour protein p53 binding protein 1
aa: amino acid
Abraxas (ABRA1/CCDC98): Coiled-Coil Domain-Containing Protein 98/BRCA1-A Complex Subunit Abraxas
ADP: Adenosine diphosphate
AID: Activation-Induced Cytidine Deaminase
APC: Adenomatous Polyposis Coli
Ape1 (REF1): Apurinic/Apyrimidinic (Abasic) Endonuclease
Artemis (SNM1C): DNA Cross-link Repair 1C
ATM: Ataxia Telangiectasia Mutated
ATP: Adenosine Triphosphate
ATR: Ataxia Telangiectasia and Rad3-Related Protein
ATRIP: ATR Interacting Protein
Aurora B (AURKB): Aurora Kinase B
BARD1: BRCA1 Associated RING Domain 1
BASC: BRCA1-Associated genome surveillance complex
BCLAF1: BCL2-Associated Transcription Factor 1
BER: Base Excision Repair
BIC: Breast Cancer Information Core
BLG: β-lactoglobulin
BLM: Bloom Syndrome, RecQ Helicase-Like
BRCA1: Breast Cancer 1, Early Onset
BRCA2: Breast Cancer 2, Early Onset
BRCC36: BRCA1/BRCA2-Containing Complex, Subunit 3
BRCT: BRCA1 C-Terminus domain
BRD7: Bromodomain Containing 7
BRE: Brain and Reproductive Organ-Expressed
BRIP1 (BACH1/FANCJ): BRCA1 Interacting Protein C-Terminal Helicase 1 (BTB and CNC Homology 1 and Fanconi Anemia Complementation group J)
BSA: Bovine Serum Albinum
C-Abl: C-Abelson Tyrosine-Protein Kinase 1
Cdc25C: Cell Division Cycle 25C
Cdc98: Cell Division Cycle 98
cDNA: complimentary DNA
Chk1: Checkpoint Kinase 1
Chk2: Checkpoint Kinase 2
CHX: Cycloheximide

CFLB: Cell Fractionation Lysis Buffer
CMG: Cdc45-Mcm2-7-GINS protein complex
c-Myc: C-Myelocytomatosis Viral Oncogene Homolog
COBRA1: Cofactor of BRCA1
CPT: Camptothecin
Cre: Cre recombinase
CRM1: Chromosome Region Maintenance 1
CSR: Class Switch Recombination
CtIP (RBBP8): CtBP-Interacting protein (Retinoblastoma Binding Protein 8)
CUL4: Cullin 4
DDR: DNA Damage Response
DMEM: Dulbeccos Modified Eagle Medium
DMSO: Dimethyl Sulfoxide
DNA: Deoxyribonucleic Acid
DNA-PKcs: DNA activated, Protein Kinase, Catalytic Polypeptide
DNMT2b: DNA (Cytosine-5-)-Methyltransferase 2b
dNTPs: Deoxynucleotide mix
DSB: Double-strand Break
DSS1: Deleted In Split Hand/Split Foot Protein 1
DUB: Deubiquitinating enzyme
ECL: Enhanced Chemiluminescence
EME1: Essential Meiotic Endonuclease 1
ER: Estrogen Receptor
ERα: Estrogen Receptor alpha
ERCC1: Excision Repair Cross-Complementation Group 1
ES: Embryonic Stem
FAAP24: Fanconi Anemia-Associated Protein of 24 kDA
FAN1: FANCD2/FANCI-Associated Nuclease 1
FANC (FA): Fanconi Anemia
FANCA: Fanconi Anemia Complementation Group A
FANCB: Fanconi Anemia Complementation Group B
FANCC: Fanconi Anemia Complementation Group C
FANCD2: Fanconi Anemia Complementation Group D2
FANCE: Fanconi Anemia Complementation Group E
FANCF: Fanconi Anemia Complementation Group F
FANCG: Fanconi Anemia Complementation Group G
FANCI: Fanconi Anemia Complementation Group I
FANCJ: Fanconi Anemia Complementation Group J
FANCL: Fanconi Anemia Complementation Group L
FANCM: Fanconi Anemia Complementation Group M

FANCO: Fanconi Anemia Complementation Group O
FBS: Foetal Bovine Serum
FOXA1: Forkhead Box A1
GADD45: Growth Arrest and DNA- Damage-Inducible
GAL4: Galactoside-Binding Lactose 4
GAPDH: Glyceraldehyde-3-Phosphate Dehydrogenase
GCNA: Germ Cell Nuclear Antigen
γH2AX: gamma (phosphorylated) Histone 2A type X
H&E: Hematoxylin and Eosin
H2A: Histone 2A
H4K20me2: dimethyl-histone 4
hCds1: human CDP-Diacylglycerol Synthease 1
HJ: Holliday Junction
hnRNP: heterogenous nuclear Ribonucleoprotein
HP1: Heterochromatin Protein 1
HR: Homologous Recombination
hTERT: human Telomerase Reverse Transcriptase
HU: Hydroxyurea
ICD-nos: International Classification of Diseases - not otherwise specified
ICL: Interstrand Crosslink Repair
Ig: Immunoglobulin
IPTG: Isoproply β-D-1-thiogalactopyranoside
IR: Ionising Radiation
IRIF: Ionising Radiation-Induced Foci
K5: Keratin 5
K14: Keratin 14
kDa: kilo Dalton
Ku70 (XRCC6): X-Ray Repair Complementing Defective Repair in Chinese Hamster Cells 6
Ku80 (XRCC5): X-Ray Repair Complementing Defective Repair in Chinese Hamster Cells 5
L3MBTL1: Lethal (3) Malignant Brain Tumour L (3)
LB: Luria Bertani
Lig1: Ligase 1
Lig3: Ligase 3
Lig4: Ligase 4
LMB: Leptomycin B
LOH: Loss of Heterozygosity
MCF10A: Michigan Cancer Foundation 10A
MDC1: Mediator of DNA-Damage Checkpoint 1
MEF: Mouse Embryonic Fibroblast
MERIT40 (NBA1): Mediator of Rap80 Interactions and Targeting 40

MHF1: FANCM-Interacting Histone Fold Protein 1
MHF2: FANCM-Interacting Histone Fold Protein 2
MMC: Mitomycin C
MMR: Mismatch Repair
Mms4 (EME1): Essential Meiotic Endonuclease 1 Homolog
MMTV-LTR: Mouse Mammary Tumour Virus – Long Terminal Repeat
MNAN: Methyl-n-amyl nitrosamine
Mre11: Meiotic Recombination 11
MRI: Magnetic Resonance Imaging
MRN: Mre11/Rad50/Nbs1 complex
mRNA: messenger RNA
Msh-2: MutS Homolog 2
Mus81: MUS81 Structure-Specific Endonuclease Subunit
NBCS: New Born Calf Serum
NBR1: Neighbour of BRCA1 Gene 1
NBR2: Neighbour of BRCA1 Gene 2
NBS1: Nijmegen Breakage Syndrome Protein 1
NCBI: National Centre of Biotechnology Information
NCS: Neocarzinostatin
NER: Nucleotide Excision Repair
NES: Nuclear Export Sequence
NHEJ: Non-Homologous End-Joining
NIH3T3: National Institute of Health 3-day transfer $3x10^5$
NF-κB: Nuclear Factor of Kappa Light Polypeptide Gene Enhancer In B-Cells
NLS: Nuclear Localisation Sequence
Nmi: NMYC Interactor
NMR: Nuclear Magnetic Resonance
NTH1: Nth Endonuclease III-Like 1
Oct-1: Octamer-Binding Transcription Factor 1
OGG1: 8-Oxoguanine DNA Glycosylase
p21: protein 21 kDa
p50: protein 50 kDa
p53: protein 53 kDa
p60: protein 60 kDa
PAGE: Polyacrylamide gel electrophoresis
PALB2: Partner and Localizer of BRCA2
PAR: Poly (ADP-ribose)
PARP: Poly (ADP-ribose) Polymerase
PARP1: Poly (ADP-ribose) Polymerase 1
PARPi: Poly (ADP-ribose) Polymerase inhibitor

PBS: Phosphate Buffered Saline
PBST: PBS with Tween
PCR: Polymerase Chain Reaction
PNKP: Polynucleitide Kinase 3'-Phosphatase
POH1: Pad 1 Homolog 1
Pol II: Polymerase II
Pol λ: Polymerase Lambda
Pol μ: Polymerase Mu
Pol ζ: Polymerase Zeta
PR: Progesterone Receptor
PTEN: Phosphatase and Tensin Homolog
PTIP: PAX Transcription Activation Domain Interacting Protein 1
Rad6: Radiation Sensitivity Gene 6
Rad18: Radiation Sensitivity Gene 18
Rad50: Radiation Sensitivity Gene 50
Rad51: Radiation Sensitivity Gene 51
RAP80: Receptor-Associated Protein 80
REV1: REV1, Polymerase (DNA Directed)
RFC1: Replication Factor C 1
RING: Really Interesting New Gene
RIF1: Rap1-Interacting Factor 1
RNA: Ribonucleic Acid
RNF8: Ring Finger Protein 8
RNF168: Ring Finger Protein 168
RNR: Ribonucleotide Reductase
RPA: Replication Protein A
SAFB2: Scaffold Attachment Factor B2
SDS: Sodium Dodecyl Sulfate
shRNA: short hairpin RNA
siRNA: short interfering RNA
SLX4: Structure-Specific Endonuclease Subunit
Spo11 (CT45): Cancer/Testis Antigen 35
SSB: Single-strand Break
ssDNA: single-strand DNA
Stat-1: Signal Transducer and Activator of Transcription 1
SWI/SNF: SWItch/Sucrose Non-Fermentable
TCR: T Cell Receptor Recombination
Tdt: Terminal Deoxynucleotidyltransferase
TLS: Translesion Synthesis
TN: Triple Negative (Estrogen, Progesterone and HER2/neu receptor negative)

TopBP1: Topoisomerase (DNA) II Binding Protein 1
U2OS: U2 Osteosarcoma
UAF1: USP1-Associated Factor 1
Ubc13: Ubiquitin-Conjugating Enzyme 13
UbcH5: Ubiquitin-Conjugating Enzyme 5
UBE2T: Ubiquitin-Conjugating Enzyme 2T
UBXN1: UBX Domain Protein 1
UHRF1: Ubiquitin-Like with PHD and Ring Finger Domains 1
USP1: Ubiquitin Specific Peptidase 1
USP26: Ubiquitin Specific Peptidase 26
USP37: Ubiquitin Specific Peptidase 37
UV: Ultraviolet
VCP: Vasolin Containing Protein
V(D)J: Variable (Diversity) Joining
VUS: Variations of unknown significance
Wap: Whey acidic protein
Wip1: Wild-Type p53-Induced Phosphatase 1
WT: Wild-type
XIST: X Inactive Specific Transcript
XPF: Xeroderma Pigmentosum Group F-Complementing Protein
XRCC4: X-Ray Repair Complementing Defective Repair in Chinese Hamster Cells 4
Zrbk-1: Zinc Finger Protein That Interacts with BRCA1

Chapter 1 – Introduction

1.1 Introduction

The Breast Cancer 1, early onset, (*BRCA1)* gene has been a topic of media attention due to high profile cases of celebrities with hereditary breast and ovarian cancer syndrome (such as Angelina Jolie). The treatments for breast cancer have developed vastly from DNA-damage-directed chemotherapies to the use of hormone-directed therapies (non-DNA-damaging), but there are still tumours in which current therapies are not effective and DNA-damaging chemotherapy must be used. Tumours can become resistant to both of these types of therapy. A better understanding of *BRCA1* using basic science could provide more clinical avenues for prevention and treatment of cancer by investigating the cellular pathways in which *BRCA1* has a function which can be clinically manipulated. This research would help all tumours, not just *BRCA1* mutation carrier tumours or breast and ovarian cancer, because unpicking tumour suppressing mechanisms can provide new targets for cancer therapy. Although there is still a great deal of research needed to understand why mutations in *BRCA1* lead to such a high risk (almost inevitable) of developing breast cancer.

1.2 Clinical *BRCA1*

1.2.1 Hereditary breast and ovarian cancer syndrome and *BRCA1*

The *BRCA1* gene was mapped to chromosome 17q21 through linkage analysis of families with hereditary breast and ovarian cancer syndrome (Hall *et al*., 1990; Miki *et al*., 1994; Narod *et al*., 1997). The presence of a heterozygote *BRCA1* or *BRCA2* mutation in the general population is between 1 in 400-800 people (Claus *et al*., 1996; Ford *et al*., 1994; Whittemore

et al., 1997) but many communities such as Ashkenazi Jews and those of African ancestry have a higher frequency of *BRCA1* mutations (Haffty *et al*., 2006; John *et al*., 2007; Liede and Narod, 2002; Olopade *et al*., 2003; Szabo and King, 1997). It is possible for mutations to occur along the entire *BRCA1* gene but clinically important cancer mutations are most commonly in the RING (Really Interesting New Gene) domains or the BRCT (BRCA1 C-Terminus) domains (Figure 1.1 taken from (Clark *et al*., 2012)).

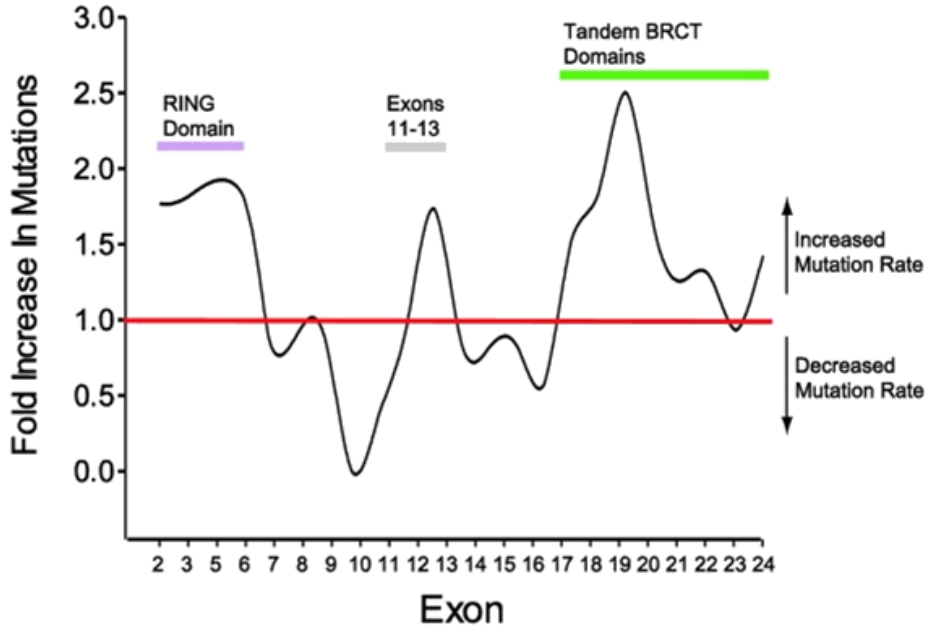

Figure 1.1 – Mutations rate across BRCA1 exons
This figure was taken from Clark et al (Clark et al., 2012). It shows the BRCA1 mutation rate found in patients with breast and ovarian cancer, pinpointing the mutations to where they lie on the gene and which protein domains these cover.

The *BRCA1* C61G mutation is the most common missense (239 cases) mutation found in *BRCA1* in all cases reported on the Breast Cancer Information Core (BIC) database and fifth most common clinically important mutation (Szabo *et al*., 2000). The majority of disease-causing mutation are truncations. The *BRCA1* C61G mutation accounts for 20% of Polish

families with breast and ovarian hereditary cancer syndrome in a study by Gorski *et al* (Gorski *et al*., 2000).

There have been only two reported cases of humans born with a mutation in both *BRCA1* alleles (Domchek *et al*., 2013; Sawyer *et al*., 2015). One patient developed ovarian cancer at 28 years old and had developmental abnormalities (Domchek *et al*., 2013). She had a truncating mutation (p.Asp821Ilefs*25) and a missense mutation (p.Val1736Ala) that affected the BRCT domain binding to BACH1 (Domchek *et al*., 2013). The second patient also had developmental anomalies that produce a Fanconi Anaemia-like syndrome and she developed breast cancer at 23 years old (Sawyer *et al*., 2015). She also has a truncating mutation (p.Ser198Argfs*35) and a missense mutation (p.Arg1699Trp) that affect the BRCT domains of BRCA1, but this single amino acid change is thought to affect the structure of BRCA1 (Sawyer *et al*., 2015). These biallelic mutations would allow for some BRCA1 protein to be made (although mutated) and this is likely to be partially functional as the developmental defects did not cause embryonic lethality, as seen in the majority of homozygote *Brca1*-mutated mice (Section 1.5.1).

It has been thought that the loss of the wild-type allele in *BRCA1* mutant carriers is the driver behind tumour development (Esteller *et al*., 2000; Neuhausen and Marshall, 1994; Smith *et al*., 1992), but this is disputed because some tumours maintain a wild-type *BRCA1* allele (Clark *et al*., 2012; Smith *et al*., 1992; Wei *et al*., 2005). It is also known that *BRCA1* is altered (mutated or altered expression) in many cases of sporadic cancer to give a clinically BRCA-like phenotype to the cancer (Neuhausen and Marshall, 1994; Smith *et al*., 1992).

1.2.2 *BRCA1* mutation carriers and cancer development

The risk of getting breast cancer by the age of 70 in a carrier of a *BRCA1* mutation is estimated to be approximately 40-90%, although this depends on the mutation that has been inherited (Antoniou *et al*., 2003; Easton *et al*., 1995; Hopper *et al*., 1999; Risch *et al*., 2006). The risk of getting ovarian cancer was shown to be approximately 24-39% by the age of 70 (Risch *et al*., 2006). Male *BRCA1* mutation carriers are at an increased risk of 1.2% of getting breast cancer by the age of 70 (Fentiman *et al*., 2006; Tai *et al*., 2007) compared to the 1 in 100,000 risk in the general male population of Europe (Sasco *et al*., 1993). Being a carrier of a *BRCA1* mutation also increases a person's risk to other cancers such as fallopian tube carcinoma (Medeiros *et al*., 2006), prostate cancer (Cybulski *et al*., 2008; Thompson *et al*., 2002), cervical cancer (Thompson *et al*., 2002), and pancreatic cancer (Lynch *et al*., 2005; Thompson *et al*., 2002).

Breast and ovarian cancer in patients with a *BRCA1* mutation occur at an earlier age and the increased risk is mostly seen in their 20-30's (Burke *et al*., 1997) compared to cases of sporadic breast cancer. The breast cancers in *BRCA1* mutation carriers tend to be triple-negative (TN) in type and the ovarian cancers are frequently serous ovarian cancers (Foulkes *et al*., 2003; Lacroix and Leclercg, 2005; Lakhani *et al*., 2005; Rakha *et al*., 2008).

The triple-negative phrase relates to these cancers being dysfunctional for three receptors; estrogen receptor (ER), progesterone receptor (PR) and HER-2/neu (Dent *et al*., 2007). TN breast cancers are associated with higher grades (typically III) of cancer, at an earlier age with signs of a more advanced cancer such as higher occurrence of metastasis and high proliferation rate of cells (Diaz *et al*., 2007; Irvin and Carey, 2008; Reis-Filho and Tutt, 2008;

Stockmans *et al*., 2008; Thike *et al*., 2010). TN cancer equates to 10-20% of the total number of breast cancer cases (Papa *et al*., 2015) and these cancers include both sporadic breast cancer and those in patients carrying a BRCA mutation. However the incidence of a BRCA mutation in TN cancers is reported to be from 16-42% which is higher than the rate of BRCA mutation in other types of breast cancer (Atchley *et al*., 2008; Gonzalez-Angulo *et al*., 2011). Although the percentage of inherited BRCA mutations is variable in TN breast cancers, a large number of TN breast cancer have dysfunctional BRCA1 protein which gives a BRCA-like phenotype, i.e. TN, in non-*BRCA1* mutation carriers (Lakhani *et al*., 2005; Turner *et al*., 2004; Turner *et al*., 2007).

1.2.3 *BRCA1* carrier cancer patient outcomes

Studies have looked at the outcomes of the patients with a *BRCA1* mutation who develop breast cancer compared to women who develop breast cancer and do not have an inherited *BRCA1* mutation, and they are inconclusive; the outcomes have been reported as better (Marcus *et al*., 1996; Porter *et al*., 1994), worse (Ansquer *et al*., 1998; Brekelmans *et al*., 2006; Foulkes *et al*., 1997; Stoppa-Lyonnet *et al*., 2000), or the same prognosis as non-BRCA carriers patients (Gaffney *et al*., 1998; Johannsson *et al*., 1998; Lee *et al*., 1999; Rennert *et al*., 2007; Verhoog *et al*., 1998; Verhoog *et al*., 1999). The outcomes for TN breast cancer is clearer in the literature than BRCA breast cancers. TN breast cancers are associated with a higher rate of cancer recurrence (Metcalfe *et al*., 2004) leading to a reduced survival rate within 5 years (Patil *et al*., 2011), especially if the cancer has metastasised (Mersin *et al*., 2008; Rodriguez-Pinilla *et al*., 2006).

TN breast cancer phenotype refers to the three receptors that are the target of hormone-targeted therapies (Tamoxifen, Herceptin and Onapristone) in breast cancer treatment and TN cancers are less responsive to these therapies than those who are positive for these receptors (Kassam *et al*., 2009; Liedtke *et al*., 2008; Rouzier *et al*., 2005). These hormone-targeted therapies have less side effects than the traditional DNA-damaging chemotherapy or radiation but these more aggressive chemotherapy options are used when tumours are unresponsive or resistant to the hormone-targeted therapies, as in TN breast cancer. A *BRCA1* mutation or an ill-functioning BRCA1 does sensitize cells to DNA-damaging agents, especially Platinum-based agents (Cass *et al*., 2003; Lafarge *et al*., 2001; Quinn *et al*., 2003; Tassone *et al*., 2003; Tassone *et al*., 2009) and PARP inhibitors (PARPi)(Farmer *et al*., 2005; Fong *et al*., 2009; Turner *et al*., 2008), due to BRCA1's role in DNA double-strand break (DSB) repair (further discussion in 5.1). However, BRCA1-driven tumours can develop resistance to these DNA-damaging agents and this may explain the variation seen in prognosis in *BRCA1*-related breast cancers.

Of all ovarian cancer cases in America in a 2005 study, 9.4% of women had a known *BRCA1* mutation (8.2% have a BRCA mutation of unknown significance) (Pal *et al*., 2005). The majority of *BRCA1*-related ovarian cancer cases were serous ovarian tumours (90%) which is higher than non-mutation carriers (50%) (Aida *et al*., 1998; Berchuck *et al*., 1998; Lu *et al*., 1999; Pal *et al*., 2005; Rubin *et al*., 1996). *BRCA1* mutation carriers have an onset age for ovarian cancer that is 8 years earlier than for patients with no underlying *BRCA1* mutation (Boyd *et al*., 2000). However, the survival outcomes for ovarian cancer patients with or without a *BRCA1* mutation has been described as the same (Brunet *et al*., 1997; Buller *et al*.,

2002; Johannsson *et al*., 1998; Zweemer *et al*., 2001) or improved (Aida *et al*., 1998; Cass *et al*., 2003; Chetrit *et al*., 2008; Tan *et al*., 2008) despite the earlier onset of ovarian cancer.

1.2.4 *BRCA1* mutation carrier: clinical intervention

A *BRCA1* mutation carrier has many options of how to manage their risk of developing cancer. There are surveillance programmes for women that are effective at identifying breast cancer by MRI (Magnetic Resonance Imaging) scan (Kriege *et al*., 2004; Kuhl *et al*., 2005; Leach *et al*., 2005; Lehman *et al*., 2005; Warner *et al*., 2004; Warner and Causer, 2005) or mammography (although less effective (Saslow *et al*., 2007)), identifying ovarian cancer women by transvaginal ultrasounds and CA-125 serum screening (Clarke-Pearson, 2009) and identifying prostate cancer in men with a *BRCA1* mutation by frequent prostate screening from the age of 40 (Burke *et al*., 1997; Mettlin *et al*., 1993). However, surveillance does not prevent cancer; it identifies it earlier.

Oral contraceptives have a protective role against ovarian cancer in *BRCA1* mutation patients of up to 33% risk reduction after 5 years of treatment (Narod *et al*., 1998; Whittemore *et al*., 2004). Breast feeding for over a year has shown a reduction in the risk of breast and ovarian cancer in *BRCA1* mutation carriers (Jernstrom *et al*., 2004), although this is disputed (Andrieu *et al*., 2006; Antoniou *et al*., 2009). Tamoxifen has also been used as a preventative agent to reduce the occurrence of cancers in *BRCA1* patients (Fisher *et al*., 1998; King *et al*., 2001; Metcalfe *et al*., 2005; Narod *et al*., 2000), although the majority of breast tumours in *BRCA1* mutation carriers develop ER-negative tumours and it was most effective at preventing ER-negative tumours (Gail *et al*., 1999).

The most effective way of preventing the development of cancer in *BRCA1* mutation carriers is by surgically removing the mostly likely tissue to develop cancer; the ovaries and the breast tissue. Bilateral prophylactic mastectomies have shown to be highly effective reducing the rate of breast cancer in *BRCA1/2* mutation carriers from 48.7% down to 1.9% or up to 90% reduction in similar studies, bringing their risk to the approximately the same as a non-carrier (Hartmann *et al*., 2001; Hartmann *et al*., 1999; Olopade and Artioli, 2004; Rebbeck *et al*., 2004). Whilst oophorectomies reduce the risk of ovarian cancer by approximately 80-96% (Kauff *et al*., 2002; Rebbeck *et al*., 2004; Rutter *et al*., 2003), they have also been shown to reduce the breast cancer incidence to 53% (Olopade and Artioli, 2004; Rebbeck *et al*., 2004). Surgical options have enormous benefit but do come at the cost of cosmetic appearance, an early menopause and can significantly affect mental health.

BRCA1 variants that are found in patients are always not known to be clinically significant and this makes it difficult to give *BRCA1* variant carrier an accurate prediction of cancer risk. This makes the decision for the patient of what or if any preventative measures should be taken to reduce this risk.

The BIC database does accumulate the known mutations and variants found in *BRCA1* and *BRCA2* in the attempt to provide more information about each mutation (Szabo *et al*., 2000). There are studies that attempt to look at specific mutations in *BRCA1* or specific regions of *BRCA1* to also provide evidence of how a variant may affect the BRCA1 protein's tumour suppressor activity (Section 1.3.1) (Loke *et al*., 2015; Starita *et al*., 2015). Despite this, many functions of BRCA1 and whether variants in *BRCA1* affect these functions still remain elusive.

The prognosis of TN *BRCA1*-related tumours remains poor and the hormone-based therapies are ineffective, leaving DNA-damaging chemotherapy as the best treatment of these tumours. Whilst poly (ADP)-ribose polymerase (PARP) inhibitors (PARPi) and platinum-based agents are proving effective in many cases, the level of resistance and recurrence is high and more therapy options are needed (Section 5.1).

1.3 *BRCA1* gene and protein

1.3.1 Protein domains

BRCA1 is a gene that translates into an 1863 amino acid protein. The main regions of BRCA1 are the N-terminal RING domain, the nuclear localisation/export sequences (NLS/NES), coiled-coil domain, a SQ cluster domain and two tandem BRCT domains at the C-terminal (Figure 1.2). *BRCA1* is a tumour suppressor and has multiple roles in maintaining genome integrity. The part of BRCA1 that is responsible for each role has been investigated through its interacting proteins, but many proteins interact with several of BRCA1's domains.

The N-terminal RING domain of BRCA1 is the only part of BRCA1 that possesses a catalytic activity. It is an E3 ubiquitin ligase that predominantly assembles lysine 6-linked (K6) polyubiquitin chains which is an unconventional linkage associated with efficient DNA repair (Morris and Solomon, 2004; Wu-Baer *et al*., 2003). The most crucial protein that the RING domain interacts with is BARD1 (BRCA1 Associated RING domain 1) (Joukov *et al*., 2001; Wu *et al*., 1996) because it is needed for the stability and catalytic function of the BRCA1 RING domain (Brzovic *et al*., 2003; Chen *et al*., 2002; Hashizume *et al*., 2001; Joukov *et al*., 2001).

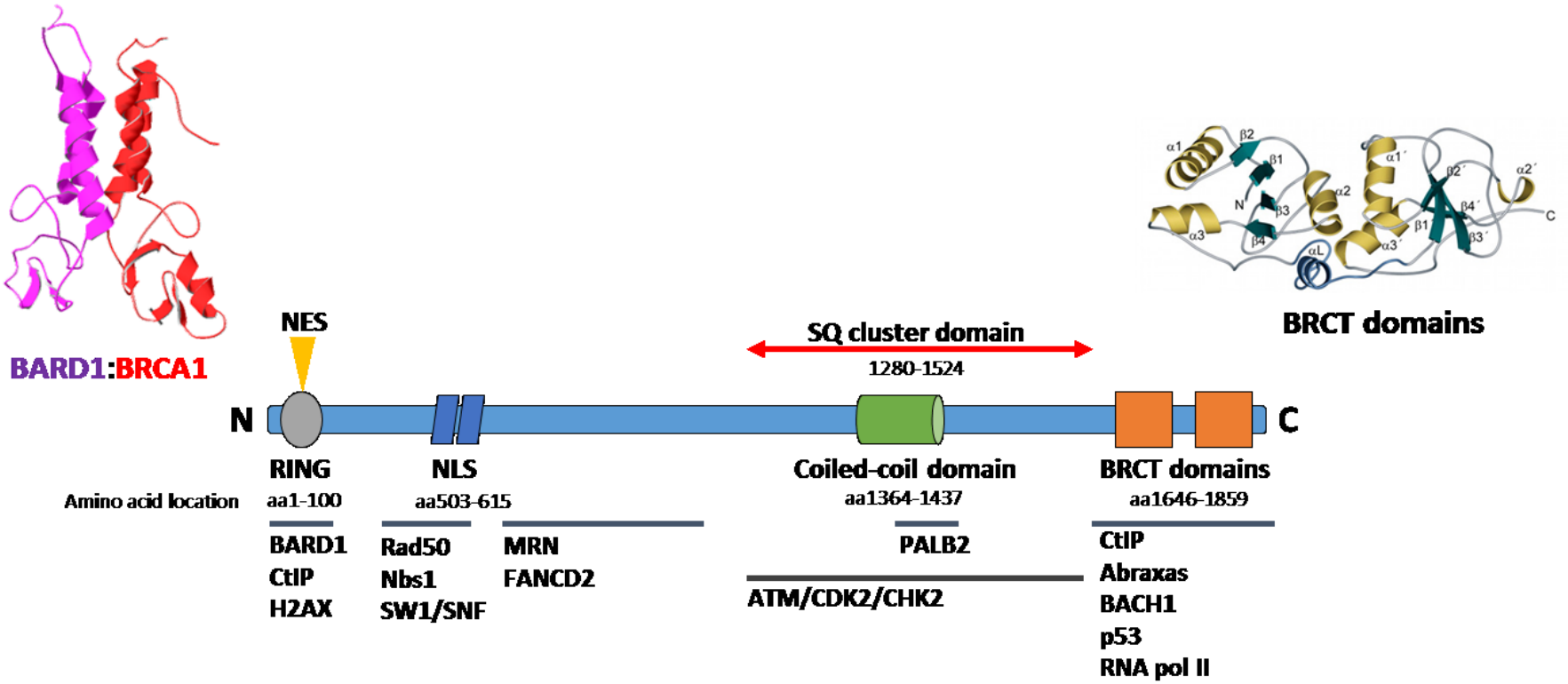

Figure 1.2 – BRCA1 domains and protein interactions

This diagram is a representation of the protein domain locations in BRCA1 and the some of the proteins that are reported to interact with these regions. The RING domain structure is from Brzovic et al (Brzovic et al., 2001b) derived through NMR and the BRCT domains structure comes from a crystal structure in Williams et al (Williams et al., 2001).

The RING domains of BRCA1 and BARD1 bind to create heterodimer (Joukov *et al*., 2001; Wu *et al*., 1996), of which there is a NMR (Nuclear magnetic resonance) structure (Brzovic *et al*., 2001b) (Figure 1.2).

A definitive list of BRCA1 substrates that influence genome stability is still not complete but multiple targets that have been reported for ubiquitination by the BRCA1:BARD1 heterodimer, and they include H2AX (Yu *et al*., 2003), Cyclin B/Cdc25C (Shabbeer *et al*., 2013), CtIP (Yu *et al*., 2006), SAFB2 (Song *et al*., 2011), progesterone receptor (Calvo and Beato, 2011) and RNA polymerase subunits (Starita *et al*., 2005; Wu *et al*., 2007).

BRCA1 has nuclear localisation sequences that are located at amino acid 501-508 (NLS1) and 606-615 (NLS2) (Chen *et al*., 1995; Fabbro *et al*., 2002; Thakur *et al*., 1997; Wilson *et al*., 1997), although deletion of NLS2 doesn't appear to affect BRCA1 localisation (Thakur *et al*., 1997). BRCA1's nuclear export sequences are recognised by the CRM1-nuclear exporter (Fabbro *et al*., 2002) and are located within the RING domain of BRCA1 (Fabbro *et al*., 2002; Rodriguez and Henderson, 2000; Rodriguez *et al*., 2003a; Rodriguez *et al*., 2004). Interruption of nuclear localisation sequences could affect BRCA1 localisation in the nucleus where most of its actions are located and therefore these localisation sequences may be important for regulation of BRCA1 roles.

The SWI/SNF complex is a chromatin remodelling complex that interacts with BRCA1 in the region spanning amino acids 260-553 (Figure 1.2) (Bochar *et al*., 2000). A subunit of this complex, BRD7, does directly bind BRCA1 and has the potential to influence BRCA1 as a transcriptional regulator (Harte *et al*., 2010).

Members of the MRN (Mre11/Rad50/Nbs1) complex, a DSB repair complex, bind around 341-748 amino acids into BRCA1 (Figure 1.2) (Wang *et al*., 2000) although this interaction relies on the BRCA1 BRCT domains binding CtIP (Yu *et al*., 1998; Yuan and Chen, 2010; Zhong *et al*., 1999).

The SQ cluster region (phosphorylation region) is a patch that includes the coiled-coil domain of BRCA1 that is phosphorylated upon DNA damage to activate BRCA1 (Figure 1.2). One such phosphorylation of BRCA1 is by Chk2 on the serine at amino acid 988 (Lee *et al*., 2000), but other proteins have the ability to phosphorylate BRCA1 such as ATR (Yoo *et al*., 2007).

The BRCA1-B complex binds through BRCA1 coiled-coil domains directly to PALB2 (Figure 1.2) (Sy *et al*., 2009; Zhang *et al*., 2009b), and this links BRCA1 and BRCA2 (Sy *et al*., 2009; Xia *et al*., 2006; Zhang *et al*., 2009a; Zhang *et al*., 2009b). It is thought that Rad51 may directly bind to BRCA1 at amino acid 758-1064, but this interaction could be indirect through the MRN complex (Garcia-Higuera *et al*., 2001).

The BRCT domains at the C-terminus of BRCA1 (aa1650-1863) (Figure 1.2) were identified by Koonin (Koonin *et al*., 1996) and the crystal structure has been solved (Williams *et al*., 2001) (Figure 1.2). Mutation in the BRCT domains, whether truncating or missense mutations, have been reported to destabilise the BRCA1 protein due to structural changes (Lee *et al*., 2010; Williams and Glover, 2003; Williams *et al*., 2003). The BRCT domains bind the sequence pSXXF (Manke *et al*., 2003; Rodriguez *et al*., 2003b; Yu *et al*., 2003) on ATM/ATR phosphorylated proteins such as BACH1/FANCJ/BRIP1 (Yu *et al*., 2003), CtIP (Buis *et al*., 2012; Yu *et al*., 2003; Yu and Chen, 2004; Yun and Hiom, 2009), and CCDC98/Abraxas (Kim *et*

al., 2007a; Wang *et al*., 2007). These proteins, when bound to BRCA1, are important for DNA repair. These complexes have the ability to recruit other DNA repair proteins and therefore whether it is a direct or indirect interaction to bind BRCA1 is unclear, for example TopBP1 which is associated with BACH1 but also thought to have a direct BRCA1 interaction (Greenberg *et al*., 2006; Karppinen *et al*., 2006). The BRCT domains are also known to bind proteins that are not phosphorylated and to bind DNA (Yamane *et al*., 2000).

BRCA1 has a role in chromatin remodelling through its interaction with BACH1 through the BRCT domains (Cantor and Andreassen, 2006) (Figure 1.2). Remodelling DNA is important to allow repair proteins to access the damaged DNA (Cantor and Andreassen, 2006). BACH1 also has a role in resolving DNA restructures during replication (Cantor *et al*., 2004; London *et al*., 2008; Wu *et al*., 2008) and BACH1-BRCA1 interaction aids the BRCA1-B complex in activating the S phase checkpoint (Cantor *et al*., 2001; Greenberg *et al*., 2006; Litman *et al*., 2005).

The BRCT domain also binds to phosphorylate cell cycle checkpoint proteins, such as Chk1 (Joughin *et al*., 2005). This interaction is needed to active the G2/M checkpoint (Yarden *et al*., 2002) to ensure DNA is repaired before mitosis.

The BRCA1-A complex involves Abraxas directly binding to the BRCT domains of BRCA1 (Figure 1.2) to recruit RAP80 (Wang *et al*., 2007) which also binds the BRCT domains (Sobhian *et al*., 2007). BRCC36 is also important for the localisation of the BRCA1-A complex to sites of DSBs (Chen *et al*., 2006). MERIT40 is needed for the stability of the BRCA1-A complex because it stabilises Abraxas (Shao *et al*., 2009a), the scaffold of the BRCA1-A

complex (Liu *et al*., 2007b), and this reduced the localisation of the whole complex to sites of DNA damage (Feng *et al*., 2009; Shao *et al*., 2009a).

CtIP binds to BRCA1's BRCT domains but may also interact with the RING domain as it is reported to be ubiquitinated by BRCA1:BARD1 heterodimer (Figure 1.2) (Yu and Chen, 2004; Yu *et al*., 2006). The BRCA1-CtIP interaction is considered to be required to promote efficient DNA end resection in homologous recombination (HR) (Buis *et al*., 2012; Chen *et al*., 2008; Sartori *et al*., 2007; Wong *et al*., 1998; Yu *et al*., 1998; Yun and Hiom, 2009; Zhong *et al*., 1999), but there are papers that suggest that CtIP enhances DNA end resection-independently of BRCA1 (Nakamura *et al*., 2010; Polato *et al*., 2014; Reczek *et al*., 2013).

UHRF1, an E3 ubiquitin ligase, was recently reported to interact with the BRCT domains of BRCA1 when phosphorylated (Zhang *et al*., 2016). This interaction and the ubiquitin ligase function of UHRF1 was reported to orchestrate the pathway choice between DSBs being repaired through homologous recombination (HR) or non-homologous end-joining (NHEJ) (Zhang *et al*., 2016).

The BRCA1 BRCT domain interaction to UBXN1 may be involved in the inhibition of the ubiquitin ligase activity of the BRCA1:BARD1 heterodimer (Wu-Baer *et al*., 2010).

These interactions described here are not all of the reported or putative interactions that are in the literature and it is clear from the multiple BRCA1 complexes through to the multiple E3 ubiquitin ligase substrates, that BRCA1 is involved in a great many important cellular functions that require its multiple domains. It is also important to note that a mutation in *BRCA1* could lead to a change that affects multiple domains or whole protein stability which could affect all of its functions.

1.3.2 Evolution of *BRCA1, BARD1* and the BRCA1:BARD1 heterodimer

The evolutionary past of *BRCA1* and *BARD1* can help us estimate the degree of conservation of the protein and its domains as an indicator of these proteins necessity in cellular functions. The conservation of the BRCA1:BARD1 heterodimer between mammals can help to understand the differences in phenotype we may see between humans and mice with the same genetic alteration. However, it does not convey the larger degree of conservation that may help us understand why the RING domain in BRCA1 is essential for cellular function through evolution.

The most distantly divergent genus with a *BRCA1* gene orthologue (*BRC-1*) is *C.elegans* (nematode) (Boulton *et al*., 2004). It was identified using the yeast-two-hybrid system through *BARD1* orthologue (*BRD-1*), because the Genefinder used by Boulton *et al* failed to predict certain exons of *BRCA1* (Boulton *et al*., 2004). This is likely due to these exons lacking similarity to the equivalent human *BRCA1* exons. BRC-1 has more similarity to the BRCA1 isoform that lacks exon 11 than the full-length human BRCA1, although it does contain a RING domain, two BRCT domains and a nuclear localisation domain (Boulton *et al*., 2004).

The ENSEMBL orthologue tree for *BRCA1* (Appendices figure I) does not identify *BRCA1* in species older than *Ciona* genus (sea squirts) (*C. intestinalis* and *C. savignyi*) (Cunningham *et al*., 2015), which diverges after *C.elegans*, and this could be due to a similar reason as stated in Boulton *et al* (Boulton *et al*., 2004) (lack of conservation in multiple exons). *Ciona* have two orthologues of *BRCA1* and yet nematodes and ancient fish (coelacanth) have one orthologue suggesting *BRCA1* has either become a single gene or diverged into two genes (also seen in platypus and the anole lizard which have two *BRCA1* othologues).

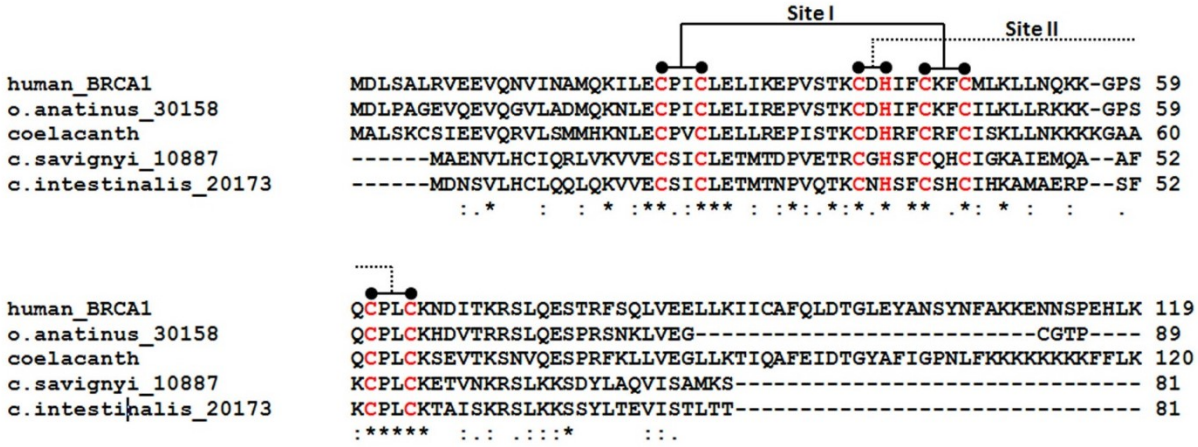

Figure 1.3 – N-terminal RING domain alignment of human BRCA1 with the RING domain containing BRCA1 orthologues.

Using CLUSTALW2 multiple sequence alignment tool and ENSEMBL, the protein sequences of the RING domain-containing BRCA1 orthologues from species with two orthologues of BRCA1 (O. anatinus_30158 =platypus, C. savignyi_10887 and C. intestinalis_20173 =sea worms identified from Appendices figure I) were aligned with human BRCA1 RING domain and its oldest common ancestor (Coelacanth= ancient fish).

Site I and Site II show the residues that contact the zinc ions that maintain the RING domain structure. The conservation of each residue and its properties is shown by the characters underneath the alignment. The characters depict the consensus between the residues in the alignment. The asterisk '' indicates a fully conserved or identical residue, the colon ':' indicates residues with highly similar properties, the period '.' indicates residues with weakly similar properties and a space ' ' indicates residues that lack conservation of residue properties.*

On closer inspection of the protein sequences in species with two *BRCA1* orthologues, it appears that one orthologue has lost one or both of the BRCT domains and kept the N-terminal RING domain, and the other orthologue does not have a RING domain and has an intact BRCT domain (Appendices figure I) (Schreiber *et al*., 2014) (refer to figure of BRCA1 domains; Figure 1.2). The presence of a RING domain containing *BRCA1* orthologue separate from the BRCT domain orthologue may suggest that the RING domain and BRCT domains may have roles that are independent of each other.

When the RING domain-containing *BRCA1* orthologues from *C. intestinalis*, *C. savignyi* and *O. anatinus* (platypus) are aligned with humans and coelacanth, it is evident that the RING domain is highly conserved as a whole and the important residues needed for holding the two structurally important zinc ions are conserved (Figure 1.3) (McWilliam *et al*., 2013). These highly conserved residues were also conserved in human BRCA1 to the *C.elegans* orthologue (Boulton *et al*., 2004).

As BARD1 and BRCA1 form a heterodimer which is important for heterodimer stability, it is essential to assess whether *BARD1* has evolved alongside *BRCA1* because this would support a conserved protein interaction. However, unlike BRCA1, the ENSEMBL orthologue tree identifies *BARD1*'s oldest orthologue in yeast (Appendices figure II) (Cunningham *et al*., 2015). On closer inspection, the oldest *BARD1* orthologues have homology of their ankyrin domain and not the RING domain. The presence of the ankyrin domain may make the evolutionary age of *BARD1* more speculative because it one of the most common domains in nature (Schreiber *et al*., 2014). BARD1 in *C.elegans* contains three Ankyrin domains, a BRCT domain and a RING domain, which is important for binding to BRCA1, and the RING domain

shows sequence similarity and conservation of functionally and structurally important residues (Boulton *et al*., 2004).

Boulton *et al* show that *C.elegans* BRC-1 and BRD-1 form a heterodimer suggesting that the relationship between the BRCA1:BARD1 heterodimer is highly conserved (Boulton *et al*., 2004). The BRC-1/BRD-1 complex was also shown to have the ability to ubiquitinate chromatin after irradiation using the UbcH5 orthologue (Polanowska *et al*., 2006). Disruption of BRC-1 or BRD-1 cause IR-sensitivity and chromosome abnormalities that are similar to the phenotype seen in human *BRCA1* and *BARD1* mutations (Boulton *et al*., 2004). This suggests that heterodimer function and E3 ubiquitin ligase activity function is highly conserved (Boulton *et al*., 2004; Polanowska *et al*., 2006).

1.3.3 RING domain function in BRCA1 roles (C61G debate)

Many papers have tried to allocate BRCA1 roles to the RING domain to better understand why mutations in the RING domain are associated with increased tumour risk in humans. As discussed previously (Section 1.3.1), BRCA1 is functionally active as an E3 ubiquitin ligase when it is in heterodimer formation with BARD1 (Figure 1.4) (Chen *et al*., 2002; Hashizume *et al*., 2001). Mutations in this area can affect one or several of the following: the structure of the RING domain, the binding of BRCA1 and BARD1 and the binding of BRCA1 to other proteins (Brzovic *et al*., 2003; Chen *et al*., 2002; Hashizume *et al*., 2001; Joukov *et al*., 2001). The C61G mutation is thought to influence all of these BRCA1 properties which dramatically reduces the ubiquitin ligase activity (Figure 1.4 Black side chain) (Brzovic *et al*., 2001a; Brzovic *et al*., 2003; Hashizume *et al*., 2001; Joukov *et al*., 2001; Mallery *et al*., 2002; Morris *et al*., 2006; Ruffner *et al*., 2001; Wu *et al*., 1996).

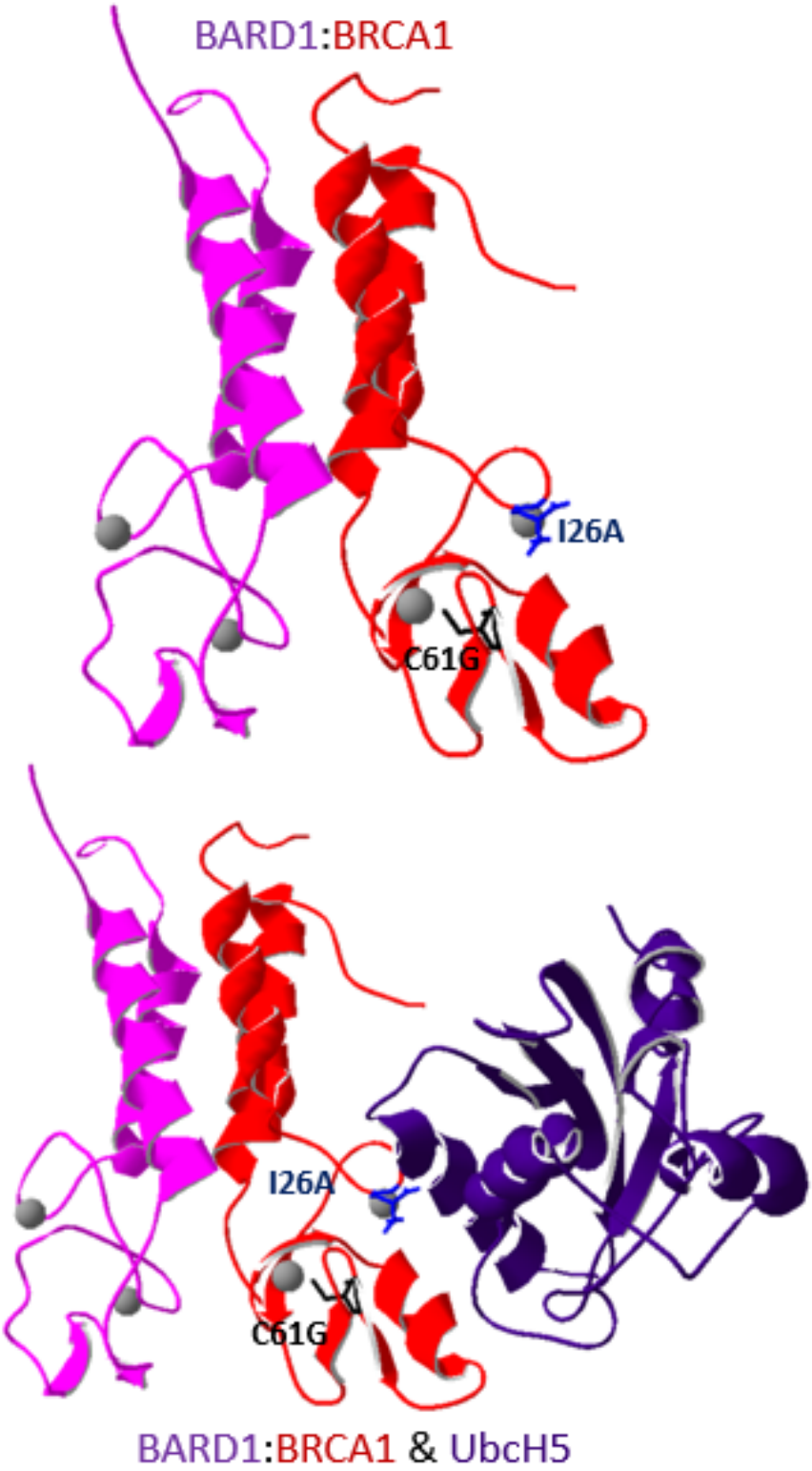

Figure 1.4 – Structure of BRCA1:BARD1 heterodimer and E2 binding
This figure shows the structure of the BRCA1:BARD1 heterodimer (red:pink) with the mutations C61G and I26A. It also shows the predictive interaction of the E2, UbcH5a (purple), with the heterodimer. Zinc ions are in grey.

There is evidence that the C61G mutation in *BRCA1* can affect the stability of the BRCA1 C61G protein, whether through destabilisation of the RING domain or reduced binding to BARD1, targeting BRCA1 for degradation assessed using both biochemical and cellular techniques (Brzovic *et al*., 1998; Brzovic *et al*., 2001b; Choudhury *et al*., 2004; Wang *et al*., 2014b). Other papers, using similar cell-based methods, suggest that the BRCA1 C61G protein is stable and at equivalent levels to wild-type BRCA1 (Campbell *et al*., 2001; Lu *et al*., 2007; Nelson and Holt, 2010).

The I26A mutation is reported to only affect the E2 conjugating enzyme (Figure 1.4 Purple structure) (UbcH5a (Dodd *et al*., 2004)) binding interface and this disrupts ubiquitin ligase activity (Figure 1.4 Blue side chain) (Brzovic *et al*., 2003), although it may not abolished (Metzger *et al*., 2014). These mutations have been used to isolate the roles of the BRCA1 N-terminal RING domain and the need of functional BRCA1 E3 ubiquitin ligase activity.

Human and mouse cell line models have shown that the *BRCA1* C61G mutation causes cell lethality (Chang *et al*., 2009; Drost *et al*., 2011), spontaneous DNA damage (Nelson and Holt, 2010), reduced HR repair (Li and Yu, 2013; Nelson and Holt, 2010; Ransburgh *et al*., 2010), centrosome amplification (Parvin and Sankaran, 2006; Sankaran *et al*., 2006) and sensitivity to ionising radiation (IR) (Li and Yu, 2013; Ruffner *et al*., 2001; Shabbeer *et al*., 2013). The *Brca1* C61G mouse model made by Drost *et al*, was embryonic lethal when homozygote, and when *Brca1* C61G was conditionally expressed alongside a *Brca1*-null allele and two *p53*-null alleles in mammary epithelial cells, tumours developed at an elevated rate (Drost *et al*., 2011). These results suggest that the C61G mutation is important for genomic stability and tumour suppression. However, it is unclear if these phenotypes are due to a defect in the E3

ubiquitin ligase activity function of BRCA1 as the C61G mutation also causes instability in the BRCA1 RING domain.

To address whether the BRCA1 E3 ubiquitin ligase activity is required for tumour suppression and genome stability, the mutation I26A is used because it is less disruptive to the RING domain structure than C61G. Cells with BRCA1 I26A (or equivalent for species) have spontaneous γH2AX foci (Zhu *et al*., 2011) and are sensitive to DNA-damaging agents, such as Camptothecin (CPT; DNA topoisomerase I inhibitor) (Sato *et al*., 2012), Neocarzinostatin (NCS; radiomimetic drug) (Shabbeer *et al*., 2013) and Mitomycin C (MMC; DNA crosslinking agent) (Tian *et al*., 2013). Although Sato *et al,* used DT40 chicken cells with V26A (equivalent to I26A) and they were not sensitive to MMC (Sato *et al*., 2012).

Reid *et al* created isogenic I26A stem cells that do not appear to produce have a defect in spontaneous DNA repair (no chromosome abnormalities) or reduction in HR levels compared to wild-type cells (Reid *et al*., 2008). Unlike C61G mice (Drost *et al*., 2011), homozygote *Brca1* I26A mice are not embryonic lethal and do not develop tumours (Shakya *et al*., 2011). These contradictory phenotypes between *Brca1* C61G and I26A N-terminal mutations, leaves the role of BRCA1's E3 ubiquitin ligase activity in genomic instability and tumour suppression as ambiguous.

Further research is needed to separate the functional role of the N-terminal RING domain of BRCA1 and BRCA1's E3 ubiquitin ligase activity and to understand why mutations in this region correlate with an increased cancer risk.

1.4 BRCA1 functions

BRCA1 has a multitude of functions across many cellular functions and many of them could share the tumour suppressing role of BRCA1 (Figure 1.5). The results of this thesis primarily investigate BRCA1's role in DNA repair.

1.4.1 DNA repair

BRCA1 has roles in the repair of multiple type of DNA damage which can be caused by natural cellular processes (such as replication or respiration), outside radiation or therapeutic drugs. Table 1.1 shows several types of DNA lesion, their repair pathway and examples of radiation or therapies that produce these types of DNA lesions.

1.4.1.1 DNA double-strand break repair

DSBs are one of the most severe types of DNA damage as they can lead to rearranged chromosomes, large scale deletions and insertions and, if the cells continue though the cell cycle with DSBs, they leads to apoptosis. There are tightly regulated pathways that control the sensing of a DSB, the choice of repair pathways and the repair of the break. These pathways are all involved in the cell cycle checkpoint response as continuing the cell cycle, i.e. into mitosis and division, with DSBs leads to daughter cells inheriting mutations.

The first responders to a DSB are the Ku70/80 heterodimer complex (Soutoglou *et al*., 2007) and the MRN complex (Lavin, 2007). The Ku70/80 complex binds directly to the end of the DNA break point and protects the ends from being resected by nucleases (Soutoglou *et al*., 2007). The MRN complex is made up of Mre11, Rad50 and Nbs1 (Lavin, 2007). Part of its function is to activate ATM (Berkovich *et al*., 2007) which phosphorylates H2AX histones around the DSB (Burma *et al*., 2001). The MRN complex is also a DNA damage sensor and

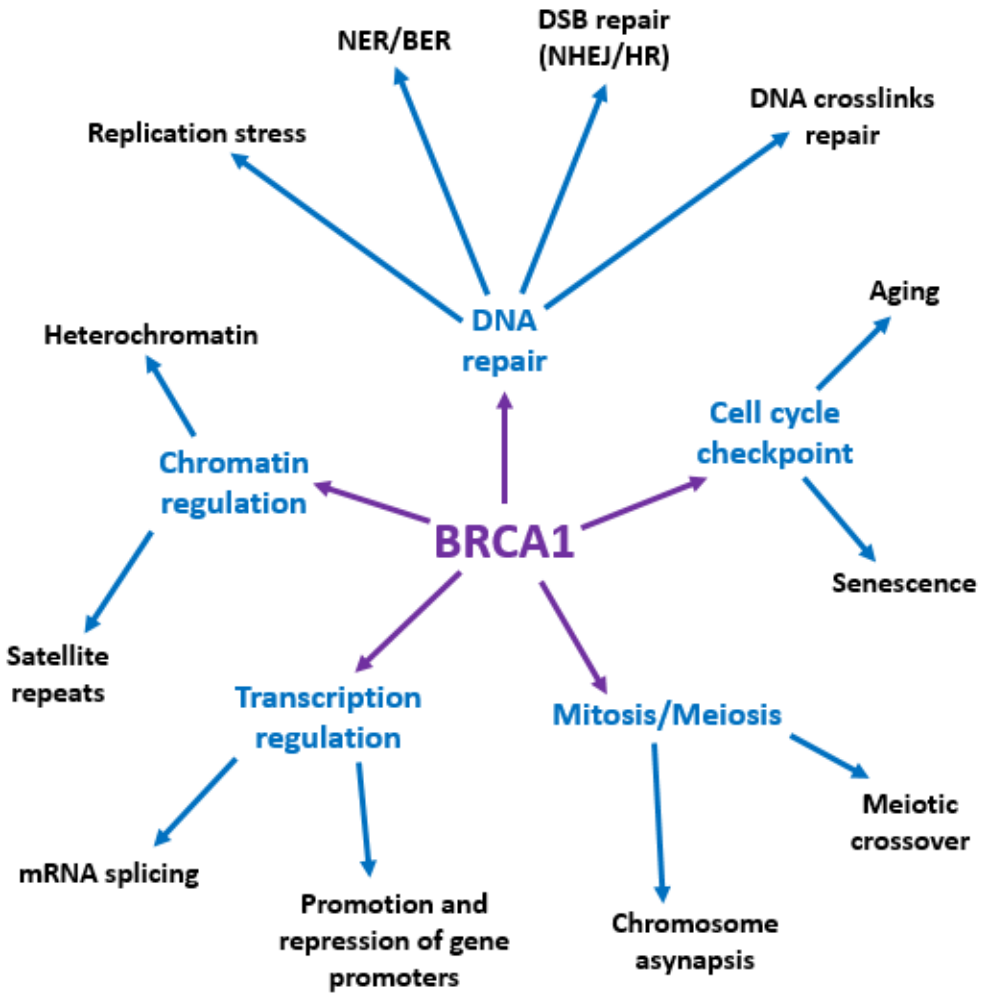

Figure 1.5 – Functions of BRCA1
This figure summarized BRCA1's more prominent roles in genome stability.

Table 1.1 – Table of DNA damage, repair and inducing agents

Type of DNA damage	Type of repair	DNA damage inducers
Double-strand break (DSB)	Non-homologous end-joining (NHEJ), Homologous recombination (HR), Microhomology, Other NHEJ variations	Ionising radiation (IR) [predominantly DSB but also other DNA damage], Topoisomerase II inhibitor - Etoposide/Doxorubicin
Single-strand lesions and single-strand breaks (SSB)	Mismatch repair (MMR), Nucleotide excision repair (NER)	Poly (ADP-ribose) polymerase inhibitors (PARPi) - Olaparib/4AN/Veliparib, Ultraviolet light (UV), Topoisomerase I inihbitors - Camptothecin (CPT)/Topotecan
DNA crosslinking repair (FANC pathway)	ICL repair (uses HR)	Mitomycin C (MMC), Nitrogen Mustard, Platinum agents - Cisplatin
Replication stress	Replication restart, Dissolution of DNA structures, DSB repair (after long period of replication stress)	Hydroxyurea (HU), Gemcitabine (Gemca), Fluorouracil (5-FU)

γH2AX acts as a beacon for further DSB repair proteins to accumulate. The first of these is MDC1 (Fau *et al*., 2003), which interacts with Nbs1, of the MRN complex (Lukas *et al*., 2004). MDC1 accumulation leads to the recruitment of RNF8 (Huen *et al*., 2007) which is an E3 ubiquitin ligase that can monoubiquitinate histones (Mailand *et al*., 2007). The signal from the monoubiquitination of histones is amplified by the creation of polyubiquitin chains (Bekker-Jensen *et al*., 2010). Histone H1 is monoubiquitinated by RNF8/Ubc13 complex (Hodge *et al*., 2016), and RNF168 or RNF8 can extend Histone H1 modifications into Lysine 63 (K63)-linked polyubiquitin chains (Hodge *et al*., 2016) that are needed for recruitment of BRCA1 (Bekker-Jensen *et al*., 2010; Hodge *et al*., 2016; Thorslund *et al*., 2015) and the Abraxas complex (Wang *et al*., 2007). RNF168 monoubiquitinates histone H2A on lysine 15

with K63-linked polyubiquitin chains, which recruits 53BP1 (Doil *et al*., 2009; Fradet-Turcotte *et al*., 2013; Gatti *et al*., 2012; Mattiroli *et al*., 2012; Stewart *et al*., 2009). Although it was previous shown that histones modified with K48 polyubiquitin chains may be required for recruitment of 53BP1 (Huen *et al*., 2007) and a recent paper suggested 53BP1 was recruited due to chromatin modification, but this could be independent of RNF8 and RNF168 (Kocylowski *et al*., 2015). L3MBTL1 binds to dimethyl-histone H4 Lysine 20 (H4K20me2) with a similar interaction site as 53BP1 (Min *et al*., 2007). In contrasting papers, the recruitment of 53BP1 has been reported to promote both NHEJ (Noon *et al*., 2010) and HR (Kakarougkas *et al*., 2013a), through promoting Kap1 phosphorylation of Serine 824 (pS824). RNF4 was recently described to be the controlling factor that degrades and localises phosphorylated Kap1 in a cell cycle-dependent manner and that pS824-Kap1 and 53BP1 colocalise after IR (Kuo *et al*., 2016). This paper suggests that pS824-Kap1 presence is a promoter of NHEJ and the accumulation of RNF4 in S/G2 phase relieves this NHEJ promotion through the degradation of Kap1 (Kuo *et al*., 2016).

Chromatin rearrangement is needed for both DSB repair pathways but 53BP1 binding to H4K20me2 (Botuyan *et al*., 2006) leads to the restriction of HR nucleases to access to the DSB (Xie *et al*., 2007). The ubiquitination of 53BP1 by Rad6-Rad18, allows 53BP1 to stably bind and be retained at chromatin, and this is specific to G1 phase of the cell cycle (Watanabe *et al*., 2009). SUMOylation of BRCA1 and 53BP1 are needed for their retention on chromatin (Galanty *et al*., 2009), and for BRCA1 E3 ubiquitin ligase activity (Morris *et al*., 2009).

Ku70/Ku80 heterodimer binds almost immediately to DSB DNA ends and forms the DNA-PK complex with DNA-PKcs (Gottlieb and Jackson, 1993). DNA-PKcs is a kinase that is activated

by the binding to DNA of Ku70/Ku80 and autophosphorylation (Hammarsten and Chu, 1998). It phosphorylates surrounding histones such as H2AX along with ATM and ATR (Kysela *et al*., 2005).

1.4.1.1.1 Homologous recombination

In S phase the DNA-PK complex is removed by VCP (Jiang *et al*., 2013b) as are K48 polyubiquitin chains on the histone (Meerang *et al*., 2011), and the DNA ends are ready for resection. K63 polyubiquitin chains, made by RNF168 and Ubc13 (Doil *et al*., 2009; Plans *et al*., 2006; Stewart *et al*., 2009; VanDemark *et al*., 2001), recruit the BRCA1-A complex (Wang and Elledge, 2007). Abraxas is the platform that holds the BRCA1-A complex together (Wang and Elledge, 2007), which is made up of Cdc98 (Liu *et al*., 2007b), BRE, MERIT40 (Wang and Elledge, 2007) and BRCC63 (Dong *et al*., 2003), a deubiuqinating enzyme (DUB). BRCC63 removed K63 polyubiquitin chains once the BRCA1-A complex is recruited allowing K6 polyubiquitin chains to be formed by BRCA1 (Shao *et al*., 2009b). The function of these K6-linked polyubiquitin chains is not clear.

End resection nucleases Mre11 (Taylor *et al*., 2010), from the MRN complex, and CtIP, in the BRCA1-C complex, resect DNA (Buis *et al*., 2012). CtIP is responsible for the majority of the resection and this activity is dependent on CtIP being phosphorylated by ATM (Yu and Chen, 2004). During end resection, the DNA is unwound by BLM helicase to elongate the 3' ssDNA (single-stranded DNA) end (Nimonkar *et al*., 2008). Phosphorylated RPA coats ssDNA to protect it from nucleases (Erdile *et al*., 1991), until it is replaced by Rad51 (Wang and Haber, 2004). The 9-1-1 clamp complex is phosphorylated in response to DNA damage signals and, alongside Rad17, is loaded onto RPA-coated ssDNA to sense DNA damage and start the recruitment of DNA damage proteins (Zou *et al*., 2002; Zou *et al*., 2003). TopBP1 is also

recruited (Kim *et al*., 2005) to ensure correct DNA repair. Rad51 is recruited by RNF8's K48 polyubiquitin chains (Ramadan, 2012) and is loaded onto ssDNA with the aid of BRCA2 (Dong *et al*., 2003) and DSS1 (Gudmundsdottir *et al*., 2004). BRCA1-B complex is made up of BRCA1, BRCA2 and PALB2. The BRCA1 and BRCA2 interaction is through BRCA1 coiled-coil domain binding to PALB2, and this recruits DSS1 (Zhang *et al*., 2009b). C-Abl phosphorylates Rad51 and this allows loading into the DNA (Yuan *et al*., 1998). Once bound to ssDNA, Rad51 forms filaments between the broken DNA strand and the sister chromatid template (Sung and Robberson, 1995; Yu *et al*., 2001) to allow the repair to be synthesised by a DNA polymerase such as Polζ-REV1 (Sharma *et al*., 2012). Once the DNA strand has been replicated and Rad51 filaments are displaced from the DNA, the template and new strand re-anneal and this can form a Holliday Junction (HJ) (Jones Petermann , 2012). HJ's are cut using Mus81/Mms4, which resolves the DNA strand structure and this can lead to sister chromatid crossover depending on the strand cut by Mus80/Mms4 (Boddy *et al*., 2001; Hanada *et al*., 2007). The cuts in the DNA backbones are ligated together by Lig1 or Lig3 (Liang *et al*., 2008).

1.4.1.1.2 Non-Homologous End-Joining

If 53bp1/DNA-PKcs/Ku complex is not removed from the DSB, DNA-PKcs is autophosphorylated (Hammarsten and Chu, 1998) and NHEJ repair is activated. DNA-PKcs also phosphorylates Artemis and RPA (Drouet *et al*., 2006). The conformational changes that occur in DNA-PKcs allow NHEJ proteins to access the DSB, such Artemis (Drouet *et al*., 2006), PNKP (Weinfeld *et al*., 2011), Tdt and pol λ and pol μ (Ramsden, 2011). Artemis is a ssDNA 5' exonuclease and has been shown, with DNA-PKcs, to have ssDNA 5' and 3' endonuclease activity (Drouet *et al*., 2006). PNKP is a 5' kinase and a 3' phosphatase and has been shown to require XRCC4 and DNA-PKcs to be active as phosphatases (Weinfeld *et al*., 2011). Artemis

is suggested to process the DNA ends for PNKP to chemically prepare the backbone of the DNA strands, and Tdt, pol λ and pol μ can replace any missing nucleotides that have created ssDNA overhang at the DSB (Ramsden, 2011). This is in preparation for Lig4, bound to XRCC4, to ligate the backbones together and fix the DSB (Kysela *et al*., 2005). NHEJ is considered to be error-prone because the DNA ends are processed before they are ligated back together and no DNA template is used to ensure there are no deletions.

1.4.1.1.3 DSB repair pathway choice

The mechanism that controls the choice of repair pathway is still being deciphered, but BRCA1 and 53BP1 remain the upstream effector proteins that orchestrate the choice of NHEJ or HR through prevention of DNA end resection and its antagonism (Figure 1.6). 53BP1 protects DSB ends from resection (Botuyan *et al*., 2006), a prerequisite for HR, and BRCA1 promotes resection (Schlegel *et al*., 2006), antagonising 53BP1's role to prevent DNA end-resection. 53bp1's prevention of end resection is orchestrated through phosphorylation-dependent interactions with RIF1 and PTIP (Callen *et al*., 2013). RIF1's role in preventing HR is less defined (Chapman *et al*., 2013; Escribano-Diaz *et al*., 2013; Zimmermann *et al*., 2013) than PTIP's but it may have a role in chromatin regulation (Dan *et al*., 2014) and RIF1 thought to act through the end-resection-inhibiting effects of REV7 (Boersma *et al*., 2015). PTIP binds 53bp1 through S/QT phosphorylation sites (Callen *et al*., 2013) and promotes end resection through recruitment of the nuclease Artemis which prepares DNA ends subsequently promoting NHEJ (Wang *et al*., 2014a). It is this that promotes the errors in NHEJ (Callen *et al*., 2013). In S phase BRCA1 BRCT domains can bind to the E3 ubiquitin ligase, UHRF1, which ubiquitinates RIF1 with K63-linked polyubiquitin chains which in turn removes 53BP1 from DSB sites (Zhang *et al*., 2016). POH1, a deubiquitinating enzyme (DUB),

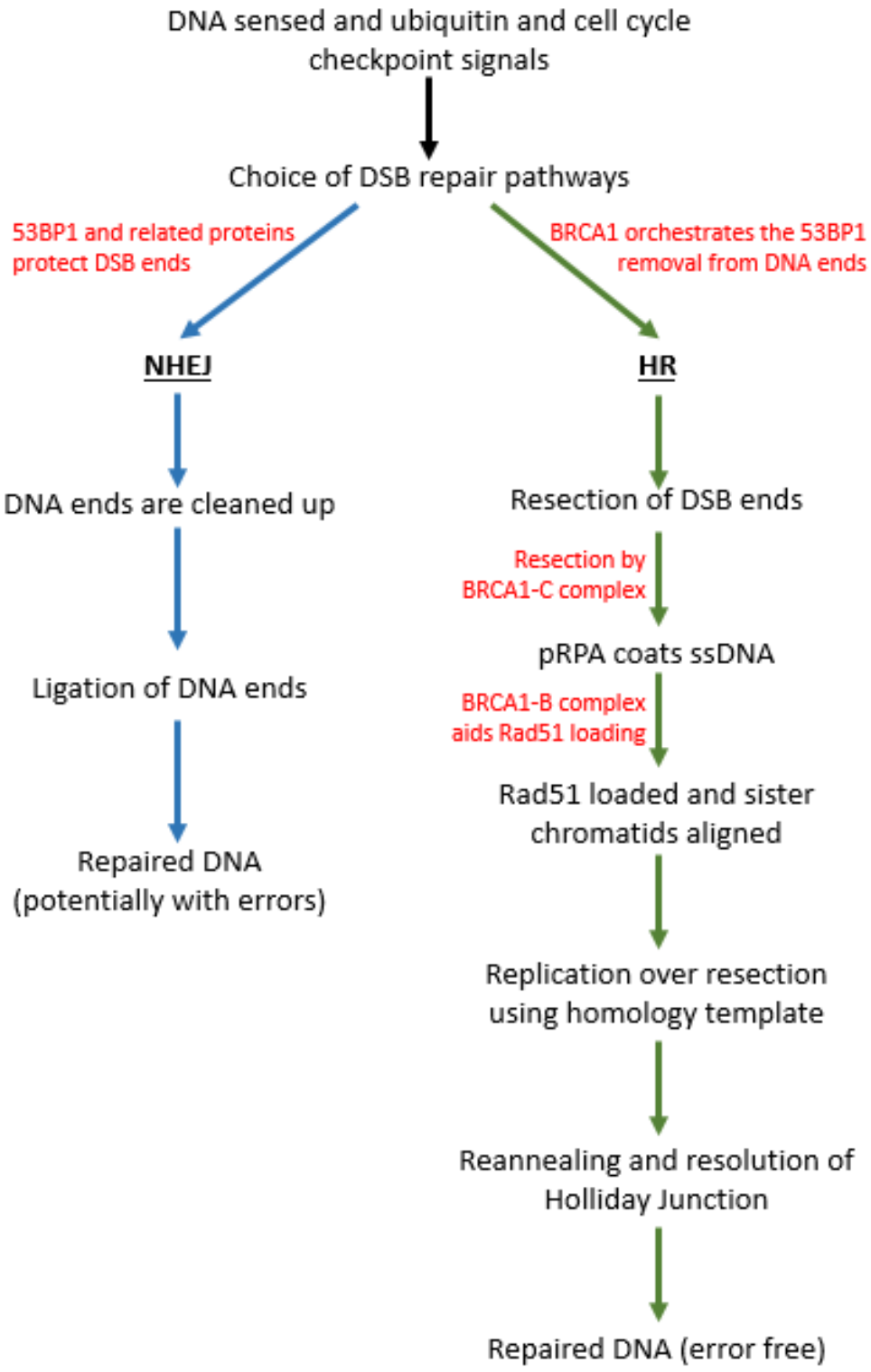

Figure 1.6 – The DSB repair pathway choice and BRCA1 roles
This simplifies NHEJ and HR, and the choice between which DSB repair pathway is used for repair. It identifies where BRCA1 has a role.

limits the presence of K63-linked polyubiquitin chains at a DSB (Butler *et al*., 2012) and this affects the accumulation of 53bp1 at the ends of the DSB (but not from the surrounding DSB area) (Kakarougkas *et al*., 2013b). The outward movement of 53BP1 from the centre of the DSB creates an increase in the 53BP1 foci size (Butler *et al*., 2012) and forms a core devoid of 53BP1 (Kakarougkas *et al*., 2013b). This devoid core is also devoid of RAP80 (Kakarougkas *et al*., 2013b). The polyubiquitin chains created by RNF8/RNF168 are removed (Butler *et al*., 2012) by USP26 and USP37 (Typas *et al*., 2015). These processes allows DNA to be nicked and resected by Mre11 and EXO1/BLM nucleases (Shibata *et al*., 2014), and allows RPA foci to form (Kakarougkas *et al*., 2013b). Shibata *et al*, suggest that it is the resection by Mre11 and EXO/BLM endonuclease activity that commits a DSB to be repair via HR (Shibata *et al*., 2014). USP26 and USP37 were also shown to promote the BRCA1 interaction with PALB2 (Typas *et al*., 2015), which is needed alongside BRCA2 to load Rad51 foci onto chromatin (Dong *et al*., 2003; Zhang *et al*., 2009b).

This removal of 53BP1 and its downstream effectors allows HR to progress although this is cell cycle-dependent (Chapman *et al*., 2012; Feng *et al*., 2013). Zhang *et al*, suggested the recruitment and phosphorylation of UHRF1 by CDK2/CyclinA, allow UHRF1 to polyubiquitinate RIF1 which leads to the disassociation of 53BP1 from sites of DSB, promoting HR (Zhang *et al*., 2016) in S/G2 phases of the cell cycle. The Ku complex has been reported to be removed from DSB ends in S/G2 phase by phosphorylation (Lee *et al*., 2016) and ubiquitination (Ismail *et al*., 2015). Many of the DSB repair proteins have phosphorylation sites that are provide control over their localisation or actions dependent on the cell cycle and as described above, these must in part contribute to the choice of repair pathway utilised at a DSB break.

1.4.1.1.4 BRCA1 roles in HR

BRCA1 has several roles in the HR repair and its functions can be seen when looking at the properties of each BRCA1 complex that is formed and localised to DSBs.

The first complex is called BRCA1-A, and contains RAP80 (Wang and Elledge, 2007), Abraxas (Wang and Elledge, 2007), ABRA1, CCDC98 (Liu *et al*., 2007b), NBA1/MERIT40 (Wang and Elledge, 2007), BRE and BRCC36 (Dong *et al*., 2003). Abraxas has coiled-coil domain which allows it to act as binding platform for proteins and its C-terminal phospho-Ser406 in its pSXXF motif interacts with the BRCT domains in BRCA1 (Wu *et al*., 2016). It also binds to RAP80, which is localised as a prerequisite for BRCA1 localisation. NBA1 has been shown to enhance the localisation of BRCA1-A complex to sites of DSB but only when ubiquitin is present (Wang and Elledge, 2007). In fact, many of the proteins in this complex are required for the localisation of BRCA1 because when they are knocked down or absent from cells, BRCA1 foci are greatly altered or decreased (Chen *et al*., 2006; Dong *et al*., 2003; Kim *et al*., 2007b; Liu *et al*., 2007b; Shao *et al*., 2009b; Sobhian *et al*., 2007; Wang *et al*., 2007). The localisation has also been shown to be influenced by ubiquitination of histones by RNF8 (Wang and Elledge, 2007) and RNF168 (Doil *et al*., 2009). However, BRCC36 is a DUB that hydrolyses K63 polyubiquitin chains, and it also is needed for BRCA1 recruitment in response to damage (Dong *et al*., 2003). This suggests that this role of BRCA1 is highly regulated by the presence and absence of ubiquitin chains. It has been suggested that the BRCA1-A complex has the ability to limit end resection at DSBs (Coleman and Greenberg, 2011) and a RAP80 knockdown in *BRCA1* mutated cells leads to increased levels of RPA in S/G2 phase cells and G1 cells are unaffected (Dong *et al*., 2003). This is interesting as BRCA1-C complex is

considered to promote HR by enhancing end resection, whilst the BRCA1-A complex limits end resection.

The BRCA1-C complex involved BRCA1/BARD1 heterodimer and CtIP. CtIP interacts with BRCA1 through its BRCT domains at its C-terminal end (Williams *et al*., 2009). CtIP, like BRCA1, is also phosphorylated by ATM and phosphorylates Chk2 (Yu and Chen, 2004; Yun and Hiom, 2009). CtIP is polyubiquitinated by BRCA1 in cells without damage, but ubiquitinated CtIP binding to chromatin in response to damage is BRCA1-dependent (Yu *et al*., 2006). Localisation of CtIP is also S and G2 phase-dependent as it is Cyclin A-dependent (Chen *et al*., 2008). CtIP is shown to resect DNA ends at a DSB, but also has been shown to promote MRE11 of the MRN complex and EXO1/BLM to complete bidirectional resection of the DSB ends (Buis *et al*., 2012; Shibata *et al*., 2014).

BRCA1 E3 ubiquitin ligase activity is needed to polyubiquitinate CtIP but the type of ubiquitin chain BRCA1 ligates onto CtIP is not known (Barber and Boulton, 2006). Unlike RNF8 or RNF168, BRCA1 predominantly ubiquitinates with K6 polyubiquitin chains (Morris and Solomon, 2004; Wu-Baer *et al*., 2003). These K6 polyubiquitin chains could provide a self-enhancement for the BRCA1/BARD1 complex ubiquitin ligase activity (Mallery *et al*., 2002) but the exact function of these K6 polyubiquitin chains is not clear and it is possible that they are placed on an unknown substrate.

BRCA1-B complex is characterised by the interaction of BRCA1 and BRCA2 through PALB2/FANCN (Sy *et al*., 2009; Zhang *et al*., 2009b). The main function of the BRCA1-B complex is to load Rad51 onto ssDNA, replacing RPA (Yu *et al*., 2001), and allowing RAD51 filaments to bring in the sister chromatid as a template for repair of the DSB via HR (Sung and Robberson, 1995). Truncated BRCA1 proteins have shown that BRCA1 C-terminus is

needed for recruitment of the BRCA1-B complex and Rad51 foci formation (Zhang *et al*., 2009b). The specific interaction of BRCA1 and PALB2 is around aa1400 (amino acid 1400) in BRCA1 at the coiled-coil domain, next to the BRCT domains and several phosphorylation sites, and between PALB2's WT40 domains. Deletion of either of these regions stops the BRCA1-BRCA2 interaction and RAD51 loading. Although it has been seen that overexpression of RAD51 can overcome BRCA1 (Martin *et al*., 2007) or BRCA2 defects (Lee *et al*., 2009). BACH1/BRIP1/FANCJ helicase (Dohrn *et al*., 2012; Kumaraswamy and Shiekhattar, 2007) also associates with the BRCA1-B complex in a BACH1-phosphorylation G2 phase cell cycle-dependent manner (Yu *et al*., 2003) and is associated with TopBP1 which is involved in the 9-1-1 complex at the polymerase step of HR DSB repair (Cotta-Ramusino *et al*., 2011).

1.4.1.1.5 BRCA1 in NHEJ

Although BRCA1 is involved in favouring HR over NHEJ DBS repair in S/G2 phase of the cell cycle, it has been shown to have a role in NHEJ in G1 (Baldeyron *et al*., 2002; Iliakis *et al*., 2004; Thompson *et al*., 2012; Wang *et al*., 2006; Zhong *et al*., 2002a; Zhong *et al*., 2002b; Zhuang *et al*., 2006). BRCA1 binds to Ku80 with its N-terminus (Jiang *et al*., 2013a), and this interaction aids rapid BRCA1 recruitment to DSBs (Wei *et al*., 2008). This interaction is independent of BARD1 and Ku80 binds to a similar region of BRCA1 suggesting competition for binding (Wei *et al*., 2008). The C-terminus of BRCA1 does not appear to be needed for this interaction or role in NHEJ (Wei *et al*., 2008). BRCA1 improves the stability of Ku80 binding to DSB ends (Jiang *et al*., 2013a). BRCA1 was reported to need active ATM/Chk2 cell checkpoint responses and kinase activity to be effect in aiding NHEJ (Wang *et al*., 2006; Zhuang *et al*., 2006). BRCA1 appears to be involved in c-NHEJ (canonical-NHEJ) (Dohrn *et al*., 2012) which provides an error-free method of repair in G1, and cells lacking BRCA1 show an

increased error-prone NHEJ repairs DNA causing more sequence deletion and chromosome aberrations in G1 cells treated with DSB-inducing agents (Jiang *et al*., 2013a).

1.4.1.2 DNA crosslink repair

1.4.1.2.1 The FANC repair pathway

The Fanconi anaemia pathway orchestrates the repair of DNA crosslinks repair and without this repair cells develop genomic instability and patients can develop cancer (Alter *et al*., 2003; Fanconi, 1964; Matthew, 2006; Tischkowitz and Hodgson, 2003). The cells from these patients are sensitive to MMC and Cisplatin, interstrand DNA crosslinking (ICL) damaging agents, and have chromosomal rearrangements (Matthew, 2006). These genetic mutations underlying Fanconi anaemia have been mapped to at least 15 genes that make up the Fanconi anaemia (FA) DNA repair pathway (de Winter *et al*., 1998; de Winter *et al*., 2000a; de Winter *et al*., 2000b; Howlett *et al*., 2002; Levitus *et al*., 2004; Levitus *et al*., 2005; Lo Ten Foe *et al*., 1996; Meetei *et al*., 2003; Meetei *et al*., 2004; Meetei *et al*., 2005; Strathdee *et al*., 1992; Timmers *et al*., 2001; Tischkowitz *et al*., 2007).

The FA pathway is activated during DNA replication where ICLs are recognised by FANCM-FAAP24 (Kim *et al*., 2008) and starts the repair by signalling the S phase checkpoint pathway via ATR (Collis *et al*., 2008) and recruiting the FA E3 ubiquitin ligase complex (Garcia-Higuera *et al*., 2001). The FA E3 ubiquitin ligase complex is made up of FANCA, FANCB, FANCC, FANCE, FANCF, FANCG, FANCL and FANCM (de Winter *et al*., 1998; de Winter *et al*., 2000a; de Winter *et al*., 2000b; Lo Ten Foe *et al*., 1996; Meetei *et al*., 2003; Meetei *et al*., 2004; Meetei *et al*., 2005; Strathdee *et al*., 1992). Once phosphorylated, FANCM is stabilised onto chromatin in association with MHF1 and MHF2 (Singh *et al*., 2010; Yan *et al*., 2010). Chk1,

from the ATR-checkpoint pathway, phosphorylates several of the FANC proteins in the complex to aid activation of the repair (Cohn and D'Andrea, 2008).

FANCL, the E3 ubiquitin ligase of the FA complex (Cole *et al*., 2010), monoubiquitinates FANCD2 and FANCI with the E2 conjugating enzyme, UBE2T, during S phase (Garner and Smogorzewska, 2011). Once FANCD2 and FANCI are ubiquitinated they are recruited, alongside FANCM/MHF complex, to the DNA lesion with the aid of BRCA1 (Bouwman *et al*., 2010; Bunting *et al*., 2012; Garcia-Higuera *et al*., 2001; Vandenberg *et al*., 2003; Zhang *et al*., 2010) to co-ordinate repair (Garner and Smogorzewska, 2011). Rad18 has also been seen to ubiquitinate FANCD2 as part of its activity in regulating translesion synthesis (TLS) (Williams *et al*., 2011). Ubiquitinated FANCD2 recruits the ubiquitin binding nucleases, FAN1 and P/SLX4, to start excision of the replicated DNA surrounding the DNA crosslink (Crossan and Patel, 2012). MUS81-EME and XPF-ERCC1 nucleases are recruited to cut the specific 'chicken foot' structure that replicated DNA has formed around the DNA crosslink (Ciccia *et al*., 2008). These nucleases lead to DSB formation that allows the cross between the two strands in the interstrand crosslink to stay attached to one strand of the DNA whilst the other is replicated via TLS (Long *et al*., 2011). The TLS of the DNA is polymerised by REV1 and pol ζ (Acharya *et al*., 2006; Hara *et al*., 2010). The remaining lesion is repair by nucleotide excision repair (NES) and DNA replication (Muniandy *et al*., 2010).

The DSBs are repaired through HR utilising BRCA1 (Bhattacharyya *et al*., 2000; Sawyer *et al*., 2015), Rad18 (Huang *et al*., 2009), BRCA2/FANCD1 (Howlett *et al*., 2002; Moynahan *et al*., 2001b), BRIP1/FANCJ (Litman *et al*., 2005; Sommers *et al*., 2009), PALB2/FANCN (Zhang *et al*., 2009b) and RAD51C/FANCO (Vaz *et al*., 2010) to promote Rad51 loading. FANCJ may have a role with BLM, as helicases for unwinding DNA to be resected by the endonucleases

(Suhasini *et al*., 2011). The inhibition of USP1 and UAF1 decreases the efficiency to HR at ICLs, suggesting that the removal of ubiquitin from FANCD2 may be needed to facilitate HR (Murai *et al*., 2011). Once USP1 and UAF1 have deubiquitinated FANCD2 and FANCI (Cohn *et al*., 2007; Cohn *et al*., 2009; Kim *et al*., 2009a; Murai *et al*., 2011; Nijman *et al*., 2005), DNA replication and the cell cycle can continue.

HR is used to repair the DSBs created in the resolution of ICLs because there is a second copy of the DNA to use a template in the form of the TLS product. The FA pathway does show a promotion of HR, over NHEJ, favouring error-free repair (Adamo *et al*., 2010; Pace *et al*., 2010). FANCD2, as a purified protein, has been suggested to be an antagonist for Ku70 activity through modifying DNA surrounding the ICL DSB (Pace *et al*., 2010).

This was shown by the successful attempts to rescue NHEJ repair in cells with defective FA repair by inhibiting NHEJ factors, such as DNA-PKcs, Lig4 and Ku70, (Adamo *et al*., 2010; Pace *et al*., 2010). However, not all NHEJ protein depletions rescue the FA pathway suggesting that the removal of NHEJ pathway is not sufficient, but there is a need for the removal of the mechanism by which FA pathway promotes NHEJ (Adamo *et al*., 2010).

1.4.1.2.2 BRCA1 roles in the FANC repair pathway

BRCA1 aids in the localisation of PALB2 and BRCA2 for Rad51 loading onto ssDNA for template repair in ICL repair. BRCA1's role with PALB2 and BRCA2 in Rad51 loading is an important component of HR, and it has been shown that in *53bp1*-null *Brca1*-defective cells, the loading of Rad51 foci at DSBs is independent of wild-type *Brca1* (Bunting *et al*., 2012; Nakada *et al*., 2012). This redundancy of BRCA1 in the loading of Rad51 would suggest that it is a 53bp1-independent role of BRCA1 that can lead to DNA crosslink sensitivity in BRCA1-defective cells (Bunting *et al*., 2012).

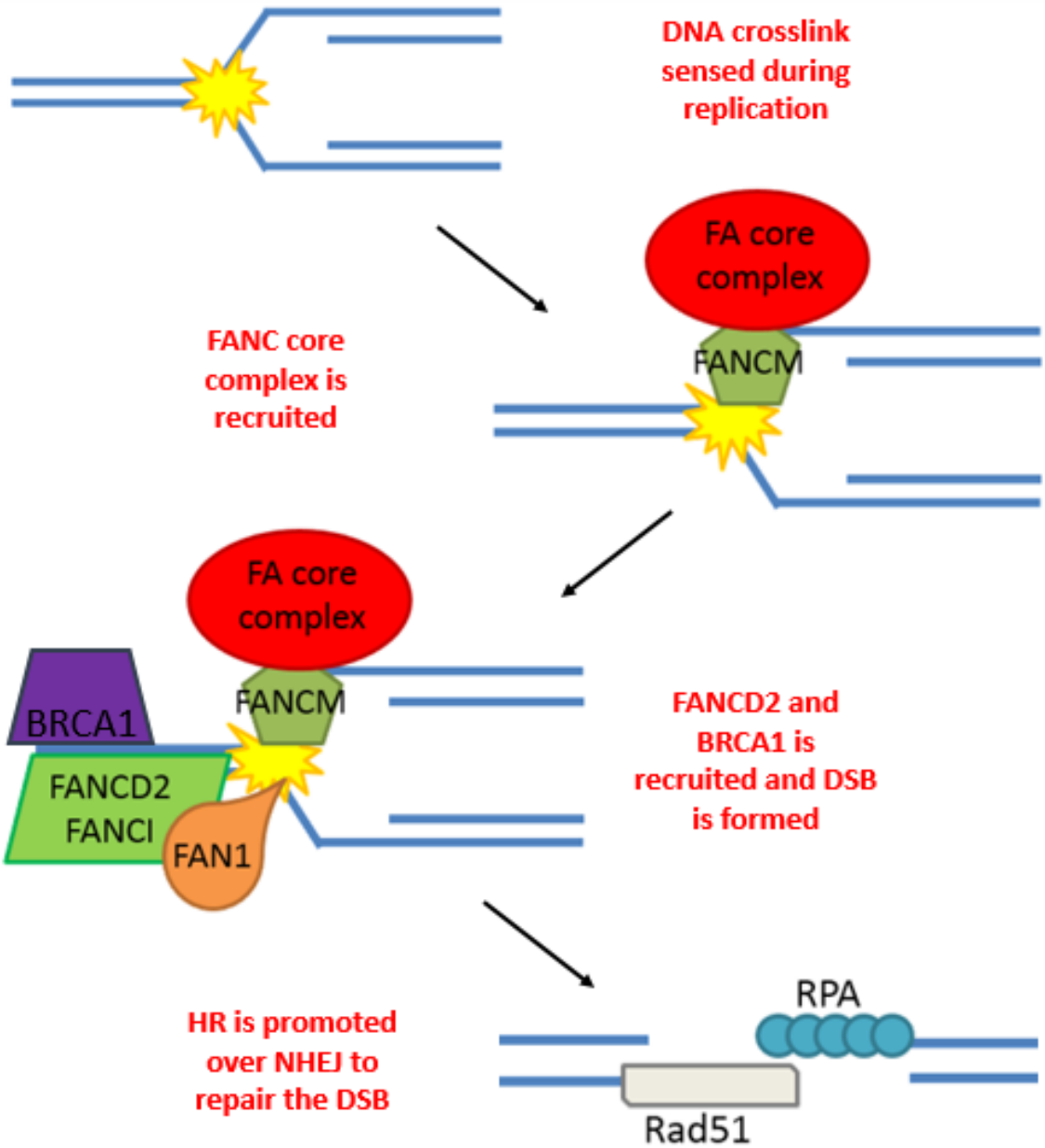

Figure 1.7 – DNA crosslink repair
This figure shows a simplified depiction of DNA crosslink repair and the involvement of BRCA1.

BRCA1 is important for the localisation of ubiquitinated FANCD2 to DNA crosslink repair foci (Figure 1.7) (Bouwman *et al*., 2010; Bunting *et al*., 2012; Garcia-Higuera *et al*., 2001; Vandenberg *et al*., 2003; Zhang *et al*., 2010) and FANCD2-FANCDI ubiquitination is essential for bringing in nucleases to start resection at ICLs (Klein Douwel *et al*., 2014; Knipscheer *et al*., 2009). *In vitro,* BRCA1/BARD1 E3 ubiquitin ligase activity has the ability to monoubiquinate FANCD2, but *in vivo* assays have shown that BRCA1 presence or E3 ubiquitin ligase activity (Exons 3&5 deleted) are not required for monoubiquitination but do lead to chromosome abnormalities (Vandenberg *et al*., 2003). FANCD2 and BRCA1 colocalize at sites of DNA damage (Garcia-Higuera *et al*., 2001; Taniguchi *et al*., 2002) and cells treated with BRCA1 siRNA or that have a *BRCA1* mutation show reduced localization of FANCD2 foci (Garcia-Higuera *et al*., 2001; Vandenberg *et al*., 2003).

A paper recently described BRCA1 in promoting the unloading of a helicase, called CMG, from replication structures (which include DNA crosslink repair structures) (Long *et al*., 2014). Long *et al* suggest that BRCA1 is localised to DNA crosslinks through ubiquitin signals and then unloads the CMG helicase which is upstream of FANCD2 recruitment or nucleases creating a DSB (Long *et al*., 2014). The BRCA1-CtIP interaction may also be important for DNA crosslink repair, as Yeo *et al* suggested that BRCA1 is essential for CtIP and FANCD2 being localised to chromatin (Yeo *et al*., 2014). It has also been shown that BRCA1 binds to FANCJ and its localisation is dependent on functioning BRCA1 ((Zhang *et al*., 2010).

These papers suggest that BRCA1 has at least one role in the DNA crosslink pathway that is upstream of Rad51 loading onto resected DNA. This upstream function supports that BRCA1 has a 53bp1-independent role in DNA crosslink repair and may explain why *53bp1*$^{-/-}$

Brca1$^{\Delta 11/\Delta 11}$ cells are sensitive to DNA crosslinking-agents but are functional in repairing DSBs through HR when caused by PARP inhibitors or IR (Bunting *et al*., 2010; Bunting *et al*., 2012).

1.4.1.3 Other DNA repair pathways

BRCA1's has DNA repair functions outside of the described roles in DSB and DNA crosslinks repair. The base excision repair (BER) pathway repairs lesions caused by oxidized DNA (Aiub *et al*., 2004; Evans *et al*., 2010) and BRCA1-deficient cells are sensitive to oxidative stress agents (Fridlich *et al*., 2015). NER involves the BASC complex (BRCA1-associated genome surveillance complex) of which BRCA1 is key (Wang *et al*., 2000). Both NER and BER can be repaired due to collisions with transcription machinery and BRCA1/BARD1 is involved in the degradation of RNA Pol II which removes proteins to allow DNA repair to proceed (Kleiman *et al*., 2005; Le Page *et al*., 2000; Starita *et al*., 2005) and is required for the transactivation of repair proteins (Hartman and Ford, 2002). UV radiation causes lesions that are repaired through TLS which is regulated by BRCA1's interaction with REV1 (Tian *et al*., 2013). It is important to note that if any of these repair mechanisms or DNA/protein structures are faulty, they can become DSBs in replication and need BRCA1-dependent HR for accurate repair.

1.4.2 Other Brca1 functions

DNA repair by BRCA1 is needed for genome stability but other cellular functions that are BRCA1-dependent are also important for the suppression of tumours.

1.4.2.1 Chromatin regulation

Loss of BRCA1 causes chromatin de-condensation on a genome-wide scale (Ye *et al*., 2001) and dysregulation of repetitive-satellite-containing heterochromatin (Zhu *et al*., 2011). This

has been reported to be through BRCA1 and BARD1's ability to ubiquitinate H2A (Zhu *et al*., 2011), but BRCA1 also interacts with chromatin remodelling proteins that could contribute to BRCA1-dependent chromatin regulation.

BRCA1 binds to histone deacetylases and the SWI/SNF chromatin remodelling complex (Chen *et al*., 2001; Harte *et al*., 2010; Yarden and Brody, 1999). It has also been reported to recruit DNA methyltransferases and interact with HP1 (a heterochromatin packaging protein) (Choi *et al*., 2012; Filipponi *et al*., 2013), which gives BRCA1 the ability to influence gene expression, as it does of Wip1 (Filipponi *et al*., 2013) and FOXA1 (Gong *et al*., 2015). Zhu *et al* suggested that the dysregulation of satellite DNA, due to *BRCA1* mutation, is enough to cause tumour development (Zhu *et al*., 2011).

1.4.2.2 Transcription regulation

BRCA1 has a role in active transcription which includes regulating mRNA splicing (Savage *et al*., 2014). Phosphorylated BRCA1 is recruited to the *BRCA1* mRNA splicing complex through its subunit BCLAF1 in response to DNA damage (Savage *et al*., 2014). BRCA1 can inhibit polyadenylation of 3' mRNA through ubiquitinating RNA Pol II and this affects the stability of mRNA (Kleiman *et al*., 2005).

BRCA1 also has the ability to resolve R-loops and aid transcription restart without the formation of DSBs (Hatchi *et al*., 2015; Hill *et al*., 2014). BRCA1-PALB2 complex is seen to be locating to actively transcribed regions of chromatin, and specifically DNA damage sites that are being transcribed (Aymard *et al*., 2014; Gardini *et al*., 2014; Tang *et al*., 2013). BRCA1 can interact with complexes containing RNA and hnRNP proteins that are formed after the DNA is damaged (Chiba and Parvin, 2001).

BRCA1 has a patch of acidic amino acid residues in the C-terminus and Miki *et al* predicted BRCA1 to be involved in transcription (Miki *et al*., 1994). It was then shown that the C-terminus fragment of BRCA1 alongside the GAL4 DNA binding domain, did have transcriptional activity (Monterio *et al*., 1996). C-terminal mutations found in patients with cancer showed that this region was essential for BRCA1 transcriptional activity (Humphrey *et al*., 1997; Monterio *et al*., 1996). BRCA1 has roles in both transcriptional regulation that promotes and inhibits gene transcription. The *BRCA1* transcriptome showed that the majority of BRCA1 gene regulation is DNA damage-induced (Gorski *et al*., 2011).

ATM/ATR-phosphorylated BRCA1 promotes the transcription of p21-dependent DNA repair and cell cycle checkpoint genes through p53 (Andrews *et al*., 2002; Fabbro *et al*., 2004a; MacLachlan *et al*., 2002). Through Oct-1 interaction, BRCA1 aids the transactivation of GADD45 which stalls the cell cycle and promotes apoptosis (Fan *et al*., 2002; Harkin *et al*., 1999) in DNA damage cells, but in undamaged cells CtIP/Zrbk-1 aids BRCA1-Oct-1 in GADD45 repression (Li *et al*., 1999; Yu *et al*., 1998; Zheng *et al*., 2000). Oct-1/BRCA1 also activated the expression of BER pathway proteins, such as NTH1, REF1/Ape1 and OGG1 (Saha *et al*., 2010). Stat-1 was found to co-activate pro-apoptotic genes with BRCA1 after interferon-γ stimulation (Buckley *et al*., 2007; Ouchi *et al*., 2000). BRCA1 also inhibits apoptosis by activating anti-apoptotic genes regulated by NF-κB pathway by recruiting p50 to promoters where BRCA1/p60 are bound (Harte *et al*., 2014).

BRCA1 can repress genes when in complex with c-Myc and Nmi, which stops hTERT and other tumour-related genes, from being expressed (Kennedy *et al*., 2005; Li *et al*., 2002). BRCA1's influence on p53-regulated genes does promote one set of genes to be expressed

but it also causes the repression of p53-regulated pro-apoptotic genes (Andrews *et al*., 2002; MacLachlan *et al*., 2002). The estrogen receptor alpha (ERα) is repressed when it binds to BRCA1 (Fan *et al*., 2001a; Zheng *et al*., 2001) and this stops the transcription of proteins that promote angiogenesis and tumour proliferation (Kawai *et al*., 2002). COBRA1 is a co-factor of BRCA1 that aids the inhibition of ERα by stalling RNA Pol II mRNA elongation (Aiyar *et al*., 2004). Oct-1 is also involved in recruiting BRCA1 to ERα (Hosey *et al*., 2007). The BRCA1/CtIP/Zbrk1 complex is known to repress genes such as RFC1, which is a DNA repair protein (Furuta *et al*., 2006).

These studies collectively show that BRCA1 has transcriptional roles that influence a great number of tumour suppressing and oncogenes that are known to aid tumour development when dysregulated.

1.4.2.3 Cell cycle checkpoint regulation

Many DSB repair proteins aid cell cycle checkpoint activation to allow the cell cycle to halt for the time it takes to repair the DNA. BRCA1 is needed to activate cell cycle checkpoint proteins but cell cycle proteins regulate its own activation.

BRCA1 mediates the ATM/ATR-dependent phosphorylation of p53 at Serine 15 after IR (Fabbro *et al*., 2004a). But to do this BRCA1 must be phosphorylated by ATM or ATR at Serine 1423 or 1524 (Fabbro *et al*., 2004a; Xu *et al*., 2001a). The phosphorylation of p53 orchestrates the G1/S phase checkpoint by transcribing p21 (Fabbro *et al*., 2004a). The phosphorylation of BRCA1 is transient and is removed once the DNA is repaired (Chen *et al*., 1996; Ruffner and Verma, 1997).

BRCA1's interaction with TopBP1 is required for the ATR activation that activates the S phase checkpoint (Xie *et al*., 2012). The BRCA1-ATRIP complex is thought to aid pRPA-coated ssDNA to activate an ATR checkpoint response (Venere *et al*., 2007; Zou and Elledge, 2003). hCds1 and Chk2 are also involved in the BRCA1-mediated replication arrest (Yarden *et al*., 2002).

The BRCA1 interacting protein ATRIP is also important for an efficient G2/M checkpoint and can be disrupted by altering the interaction between the BRCT domains of BRCA1 and phosphorylated Serine 239 in ATRIP (Venere *et al*., 2007). It has been reported that BRCA1 ubiquitinates Cyclin B/Cdc25C which is degraded (Shabbeer *et al*., 2013), and this stops their accumulation and the entry into mitosis (Kostyrko *et al*., 2015; Yarden *et al*., 2002).

The G2/M checkpoint requires both ATM and BRCA1 to be fully functional (Draga *et al*., 2015; Yarden *et al*., 2002). BRCA1 S1423 is phosphorylated by ATM and prolongs the phosphorylation of Chk1 which when activated arrests the cells in G2 phase (Draga *et al*., 2015; Yarden *et al*., 2002). BRCA1 requires ABRAXAS to achieve this G2 arrest (Draga *et al*., 2015).

The presence of a functional checkpoint response is important for correct DNA repair. In the case of BRCA1's role in DSBS repair end resection, if Chk2 is not phosphorylated in response to DNA damage, there is a delay in DSB end resection and BRCA1 foci are retained for longer at DSBs (Parameswaran *et al*., 2015).

BRCA1 mutated cells have different cell cycle defects dependent on the mutation. Cells that only express the BRCA1 Exon 11 (Δ11) isoform have a defective G2/M checkpoint but have a functional G1/S phase checkpoint (Larson *et al*., 1997; Xu *et al*., 1999b). Mutation of Serine 1423 on BRCA1 abolishes ATM phosphorylation and this causes a G2/M checkpoint defect,

but does not affect the S phase checkpoint arrest (Xu *et al*., 2001a). Shabbeer *et al* suggest that the ubiquitin ligase activity of BRCA1 is also important for a G2/M cell cycle arrest (Shabbeer *et al*., 2013). Overexpressing BRCA1 has also been seen to arrest cells in G0/1 (Campbell *et al*., 2001) and G1/2 (Somasundaram *et al*., 1997).

Without functional BRCA1 (or a BRCA1 that cannot be phosphorylated correctly), cells display the signs of DNA damage being present throughout the cell cycle and through mitosis and this leads to sensitivity to DNA-damaging agents (Cortez *et al*., 1999; Wiltshire *et al*., 2007). This also leads to mitotic problems and daughter cells that can inherited mutations or loose/gain chromosome arms. Therefore BRCA1 cell cycle roles are important for maintaining genomic stability.

1.4.2.4 Centrosome

Centrosomes are the main microtubule organising centres during mitosis and they are important for the correct segregation of chromosomes to ensure genome integrity. In normal cells BRCA1 colocalises with centrosomes (Di Paolo *et al*., 2014; Hsu and White, 1998; Sankaran *et al*., 2005) and BRCA1-deficient cells show an amplification of centrosomes, abnormal chromosome segregation and aneuploidy (Di Paolo *et al*., 2014; Starita *et al*., 2004; Xu *et al*., 1999b). BRCA1 interacts with proteins that are involved in the spindle assembly checkpoint (Bae *et al*., 2005; Chabalier *et al*., 2006; Wang *et al*., 2004a) and spindle pole proteins (Jin *et al*., 2009; Joukov *et al*., 2006). The loss of BRCA1 protein causes an increased distance between interkinetochores and less centromeric cohesion (Di Paolo *et al*., 2014). This may be due to BRCA1 being important for the full accumulation of Aurora B

kinase at centromeres, through its role in hypomethylation by recruiting DNMT2b, a DNA methyltransferase (Di Paolo *et al*., 2014).

1.5 *Brca1* mouse models

Due to the clinical nature of *BRCA1* mutations, mouse models with *Brca1* mutation have been explored to help provide more information about the human *BRCA1* mutation and how they could leave to cancer development. Mice are used as a model organism from human disease because they are a mammal, therefore are closely related in evolution, and because they can be genetically altered to mimic genetic disorders and their progression. Brca1 in mice is 75.22% (Clustal 2.1) similar to human BRCA1 and important residues and domains are conserved (Intro 1.3.2 and Chapter 3.2).

1.5.1 *Brca1* mouse mutations and embryonic lethality

The various mouse models that have been made encompass several different mutations in *Brca1* and the defects and phenotypes of the mice vary. This variety is likely to be due to the disruption of a region of Brca1 altering a function of Brca1 that is actioned by that region. Figure 1.8 maps out previously studied mouse mutations and their positions in Brca1 domains to indicate the possible impact each mutation has on the protein structure of *Brca1* and some of the phenotypes seen in these mice.

Some *Brca1* mouse models have used a flox system that encompasses Exon 11 (Δ11) of *Brca1* creating a large deletion of the gene (Cressman *et al*., 1999b; Gowen *et al*., 1996; Liu *et al*., 1996; Shen *et al*., 1998; Xu *et al*., 1999a). The Flox system consists of flanking a region with two flox domains which allow for recombination of that region. However, certain Exon 11

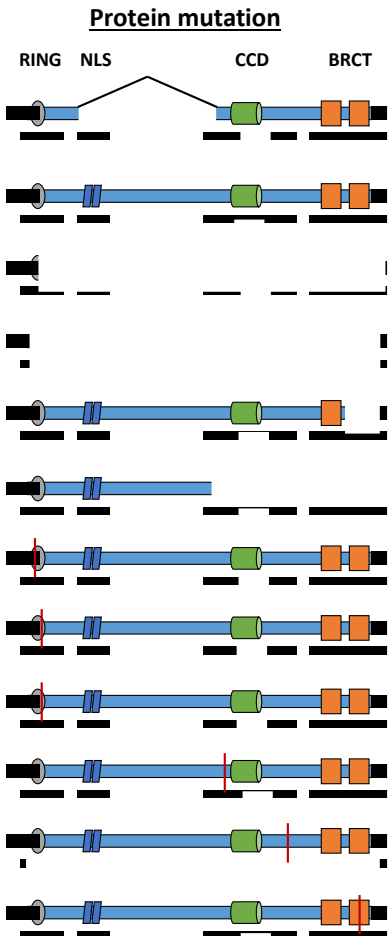

Mutation	Embryonic Lethal	Protein	Fertility	Tumours	Reference
Exon 11 (Δ11)	Yes	Δ11 isoform	-	-	(Cressman et al., 1999b; Gowen et al., 1996; Liu et al., 1996; Xu et al., 1999)
Full-length only (FL)	No	FL only, no Δ11 isoform	Normal	Yes	(Kim et al., 2006)
Exon 5-6 (Δ5-6)	Yes	No protein, frameshift	-	-	(Hakem et al., 1997)
Exon 2 (Δ2)	Yes	Unstable	-	-	(Ludwig et al., 1997)
Truncation at amino acid 1700 (Tr aa1700)	Yes	Truncated	-	-	(Hohenstein et al., 2001)
Truncation at amino acid 924 (Tr aa924)	No	Truncated (Δ11 normal)	Male infertile	Yes	(Ludwig et al., 2001)
Ile26Ala (I26A)	No	Normal	Male infertile	No	(Shakya et al., 2011)
Cys64Gly (C64G)	Yes	aa22 frameshift	-	-	(Yang et al., 2003)
Cys61Gly (C61G)	Yes	Normal in tumours	-	-	(Drost et al., 2011)
Ser971Ala (S971A)	No	Normal	Normal	Yes	(Kim et al., 2004)
Ser1152Ala (S1152A)	No	Normal	Normal	Yes	(Kim et al., 2009)
Ser1598Phe (S1598F)	No	Normal	Male infertile	Yes	(Shakya et al., 2011)

Figure 1.8 – Brca1 mouse mutations and phenotype

This figure shows Brca1 mutation mouse models and their position in the Brca1 protein. It also comments on the embryonic lethality, fertility and tumour risk phenotype of these mice. The red line depicts the approximate location of the point mutation. Domains are further detailed in figure 1.2.

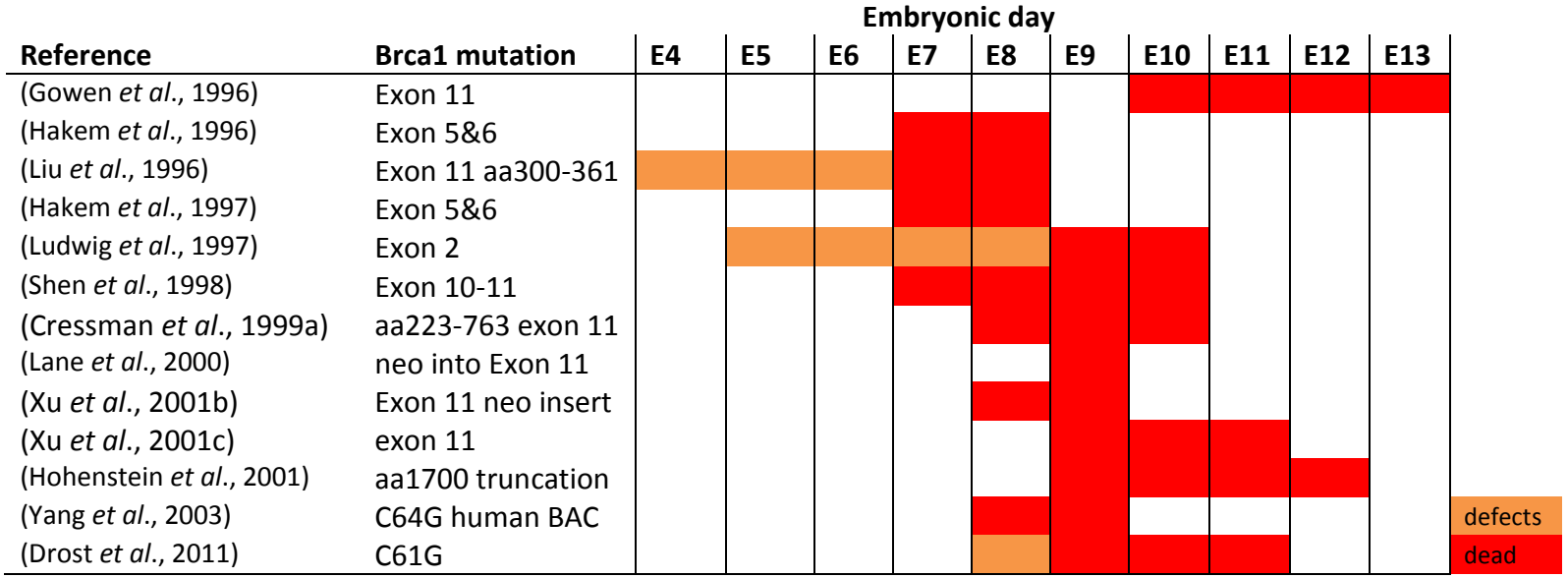

Figure 1.9 – Mouse Brca1 mutations and the embryonic lethality timing

This figure shows the Brca1 mutations that caused embryonic lethality in mice and the embryonic day at which defects (orange) and death (red) was identified.

flox vectors do not include the Brca1 has a splice acceptor site and therefore the isoform of Brca1 created by alternative splicing is not affected in these Exon 11 mutations (Gowen *et al*., 1996; Liu *et al*., 1996). The isoforms function was separated from full-length Brca1 by blocking the acceptor site (Kim *et al*., 2006). Mice that only express full-length Brca1 (no Exon 11 deletion isoform) were born healthy but showed altered mammary gland development and increased proliferation and tumourigenesis of the uterus (Kim *et al*., 2006). This suggests that the Exon 11 isoform of Brca1 is involved in genome stability and hormonal driven development in mice. Interestingly, the tumours from Exon-11-isoform-deleted mice did not have full-length Brca1 protein suggesting that full-length Brca1 is still needed to prevent cancer development (Kim *et al*., 2006).

Other mutations to in *Brca1* mouse have included the deletion of Exons 5 and 6 (Δ5-6) (Hakem *et al*., 1996; Hakem *et al*., 1997), Exon 2 (Δ2) (Ludwig *et al*., 1997), Exon 21-24 (Δ21-24) (McCarthy *et al*., 2007) and truncation at aa1700 (tr1700) (Chandler *et al*., 2001; Hohenstein *et al*., 2001) and they have all been embryonic lethal like Exon 11 (aa300-361 (Liu *et al*., 1996) and aa233-763 (Cressman *et al*., 1999a)). The phenotypes in these embryos are all similar, but they do have some variability between them in the morphological defects and in the embryonic day they are reabsorbed (Figure 1.9).

One truncation mutation of *Brca1* (aa924) was not embryonic lethal but were born at reduced Mendelian rations (4% instead of 25%) (Ludwig *et al*., 2001). The mutation in *Brca1* was caused by a knock-in of 50bp insert into Exon 11 which causes a stop codon due to the frameshift (Ludwig *et al*., 2001). In cells of this genotype full-length *Brca1* is not detected and there is a reduction in the truncated *Brca1* mRNA (Ludwig *et al*., 2001). However, the splicing variant of Brca1 was detected at wild-type levels (Ludwig *et al*., 2001). The mice that

were born had defects in skin pigmentation, growth rate, tail formation and male spermatogenesis (Ludwig *et al*., 2001). At the time of death, 26% of control mice had developed tumours compare to the 85% of homozygous mutant mice that developed a range of tumours, including lymphomas, sarcomas, ovarian teratoma and carcinomas of the breast, lung, liver, uterus and colon (Ludwig *et al*., 2001). The non-lethal phenotype of the truncation could suggest that the C-terminal of *Brca1* is not the cause of the embryonic lethality in other *Brca1* mutants however there still is a presence of the *Brca1* Exon 11 isoform. Isoform protein levels are approximately a fifth of full-length Brca1 protein levels, but could have a functional C-terminus. This would mean that the functional absent region of Brca1 in these mice is from aa924 to Exon 10 (aa1365).

To divide the functions of BRCA1, mutations can be made that alter a region-associated function. I26A, C64G, C61G, S971A, S1152A and S1598F are all missense mutations in important residue that are targeted to affect a specific activity of BRCA1. S1598F changes a serine residue to a proline, which disrupts the BRCT domain binding to BACH and FANCJ (Shakya *et al*., 2011). This mutation, when homozygote, was also not embryonic lethal but the mice did develop tumours and the male mice were sterile (Shakya *et al*., 2011). This suggests that the BRCT domain interaction with BACH and FANCJ are not important in embryonic lethality, but may be for tumour development (Shakya *et al*., 2011).

S971A and S1152A both change a serine to an alanine. S971 relates to S988 in human BRCA1 and it known to be a Chk2 phosphorylation site. The mice were born at expected ratios but still developed uterus and ovarian tumours by 2 years of age showing underlying genomic instability (Kim *et al*., 2004). This mouse can be compared to the *Chk2*-deficient *Brca1*-deficient mice (Cao *et al*., 2006), as S971A functions the same as the removal of *Chk2* in the

ATM-p53-Chk2 checkpoint pathways. The mutation does not cause embryonic lethality which suggests that it is not responsible for the developmental defects, but still causes checkpoint defects that lead to tumourigenesis (Kim *et al*., 2004). S1152, which is S1189 in humans, is phosphorylated by ATM in response to DSBs. Like the S971A mice, S1155A mice were born at the expected ratio and at 18 months old, developed tumours, however S1152A mice has a severe phenotype with higher levels of apoptosis and growth retardation (Kim *et al*., 2009b). The lack of ATM-BRCA1 interaction is also not responsible for the embryonic lethality in *Brca1*-deficient mice, but shows control in growth and genome stability. Both of these mutations target the ATM-p53-Chk2 cell cycle checkpoint, which has been shown to allow the rescue of embryonic lethality in *Brca1*-deficient mice (Cao *et al*., 2003; Cao *et al*., 2006; Cao *et al*., 2007; Cressman *et al*., 1999a; Mak *et al*., 2000; Xu *et al*., 1999a; Xu *et al*., 2001c), but the lack of embryonic lethality suggests that neither missense mutation solely controls the checkpoint or the checkpoint defect is not enough to cause the developmental defects.

C61G and C64G missense mutations both change cysteines into glycines in Site II of the zinc ligating region and I26A mutation changes an isoleucine to an alanine in Site I of the zinc ligating region, of the RING domain in BRCA1. The BRCA1 RING domain is highly conserved and these missense mutations have been shown to reduce the BRCA1 E3 ubiquitin ligase activity using an *in vivo* ubiquitination assay (Brzovic *et al*., 2003). C61G and C64G mutations alter zinc ligation and BARD1 binding and this is what causes the reduction in ubiquitin ligase activity (Brzovic *et al*., 2003; Hashizume *et al*., 2001; Mallery *et al*., 2002; Ruffner *et al*., 2001; Wu *et al*., 1996). I26A does not alter zinc ligation but does alter the binding of an E2 conjugating enzyme which causes the reduced ubiquitin ligase activity (Brzovic *et al*., 2003).

Brca1$^{I26A/\Delta 2}$ embryonic stem (ES) cells show differentiation and colony formation showing that I26A ES cells are viable, but do show male sterility and a decreased body weight (Shakya *et al*., 2011). The *Brca1*$^{I26A/\Delta 2}$ mice were viable and did not develop tumours (Shakya *et al*., 2011). C61G (Drost *et al*., 2011) and C64G mice (Yang *et al*., 2003) were both embryonic lethal. C64G mutation of a G-T at nucleotide 309 has been shown to produce a 22-nucleotide deletion from *Brca1* mRNA transcript due to the interruption of splicing site (Yang *et al*., 2003). C61G mice are also embryonic lethal but showed Brca1 C61G protein levels similar to wild-type Brca1 protein levels in tumour cells (Drost *et al*., 2011). This could suggest that the C61G mutation lethality is caused by the single amino acid change affecting the E3 ubiquitin ligase activity (Drost *et al*., 2011) rather than affecting the amount of Brca1 protein. There is other evidence, mostly cell-based, that suggests Brca1 C61G protein is stable (Campbell *et al*., 2001; Lu *et al*., 2007; Nelson and Holt, 2010) and evidence that disagrees with this (Brzovic *et al*., 1998; Brzovic *et al*., 2001b; Choudhury *et al*., 2004; Wang *et al*., 2014b) which is both biochemical and cell-based research. The difference in phenotypes produced by these three N-terminal RING domain mutations suggests more research is needed to explain why specific mutations lead to specific phenotypes, and how this relates to the function of the RING domain.

1.5.2 Tissue-specific *Brca1* mutations in mice

A tissue-specific *Brca1* mutation can be used to study *Brca1* homozygote mutations in mice without the problem of embryonic lethality. This uses a tissue-specific genome editing system that will create a *Brca1* homozygote mutation using a promoter that is only expressed in the specific cell type. A T cell-specific *Lck* promoter with *Cre* recombinase ability was bred with *Brca1*$^{fl5\text{-}6}$ to investigate Brca1 function in T cell-lineage development (Mak *et*

al., 2000). There was 90% less thymocytes in the *Brca1*-defective mice compared to WT mice showing *Brca1* to be essential for T cell lineage development. *p53*-rescued *Brca1*-deficient mice have some levels of T cell lineage depletion but not to the extent of the conditional *LckCre Brca1*-defective mice, suggesting that a p53-dependent Brca1 pathway causes the cell death in T cells (Mak *et al*., 2000).

Ovarian cancer occurs at high prevalence in hereditary *BRCA1* mutation families. A *Fshr-Cre* Exon 11 deletion in *Brca1* was made which creates a *Brca1* homozygous mutation in granulosa cells (Chodankar *et al*., 2005). 68% of these mice develop ovarian and uterine cysts between 12-20 months and the majority of cysts were cancerous (Chodankar *et al*., 2005). The tumours in these mice show similar histology and genomic rearrangements that are seen in human ovarian serous carcinoma and cells were of non-granulosa, epithelial origin (Chodankar *et al*., 2005). This paper suggests that it may not be the DSB repair defect caused by *Brca1* deficiency that starts the tumour development, but faulty or lack control of the ovarian and uterine growth via Brca1, possibly through the oestrus cycle (Chodankar *et al*., 2005).

Brca1 is expressed in highly proliferative epithelial tissue the several conditional *Cre* recombinase mouse models have been made to remove *Brca1* specifically from epithelial tissues. Whey acidic protein (*Wap*), mouse mammary tumour virus-long terminal repeat (*MMTV-LTR*), β-lactoglobulin (*BLG*), keratin 5 (*K5*) and keratin 14 (*K14*) are all promoters expressed in mammary epithelial cells, but some are not exclusive to mammary tissue. *K5* promoter is found in the oral and sinus cavity, esophagus, bladder, prostate, vagina, skin basal layer and mammary gland epithelial cells (Ramirez *et al*., 1994). *K14* is specific to squamous epithelia and epidermal keratinocytes mainly involving breast tissue and skin

(Vassar *et al*., 1989). *MMTV-LTR* is expressed in mammary epithelial cells and ductal cells of the salivary gland (Wagner *et al*., 1997). *Wap* promoter is specific to the alveolar epithelial mammary cells (Wagner *et al*., 1997). *BLG* is expressed in secretory epithelial cells in the mammary glands and at low levels in salivary glands (Whitelaw *et al*., 1992).

Brca1$^{\Delta 11}$*K5-Cre* mice showed apoptotic skin epithelial from 6 weeks old and at 88 weeks mice developed a variety of cancers such as lymphoma, ear, oral cavity, stomach, skin and vagina (Berton *et al*., 2003). *Brca1*$^{\Delta 21\text{-}24}$*BLG-Cre* (McCarthy *et al*., 2007), *Brca1*$^{\Delta 5\text{-}13}$*K14-Cre* (Liu *et al*., 2007a) and *Brca1*$^{F/C61G}$ *K14-Cre* (Drost *et al*., 2011) mice developed breast tumours when combined with one or two mutations in *p53*. *Brca1*$^{\Delta 11}$*Wap-Cre* and *Brca1*$^{\Delta 11}$*MMTV-LTR-Cre* mice showed abnormal mammary and fat pad development and mammary tumours around 1 year of age, but the tumour development was be sped up by a *p53* heterozygous mutation (Brodie *et al*., 2001). The *Wap-Brca1* and *K14-Brca1* mouse mammary tumours resembled human BRCA1 breast cancer histology (Brodie *et al*., 2001; Drost *et al*., 2011).

1.5.3 *Brca1* mutant mice with a second gene mutation

A second method of evading the homozygote *Brca1* mutation embryonic lethality is by removing a second gene (or one allele of another gene) to compensate for the defects that cause developmental problems.

Chk2 and *p53* mutated rescue of *Brca1*-deficient mice leads to the development of various types of cancer (Cao *et al*., 2003; Cao *et al*., 2006; Cao *et al*., 2007; Hakem *et al*., 1997; Xu *et al*., 1999a). *p53* rescue leads to lymphoma (Cressman *et al*., 1999a), breast (Xu *et al*., 1999a), oesophageal and stomach cancer (Cao *et al*., 2007), but the mice have other phenotypes such as premature aging and high levels of senescence (Cao *et al*., 2003). *Chk2* rescued mice produce mainly breast and ovarian tumours and show a reduced, but not normal, level of

apoptosis and senescence (Cao *et al*., 2006) compared to *p53* rescued mice (Cao *et al*., 2007). Cells from both rescued *Brca1*-deficient mice still show premature aging and genomic instability (Cao *et al*., 2003; Cao *et al*., 2006). *Chk2* and *p53* are part of the ATM-Chk2-p53 cell cycle checkpoint signalling pathway that is activated in response to DNA damage to stop cells from replicating with unresolved DNA damage (Iliakis *et al*., 2003). *Brca1* deficiency leads to unrepaired damage due to a HR defect and this triggers the ATM-Chk2-p53 checkpoint and cells senescence or become apoptotic (Xu *et al*., 2001c). Without a second mutation in this checkpoint pathway cells cannot proliferate and this could be why *Brca1*-deficient embryos stop growth and show very high levels of senescence (Xu *et al*., 2001c). With a mutation in *p53* or *Chk2*, *Brca1*-deficient cells still show some senescence and a DNA damage repair defect with chromosomal abnormalities leading to tumourigenesis, but cells do manage to proliferate allowing development past embryogenesis (Bachelier *et al*., 2003; Cao *et al*., 2003; Cao *et al*., 2006; Cao *et al*., 2007; Cressman *et al*., 1999a; Xu *et al*., 2001c). Mutations in genes with similar functions have been made to attempt to rescue *Brca1*-deficient mice. p21 is a downstream regulator of the p53-dependent cell cycle checkpoint that controls G1-S transition in the cell cycle, therefore if *p21* were mutated this could overcome the checkpoint and allow proliferation (Mak *et al*., 2000). *Brca1;p21*-deficient embryos do show reduced levels of senescence and survive until birth, however they die within 24 hours (Hakem *et al*., 1997; Mak *et al*., 2000). This suggests that p21 is part of the pathway is involved in the *Brca1*-deficient embryonic lethality but p53 is upstream of p21 and therefore a *p53* mutation allows for a more complete rescue of embryonic development.

Chk1, is part of a cell cycle checkpoint response called ATR-Chk1-p53 signalling pathway and it control the DNA replication checkpoint (Cao *et al*., 2006). *Chk1*-null homozygote mice are embryonic lethal at day E4.5, therefore a heterozygous mutation of *Chk1* was bred to produce a *Brca1*-deficient mouse (Cao *et al*., 2006). There was a partial rescue as 80% of *Brca1*-deficient *Chk1*-null heterozygous mice survived until birth, but they died within 24 hours (Cao *et al*., 2006). This suggests, similarly to p21, that there is a postnatal development defect that is not rescued by mutated *Chk1*, because of Chk1-independent Chk2-dependent pathway.

Other proteins that are involved in p53 cell cycle regulation and DNA damage repair pathways have be used to attempt to rescue embryo development in the *Brca1* homozygote mice but they have not succeeded; proteins such as PTEN (Cao *et al*., 2006), Gadd45a (Wang *et al*., 2004b), APC, Msh-2 (Hohenstein *et al*., 2001) and PARP1 (Cao *et al*., 2006).

DNA repair genes have also been mutated in attempt to rescue the development of *Brca1*-deficient mice. The most successful was a null mutation in the NHEJ promoting protein *53bp1* which alleviated the embryonic lethality of $Brca1^{\Delta 11/\Delta 11}$ mice (Bunting *et al*., 2010; Bunting *et al*., 2012; Cao *et al*., 2009). *53bp1*-null mice are born at normal Mendelian ratios, but have a suppressed immune system, IR sensitivity, chromosome abnormalities, thymic lymphoma and slowed growth (Morales *et al*., 2003; Ward *et al*., 2003b). The suppressed immunity is caused by faulty end-joining in V(D)J recombination which affects CSR (class switch recombination). CSR utilises NHEJ in AID (Activation-Induced Deaminase) during G1 to create variety in switch regions in immunoglobulin heavy-chains and this allows Ig's to have more diversity producing a more effective immune system, and therefore *53bp1*-deficient mice have the phenotype of weakened immunity (mice die from unknown causes,

suggestive of succumbing to infection) (Morales *et al*., 2003). Chromosome abnormalities are a phenotype evident of errors in DSB repair and having dysfunctional telomeres and chromosome segregation that is seen in *53bp1*$^{-/-}$ mice (Ward *et al*., 2003b). 53BP1 acts to protect DSB and telomere ends by binding to dimethyl-histone 4 (H4K20me2) which prevents the relaxation of the histones, stopping the endonucleases from access to the DNA ends (Botuyan *et al*., 2006; Xie *et al*., 2007). This protects chromosome ends from being degraded which leads to DNA and, possibly, gene loss and stops end resection at DSB breaks from promoting HR (Xie *et al*., 2007).

In *Brca1*-deficient mice, the *53bp1* knockout rescues the embryonic lethality and the *53bp1*$^{-/-}$ *Brca1*$^{\Delta 11/\Delta 11}$ mice are born at Mendelian ratios and have a normal lifespan without elevated tumour incidence (Bunting *et al*., 2010; Bunting *et al*., 2012; Cao *et al*., 2009). Chromosome exchanges and radial chromosomes were reduced in *53bp1*$^{-/-}$*Brca1*$^{\Delta 11/\Delta 11}$ cells in comparison to *Brca1*$^{\Delta 11/\Delta 11}$*p53*$^{-/-}$ cells (Bunting *et al*., 2010). *Brca1*-deficient cells with a *p53* mutation show sensitivity to DSB and DNA crosslinking damaging agents (Bunting *et al*., 2012) but *53bp1*$^{-/-}$*Brca1*$^{\Delta 11/\Delta 11}$ MEFs show a rescue of the Brca1-dependent sensitivity to PARPi, CPT, and IR which all cause DSBs (Bunting *et al*., 2010). PARPi inhibit PARP, a single-strand DNA break (SSB) repair protein (Altmeyer *et al*., 2009), and CPT inhibits topoisomerase I, a ssDNA exonuclease, causing an accumulation of single-stranded breaks (Hsiang *et al*., 1985). These ssDNA breaks are converted into DSB during DNA replication (Liu *et al*., 2008; Satoh and Lindahl, 1992). IR causes multiple types of DNA damage but the majority are DSBs (Painter, 1974; Yamamoto *et al*., 1985). The rescue of sensitivity in *53bp1*$^{-/-}$*Brca1*$^{\Delta 11/\Delta 11}$ MEFs suggests that DSB repair is possible in these cells.

53bp1$^{-/-}$*Brca1*$^{\Delta 11/\Delta 11}$ MEFs show sensitivity to crosslinking agents such as Cisplatin and MMC (Bunting *et al*., 2012) suggesting that although DSB repair is possible, DNA crosslink repair is defective (Bunting *et al*., 2012). Brca1 has a 53bp1-independent role of the crosslinking repair pathway (Section 1.4.1) and therefore the deletion of 53bp1 does not rescue the ICL repair pathway.

The deletion of other HR proteins, such as *Brca2* and *Xrcc2* (Bunting *et al*., 2010), do not replicate the HR rescue phenotype with the removal of *53bp1*, and the deletion of NHEJ proteins, such as *Ku70*, *DNA-PKcs* (Bunting *et al*., 2012) and *Lig4* (Bunting *et al*., 2010), show no or only partial rescue of the *Brca1*-deficient phenotype. Deletion of proteins in multiple DNA repair pathways often leads to synthetic lethality due to the cells being unable to repair DNA damage leading to cell death (Mohni *et al*., 2015; Somyajit *et al*., 2015; Turner *et al*., 2008). Synthetic viability is the alleviation of a mutated genes' lethal phenotype due to the deletion of a second protein. This is true for *53bp1*-null homozygote *Brca1* Δ11 mice which develop to maturity (Bunting *et al*., 2010; Bunting *et al*., 2012; Cao *et al*., 2009).

1.5.4 Male infertility

DNA repair proteins have been known to be involved in the resolution and control of meiotic crossover involving DSB repair (Boateng *et al*., 2013; Cressman *et al*., 1999a; Kopanja *et al*., 2011; Lou *et al*., 2006; Santos *et al*., 2010; Schaetzlein *et al*., 2013; Simhadri *et al*., 2014; Xu *et al*., 2003; Xu *et al*., 1996) and chromatin control, including meiotic sex chromosome inactivation and sex body control (Adamo *et al*., 2008; Fernandez-Capetillo *et al*., 2003; Santos *et al*., 2010). Mutations in DNA damage repair proteins have been shown to cause male infertility in humans (Ji *et al*., 2013) and this is replicated in mouse models mutated in DSB repair genes such as *MDC1* (Lou *et al*., 2006), *RNF8* (Li *et al*., 2010; Lu *et al*., 2010;

Santos *et al*., 2010), *PALB2* (Simhadri *et al*., 2014) and *CUL4* (Kopanja *et al*., 2011). Although these gene mutations cause male infertility, some DNA repair proteins cause male and female sterility such as mutations in *BRCA2* (Friedman *et al*., 1998), *ATM* (Xu *et al*., 1996) and *Exo1* (Schaetzlein *et al*., 2013). Other DSB repair proteins show no effect on fertility (Chapman *et al*., 2013; de Murcia *et al*., 1997; Gu *et al*., 1997; Ward *et al*., 2003b; Zhu *et al*., 1996), and *53bp1* is one of these proteins (Ward *et al*., 2003b). Mus81 is an exonuclease needed to resolve collapsed replication forks (Boddy *et al*., 2001; Hanada *et al*., 2007) and mice with homozygote null mutations in *Mus81* are fertile (Dendouga *et al*., 2005; Holloway *et al*., 2008; McPherson *et al*., 2004) but do show dysregulated crossovers in meiosis (Holloway *et al*., 2008). These results suggest that mutations in DNA repair proteins may cause different effects on fertility depending on the functional change they have on meiosis. The reasons behind the sex-specific infertility is not completely understood but one theory is that it is the inactivation of the meiotic XY sex chromosomes that affects spermatogenesis (Royo *et al*., 2010).

Brca1 mice with mutations affecting the BRCT domains or the RING domain ubiquitin ligase function cause male-specific infertility (*Brca1* null mutation lacking *53bp1* (Bunting *et al*., 2012), truncating mutation (Ludwig *et al*., 2001), I26A (Shakya *et al*., 2011), Δ223-763 (Cressman *et al*., 1999a) and Δ11 with either $p53^{+/-}$ (Xu *et al*., 2003) or $Chk2^{-/-}$ (Cao *et al*., 2006)). However *Brca1* point mutations not affecting these domains (S1152A (Kim *et al*., 2009b) and S971A (Kim *et al*., 2006)) and *Brca1* mice which only express full-length Brca1 (Kim *et al*., 2004) do not show any infertility. This suggests that the function of Brca1 in meiosis involves both the BRCT domains and a catalytically active E3 ubiquitin ligase RING domain.

BRCA1 is important for resolution of meiosis crossovers in which DSBs are created and repaired (Cressman *et al*., 1999a; Simhadri *et al*., 2014; Xu *et al*., 2003), and is involved in the chromatin regulation and sex body inactivation since BRCA1 binds to unsynapsed meiotic chromosomes and inactivated sex chromosomes (Adamo *et al*., 2008; Ganesan *et al*., 2002; Turner *et al*., 2004; Turner *et al*., 2005; Xu *et al*., 2003). Xu *et al* suggest that the meiotic defects associated with BRCA1 occur in Prophase I when there is a high level of DSBs created for crossovers to occur (Xu *et al*., 2003). Specifically, BRCA1-defective cells arrest in pachytene stage and maintain a prolonged γH2AX signal (a DNA damage sensor) and prolonged GCNA protein presence which does not allow for the continuation of meiosis (Xu *et al*., 2003). Spo11 is the exonuclease that creates DSBs during meiotic crossover (Bellani *et al*., 2010; Boateng *et al*., 2013; Romanienko and Camerini-Otero, 2000) and *Spo11/Brca1* double mutant in *C.elegans* shows infertility even though DSBs are not created in meiosis (Adamo *et al*., 2008). Adamo *et al* suggests that the *Brca1* defect in meiosis is not caused by faulty DSB repair (Adamo *et al*., 2008) and therefore it may be BRCA1's role in asynapsed chromosomes and sex body inactivation through its interaction with XIST RNA (Ganesan *et al*., 2002; Royo *et al*., 2010) that causes the male-specific infertility in *Brca1*-mutated mice.

1.6 Aims of this thesis

Despite the substantial amount of current literature, more information is required about the functions of BRCA1 and how variants or pathogenic mutations affect BRCA1's roles in tumour suppression. This thesis investigates the effects of the C61G mutation on mouse Brca1, including its E3 ubiquitin ligase activity *in vitro*, how cells with two copies of the *Brca1* C61G allele respond to DNA-damaging agents. Homozygote *Brca1* C61G mice are embryonic lethal (Drost *et al*., 2011) and this thesis will describe the breeding of these mice with *53bp1*-

null mice to produce living *53bp1*$^{-/-}$*Brca1*$^{C61G/C61G}$ offspring. MEFs were isolated from these mice and were used to further study Brca1-related cellular functions, but also a mouse model provided an organism in which the *Brca1* C61G mutation could cause tumour development.

This project investigated the effect of the *Brca1* C61G mutation on mouse protein, mouse cells and the mouse as an organism and this has provided valuable information into the degree at which the C61G mutation effects *Brca1*-dependent genome stability. This information will contribute to a better understanding of why cancer risk is high in *BRCA1* C61G carriers and potentially, which drugs are effective in treating BRCA1-C61G tumours (specifically tumours which also have 53bp1 dysregulation).

Chapter 2 – Materials and methods.

Materials

2.1 Drug and radiation treatments

2.1.1 Ionising Radiation

Cells were placed inside the irradiator case. The machine was programmed with the number of seconds (5 Gray= 157 seconds) that gave the desired level of exposure (measured in Gray) to the ^{137}Caesium source. Cells were returned to the 37°C incubator.

2.1.2 Drug treatments

The following table (Table 2.8) contains the DNA-damaging drugs (Cisplatin, CPT, HU, Olaparib, Veliparib, MMC) and the cell manipulation drugs (LMB and CHX). These were used at the doses specified in the each experiment for the time stated (Table 2.8).

Table 2.1 – Drug treatments

Drug	Stock concentration	Solution	Company
Cisplatin	Made up fresh	Saline	Sigma
Camptothecin (CPT)	10mM stock	DMSO	Sigma
Hydroxyurea (HU)	1M stock	H_2O	Sigma
Olaparib	50mM	DMSO	Santa Cruz Biotechnology
Veliparib	50mM	DMSO	Santa Cruz Biotechnology
Mitomycin C (MMC)	make up fresh	H_2O	Abcam
Leptomycin B (LMB)	10ng/ml	Ethanol	Sigma
Cycloheximide (CHX)	100mg/ml	DMSO	Sigma

2.2 Microscopy

Images were taken using a Leica DM6000B microscope with Leica LAS software and a HCX 100x/1.4 oil lens. This Leica uses a HBO lamp with a 100W mercury short arc UV bulb light source and four filter cubes, A4, L5, N3 and Y5. The filters that were used in this thesis were to produce excitation at the wavelengths 488 and 555, and the UV bulb excited the Hoechst stain.

2.3 PCR mutagenesis primer sequences

Primer sequences were designed to be of 15 bp or more with either a C or G base. They matched the cDNA of the vector used but contained base pair changes that created the codon for the desired change to sequence (Table 2.9). Primers were diluted in dH_2O.

Table 2.2 – PCR mutagenesis primer sequences

Primer name	Primer sequence
C61G Forward	GCCCGTCGCAGGGGCCGCTGTGTAAAAATGAAATTACC
C61G Reverse	GGTAATTTCATTTTTACACAGCGGCCCCTGCGACGGGC
I26A Forward	CCTGGAATGCCCGGCCTGCCTGGAACTGATTAAAGAACC
I26A Reverse	GGTTCTTTAATCAGTTCCAGGCAGGCCGGGCATTCCAGG
P62R Forward	CGTCGCAGTGCCGCCTGTG
P62R Reverse	CACAGGCGGCACTGCGACG
L82R Forward	CGCTTTTCTCAGCGCGCGGAAG
L82R Reverse	CTTCCGCGCGCTGAGAAAAGCG
R93A Forward	CCTCAAGATAAACGCACAATTGGACAGC
R93A Reverse	GCTGTCCAATTGTGCGTTTATCTTGAGG
R93E Forward	CCTCAAGATAAACGCACAATTGGACAGC
R93E Reverse	GCTGTCCAATTGTGCGTTTATCTTGAGG

2.4 Antibodies

Primary and secondary antibodies used in the western blotting and immunofluorescent experiments are detailed in table 2.10 and 2.11 below. They were used at the stated dilutions in Milk or 10% FBS:PBS.

Table 2.3 – Primary antibodies

Protein	Animal	Supplier	Dilution	IF/WB
53bp1 (ab172580)	Rabbit	Abcam	1:2000	IF
β-tubulin (ab6046)	Rabbit	Abcam	1:5000	WB
β-actin (ab8226)	Rabbit	Abcam	1:4000	WB
γH2AX (ab2893)	Rabbit	Abcam	1:4000	IF
γH2AX (ab184520)	Mouse	Abcam	1:4000	IF
Brca1 (GH118)	Mouse	gift from Jos Jonkers	neat	IF/WB
CtIP (AC-R0192-1)	Rabbit	Millipore	1:2000	WB
Cyclin A (ab38)	Mouse	Abcam	1:1000	IF/WB
FANCD2 (NB100-182)	Rabbit	Novus	1:2000	IF/WB
Flag-tag (M2, F3165)	Mouse	Sigma	1:4000	WB
GAPDH (ab8245)	Mouse	Abcam	1:2000	WB
HA-tag (H3663-7)	Mouse	Sigma	1:4000	WB

His-tag (SAB2702218-GT359)	Rabbit	Sigma	1:1000	WB
Histone 4 (ab10158)	Rabbit	Abcam	1:5000	WB
Hoechst (94403)	N/A	Sigma	1:20000	IF
Rad51 (H-92, sc-8349)	Rabbit	Santa Cruz	1:1000	IF
Ubiquitin (P4D1, sc-8017)	Mouse	Santa Cruz	1:2000	WB

Table 2.4 – Secondary antibodies

Secondary antibody	Animal	Supplier	Dilution	IF/WB
Goat anti-Mouse Alexa Fluor 555	Goat	Life technologies	1:2000	IF
Goat anti-Rabbit Alexa Fluor 488	Goat	Life technologies	1:2000	IF
Donkey anti-Mouse Alexa Fluor 488	Donkey	Life technologies	1:2000	IF
Donkey anti-Rabbit Alexa Fluor 555	Donkey	Life technologies	1:2000	IF
Rabbit anti-Mouse HRP	Rabbit	DAKO	1:5000	WB
Swine anti-Rabbit HRP	Swine	DAKO	1:5000	WB

2.5 Buffers

LB broth – 10g LB broth powder (Sigma) in 500ml H_2O

LB agar – 1 LB agar capsule (Thermo Fisher) in 500ml H_2O

50x TAE buffer – 2M Tris base, 17.5% acetic acid (Glacial), 10% 0.5M EDTA pH8

Urea buffer – 0.25M Tris pH6.8, 8% SDS, 40% Glycerol, 6M Urea, 10% β-mecaptoethanol

PBS – 1 PBS tablet (Sigma) in 200ml H_2O

SDS running buffer – 10% 10x Tris/Glycine/SDS in 90% H_2O

Transfer buffer – 10% 10x Tris/Glycine, 10% methanol, 80% H_2O

Lysis buffer – 50mM sodium phosphate pH7, 300mM sodium chloride, 5% glycerol, 10mM β-mercaptoethanol

Wash buffer – 50mM sodium phosphate pH7, 300mM sodium chloride, 5% glycerol, 10mM β-mercaptoethanol, 50mM imidazole

Dialysis buffer – 25mM Tris-HCl pH7.5, 10% glycerol, 2mM DTT, 150mM potassium chloride

10x Ubiquitin ligase buffer – 0.5M Tris-HCl pH7.5, 50mM magnesium chloride, 5mM DTT

4x SDS sample loading buffer – 0.25M Tris pH6.8, 8% SDS, 40% Glycerol, 6M Urea, 10% β-mecaptoethanol, dyes to colour desired

Cell fractionation buffer 1 – 50mM Hepes-KOH pH7.5, 140mM sodium chloride, 1mM EDTA, 10% glycerol, 0.5% NP40, 0.25% Triton X

Cell fractionation buffer 2 – 10mM Tris-HCl pH8, 200mM sodium chloride, 1mM EDTA, 0.5mM EGTA

Cell fractionation buffer 3 – 10mM Tris-HCl pH8, 100mM sodium chloride, 1mM EDTA, 0.5mM EGTA, 0.1% Na-Deoxycholate, 0.5% N-Lauroylsarcosine

Crystal Violet stain – 0.5% Crystal Violet, 50% Methanol, 49.5% H_2O

Methods

2.6 Bioinformatic techniques

2.6.1 Sequence retrieval and alignments

Gene and protein sequences were taken from Ensembl (Cunningham *et al*., 2015) and aligned using BLAST (Camacho *et al*., 2009).

2.6.2 Molecular structure alignment

1JM7 is the solution structure of human BRCA1:BARD1 RING domain heterodimers (Brzovic *et al*., 2001b). This structure and SWISS-MODEL (Biasini *et al*., 2014) was used to thread the mouse Brca1:Bard1 RING domain sequences to predict the structure used in this thesis. 2C4P is the crystal structure of human ubiquitin-conjugating enzyme UbcH5a (Dodd *et al*., 2004) and it was used to map on the E2 predicted binding surface onto Brca1:Bard1. SWISS Pdb-Viewer was used to visualise and manipulate molecular structures (Guex and Peitsch, 1997).

2.6.3 Measuring WB protein band density

Using ImageJ (Schneider *et al*., 2012), protein band from scanned western blot films were measured for density. The area of these plotted density peaks from these bands was measured and used to correlate to the amount of protein detected by the antibody on the western blot.

2.7 Molecular Biology

2.7.1 Bacterial transformations

For DNA production, performed under sterile conditions, 10µl of *Escherichia coli* DH5α (Bioline) was pipetted into pre-chilled Eppendorf's alongside 1-50ng of the desired DNA plasmid. These were incubated on ice for 15 minutes and heat shocked for 30 seconds at 42°C. Eppendorf's were placed on ice for 2 minutes before 100µl of Luria Bertani (LB) was added to the tube and gentle mixed through flicking. These cultures were placed into a 37°C incubator for 45-60 minutes. The cultures were next spread onto LB agar plates containing the relevant antibiotics and incubated overnight at 37°C. This thesis utilises vectors with either Ampicillin or Kanamycin antibiotic resistance, and LB agar plates contain either 50µg/ml of Ampicillin or Kanamycin.

For protein production culture under sterile conditions, 5-10µl of Escherichia coli BL21 (DE3) were placed in a pre-chilled Eppendorf alongside 100ng of the desired protein producing vector. This remained on ice for 20-40 minutes before exposing the Eppendorf to 42°C for 45 seconds. This is returned to ice for 2 minutes prior to 100µl of LB is added to the tube and flicked to mix. The tube was incubated for 45 minutes (or overnight for two vectors) and spread onto LB agar plates with the correct antibiotic(s) matching the antibiotic resistance gene in the DNA vector(s).

2.7.2 Plasmid DNA preparation

Half of a single bacterial colony was picked from the LB antibiotic agar plate and placed into either a 5ml (Miniprep), 20-100ml (Midiprep) or 500-1000ml (Maxiprep) of LB with 50µg/ml of the antibiotic matching the antibiotic resistance gene in the DNA vector. This culture was

incubated overnight at 37°C. Using a centrifuge, the bacterial was separated from the LB by spinning at 3000rpm for 30 minutes. DNA was extracted from the bacterial pellet using GeneJET Miniprep, Midiprep or Maxiprep kits (ThermoFisher) following the manufacturer's protocol.

2.7.3 Quantification of nucleic acids

DNA quantification was performed using ND-1000 software and a Labtech Spectrophotometer. dH_2O or TE buffer (GeneJET kit, ThermoFisher) was used as a blank measurement.

2.7.4 PCR mutagenesis

PCR was used to amplify and mutate DNA vectors using primers that contained a mutation directed to a specific site in the vectors gene. dNTPs (Bioline) and Pfu DNA polymerase (Thermo) were used using the following recipe (Table 2.1) and PCR programme (Table 2.2) for PCR mutagenesis.

Table 2.5 – PCR mutagenesis DNA polymerase mastermix

Ingredient	Stock concentration	Final concentration	Volume in 50µl
DNA	variable	1ng	-
Pfu buffer	10x	1x	5µl
dNTPs	10mM	200µM	1µl
PfU	2.5 Units/µl	2.5 Units	0.5µl
Forward primer	20µM	0.8µM	2µl
Reverse primer	20µM	0.8µM	2µl
dH_2O	-	-	made up to 50µl

Table 2.6 – PCR mutagenesis amplification programme

Step	Temperature (°C)	Time	Cycles
Starting denaturing	98	2 minutes	1
Denaturing	98	1 minute	18
Annealing of primers	65	30 seconds	18
Extension of DNA	72	10 minutes	18
Finalising extension	72	5 minutes	1
Hold	4	∞	-

PCR programme times in table 2.2 were adjusted to 5°C less than the lowest optimum annealing temperature for the primers and the length of the DNA vector.

2.7.5 Restriction enzyme digest

DNA vector solutions that were subject to mutation through PCR mutagenesis were treated with Dpn1 restriction enzyme. 2µl of Dpn1 restriction enzyme was added to 25µl of PCR mutagenesis solution (50µl total) and stored at 37°C for 1 hour. 10µl of both the Dpn1 treated and untreated were run on a DNA electrophoresis gel.

Mouse genotyping samples that were amplified using the Brca1 C61G loci primers were treated with EcoNI restriction enzyme for 1 hour at 37°C. Some samples were exposed to 65°C for 20 minutes to stop the EcoNI enzyme action. 10µl of the untreated and EcoNI treated samples were run on a DNA electrophoresis gel to separate and visualise the DNA bands.

2.7.6 Agarose gel electrophoresis

DNA electrophoresis gels were made with 2% agarose gel for separating mouse genotyping samples and 1% for PCR mutagenesis DNA vector samples. Agarose gels were made with agarose, 1x TAE buffer and a 1:100,000 dilution of ethidium bromide (final concentration 0.1µg/ml). Bioline HyperLadders 100bp or 1kb were used to measure the length of the DNA bands produced. 10µl of sample and 2µl of loading buffer (QIAGEN) (5µl of DNA ladder was loaded) were run on either the 2% agarose gel for 45 minutes at 110V or the 1% gel for 120V for 30 minutes. The separate DNA bands were visualised on GeneSnap by Syngene, using UV light.

2.7.7 DNA sequencing

PCR mutagenesis samples were sequenced to confirm the desired mutation by diluting the sample to 10ng/µl and sent to be used with T7 forward and reverse primers to Source Biosciences. Source Bioscience use Sanger sequencing and the results were analysed using SeqMan software.

2.8 Protein methods

2.8.1 Bradford assay

Cells were harvested in 8M urea buffer (without dye) and sonicated using the Misonix Microson ultrasonic cell disruptor XL2000). The typical sonication treatment for a 200µl sample was using ~6 watts for 40 second, repeated twice with a wait step on ice in between sonication but the treatment depended on the viscosity and volume of the protein solution. Part of the sonicated protein extract was diluted 1 in 10 and 10µl were added to wells in a clear 96 well plate in triplicate. A range of known BSA (Bovine Serum Albinum) standards were also added to wells in triplicate to measure alongside the experimental samples. 200µl of Bradford reagent (Sigma) was added to each well. This plate was read at 595nm on a Victor plate reader. The approximate concentration of protein in each experimental sample was estimated using the reading from the known BSA concentrations. The triplicates were averaged and this was used for dilution so that all samples could be equally loaded onto a Western blot.

2.8.2 SDS Polyacrylamide Gel Electrophoresis (SDS PAGE)

Polyacrylamide gels were made using Bio-Rad gel casting equipment using the following recipe table (Table 2.3). Both 6% and 15% acrylamide gels were topped with a 5% stacking

gel. Resolving gels were covered in water-saturated isobutanol to set and then removed, before the stacking gel was added with a well comb.

Table 2.7 – SDS Polyacrylamide gel recipes

Ingredient (ml)	Resolving gel		Stacking gel
	6%	**15%**	**5%**
dH_2O	8.5	3.7	2.7
30% polyacrylamide mix	3.2	8	0.67
1.5M Tris pH8.8	4	4	-
1.0M Tris pH6.8	-	-	0.5
10% SDS	0.16	0.16	0.04
10% APS	0.16	0.16	0.04
TEMED	0.016	0.016	0.004
Total volume	16ml	16ml	4ml

Once polyacrylamide gels were set they were placed in corresponding Bio-Rad tanks with another gel or a buffer holding plate. The space between the gels and the tanks were then filled with 1x SDS Running buffer before samples were loaded alongside 10µl PageRuler Plus Prestained Protein Ladder.

Ubiquitin ligase assay samples were run on either a 15% gel or a Novex 4-20% Tris-Glycine Mini Protein Gel and run for 90 minutes at 150V. All other protein lysates were run on a 6% or 15% gel depending on the size of protein that was being blotted. They were run at either 90 or 120V for varying times depending on the size of desired protein. Gels were Western blotted.

2.8.3 Western blotting

Protein samples run on SDS PAGE gels were transferred into membrane (PVDF immobillon) using electrophoresis. The transfer cassettes were set up with transfer buffer soaked sponges and 3mm filter paper. Methanol was used to activate the membrane and washed with transfer buffer before being place onto the SDS PAGE gel. The gel/membrane was

placed onto the prepared cassette, the loaded cassette was put into the transfer tank and filled with 1x transfer buffer. This was run at either 90 volts for 90 minutes to blot for Brca1 and FANCD2, or at 100 volts for an hour for all other proteins. The membrane with proteins bound was placed into 5% milk (Marvel) made with 0.1% Tween in PBS (PBST) for 1 hour to block. The membrane was washed with PBST 3 times for 5-10 minutes and then placed into the primary antibody (Table 2.10). The membrane was washed in the same manner as before and after being placed in secondary antibodies conjugated with HRP (or two consecutive secondary antibodies for Brca1) (Table 2.11). Once washed the membrane was exposed to an ECL mix (either ECL Prime Western Blotting Detection Reagent, Amersham, or Clarity Western ECL Blotting substrate (Bio-Rad). X-ray film (Fuji X-ray film, Fisher Scientific) was exposed to the membrane for varying lengths of time and developed using a Xograph Compact X4 developer.

2.8.4 Protein expression

Transformed bacterial colonies with the desired protein expression vector(s) were picked from agar plates and placed into 50ml LB broth containing the corresponding antibody (concentrations of antibody stated in 2.2.1) to the vector(s). This was left overnight at 37°C. In the morning, 1ml of the culture was taken and added in a 1:1 ratio with 80% glycerol to create a 40% glycerol stock of the desired colony, to be stored at -80°C. This glycerol stock was then be used to pick from instead of an agar plate. The remaining culture was added to 1 litre of LB broth with the correct antibiotics and placed at 37% for 1-2 hours to grow. After this time, IPTG (200mM final concentration) was added to induce the bacterial to produce protein and incubated overnight at 25°C in a shaking incubator.

2.8.5 His-tag protein isolation

The protein expressing bacterial culture (Section 2.2.1) was centrifuged at 300rpm for 15 minutes and the supernatant removed. The pellet of bacteria was suspended and lysed using Lysis buffer and left on ice for 2 minutes. The lysed bacteria was sonicated twice for 40 seconds on 20% intensity with a rest step on ice in between sonications. This lysate was centrifuged for 15 minutes at 13000rpm to pellet the cell debris before adding the supernatant to 500µl of Nickel beads (Qiagen). This was rotated at 4°C overnight. The beads were washed three times using ice-cold Wash buffer for 10 minutes at 4°C. The beads were pelleted between washes and after the final wash. The supernatant was removed and replaced with 400µl of ice-cold Lysis buffer with 500mM of Imidazole and placed on ice for 1 hour. The beads were pelleted by centrifuge for 2 minutes at 1000rpm. The supernatant was placed into a dialysis column and placed in Dialysis buffer at 4°C overnight. The protein solutions were aliquoted and stored at -80°C.

2.8.6 Ubiquitin ligase activity assay

Purified E3 enzyme (or E3 heterodimer as is BRCA1 and BARD1) and any experimental mutated E3 enzyme were diluted to equal concentrations and 10µl was added into two tubes (two tubes to each purified enzyme). The first tube of each had 10µl of ubiquitin ligase buffer (Section 2.11) added to it, and the second tube had 10µl of Ubiquitin ligase mix (Table 2.4) added to it. This was timed with 15 second intervals until all tubes had contained 20µl of solution. Samples were kept at 37°C for 30 minutes, at which time (with 15 second intervals and in the same order) 10µl of pre-warmed SDS sample loading buffer was added to stop the reaction. These were kept at 95°C for 5 minutes before loading onto a SDS PAGE gel for Western blotting.

Table 2.8 – Ubiquitin ligase mix

	Stock	Final concentration	Volume per reaction (µl)
ATP	100mM	10mM	1
E1 enzyme	400µl/ml	10µl/ml	1
E2 enzyme	1.25µl/ml	0.25µl/ml	1
Ubiquitin	2.5µl/ml	0.0125µl/ml	0.5
Ubiquitin ligase buffer	10x	1x	1
dH_2O	-	-	5.5
			10µl total

2.9 Cell Biology

2.9.1 Tissue culture

Primary MEFs were kept in 1% gelatin-coated flasks and dishes until immortalised. MEFs were grown in DMEM (Dulbeccos Modified Eagle Medium) with 1% Penicillin/Streptomycin and 10% FBS (Fetal Bovine Serum). The NIH3T3 cell line was kept in DMEM with 1% Penicillin/Streptomycin and 10% NBCS (New Born Calf Serum). They were incubated at 37°C with 5% CO_2 in Corning Flasks (T25/T75/T150). Cells were passaged when 70-80% confluent using 1xTrypsin/EDTA, and resuspended in media. The percentage of cell-suspended media was transferred to a new flask depended on the size of flask or dish they were going to grow in.

2.9.2 Thawing cells

Frozen cell aliquots were placed into a 37°C water bath. Once thawed, they were immediately transferred into a 15ml tube and gently resuspended with 5ml of pre-warmed media. Cells were spun at 1400rpm for 5 minutes and the supernatant was removed. Again, the cell pellet was resuspended gently in 5ml of pre-warmed media and pipetted into a T25 flask (Corning). The cells were placed into the cell culture incubator to settle.

2.9.3 Freezing cells

Trypsinised cells from a 90% confluent flask were spun down at 1500rpm for 5 minutes. The pellet was resuspended in freezing medium (80% FCS:20% DMSO or 80% NBCS:20% DMSO) allowing 1ml for each cryovial. The cryovials were placed in an isopropanol freezing box and placed at -80°C for 24 hours, before being transferred to liquid nitrogen for long storage.

2.9.4 Isolation of MEFs

Female mice that were pregnant at embryonic day 14.5 (E14.5) were euthanized using a CO_2 euthanasia chamber. The pregnant female was dissected using a laparotomy surgery, her uterine horn was excised and each embryo was dissected out of the horn. The embryos were washed in 1xPBS and all tissues from the mother were removed. Embryos were placed in individual 10cm petri dishes and macerated with forceps and scalpels as small as possible. These cells were collected in PBS and spun at 1000rpm for 3 minutes, the supernatant was discarded and the pellet of cells was resuspended in 1xTrypsin for 5 minutes at 37°C. The cells were centrifuged at 1500rpm for 3 minutes and the supernatant was discarded. Fresh media (supplemented DMEM) was used to resuspend cells and they were placed in a 10cm petri dish coated in 1% gelatin. This was considered passage 0 and cells were labelled with their embryo number. Whilst passaging these fast growing MEFs, cells were taken in passage 1 for DNA isolation and genotyping. MEFs were kept in the same conditions and in the same media as stated in section 2.4.1.

2.9.5 Immortalisation of MEFs

MEF (passage 2) cells were plated at three varying densities (2, 2 or 3 x10^5 cells) in a gelatin (1% gelatin in sterile H_2O) -coated 6-well dish and left to grow overnight. 7μg of SV40 Large T

antigen vector (pBsSVD2005, AdGene) was transfected into each 6-well containing the MEFs using Lipofectamine LTX reagent and PLUS reagent (ThermoFisher) as per manufacturer's instructions. The media was replaced 16 hours after treatment and cells were passaged when they became confluent.

Once cells had senesced, they were no longer passaged and media was replaced every other day. Once the cells started to grow again and changed morphology, passaging resumed as a normal immortal cell line.

2.9.6 Cell fractionation

Trypinised cells were pelleted before being gently suspended in 200µl of Cell Fractionation Lysis Buffer 1 (CFLB1) and kept on ice for 10 minutes. Cells were centrifuged at 4000rpm for 1 minute to pellet the nuclei and the supernatant was kept as the cytoplasmic fraction. The nuclei pellet was resuspended gently in 200µl of CFLB2 and kept at room temperature for 10 minutes. The nuclei mix was centrifuged at 4000rpm for 1 minute and the supernatant discarded. The remaining pellet was resuspended in 200µl of ice-cold CFLB3. This is the nuclear fraction and was sonicated (~4 watts for 30 seconds with a minute wait step on ice in between the two sonications) before run on an SDS PAGE gel and western blotted.

2.9.7 Immunofluorescent staining

Cells (approximately $2x10^4$) were grown in each 24-well, with a coverslip overnight. Cells were untreated or treated depending on the experiment. Cells to be stained for Brca1/γH2AX and 53bp1/γH2AX were treated with 4% PFA for 10 minutes, 1 hour after treatment with 5 Gray IR. They were permeablised with 0.5% Triton/PBS solution for 5 minutes before washing with PBS and storing in PBS. Cells to be stained for FANCD2 were

permeablised and fixed after being treated with 250ng/ml of MMC for 24 hours (no release from MMC). These cells were first pre-extracted with 0.2% Triton/PBS for 2 minutes before being fixed with 4% PFA for 10 minutes. These cells were further extracted using 0.5% Triton/PBS for 5 minutes before washing with and stored in PBS. Cells to be stained with Rad51/Cyclin A were fixed at 4 hours after 5 Gray IR or at the 24 hour time point of 250ng/µl MMC treatment. Cells were fixed in 4% PFA for 10 minutes, before being treated with -20°C Methanol and kept at -20°C for 10 minutes. After this permeabilisation cells were washed with PBS and stored in PBS. Cells were stored for up to three days before the antibodies were applied.

Prepared cells in PBS were washed with PBS/FCS (80% 1xPBS:20% FCS) before blocking in PBS/FCS for 5-30 minutes. Primary and secondary antibodies (Table 2.10/11) were made up to specified dilution (unless neat) in PBS/FCS. Cells were incubated with primary antibody solutions from 1 hour to overnight at 4°C. Before the secondary antibody solution was added to cells, the cells were washed with PBC/FCS 3 times. The secondary antibodies were conjugated to a be excited at specific wavelengths for visualisation, and to prevent weak signals cells were kept in the dark at 4°C whist being were treated with secondary antibodies. After secondary antibodies were left on for 1-2 hours, the cells were washed three times with PBS and treated with 4% PFA for 10 minutes. Cells were washed with PBS and treated with Hoechst (Table 2.10) for 3 minutes before again washing in PBS. The cells were stored in PBS in the dark at 4°C until they could be mounted onto slides.

Slides were mounted in Immunomounting media (DAKO) and kept in the dark at 4°C until visualised with a microscope.

2.9.8 Colony survival assays

Cells were plated in 6 well dishes with 20,000 cells in each well and grown overnight in the tissue culture incubator. Cells were treated with the specific drugs or irradiated, the next day (Table 2.5). After treatment cells were washed and trypsinised to be re-plated at 2 cell densities (two plates of each density) (Table 2.6). Re-plated cells were kept in an incubator for either 10 or 14 days (*Brca1* C61G MEFs – 10 days, *Brca1* Δ11 MEFs – 14 days) before fixing and staining with Crystal violet. This was washed off with PBS and dried before counting the number of colonies. The number of untreated colonies was used to measure the survival of treated cells.

Table 2.9 – Colony assay treatments

Treatment	Doses	Treatment length
Ionising radiation (IR)	1, 3, 5, 8 Gray	n/a
Cisplatin	5,10, 20, 30 µM	1 hour
Camptothecin (CPT)	20, 40, 80, 100 µM	16 hours
Hydroxyurea (HU)	0.2, 0.4, 0.8, 1 mM	16 hours
Olaparib	2, 4, 10, 20 µM	90 minutes
Veliparib	2, 4, 10, 20 µM	90 minutes

Table 2.10 – Colony assay plated cell numbers

Drug	Number of cells used in duplicate at each dose				
Gray	**Untreated**	**1**	**3**	**5**	**8**
IR	100x4	100x2, 200x2	200x2, 500x2	500x2, 1000x2	1000x2, 2000x2
µM	**Untreated**	**5**	**10**	**20**	**30**
Cisplatin	100x2, 200x2	100x2, 200x2	200x2, 500x2	500x2, 1000x2	1000x2, 2000x2
µM	**Untreated**	**20**	**40**	**80**	**100**
CPT	50x2, 100x2	50x2, 100x2	50x2, 100x2	50x2, 100x2	50x2, 100x2
mM	**Untreated**	**0.2**	**0.4**	**0.8**	**1**
HU	50x2, 100x2	50x2, 100x2	50x2, 100x2	50x2, 100x2	50x2, 100x2
µM	**Untreated**	**2**	**4**	**10**	**20**
Olaparib	100x2, 200x2	100x2, 200x2	100x2, 200x2	100x2, 200x2	100x2, 200x2
µM	**Untreated**	**2**	**4**	**10**	**20**

Veliparib	100x4	100x4	100x4	100x2, 200x2	100x2, 200x2

2.10 Mouse breeding and dissection

2.10.1 Mice creation

2.10.1.1 Brca1 C61G *mice*

The *Brca1* C61G allele in mice was created by Drost *et al* and the mutation in the 61st codon of TGT to GGT substituted a glycine to a cysteine (Figure 2.1a) in the targeting vector (Drost *et al*., 2011). It also created an EcoNI restriction enzyme cut site due to the nucleotide change. The targeting vector, which contained the *Brca1* region spanning exon 3 and exon 5, was electroporated into mouse embryonic stem cells (ES cells) where it recombined within the *Brca1* locus of the genome (Figure 2.1b). The targeted vector contained two LoxP sites

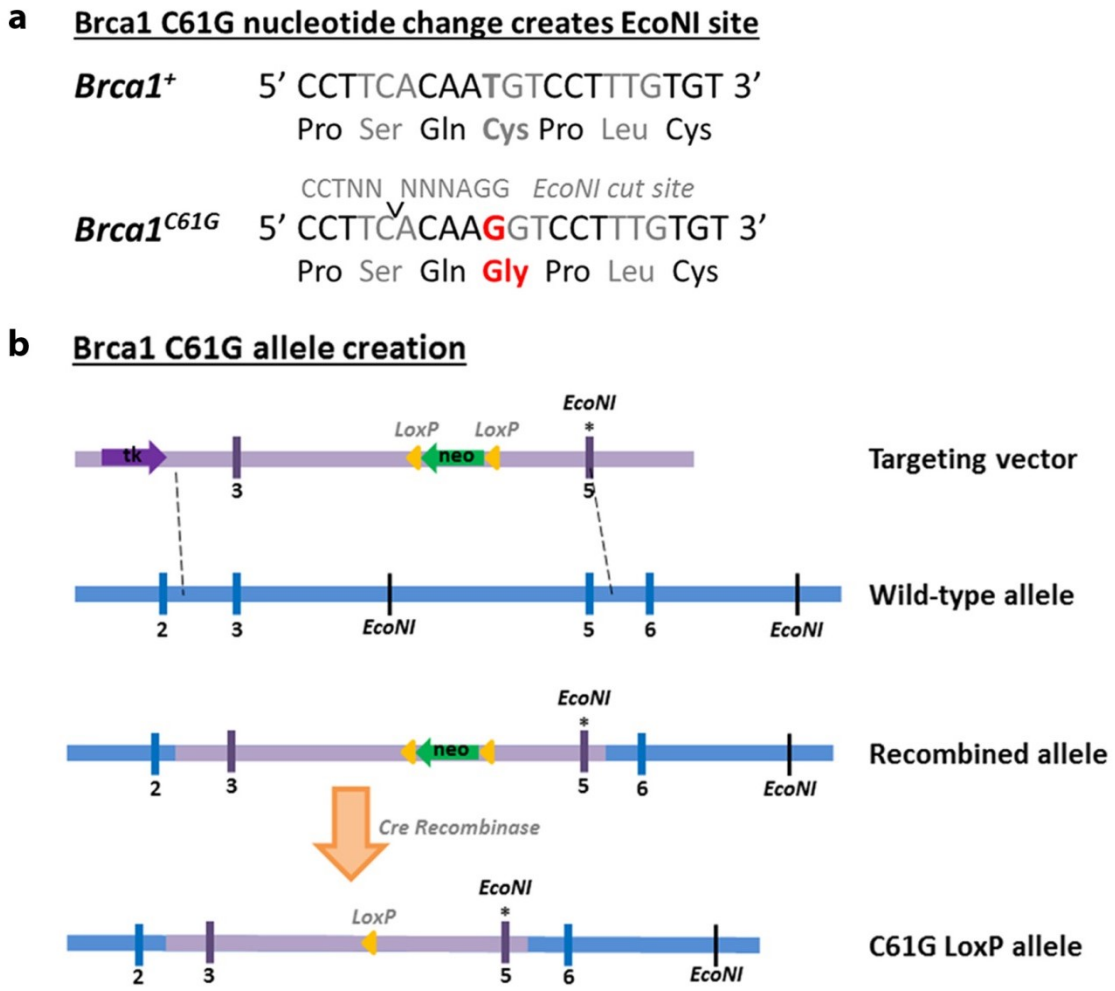

Figure 2.1 – The creation of the Brca1 C61G allele

[a] shows the nucleotide sequences of the region surrounding the 61st codon, of the wild-type (Brca1+) and the mutated allele (Brca1C61G). It shows in red the change T>G that causes the cysteine, the 61st amino acid, to become a glycine. It also shows the EcoNI cut site created by this nucleotide change. Alternate codons are shown in black and grey. [b] shows the cloning strategy used by Drost et al (2), to create the Brca1 C61G allele in mice. The targeting vector (purple) contained exons 3 and 5 and a neomycin gene (green arrow) flanked by 2 LoxP sites (yellow arrowheads). Cells successfully identified as having the target vector recombined into the genomic DNA (blue) were treated with Cre recombinase which removed the Neomycin gene and left a single LoxP site.

flanking the *neomycin* gene which was used for selection of successful recombination. The neomycin gene and one of the Lox P sites were removed from the genome by treatment with Cre recombinase. This left the *Brca1* C61G allele that contains the C61G mutation, the EcoNI cut site and a remaining LoxP site.

2.10.1.2 53bp1-null mice

The *53bp1*-null mice were created by Ward *et al*, by removing exon 5 of *53bp1* using the BamH1 and Xho restriction enzymes (Figure 4.1c) (Ward *et al*., 2003a). This was replaced by a *neomycin* gene and this gene was used for selection of successful creation of the *53bp1*-null allele.

2.10.2 Mouse breeding

The mice were bred on the University of Birmingham BMSU licence (Caroline Chadwick breeding licence (70/8198)) and all practices complied with the Home Office Animal (Scientific Proceedures) Act 1986. Mice were monitored daily by fully trained staff of the BMSU who maintain the breeding colonies to the standards of the Home Office guidelines. Mice were culled by neck dislocation or CO_2 euthanasia chamber if found to be showing signs of pain, distress, discomfort or any signs of morbidity (or if at the time limits of the project licence). My personal licence (PIL) is 70/25120.

Timed matings were set up through members of the animal house who separated the specific animals from the colony. These animal were placed in a cage together and observed for the presence of a vaginal plug, once this was seen the stud male was removed from the cage. This would allow for the taking of MEFs at embryonic day 14.5 (E14.5).

Colony breeding for multiplying numbers or for setting up the breeding crosses to test fertility, were set up by placing the mice of the desired genotype in a new cage (now the breeding cage) and allowed to breed unmanaged (i.e. they were not watched for the presence of a vaginal plug and the male was not removed from cage). Litters born to these mice were sexed and had ear clipping taken at approximately two weeks old. The ear clippings were used to isolate DNA for genotyping. At three weeks, the mice were weaned and placed in segregated male or female cages. Mice were monitored by the animal house staff and all procedures and care upheld Home Office regulations and recommended practice.

2.10.3 Mouse Genotyping methods

Ear clippings were taken at 2 weeks from the offspring of mated mice and DNA was isolated from these samples. The DNA was isolated using DirectPCR Lysis Reagent (Mouse Tail) (Viagen Biotech) using their recommended protocol (25:1 ratio buffer to Proteinase K).

The remaining LoxP site in the *Brca1* C61G mouse gene and EcoNI site created by the T>G nucleotide change have allowed two ways of PCR genotyping using either of these molecular signatures. The first strategy used PCR primers in *Brca1* intron 4 that are either side of the LoxP site, creating either an approximately 200 (wild-type allele) or 300 (C61G allele) base pair (bp) DNA product and this size increase allowed for differentiation between the alleles (Figure 2.1a and figure 4.1a and b). The second strategy used PCR primers in *Brca1* that span from intron 4 into exon 5 (Figure 2.1b and figure 4.1a and b). This region included codon 61 in which the C61G mutation has been created and therefore it included the EcoNI restriction enzyme cut site. Once this region was amplified by PCR, the DNA product was cut by an

EcoNI enzyme and the resulting DNA products were examined for size to differentiate the alleles. If the 931 bp PCR product was uncut then it did not contain the C61G mutation and was wild-type. If the PCR product was cut and produced two bands of approximately 640 and 290 bps then the allele contained the C61G mutation (Figure 2.1b).

The *53bp1* alleles of the mice were genotyped using PCR primers that amplified across the exon 5 and created either a band of 465bp representing the wild-type *53bp1* allele and a band of 270bp representing the *53bp1* allele with exon 5 deleted and the remaining neomycin gene in its place (Figure 4.1c).

All three methods of genotyping used GoTaq Green Master Mix (Promega) and the following PCR recipe (Table 2.6) and PCR programme (Table 2.7).

Table 2.11 – Mouse genotyping DNA polymerase mastermix

Ingredient	Stock concentration	Final concentration	Volume in 50µl
DNA	variable	1µg	-
GoTaq buffer	2x	1x	5µl
Forward primer	10µM	0.4µM	2µl
Reverse primer	10µM	0.4µM	2µl
Middle primer (53bp1 only)	10µM	0.4µM	2µl
dH_2O	-	-	made up to 50µl

Table 2.12 – Mouse genotyping PCR programme

Step	Temperature (°C)	Time	Cycles
Starting denaturing	98	2 minutes	1
Denaturing	98	1.5 minutes	35
Annealing of primers	55	1 minutes	35
Extension of DNA	72	30 seconds	35
Finalising extension	72	5 minutes	1
Hold	4	∞	-

The resulting PCR products were run on a 1% agarose electrophoresis gel (Section 2.2.6) to separate the PCR products by size for genotyping.

2.10.4 Mouse sterility

Mice were set up according to normal breeding cross procedure and the lack of litters after 3 months was assumed to be due to infertility (all genotype crosses except this including male *53bp1*$^{-/-}$*Brca1*$^{C61G/C61G}$ mice produced offspring in this time). 4 male *53bp1*$^{-/-}$*Brca1*$^{C61G/C61G}$ mice were placed with proven fertile-genotype females and none produced offspring.

Male littermates with varying genotypes were dissected at a range of ages and their testes examined and compared. These were dissected as in 2.2.5, 8 males of each genotype were dissected; the organs from half of each genotype were formalin (4%) fixed and stored at 4°C and the other half of mice had their organs frozen in liquid nitrogen and stored at -80.

2.10.5 Dissection

Mice were culled using a CO_2 Euthanasia chamber or through neck dislocation and the Home Office regulated procedure. Mice were dissected through a laparotomy surgical cut and the following organs were examined and formalin fixed; intestines, spleen, stomach, liver, ovaries and uterine horn or testes and seminiferous tubules, kidneys, lungs, heart and thymus. During dissection other organs were examined for any other abnormalities but not taken unless abnormal, such as mammary glands, lymph nodes and skin. All tissues were fixed in 4% formalin solution and stored at 4°C.

2.10.6 Tumour histology

Fixed tumours were kept in formalin and sent to HistologiX, an independent immunohistochemistry and contract histology laboratory (Nottingham, UK), where they were embedded in wax and sectioned. Slides were stained with H&E and imaged. Images, tissues and slides were returned alongside a report from their pathologist (David Fairley,

human and mouse tissue pathologist). This report identified which abnormal organs were cancerous and the likely type of tumour, or what kind of abnormality if not cancer.

2.11 Statistics

All results that were tested were between means from two genotypes to see if there was a significant difference between genotypes response in the experiment. Mean results are the average of at least three repeated experiment means, of which each experiment had 3 or more individual repeats. Any outliers were eliminated only when they met the criteria after a Grubbs test. A Type 2 two-tailed student t-test was used as the means are from two non-paired normally distributed samples.

Kaplan-Meier statistical method was used to assess the survival analysis/tumour formation of the mice, but the sample size (n=9) is too small to be significant.

Chapter 3 – The BRCA1 RING domain is highly conserved and its ubiquitin ligase activity is comparable between mice and humans.

3.1 Introduction

Mouse models provide an invaluable platform for exploring genetic diseases and are essential for the development of therapies. Mice are a genetically alterable mammal that has a short life span and can be kept in a relatively small space. This allows for large numbers of mice in each study and the duration of the study to be short. Mice are also easy to treat with therapies and since they age quicker, there is more potential to identify any long-term effects of treatments.

There have been many mouse models created to look at breast cancer and to look at the progression of disease when the *Brca1* gene is mutated. As discussed in section 1.5, many homozygote mutations in *Brca1* are embryonic lethal or cause tumourigenesis (Figure 1.8) suggesting *Brca1* is needed for embryonic development and genome integrity.

The desired reproduction of a human disease in the mouse is not always achieved and this can be due to the differences between mice and humans. For example, the affected protein may have a different role, interact with different protein pathways, or have a different catalytic rate in mice compared to humans. Therefore it is important to start by identifying the similarities and differences between mouse and human BRCA1 protein.

BRCA1's most prominent features include a RING domain at its N-terminus and two BRCT domains at the C-terminus (Figure 1.2). The N-terminal RING domain of BRCA1 forms a heterodimer with the N-terminal RING domain of BARD1 (Figure 1.4) (Hashizume *et al*.,

2001; Morris *et al*., 2002; Wu *et al*., 1996), and this interaction is crucial for the stability of BRCA1 (Brzovic *et al*., 2003; Hashizume *et al*., 2001; Joukov *et al*., 2001) (see section 1.3). The N-terminal RING domain of BRCA1 and the formation of the BRCA1:BARD1 heterodimer is essential for the only known catalytic function of BRCA1, its E3 ubiquitin ligase activity (Chen *et al*., 2002; Hashizume *et al*., 2001). BARD1 is not currently recognised (in the literature, Morris lab results suggest otherwise) to have any contribution in the production of polyubiquitin chains aside from aiding BRCA1 stability (Brzovic *et al*., 2003; Hashizume *et al*., 2001; Joukov *et al*., 2001). BARD1 has 2 tandem BRCT domains at the C-terminus, as does BRCA1, and the BRCT domains in both BRCA1 and BARD1 enable the heterodimer complex to be recruited into the nucleus and to sites of double-strand breaks (DSBs) (Chen *et al*., 2006; Fabbro *et al*., 2002; Kim *et al*., 2007b; Liu *et al*., 2007b; Rodriguez *et al*., 2004; Sobhian *et al*., 2007; Wang *et al*., 2007; Wang and Elledge, 2007).

The importance of BRCA1's E3 ubiquitin ligase function in the development of cancer is controversial and the role of the E3 ubiquitin ligase function in cells is not understood (Section 1.3.3). As discussed in the introduction (Section 1.2.1-2), there are *BRCA1* N-terminal missense mutations found in patients that correlate with cancer incidence and this implies there is a role for the N-terminus RING domain in tumour suppression. However it is not known whether it is the alteration of the catalytic activity of BRCA1 that is the driver behind this tumourigenesis.

This chapter will start by comparing the amino acid sequences between mouse and human BRCA1 and BARD1 RING domains to identify any significant differences that could affect the ubiquitin ligase function of the heterodimer. Finally, the ability of the wild-type and mutated

mouse N-terminal Brca1:Bard1 heterodimer to replicate the rate of *in vitro* polyubiquitin chain formation of the human N-terminal BRCA1:BARD1 heterodimer will be assessed.

3.2 Mouse and human *BRCA1* have a conserved N-terminal RING domain

Human *BRCA1* is located on the reverse strand of chromosome 17 and mouse *Brca1* is located on the reverse strand of chromosome 11 (Table 3.1). Human *BRCA1* is longer than mouse *Brca1* but they have the same number of exons (Table 3.1). At a nucleotide level, mouse *Brca1* has a similarity of 75.22% (Clustal 2.1) to human *BRCA1* and they are 56% identical in their amino acid transcript. The N-terminal RING domain (aa1-103) in BRCA1 is 83.5% identical in mice to humans (Figure 3.1a).

Table 3.1 – BRCA1 gene and protein comparison between mice and humans

BRCA1	Chromosome	Nucleotides	Exons	Amino acids
Human	17	7094	24	1863
Mouse	11	6572	24	1812

To investigate the molecular structure of mouse Brca1 and Bard1 N-terminal RING domains the NMR (Nuclear magnetic resonance) structure that was resolved for the human BRCA1:BARD1 RING domains (Brzovic *et al*., 2001b) (Figure 1.2 and 1.4) was used as a template to produce the predicted molecular structure that is used in this thesis. The RING domain equips BRCA1 with its ability to function as an E3 ubiquitin ligase (Chen *et al*., 2002). It is made up of two α-helices at either end of the domain and in the centre there are two loops that are held in position by two zinc ions and a small helix (Figure 3.1c). The zinc ions are held by regions of cysteine and histidine residues on the two loops and these are referred to as Site I and Site II (Figure 3.1a) which are highly conserved due to their

a

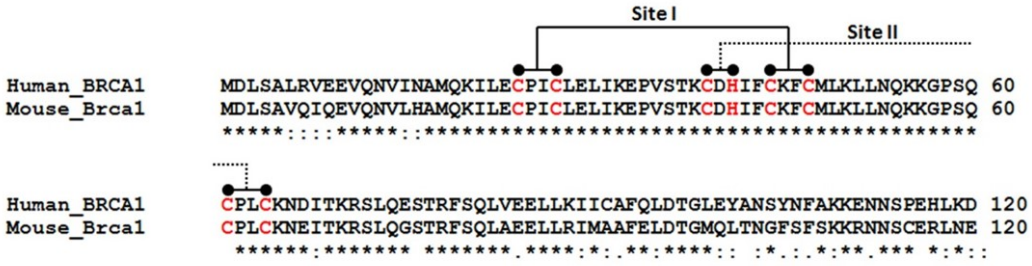

b

Humans	Mice	Grantham
LEU6	VAL6	32
ARG7	GLN7	43
VAL8	ILE8	29
GLU9	GLN9	29
ILE15	LEU15	5
ASN16	HIS16	68
ASP67	GLU67	45
GLU75	GLY75	29
VAL83	ALA83	64
LYS88	ARG88	26
ILE90	MET90	10
CYS91	ALA91	195
GLN94	GLU94	29
LEU99	MET99	15
GLU100	GLN100	29
TYR101	LEU101	36
ALA102	THR102	58

c

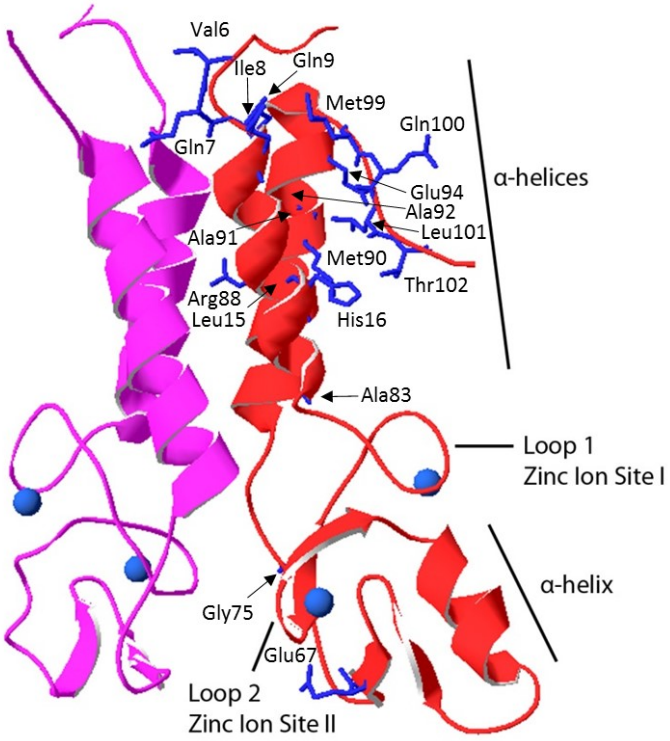

Figure 3.1 – BRCA1 N-terminal RING domain comparison between human and mouse protein

ENSEMBL protein sequences and CLUSTALW2 multiple sequence alignment tool were used to align the human and mouse BRCA1 N-terminal RING domain protein sequences [a]. Site I and Site II show the residues that hold the zinc ions that maintain the RING domain structure (red letters). The characters depict the consensus between the residues in the alignment. The asterisk '' indicates a fully conserved or identical residue, the colon ':' indicates residues with highly similar properties, the period '.' indicates residues with weakly similar properties and a space ' ' indicates residues that lack conservation of residue properties.*

[a] shows the differences in the mouse BRCA1 RING domain amino acid sequence compared to human BRCA1 RING domain amino acid sequence. [b] identifies the specific residue differences and the predicted effect of the residue change is scored using the Grantham scale. [c] shows the mouse Brca1 and Bard1 RING domain heterodimer modelled on the NMR structure of the human BRCA1:BARD1 heterodimer. Brca1 (red) has two contacting α-helices with two zinc loops and a small helix making up the RING domain structure. Bard1 is shown in purple. Zinc ions are shown as blue spheres and the side chains of the residues that differ in humans are shown in blue.

importance for maintaining the RING domain structure. There are 17 residue differences between the mouse and human BRCA1 RING domain and these residues mostly have low impact as determined by the low Grantham score (Figure 3.1b, c)(Grantham, 1974). The Grantham score gives a number to the physiochemical differences between two amino acids which is used to indicate the degree of change when a residue is substituted (Grantham, 1974). This conservation of the RING domain is indicative that it is an important functional region.

3.3 Mouse and human *BARD1* have a conserved N-terminal RING domain

Since BRCA1 is part of a heterodimer with BARD1 and is required for the protein stability and N-terminal function of BRCA1 (Brzovic *et al*., 2003; Hashizume *et al*., 2001; Joukov *et al*., 2001), it is important to examine the similarity between mouse and human BARD1 when looking at BRCA1.

Table 3.2 – BARD1 gene and protein comparison between mice and humans

BARD1	Chromosome	Nucleotides	Exons	Amino acids
Human	2	5499	13	777
Mouse	11	5659	11	765

Mouse *BARD1* nucleotide sequence is 79.53% identical to human *BARD1* (Clustal 2.1) and 70% identical in amino acid sequence. The C-terminus of BARD1 contains two BRCT domains and there is an ankyrin repeating domain on the N-terminal side of the BRCT domains. The N-terminus of BARD1 contains a RING domain but this has no known E3 ubiquitin ligase function and is reported to be the non-catalytic partner of the heterodimer (Wu *et al*., 1996) despite the RING domain in BARD1 having a similar molecular structure to BRCA1 (Figure 3.2a, c). It does not contain a small helix between the zinc ion loops as in the BRCA1 RING

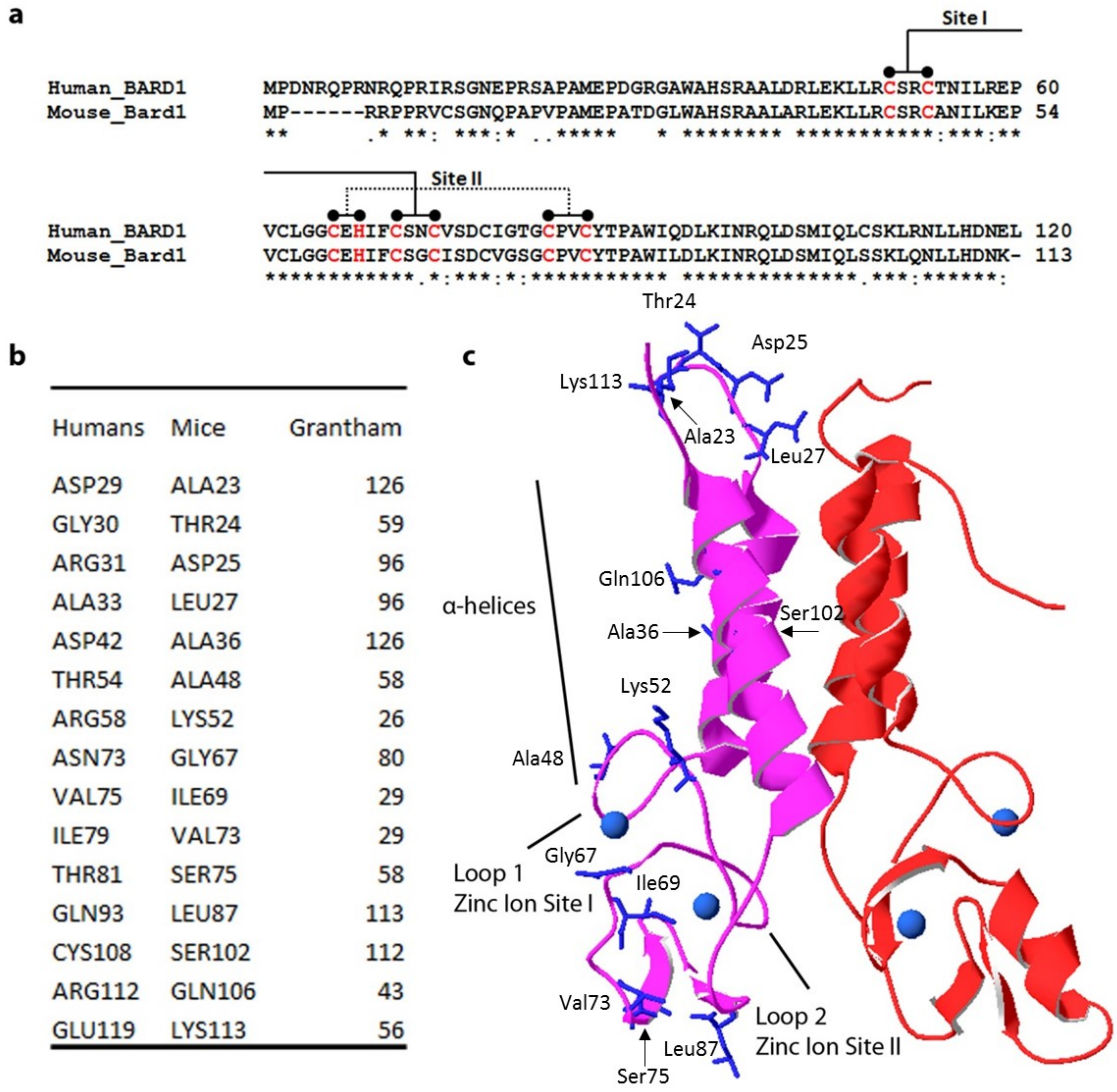

Figure 3.2 – BARD1 N-terminal RING domain comparison between human and mouse protein

ENSEMBL protein sequences and CLUSTALW2 multiple sequence alignment tool were used to align the human and mouse BARD1 N-terminal RING domain amino acid sequences [a]. Site I and Site II show the residues that hold the zinc ions that maintain the RING domain structure (red letters). The characters depict the consensus between the residues in the alignment. The asterisk '' indicates a fully conserved or identical residue, the colon ':' indicates residues with highly similar properties, the period '.' indicates residues with weakly similar properties and a space ' ' indicates residues that lack conservation of residue properties. [a] shows the differences in the mouse BARD1 RING domain compared to human BARD1 RING domain sequence. [b] identifies the specific residue changes and the predicted effect the residue change is scored using the Grantham scale. [c] show the mouse Brca1 and Bard1 RING domain heterodimer modelled on the NMR structure of the human BRCA1:BARD1 heterodimer. Bard1 (purple) has two contacting α-helices with two zinc loops making up the RING domain structure. Brca1 is shown in red. Zinc ions are shown as blue spheres and the side chains of the residues that differ in humans are shown in blue.*

domain but does have two sites that hold zinc ions in place (Figure 3.2a, c). There are 15 amino acids that are different in the mouse transcript but most have a low impact as determined by the Grantham Score (Figure 3.2b)(Grantham, 1974). This similarity between the RING domains in mice and humans is indicative of a conserved function between these species (Joukov *et al*., 2001).

3.4 *In vitro* ubiquitin ligase assay considerations

There are several components needed to form polyubiquitin chains in an *in vitro* ubiquitin ligase assay; E1 ubiquitin-activating enzyme, E2 ubiquitin-conjugating enzyme, E3 ubiquitin ligase enzyme, ubiquitin and ATP (Hershko *et al*., 1983). The reaction also needs a substrate on which the ubiquitin is bound, unless the E3 ubiquitin ligase has the ability to make free polyubiquitin chains or self-ubiquitinate. This substrate can be a targeted protein or an ubiquitin moiety to form chains of polyubiquitin. E1 enzymes-activate ubiquitin and load this onto the E2 conjugating-enzyme (Haas and Siepmann, 1997). The conjugated ubiquitin-E2 complex then associates with an E3 ubiquitin enzyme which transfers the ubiquitin onto a specific substrate forming an isopeptide bond (Pickart and Eddins, 2004).

It is important to consider the human-to-mouse conservation of the purified enzymes that are being used in the *in vitro* ubiquitin ligase activity, as the combination of mouse and human proteins could alter the rate of polyubiquitin chain production. Ubiquitin is a highly conserved protein and is identical in humans and mice. E1 enzymes do not contact E3 enzymes so there is no human protein-mouse protein contact. E2 enzymes do contact the E3 enzyme so there may be a problem if the E2 used is not conserved in mice. Conjugating E2

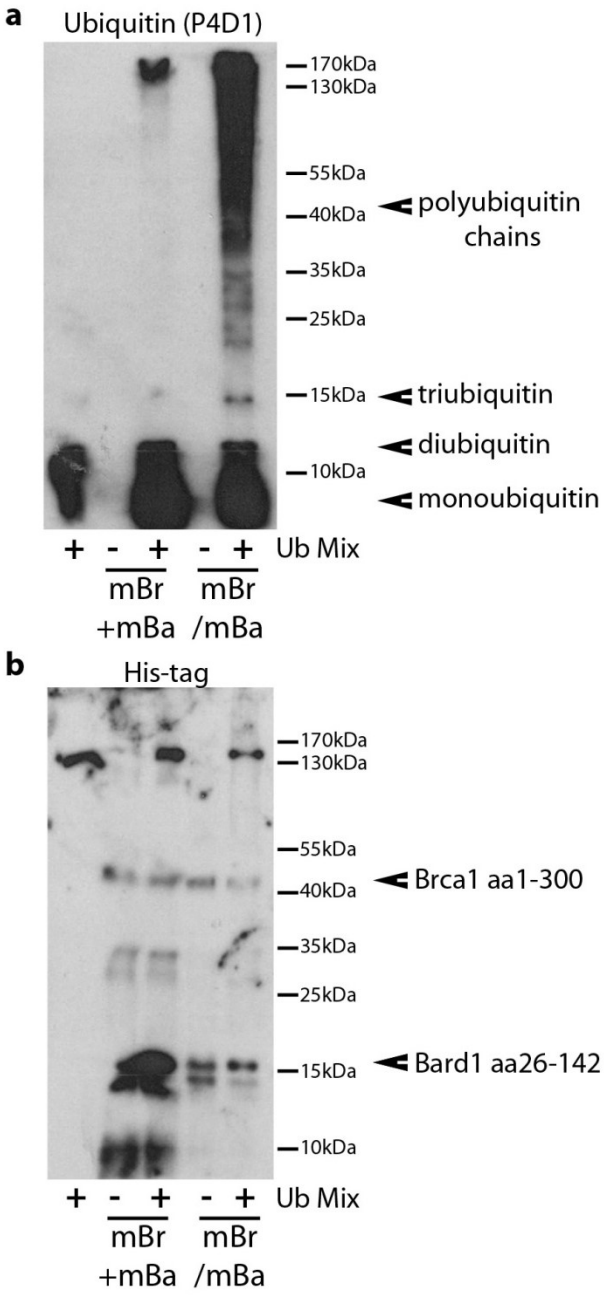

Figure 3.3 – In vitro ubiquitin ligase assay using Brca1:Bard1 heterodimer produced from co-expression or single protein expression

An in vitro ubiquitin ligase assay western blot probed with the ubiquitin antibody (P4D1) and a His-tag antibody. [a] shows the size shift in ubiquitin caused by the production of polyubiquitin chains in the assay. The His-tag blot [b] shows the sizes and relative amount of His-tagged Brca1 (aa1-300) and His-tagged Bard1 (aa26-142). The ubiquitin mix (+) contains ubiquitin, ATP, E1 enzyme and UbcH5a. mBr+mBa represents mouse Brca1 (mBr) and mouse Bard1 (mBa) N-terminal protein purified from separate cultures. mBr/mBa represents mouse Brca1 and mouse Bard1 N-terminal protein purified from a culture expressing both proteins.

enzyme UbcH5α was used in all *in vitro* ubiquitin ligase experiments in this thesis as it has been shown to be important for Brca1 E3 ubiquitin ligase activity *in vitro* (Brzovic *et al*., 2003; Mallery *et al*., 2002). Mouse *UbcH5a* has 40 silent differences in its nucleotide sequence compared to human *UbcH5a* therefore the protein is identical and is predicted not to alter the rate of activity in an *in vitro* ubiquitin ligase assay.

Mouse *Brca1* and mouse *Bard1* RING domain cDNA sequences have been produced in individual vectors with different antibiotic resistance genes. The mouse *Brca1* RING domain sequence for protein purification consists of amino acids 1-300 and is His- and Flag-tagged and the vector has an ampicillin resistance gene. The mouse *Bard1* RING domain for protein purification consists of amino acids 26-142 and is His- and HA-tagged and has a kanamycin resistance gene.

When first attempting to make purified protein of the N-terminus Brca1 and Bard1, *E. coli* colonies producing either Brca1 (mBr) or Bard1 (mBa) RING domain were used and the resulting proteins were combined (mBr+mBa) (Figure 3.3). The resulting mix of Brca1 and Bard1 heterodimer did not have E3 ubiquitin ligase function. Due to the separation of Brca1 and Bard1 RING domains in two vectors with different antibiotic resistance genes, it was possible to isolate *E. coli* colonies with both vectors by selecting with both antibiotics. These colonies were used to make purified Brca1/Bard1 heterodimer (mBr/mBa). This protein had E3 ubiquitin ligase function (Figure 3.3) suggesting that heterodimer ubiquitin ligase activity is dependent on translation of Brca1 and Bard1 in the same cell. Unpublished data (Morris lab) and the literature (Hashizume *et al*., 2001; Joukov *et al*., 2001) suggest that when BARD1 is over expressed in cells, more BRCA1 protein is stable and that this

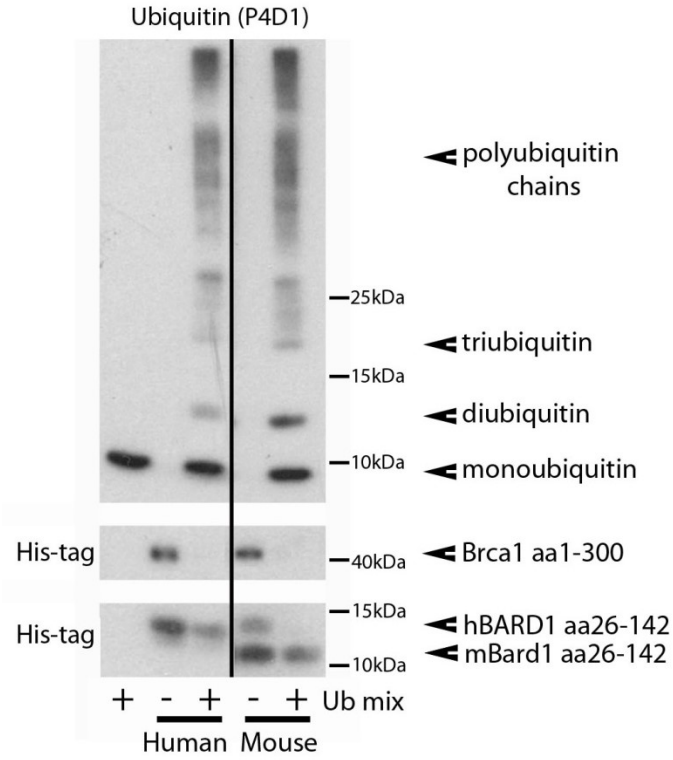

Figure 3.4 – In vitro ubiquitin ligase assay comparing the ubiquitin ligase activity of human and mouse wild-type Brca1:Bard1 heterodimer

An in vitro ubiquitin ligase assay western blot using the ubiquitin antibody (P4D1) and a His-tag antibody. The black line indicates the removal of lanes from the blot. The ubiquitin blot shows the size shift caused by the production of polyubiquitin chains in the assay. The His-tag blots shows the sizes and relative amount of human (h) and mouse (m) His-tagged Brca1 (aa1-300) and His-tagged Bard1 (aa26-142). The ubiquitin mix (+) contains ubiquitin, ATP, E1 enzyme and UbcH5a.

relationship is not the same for the contrary situation. The fact that only co-expressed Brca1:Bard1 has catalytic activity in figure 3.3 supports the idea that Bard1 stabilises Brca1. This highlights the need for the Brca1:Bard1 heterodimer to be formed for Brca1 stability and for Brca1 to function as an E3 ubiquitin ligase.

3.5 Comparing mouse and human *in vitro* ubiquitin ligase activity

Due to the differences in the human and mouse Brca1:Bard1 RING domains, it is important to investigate if the heterodimers from both species have the same efficiency at ligating polyubiquitin chains.

An *in vitro* ubiquitin ligase assay using equivalent amounts of wild-type human and mouse Brca1 and Bard1 proteins showed that the mouse and human heterodimers make a comparable amount of polyubiquitin chains within 30 minutes (Figure 3.4). This suggests that both species heterodimers have a similar efficiency as an E3 ubiquitin ligase *in vitro*. This is important for any results that compare the human and mouse Brca1:Bard1 heterodimer ubiquitin ligase activity *in vitro* and may allude to having similar activity in cells.

3.6 *BRCA1* C61G patient mutation causes a reduction in *in vitro* ubiquitin ligase activity of mouse protein

BRCA1 C61G is a patient mutation that correlates with cancer incidence in families with hereditary breast and ovarian cancer (Gorski *et al.*, 2000). It is a nucleotide mutation that causes a change in the 61st amino acid from a cysteine to a glycine. This residue is important for maintaining a zinc ion that is required for the RING domain structure (Figure 3.5 and 3.6a) (Brzovic *et al.*, 2001b; Brzovic *et al.*, 2003; Joukov *et al.*, 2001; Ruffner *et al.*, 2001) and

this mutation is known to alter BRCA1:BARD1 heterodimer binding (Brzovic *et al*., 2003; Hashizume *et al*., 2001; Joukov *et al*., 2001; Morris *et al*., 2006; Wu *et al*., 1996). The BRCA1

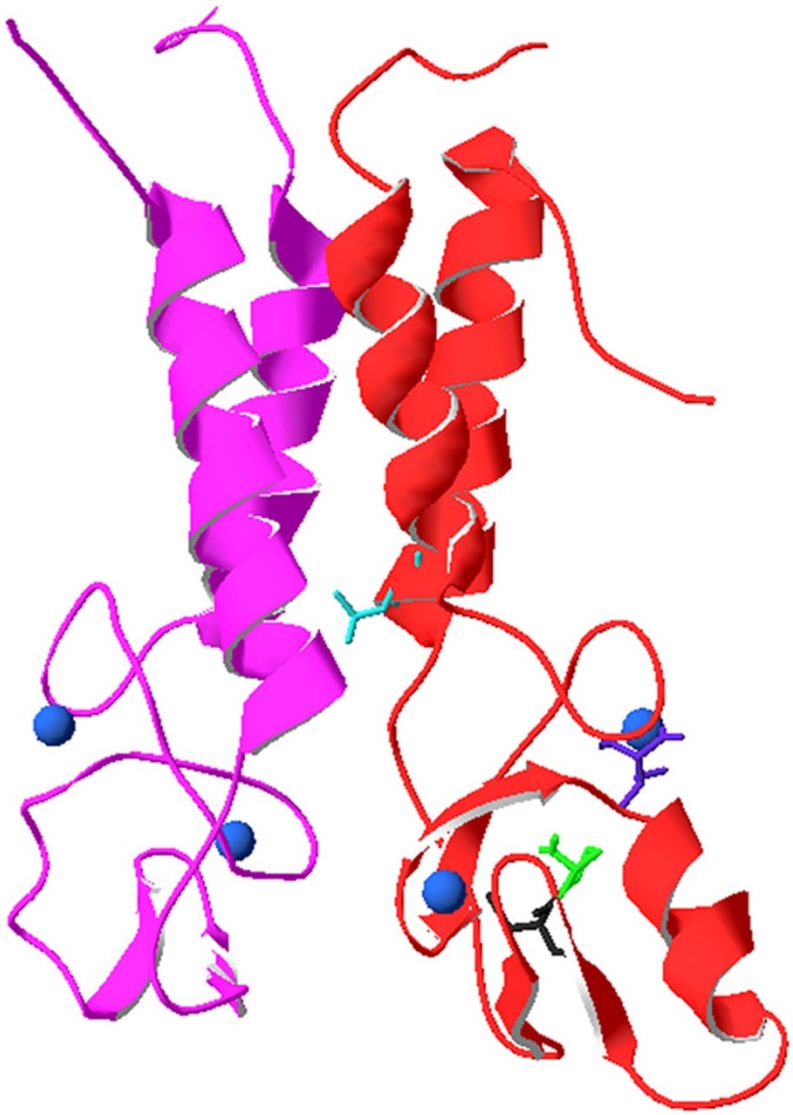

Figure 3.5 – Molecular modelling of Brca1 residue substitutions
This figure shows the mutated residues used to explore the ubiquitin ligase activity were modelled using the predicted molecular structure of mouse Brca1:Bard1 heterodimer. Brca1 is shown in red and Bard1 is shown in grey. Zinc ions are shown as blue spheres. C61 is shown in black, I26 is shown in blue, P62 is shown in green and L82 is shown in light blue.

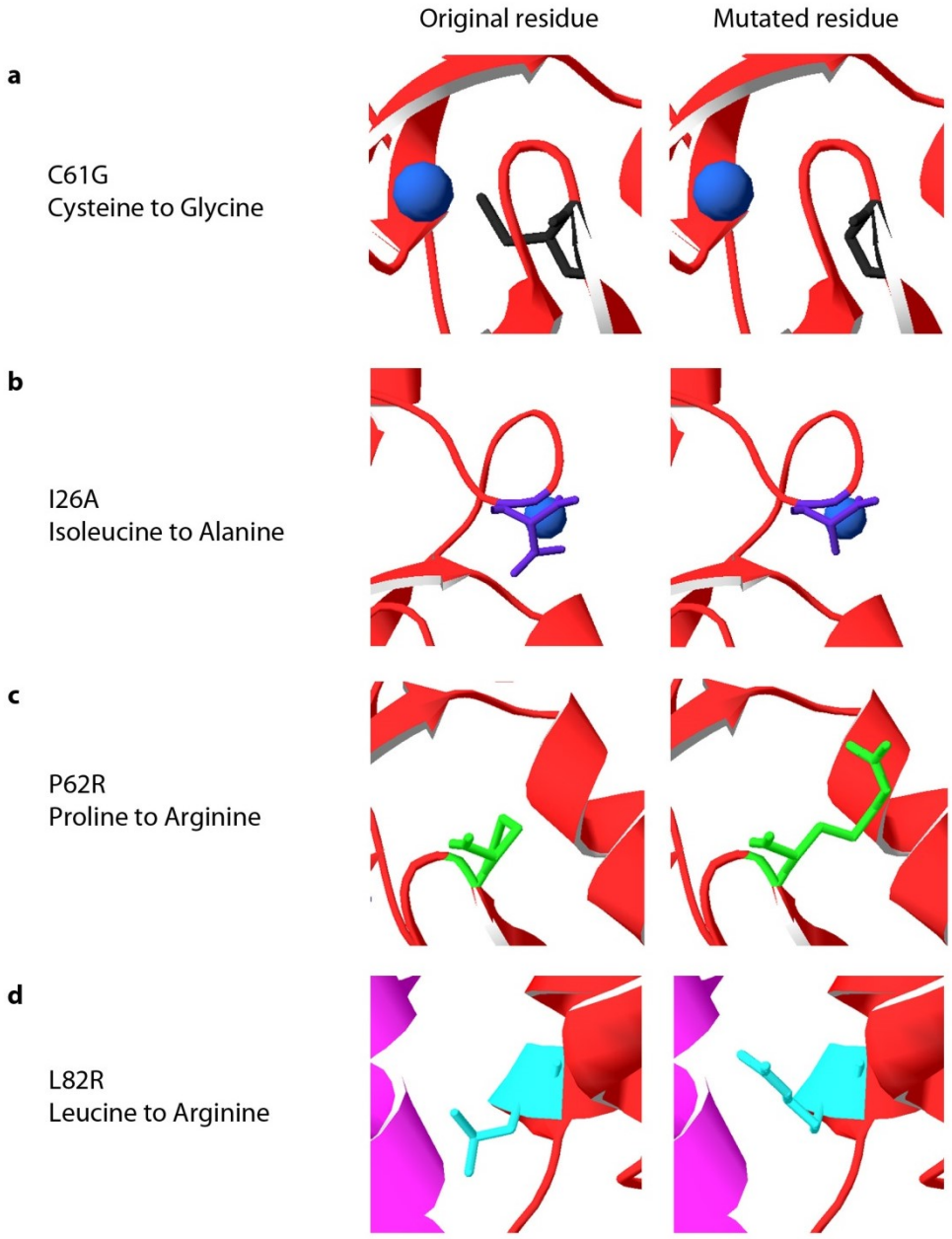

Figure 3.6 – Brca1 structural models of the residue changes C61G, I26A, P62R and L82R
The mutated residues used to explore the ubiquitin ligase activity were modelled using the predicted molecular structure of mouse Brca1:Bard1 heterodimer. Brca1 is shown in red and Bard1 is shown in purple. Zinc ions are shown as blue spheres.
[a] show the side chain alteration of residue 61 from a cysteine to a glycine (C61G), shown in black. [b] show the side chain alteration of residue 26 from an isoleucine to an alanine (I26A), shown in blue. [c] show the side chain alteration of residue 62 from a proline to an arginine (P62R), shown in green. [d] show the side chain alteration of residue 82 from a leucine to an arginine (L82R), shown in light blue.

C61G mutation has been used in the literature as a mutation that reduces ubiquitin ligase activity (Brzovic *et al*., 2003; Hashizume *et al*., 2001; Mallery *et al*., 2002; Morris *et al*., 2006; Ruffner *et al*., 2001). The residue, C61, cannot be determined as directly influential to the ubiquitin ligase activity of BRCA1 because it cannot be separated from its necessity in the RING domain structure and heterodimer binding.

I26A is also a substitution shown to reduce the ubiquitin ligase function of BRCA1 but it does not alter the BRCA1:BARD1 heterodimer binding (Brzovic *et al*., 2003). Therefore it has been associated with the ability to separate the functional importance of BRCA1 ubiquitin ligase activity and the structural importance of the BRCA1:BARD1 heterodimer binding on BRCA1 stability. It changes the 26th amino acid from an isoleucine to an alanine (Figure 3.5 and 3.6b) and this residue change is reported to affect the binding between BRCA1 and the E2 conjugating enzyme (Brzovic *et al*., 2003).

P62R is a substitution in the RING domain loop that does not alter the zinc binding sites. This substitution can show that other residues in the zinc ion loops may be functionally important without directly altering zinc ion binding residues. It changes a proline to an arginine at amino acid 62 (Figure 3.5 and 3.6c).

L82R is a substitution at the bottom of the paired α-helices that is used to alter the binding between BRCA1 and BARD1. It changes a leucine to an arginine at amino acid 82 (Figure 3.5 and 3.6d).

The BRCA1 P62 residue was suggested to have significance in BRCA1's interaction with the E2 conjugating enzyme after the NMR structure of BRCA1 was compared with cCbl

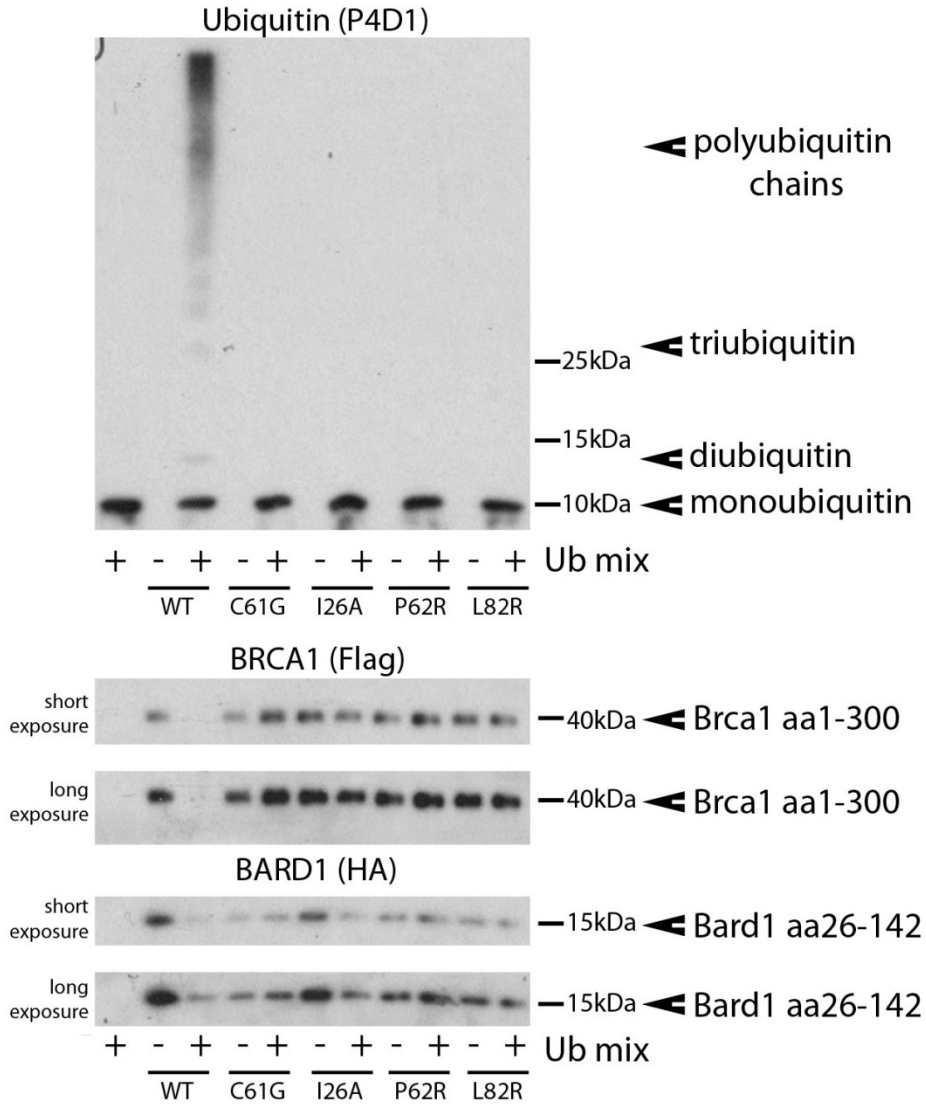

Figure 3.7 – Residue alterations in mouse Brca1 that reduce the formation of polyubiquitin chains produced by the Brca1:Bard1 heterodimer

This figure shows an in vitro ubiquitin ligase assay western blot using the ubiquitin antibody (P4D1) and the Flag- and HA-tag antibodies. The ubiquitin blot shows the size shift caused by the production of polyubiquitin chains in the assay. The ubiquitin mix (+) contains ubiquitin, ATP, E1 enzyme and UbcH5a. The Flag blots show the sizes and relative amount of mouse Brca1 (aa1-300) and the HA blots show the sizes and relative amounts of mouse Bard1 (aa26-142). WT (wild-type), C61G, I26A, P62R and L82R show the substitution status of Brca1.

(Brzovic *et al*., 2001b). The equivalent residue of P62 in cCbl was predicted to have van de Waals interactions with UbcH7, an E2 conjugating enzyme (Brzovic *et al*., 2001b). In the same study, the BRCA1 L82 residue was shown to be a hydrophobic interfacing residue in the helices bundle that is the contact surface for BRCA1 and BARD1 (Brzovic *et al*., 2001b). Any substitution of the P62 residue is likely to reduce the stability of the RING domain structure and a substitution at P82 is likely to affect the strength of the binding between BRCA1 and BARD1. P62R and L82R were used as substitutions in a yeast-2 and yeast-3-hybrid experiment (unpublished data, James Beesley, Morris lab) that showed that they both reduced the binding between BRCA1 and BARD1, and the binding of the heterodimer to UbcH5a, an E2 conjugating enzyme.

C61G, I26A, P62R, L82R are shown in their positions in the mouse Brca1:Bard1 heterodimer in figure 3.6. These residue alterations were made in mouse Brca1 protein to investigate *in vitro* whether they reduce the efficiency of the mouse Brca1:Bard1 heterodimer to produce polyubiquitin chains. Figure 3.7 shows an ubiquitin ligase assay using equivalent levels of Brca1 and Bard1 mouse protein that is wild-type (WT) or has the described residue substitutions (C61G, I26A, P62R, L82R). It shows that in comparison to wild-type Brca1 protein, these substitutions show a reduced ability for form polyubiquitin chains and that these residues are essential for ubiquitin ligase activity.

This experiment infers that these specific residues in the Brca1 RING domain, the structure of the Brca1 RING domain, the Brca1:Bard1 heterodimer binding and the interaction between Brca1 and the E2 conjugating enzyme are all essential for E3 ubiquitin ligase activity. However it does not identify in which way the patient mutation C61G alters the

ubiquitin ligase activity and it also does not infer that these substitutions would have the same effect on the heterodimer structure and binding, or the ubiquitin ligase activity *in vivo*. It would therefore be important to use cell-based techniques such as an immunoprecipitation with tagged-Brca1 to assess the ability of Bard1 to bind to Brca1 and whether this heterodimer complex formed *in vivo* would display a similar reduction in ligase activity.

3.7 *Bard1* variant causes a reduction in *in vitro* ubiquitin ligase activity of the mouse Brca1:Bard1 heterodimer.

Unpublished data from Dr Ruth Densham (Morris lab) has isolated a residue change in human BARD1 (R99A/E) that does not affect the binding ability of the BRCA1:BARD1 heterodimer, but does alter the *in vitro* ubiquitin ligase activity of the heterodimer in humans. The residue in human BARD1 is amino acid 99 which is an arginine, the corresponding residue in the mouse Bard1 protein is amino acid 93 which is also an arginine (Figure 3.8). This conserved arginine residue lies on the Bard1 α-helix at the front of the protein (Figure 3.8b-i) and the R side chain sticks out of the heterodimer complex and slightly towards Brca1 (Figure 3.8b-i, ii). Upon further modelling Densham *et al*, suggest that this residue would interact with the ubiquitin in a loaded ubiquitin-E2 complex as it was interacting with BRCA1. When the R99 residue is substituted by an alanine residue (R99A) or a glutamic acid residue (R99E), this alters the ubiquitin ligase activity of the BRCA1:BARD1 heterodimer. The R99E residue replacement greatly reduces the ubiquitin ligase activity of the heterodimer compared to a milder reduction caused by the R99A substitution. This shows that this BARD1 residue has a role in the ubiquitin ligase activity of the BRCA1:BARD1

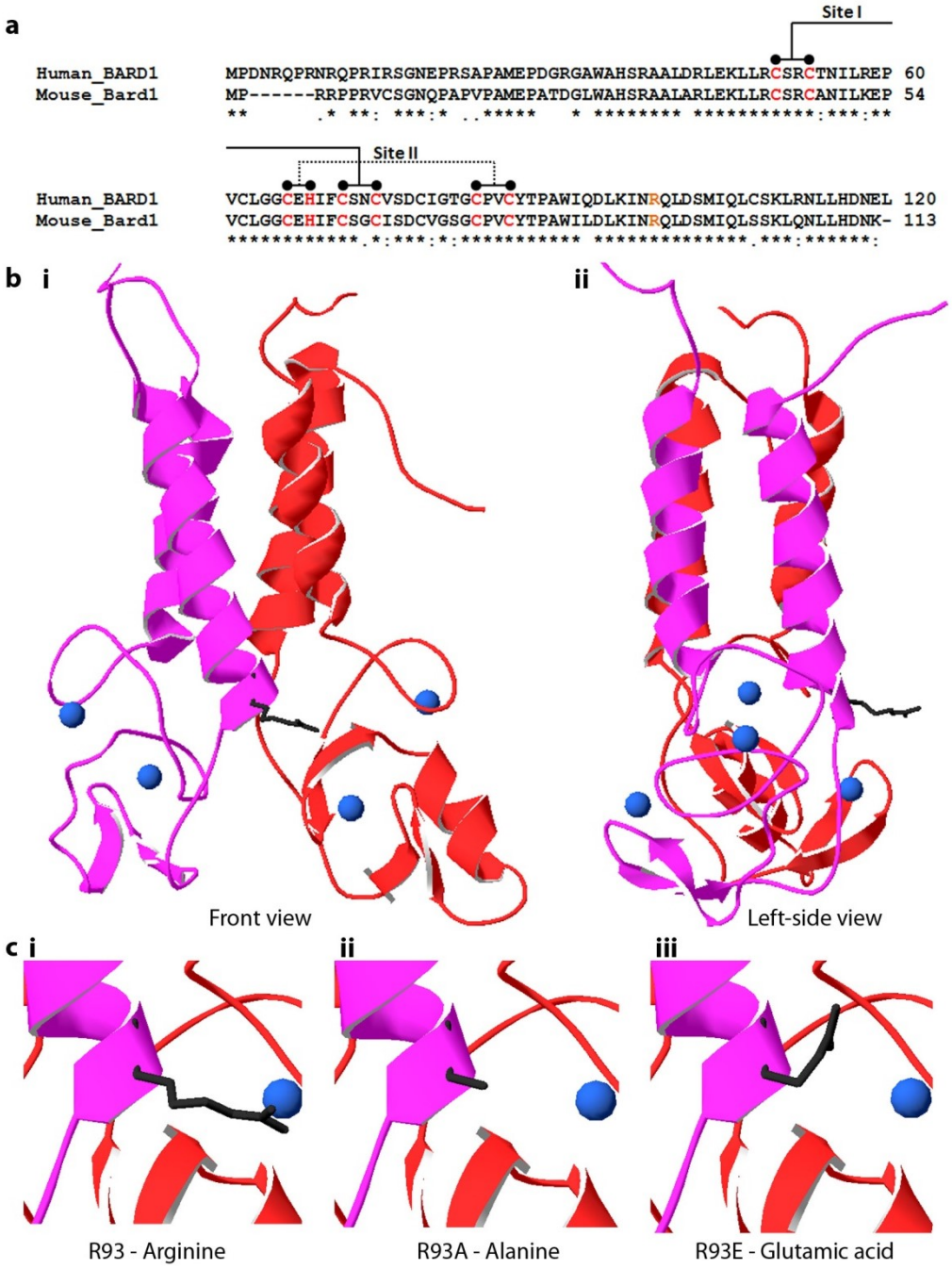

Figure 3.8 – R93/R99 residue in human and mouse Bard1 RING domain

ENSEMBL protein sequences and CLUSTALW2 multiple sequence alignment tool were used to align the human and mouse BARD1 N-terminal RING domain protein sequences [a]. The characters depict the consensus between the residues in the alignment. The asterisk '' indicates a fully conserved or identical residue, the colon ':' indicates residues with highly similar properties, the period '.' indicates residues with weakly similar properties and a space ' ' indicates residues that lack conservation of residue properties. The arginine residue at position 99 in humans and 93 in mice is shown in orange. Red letters show the residues that hold the zinc ions; site I and site II. [b] shows the R93 residue used was modelled using the predicted molecular structure of mouse Brca1:Bard1 heterodimer. Brca1 is shown in red and Bard1 is shown in purple. Zinc ions are shown as blue spheres. [b and c] shows the side*

residue of R93 (black). [b, i] shows R93 in the Brca1:Bard1 heterodimer from the front view and [b, ii] shows R93 in the Brca1:Bard1 heterodimer from the left-side view, through Bard1. [c, i] shows a close up view of the arginine side chain of R93. [c, ii] shows the side chain alteration when R93 is changed to an alanine (R93A). [c, iii] shows the side chain alteration when R93 is changed to a glutamic acid residue (R93E).

heterodimer and the affect caused by the R99E residue charge reverse shows the side chain is important for BARD's role. A model of the R99 residue change in mouse Bard1 using the NMR-resolved human heterodimer, displays the physical effect changing the arginine residue at amino acid 93 to alanine or glutamic acid. It shows the modification of size and angle of the residue side chain (Figure 3.8c-i, ii, iii). The R93A change would reduce the amino acid side chain size dramatically which would reduce its protrusion from the heterodimer. The R93E change would cause the side chain to be angled in towards the heterodimer. Both of these changes would be predicted to alter its ability to bind to E2-loaded ubiquitin as Densham *et al* suggest. Purified mouse Brca1:Bard1 heterodimer was made with the R93A and R93E mutation and used to perform an *in vitro* ubiquitin ligase activity assay. Equivalent levels of Bard1 wild-type, R93A and R93E protein in complex with wild-type Brca1, shows that the ubiquitin ligase activity of the mouse Brca1:Bard1 heterodimer is reduced slightly by the R93A residue change and dramatically reduced, but not abolished, by the R93E residue change (Figure 3.9). This demonstrates that the R93 substitution has the same effect on mouse Brca1:Bard1 heterodimer ubiquitin ligase activity as the human heterodimer suggesting the mechanism of Bard1 interaction with an E2-loaded ubiquitin is likely to be conserved.

3.8 Discussion

This chapter has shown that the N-terminal RING domains of BRCA1 and BARD1 are highly conserved between humans and mice with a similar ability to form polyubiquitin chains and

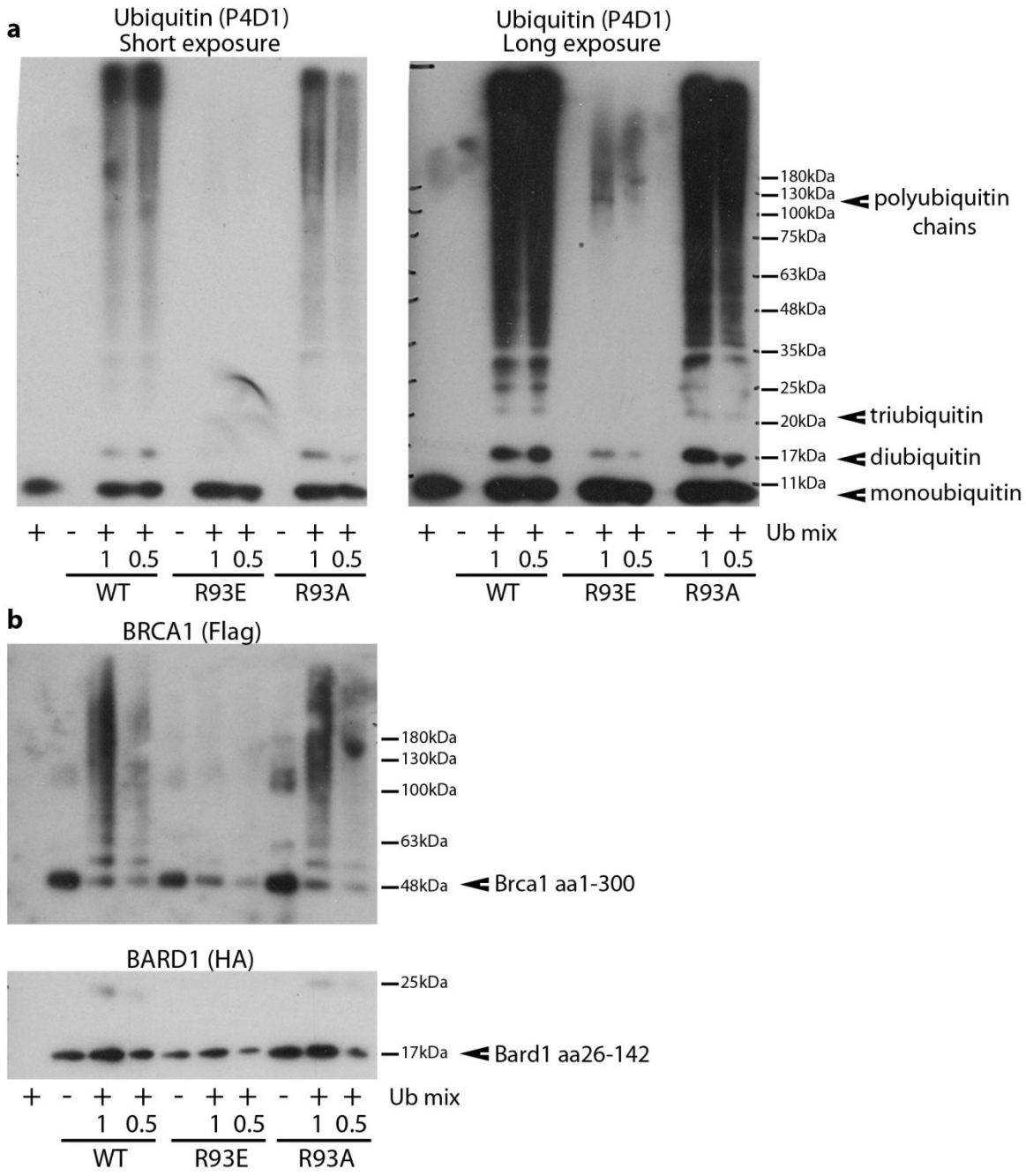

Figure 3.9 – R93 residue alterations in mouse Bard1 that reduce the ubiquitin ligase activity of the Brca1:Bard1 heterodimer

An in vitro ubiquitin ligase assay western blot using the ubiquitin antibody (P4D1) [a] and the Flag- and HA-tag antibodies [b]. [a] shows is the ubiquitin blot showing the size shift caused by the production of polyubiquitin chains in the assay. The ubiquitin mix (+) contains ubiquitin, ATP, E1 enzyme and UbcH5a. The Flag blots shows the sizes and relative amount of mouse Brca1 (aa1-300) and the HA blots show the sizes and relative amounts of mouse Bard1 (aa26-142) [b]. WT (wild-type), R93E and R93A show the mutation status of Bard1. The assay was loaded twice, the first lane with the neat output of the assay (1) and with second lane being diluted 1:1 (0.5).

the RING domains of Brca1 and Bard1 are both important for *in vitro* ubiquitin ligase activity of the Brca1:Bard1 heterodimer. This activity can be altered by the destabilisation of Brca1 zinc ion loop structure (C61G and P62R), the disruption of the heterodimer binding (Brca1 L82R), and the alteration of specific residues important for binding to ubiquitin ligase components (Bard1 R93A/E) or to the E2 conjugating enzyme (Brca1 I26A).

There are several substrate suggestions onto which the ubiquitin is ligated by the BRCA1:BARD1 heterodimer complex (Section 1.3.1) but it is not fully understood if any of these are important for the tumour suppression function of BRCA1. In the *in vitro* ubiquitin ligase assay, the substrate is ubiquitin to form polyubiquitin chains or the Brca1:Bard1 complex, i.e. autoubiquitination. It has been shown that BRCA1 is predominantly associated with the formation of K6-linked polyubiquitin chains (Morris and Solomon, 2004; Wu-Baer *et al*., 2003), and the cause for this specificity for chain type or specificity of what substrate on which these chains form is also unknown. The specificity of an E3 ubiquitin ligase for its substrate is suggested to be conferred by the E3 enzyme (Berndsen and Wolberger, 2014; Plechanovova *et al*., 2012) and it is the structural configuration of the ubiquitin loaded-E2, E3 enzyme and substrate that is suggested to induce a particular polyubiquitin chain type (Chen and Pickart, 1990; Hofmann and Pickart, 1999; van Nocker and Vierstra, 1991).

This data shows that BARD1 has a role in BRCA1's catalytic function and this suggests that BARD1 may also have tumour suppressive properties through this role. This could emphasise the importance for more widespread *BARD1* sequencing in patients that have hereditary breast and ovarian cancer (De Brakeleers *et al*., 2016; Gonzalez-Hormazabal *et al*., 2012; Klonowska *et al*., 2015; Liu *et al*., 2013; Ratajska *et al*., 2012). These results provide more

information for helping to predict the effects of *BRCA1* variation of unknown significance (VUS) (section 1.2.1) seen in patients with cancer and can help them make more informed choices on potential therapies and prophylactic actions (section 1.2.4).

These results can help us predict the residues that can alter the catalytic activity of the Brca1:Bard1 heterodimer but it does not allude to the function of the ubiquitin ligase activity in a cell, or what these residue changes would alter in the molecular pathways in cells.

The comparisons between mouse and human BRCA1 and BARD1 are crucial to understanding the phenotypes we see in *BRCA1* mouse models and understanding the scope to which animal models can help with investigating *BRCA1* mutations. The strong conservation of the RING domain and similar *in vitro* ubiquitin ligase activity seen in this chapter suggest that molecularly Brca1 and Bard1 are comparable in humans and mice. The only way to know if human *BRCA1* patient mutations can replicate human disease is to create the genetic mutation in mice.

Chapter 4 – The Brca1 C61G protein is degraded by the proteasome and is less efficient at recruiting to double-strand DNA breaks.

4.1 Introduction

As discussed in the introduction, *BRCA1* C61G mutation is a common missense mutation found to correlate with a high risk of tumourigenesis in families with hereditary breast and ovarian cancer (Section 1.2). Many studies on the alteration of BRCA1 protein caused by the C61G amino acid substitution have been published and the results have been varied (see section 1.3.3). Unfortunately, there isn't a human cancer cell line that contains the *BRCA1* C61G mutation available and previously *BRCA1* C61G DNA vectors have been expressed in breast or cancer cell lines. There are several problems with this approach. Firstly, cancer cell lines contain multiple mutations which allow the cells to become immortal and it is difficult to predict if these existing mutations affect how BRCA1 or BRCA1 C61G functions. Secondly, normal breast cells are difficult to work with because they do not have the same proliferative potential as cancer cells and can be hard to transfect DNA and RNA for expression. Thirdly, cDNA vectors cannot always be expressed at a level that is relative to endogenous and therefore may not be regulated as endogenous protein.

Despite these caveats, research into BRCA1 has shed light on the regulation and expression of BRCA1 protein, its localisation and degradation, and the recruitment or changing localisation of BRCA1 protein (Section 1.3.1).

Genetically altering the mouse genome has greatly helped in evading some of these problems. The mouse genome is relatively consistent in a colony and can be altered without resulting mutations in unknown genes occurring. However mice can still develop

spontaneous gene alterations that could lead to a phenotype. Mouse embryonic fibroblasts (MEFs) isolated from genetically engineered embryos are highly proliferative in the first few passages of culture before they senesce. There are methods of immortalising MEFs using an alteration of a tumour suppressor gene or oncogene that allow the cells to proliferate an indefinite number of times, and the effects of these gene changes are well studied.

As discussed in section 1.5, many *Brca1* mouse models have been created and they have provided a full organism and cells in which to study the effects of a *Brca1* mutation. The majority of homozygote *Brca1* mutations are embryonic lethal (Section 1.5.1 and figure 1.8) and the deletion of *53bp1* from *Brca1* Δ11-*deleted* and *Brca1*-null mice has been shown to rescue this embryonic lethality (Cao *et al*., 2009).

The *Brca1* C61G mutation has been genetically engineering into mice to study the specific effects of this common patient mutation in cells with the hope to understanding the path of tumourigenesis (Drost *et al*., 2011). *Brca1* C61G homozygote mice are embryonic lethal and MEFs could not be isolated from the embryos (Drost *et al*., 2011). With the discovery that the depletion or deletion of the 53bp1 protein can rescue the lethality of the homozygote *Brca1* Δ11 mutation, $53bp1^{-/-}Brca1^{C61G/C61G}$ mice were bred with *53bp1*-null mice in attempt to rescue the embryonic lethality of these mice.

This chapter investigates the creation of MEFs from $53bp1^{-/-}Brca1^{C61G/C61G}$ mouse embryos, and uses these MEFs to look at the Brca1 C61G protein in the cell. This includes the levels of Brca1 protein, its localisation, its degradation and the recruitment of BRCA1 protein to sites of DNA double-strand break repair.

4.2 The creation and detection of the *Brca1* C61G and *53bp1*-null alleles

Dr Jo Morris created the *Brca1* C61G mice which were published in Drost *et al* (Drost *et al*., 2011). The C61G change was created in a targeting vector by genetically mutating the 61st codon from TGT to GGT which also created an EcoNI restriction enzyme (see Chapter 2.5.1 and 2.5.3). This vector was then recombined into the genome and the neomycin selection gene was removed using *Cre* recombinase and flanking *LoxP* sites. The *Brca1* C61G allele can be genotyped by PCR amplification using either the remaining *LoxP* (larger fragment) or the EcoNI site (ability to be cut) to separate from the wild-type allele (Figure 4.1a,b).

Ward *et al* (Ward *et al*., 2003b) created the *53bp1*-null allele by the excision of exon 5 using BamH1 and Xho restriction enzyme cut sites, and replacing the region with a *neomycin* gene that was used for the selection of successful clones (Figure 4.1c and section 2.5.1). The region that was excised was approximately 450 bps in length and the *neomycin* replacement DNA region is approximately 250 bps in length. PCR amplification over this region created a wild-type allele band of 465 bps and the *53bp1*-null allele created a band of 270 bps (Figure 4.1c).

4.3 The creation of the *53bp1*$^{-/-}$*Brca1*$^{C61G/C61G}$ mice and cells

As discussed in the introduction (Section 1.5.3) the homozygote *53bp1*-null mice are not embryonic lethal (Ward *et al*., 2003b) and the homozygote *Brca1* C61G mice are embryonic lethal (Drost *et al*., 2011), the background of all the breeding mice had to be *53bp1*-null. We started the project by crossing *53bp1*$^{-/-}$ mice with mice that were heterozygote for the *Brca1* C61G allele

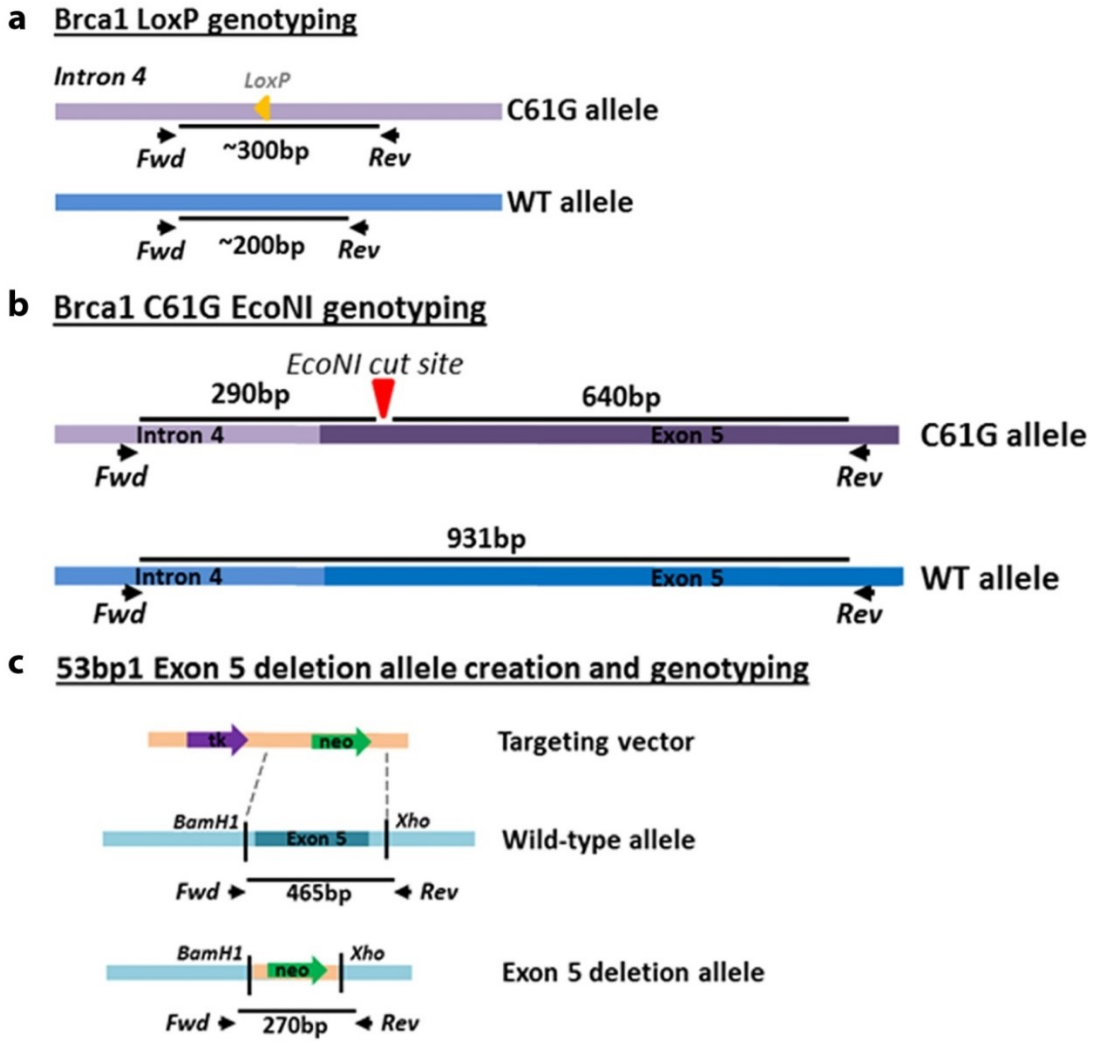

Figure 4.1 – Genotyping the Brca1 and 53bp1 allele

[a] shows the Brca1 allele genotyping method that uses the presence of the remaining LoxP site in the allele to identify the Brca1 C61G allele. The black arrows represent the location of the forward (Fwd) and reverse (Rev) primers used to PCR this region in intron 4 of Brca1. The wild-type allele (blue) produces an approximately 200 base pairs DNA product after PCR and the insertion of the LoxP site (yellow arrowhead) causes the Brca1 C61G allele (purple) PCR product to be approximately 300 base pairs in length. [b] shows the genotyping method that uses the EcoNI cut site (red arrowhead) for recognition of the Brca1 C61G allele. The black arrows represent the location of the forward (Fwd) and reverse (Rev) primers used to PCR across this region, encompassing part of intron 4 and part of exon 5 of Brca1. The PCR reaction with these primers creates a DNA product of 931 base pairs. The Brca1 C61G allele (purple) contains an EcoNI site which is cut when treated with EcoNI restriction enzyme to produce two DNA products; one is 640 base pairs in length and the other is 290 base pairs. The wild-type allele (blue) remains uncut as the EcoNI site is absent. [c] shows the cloning strategy of creating the 53bp1-null allele and how it is genotyped. The use of the normally occurring BamH1 and Xho restriction enzyme sites in the wild-type 53bp1 allele (blue) were used to excise a region of 53bp1 encompassing exon 5. A targeting vector (orange) containing a neomycin gene (green) was inserted into this region creating the 53bp1-null

allele. The black arrows represent the location of the forward (Fwd) and reverse (Rev) primers that are used to PCR amplify exon 5 and its surrounding region. The DNA product created by the wild-type allele is 465 base pairs in length and contains exon 5. The 53bp1-null allele produces a DNA product that is 270 base pairs in length and contains the neomycin gene.

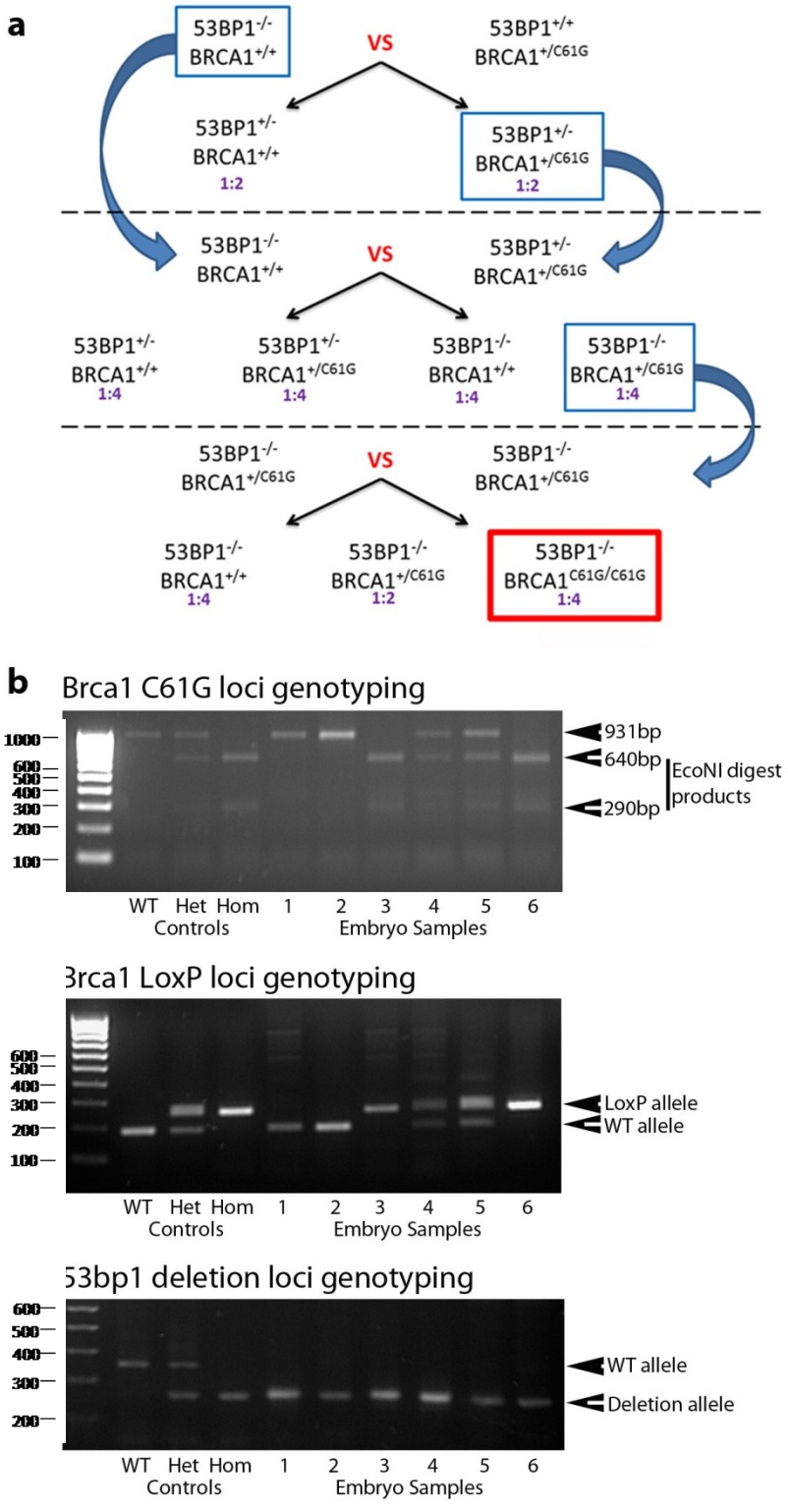

Figure 4.2 – Breeding crosses and genotyping of 53bp1$^{-/-}$ Brca1$^{C61G/C61G}$ mice

[a] shows the three breeding crosses (separated by dashed lines) and their offspring that was needed to create a mouse with the desired phenotype (53bp1$^{-/-}$ Brca1$^{C61G/C61G}$). The first cross is needed to create mice with both the 53bp1-null allele and the Brca1 C61G allele. The second cross involved the offspring of the first cross (blue box and arrow) breeding with a homozygote 53bp1-null mouse to create offspring which are homozygote for the 53bp1-null allele and heterozygote for the Brca1 C61G allele. These mice are then bred together as the third cross in which it is possible to create mice which are 53bp1$^{-/-}$ Brca1$^{C61G/C61G}$ (red box). The purple numbers are the predicted ratio at which the genotype is expected from the parental cross. [b-d] show the genotypes of mouse embryonic fibroblasts (MEFs) isolated from the third cross in [a]. [b] and [c] show the Brca1 allele genotyping results and [d] shows the 53bp1 genotyping results. (WT= wild-type allele, Het= heterozygous for

the mutant allele and Hom= homozygote for the mutant allele). [b] show the DNA products after EcoNI restriction enzyme digest from a PCR using the EcoNI digest PCR genotyping method and [c] shows the DNA products from a PCR using the LoxP PCR genotyping method described in figure 4.2. Both Brca1 genotyping methods shows that embryo samples 1 and 2 contain only wild-type allele of Brca1, embryo samples 4 and 5 are heterozygote for the Brca1 C61G allele and embryo samples 3 and 6 and homozygote for the Brca1 C61G allele. [d] shows the DNA products from a PCR using the 53bp1-null allele genotyping method (Ward et al., 2003b). It shows that all embryo samples are homozygote for the 53bp1-null allele. The first and second cross were started by Dr Jo Morris and James Beesley. James Beesley aided in genotyping mice for part of my time on this project.

(Figure 4.2a) to create the *53bp1*$^{+/-}$*Brca1*$^{+/C61G}$ mice for the next parental pairing. The second cross backcrossed the *53bp1*$^{+/-}$*Brca1*$^{+/C61G}$ mice with *53bp1*-null mice to product mice that were heterozygote for the *Brca1* C61G allele with two deleted copies of *53bp1*. This created the parents for the final cross of two *53bp1*$^{-/-}$*Brca1*$^{+/C61G}$ mice which should produce the expected Mendelian ratio of 1:4, resulting the desired *53bp1*$^{-/-}$*Brca1*$^{C61G/C61G}$ mouse. This cross produced *53bp1*$^{-/-}$*Brca1*$^{C61G/C61G}$ mice that lived to adulthood and MEFs were isolated from the mother at embryonic day 14 (Section 2.4.4) from the *53bp1*$^{-/-}$*Brca1*$^{+/C61G}$ parental cross.

Table 4.1 – Summary of the mouse embryonic fibroblasts genotypes

	***53bp1*-null**	***Brca1* C61G**	***Brca1* Δ11**	**Immortalized**
53bp1$^{+/-}$***Brca1***$^{+/C61G}$	Heterozygote	Heterozygote	-	SV40 Large T antigen
53bp1$^{-/-}$***Brca1***$^{+/+}$	Homozygote	Wild-type	-	SV40 Large T antigen
53bp1$^{-/-}$***Brca1***$^{+/C61G}$	Homozygote	Heterozygote	-	SV40 Large T antigen
53bp1$^{-/-}$***Brca1***$^{C61G/C61G}$	Homozygote	Homozygote	-	SV40 Large T antigen
53bp1$^{+/+}$***Brca1***$^{Δ11/Δ11}$	Wild-type	-	Homozygote	Spontaneous (Xu *et al*., 2001c)
53bp1$^{-/-}$***Brca1***$^{Δ11/Δ11}$	Homozygote	-	Homozygote	Spontaneous (Bunting *et al*., 2010)

The mice and MEFs produced from these breeding crosses were all genotyped using the discussed methods in the above section 4.2. The timed breeding cross to isolate MEFs produced 6 embryos that included all 3 expected genotypes (Figure 4.2b-d). Both methods

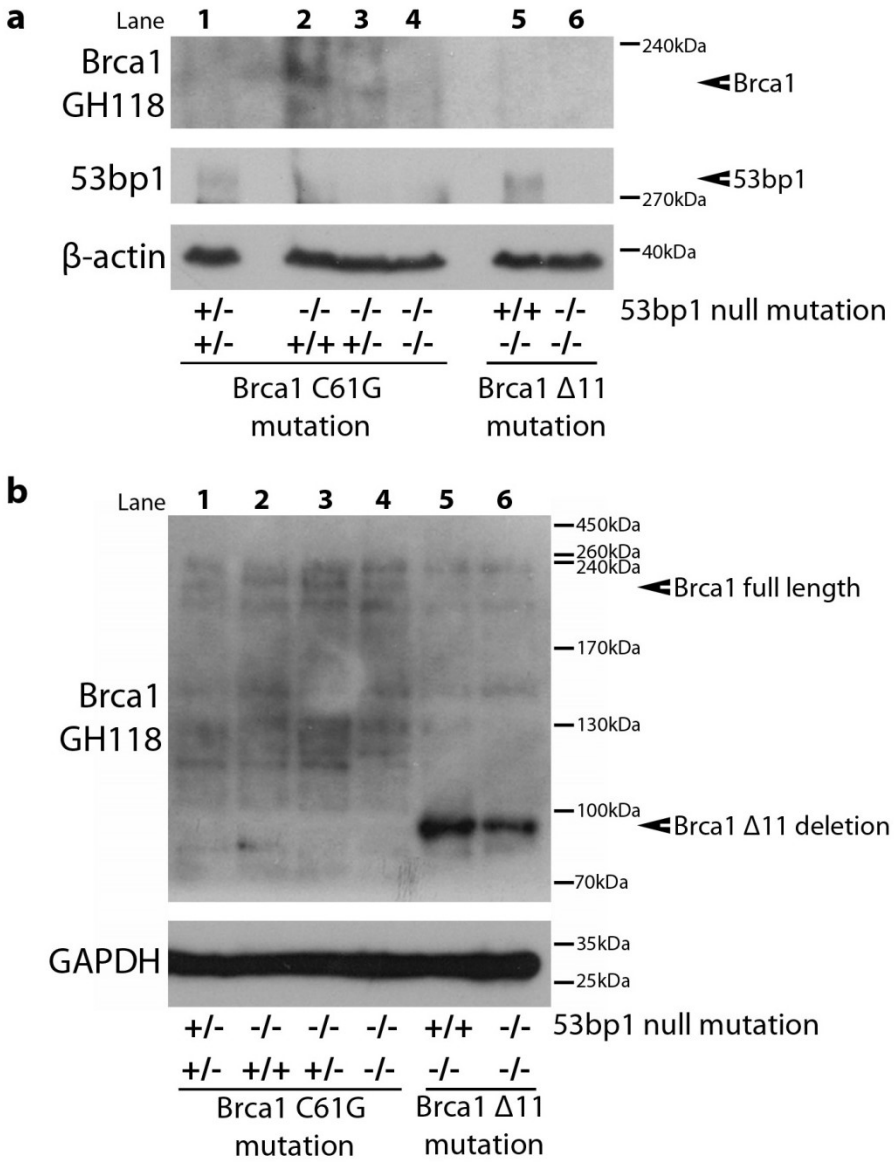

Figure 4.3 – Whole cell protein extracts from mouse embryonic fibroblasts

This figure shows two western blot results of whole cell protein extracts from MEFs with their genotypes depicted below. – represents the mutant allele (53bp1-null or Brca1 C61G) and the + represents the wild-type allele. The molecular weights are predicted using Prestained PageRuler protein ladder and shown on the right of the blot. The bands predicted to be the Brca1 or 53bp1 are shown using arrows (far right). [a] shows three blots; the first blot was probed with the mouse Brca1 antibody GH118, the second blot was probed with a 53bp1 antibody and the third blot was probed with a β-actin antibody. [b] shows two blots; the first blot was probed with the mouse Brca1 antibody GH118 and the second blot was probed with GAPDH antibody. Further details of the protocol are in section 2.3 and 2.10.

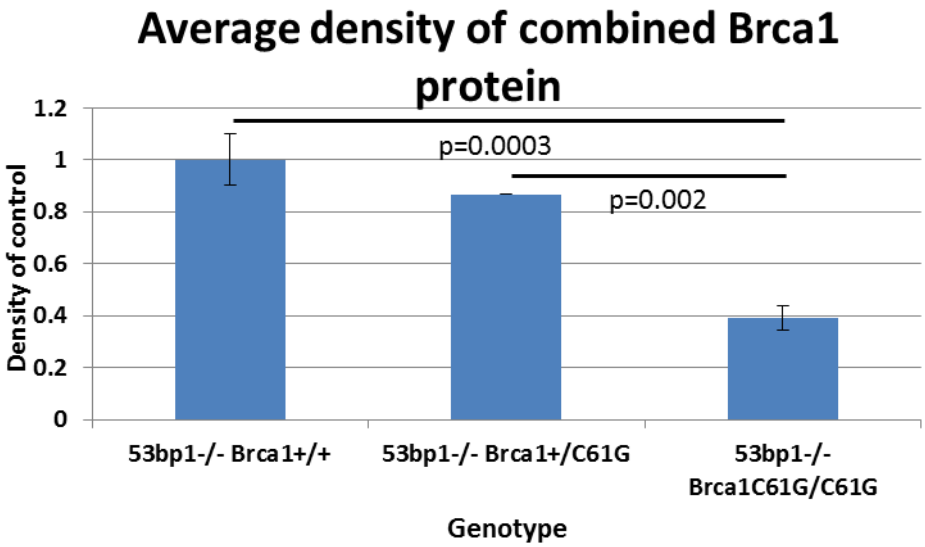

Figure 4.4 – Average density of combined Brca1 protein bands from cytoplasm and nuclear fractionation western blots
This figure shows a bar chart of the comparative levels of combined Brca1 protein in cytoplasmic and nuclear extracts from 3 western blots using fresh lysates. Each Brca1 blot was treated with the Brca1 GH118 antibody. Protein levels were measured using ImageJ analysis of the density of bands from western blot films. The error bars shows standard error and the labelled significant p value from the t-test (type 2 two-tailed student t-test) is indicated between the samples.

of PCR genotyping the *Brca1* C61G allele showed that embryos 1 and 2 were wild-type for Brca1, embryos 4 and 5 were heterozygote for the *Brca1* C61G allele, and embryos 3 and 6 were homozygote for the *Brca1* C61G mutation (Figure 4.2b-c). The *53bp1* PCR genotyping of the *53bp1* allele showed that all the embryos were homozygote for the *53bp1*-null mutation (Figure 4.2d). These embryos were cultured to produce MEFs and were immortalised using the *SV40 large T antigen* gene (details in methods 2.4.5). Table 4.1 shows the genotypes of the MEFs that are discussed in this chapter.

4.4 The determination of Brca1 C61G protein levels in cells

The immortalised MEFs were then used to investigate the effect of the C61G mutation on the cell as a whole, starting with Brca1 C61G protein. Figure 4.3a and b are the results of two western blots showing levels of Brca1 protein in whole cell extracts from the above

described MEFs and *Brca1* Δ11-deleted MEFs (with and without *53bp1* wild-type allele) (gift from Andre Nussenzweig). Full-length BRCA1 has been shown to be approximately 220 kDa in humans (Chen *et al*., 1995; Chen *et al*., 1996; Huber *et al*., 2001; Ruffner and Verma, 1997; Scully *et al*., 1996) and approximately 210 kDa in mice (Huber *et al*., 2001). The *Brca1* Δ11 MEFs have no full-length Brca1 but do produce an approximately 92 kDa fragment like the Brca1 isoform that is recognised by this Brca1 antibody (Figure 4.3a, b: lanes 5 and 6) (Huber *et al*., 2001). The GH118 Brca1 antibody was made using an epitope from the C-terminal end of the Brca1 protein. Human BRCA1 isoforms are predicted to be 96 and 110 kDa (Huber *et al*., 2001; Qin *et al*., 2011; Thakur *et al*., 1997).

Figure 4.3a and b show the varied nature of the GH118 antibody on whole cell extract samples run on a western blot. Due to this, the Brca1 protein levels were measured by estimating the band density using ImageJ of the cell and nuclear fractions of the Brca1 C61G MEFs and combining the totals. This was done for three separate experiments and compared in figure 4.4. This shows that in cells with one copy of *Brca1* C61G there is a reduction in Brca1 levels and when both copies of *Brca1* are mutated, there is a further reduction in Brca1 protein.

When used for western blotting, the Brca1 antibody (GH118) produces a weak signal and produces multiple non-specific bands and requires a large amount of protein to be loaded to be visible. The digestion of a large number of cells into a small volume allowing a large amount of protein to be loaded for this experiment, may be responsible for some of the variety in protein levels and why it is less variable when the cytoplasm and nuclear fractions are run as separate samples, however it could be due to varying Brca1 protein levels in the

MEFs themselves. The use of multiple other antibodies (List in Table 2.10 and 2.11) that target Brca1, unfortunately, did not produce any band that correlating with the size of Brca1 protein. There are papers that suggest BRCA1 levels vary during the cell cycle (Chen *et al*., 1996; Choudhury *et al*., 2004; Croke *et al*., 2013; Gudas *et al*., 1996; Hayami *et al*., 2005; Liu *et al*., 2010; Ruffner and Verma, 1997; Scully *et al*., 1997b; Vaughn *et al*., 1996; Wu *et al*., 2010), but not all papers have replicated this (Escribano-Diaz *et al*., 2013). The multiple ways in which BRCA1 is degraded have been published (Blagosklonny *et al*., 1999; Hammond-Martel *et al*., 2010; Liu *et al*., 2010; Lu *et al*., 2007; Lu *et al*., 2012; Peng *et al*., 2015; Qin *et al*., 2011; Stebbing *et al*., 2015; Wang *et al*., 2014b; Wu *et al*., 2010; Xian Ma *et al*., 2003; Zhang *et al*., 2012), and some papers that show the altered-C61 residue can cause BRCA1 to be readily degradable (Brzovic *et al*., 1998; Brzovic *et al*., 2001a; Choudhury *et al*., 2004; Wang *et al*., 2014b), but not all agree (Campbell *et al*., 2001; Lu *et al*., 2007; Nelson and Holt, 2010). Further investigation is needed to explain this variety.

Figure 4.3a also shows the absence of 53bp1 protein in MEFs with two copies of the *53bp1*-null allele, and the presence of 53bp1 protein in MEFs with one or two copies of the *53bp1* wild-type allele, confirming the removal of full-length 53bp1 protein in these cells.

4.5 Brca1 C61G protein levels in the nucleus and cytoplasm

BRCA1 has nuclear localisation sequences (NLS) (Chen *et al*., 1996; Fabbro *et al*., 2002; Thakur *et al*., 1997; Wang *et al*., 2014b; Wilson *et al*., 1997) and nuclear export signals (NES) (Fabbro *et al*., 2002; Rodriguez and Henderson, 2000; Rodriguez *et al*., 2003a; Rodriguez *et al*., 2004) that regulate the localisation of BRCA1 protein. BRCA1-interacting proteins have roles in BRCA1 localisation, such as BARD1 and Abraxas

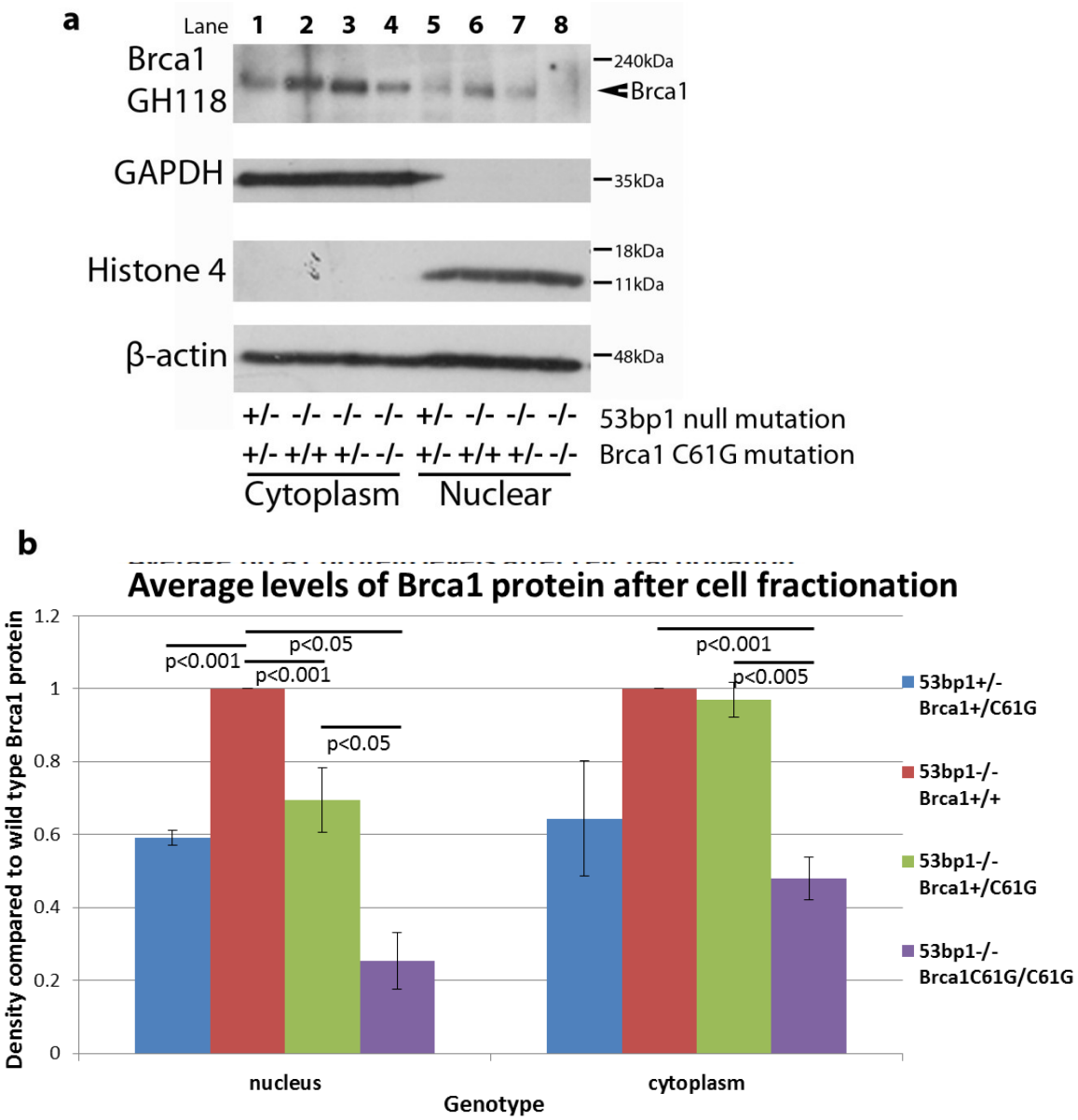

Figure 4.5 – Nuclear and cytoplasm separation of mouse embryonic fibroblasts

[a] shows a western blot results from a nuclear and cytoplasm fractionation of MEFs with their genotypes depicted below. The molecular weights are predicted using Prestained PageRuler protein ladder and shown on the right of the blot. The Brca1 protein band is shown with an arrow. The first blot is probed with mouse Brca1 antibody GH118, the second blot is probed with a GAPDH antibody, the third blot is probed with an antibody recognising Histone 4 and the final blot was probed with a βactin antibody. Samples 1-4 are the samples from the cytoplasm fraction and samples 5-8 are samples from the nuclear fraction. Further details of the protocol are in section 2.4.6. [b] shows a bar chart showing the average levels of Brca1 protein from 3 separate experiments from each MEF genotype compared with the 53bp1$^{-/-}$ Brca1$^{+/+}$ sample. The first section shows the level of Brca1 protein in the nuclear fractions and the second section shows the level of Brca1 protein in the cytoplasmic fractions. The error bars shows standard error and the significant p values from a t-test (type 2 two-tailed student t-test) are indicated. Protein levels were measured using ImageJ analysis of the density of bands from western blot films.

(Fabbro *et al*., 2002; Rodriguez and Henderson, 2000; Rosen *et al*., 2006; Vikrant *et al*., 2015). BRCA1 NES (aa81-99) is enclosed by the BRCA1:BARD1 heterodimer interface and the exposure of the NES (aa81-99) (Rodriguez and Henderson, 2000) in BRCA1 N-terminus is predicted to export BRCA1 through the CRM1 nuclear export channel for degradation in the cytoplasm (Fabbro *et al*., 2004b; Rodriguez and Henderson, 2000). Since the *BRCA1* C61G mutation has been shown to alter the structure of the RING domain (Brzovic *et al*., 1998; Brzovic *et al*., 2001a; Wang *et al*., 2014b) potentially exposing the NES (Rodriguez and Henderson, 2000), nuclear/cytoplasm fractionation was used to investigate Brca1 C61G protein levels in the nucleus. Figure 4.5a shows that the levels of Brca1 in MEFs with one copy of *Brca1* C61G (lanes 1, 3, 5 and 7) are reduced compared to homozygote wild-type *Brca1* MEFs (lanes 2 and 6), in both the cytoplasmic (lanes 1-4) and the nuclear (lanes 5-8) fractions. Further reduction of Brca1 levels are seen in the cytoplasm and nucleus when MEFs are homozygote for the *Brca1* C61G mutation (lanes 4 and 8). The presence of Histone 4 and GAPDH in each extract shows the fractionation of nuclear and cytoplasmic proteins and β-actin is the loading control.

This experiment was repeated 3 times and the densitometry of the Brca1 protein bands were measured using ImageJ (Section 2.1.3). The MEFs with only wild-type Brca1 were set as one in each experiment and used to compare against Brca1 levels in the other MEFs. Figure 4.5b shows the average of these comparative Brca1 protein level values from the three experiments and the p values from the t-test statistics on these results is in Table 4.4. These results show that the reduction in Brca1 in the nuclear fraction is significantly different in cells with one or two copies of *Brca1* C61G from cells with only wild-type Brca1 protein. In the cytoplasmic fractions, there is a significant reduction between the MEFs with one or two

copies of *Brca1* C61G in a *53bp1*-null background compared to the *53bp1*$^{-/-}$*Brca1*$^{+/+}$ MEFs. This suggests that the homozygote C61G mutation in *Brca1* does reduce the levels of Brca1 protein present in the nucleus and in cytoplasm in 53bp1-null cells.

Table 4.2 – P values from a t-test performed on the comparable Brca1 protein levels in the nucleus and cytoplasm

	Nuclear			Cytoplasm		
	***53bp1*$^{-/-}$ *Brca1*$^{+/+}$**	***53bp1*$^{-/-}$ *Brca1*$^{+/C61G}$**	***53bp1*$^{-/-}$ *Brca1*$^{C61G/C61G}$**	***53bp1*$^{-/-}$ *Brca1*$^{+/+}$**	***53bp1*$^{-/-}$ *Brca1*$^{+/C61G}$**	***53bp1*$^{-/-}$ *Brca1*$^{C61G/C61G}$**
***53bp1*$^{+/-}$ *Brca1*$^{+/C61G}$**	**0.00004**	0.327748	**0.013292**	0.087849	0.119967	0.38464
***53bp1*$^{-/-}$ *Brca1*$^{+/+}$**	-	**0.026241**	**0.000646**	-	0.557874	**0.00087**
***53bp1*$^{-/-}$ *Brca1*$^{+/C61G}$**	-	-	**0.020137**	-	-	**0.002835**

If there was an increase of Brca1 protein in the cytoplasm that matched the decrease in protein in the nucleus, this would suggest that Brca1 C61G is exported from the nucleus. However, as we see a decrease of Brca1 protein in the cytoplasm of *53bp1*-null MEFs, there are three possibilities: Brca1 C61G protein is highly degradable in both the nucleus and the cytoplasm, Brca1 C61G protein is exported from the nucleus and then rapidly degraded, or Brca1 C61G protein is not made to the same levels wild-type protein. If mRNA were unstable and less Brca1 protein was made, then it would be unlikely to see the same levels of Brca1 protein across the MEF genotypes (Section 4.4 and figure 4.4) or papers in the literature suggesting C61G does not alter BRCA1 protein levels (Campbell *et al*., 2001; Lu *et al*., 2007; Nelson and Holt, 2010). Previous papers have looked at BRCA1 degradation and have not suggested a correlation in *BRCA1* mRNA and BRCA1 protein degradation (Blagosklonny *et al*., 1999; Choudhury *et al*., 2004; Gudas *et al*., 1996; Joukov *et al*., 2001; Liu *et al*., 2010; Lu *et al*., 2007; Stebbing *et al*., 2015; Vaughn *et al*., 1996; Xian Ma *et al*., 2003), and Drost *et al*,

show *Brca1* C61G mice tumours have the expected levels of *Brca1* mRNA expression (Drost *et al*., 2011).

4.6 The nuclear export of Brca1 C61G protein

As discussed, BRCA1 has several NES sequences that are recognised by the CRM1 nuclear export protein and CRM1's action can be blocked using Leptomycin B (LMB) (Ossareh-Nazari *et al*., 1997; Wolff *et al*., 1997). Previous literature can be split into papers that show LMB is effective in stopping BRCA1 from being exported from the nucleus (Brodie *et al*., 2001; Rodriguez and Henderson, 2000; Rodriguez *et al*., 2004) and papers that show LMB does not alter BRCA1 localisation (Blagosklonny *et al*., 1999; Nelson and Holt, 2010). Nelson *et al*

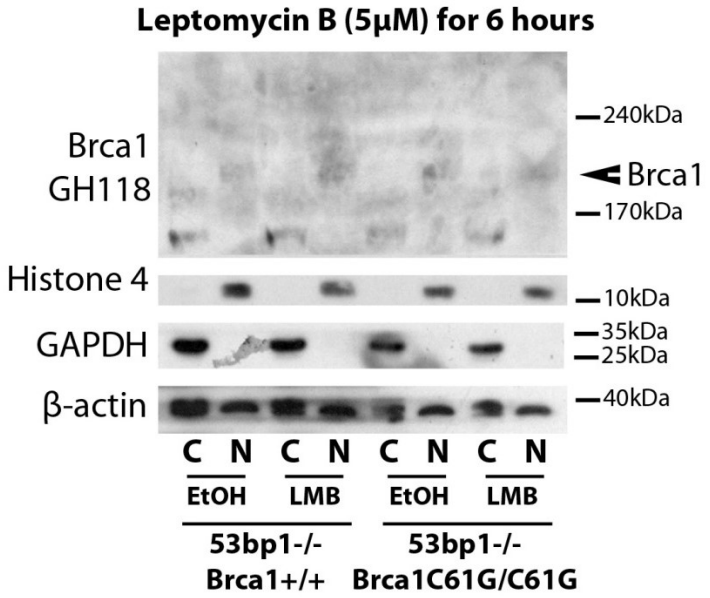

Figure 4.6 – Ratio of Brca1 protein in nuclear to cytoplasm and LMB treatment
This figure shows a nuclear (N) and cytoplasm (C) fractionation of MEFs treated with ethanol (EtOH) or treated with 5 μM Leptomycin B (LMB) for 6 hours. The molecular weights are predicted using Prestained PageRuler protein ladder and shown on the right of the blot. The band predicted to be the Brca1 are shown using arrows (right). The genotype of the samples is depicted below. The first blot was probed with the mouse Brca1 GH118 antibody, the second blot was probed with an antibody specific to Histone 4, the third blot was probed with a GAPDH antibody and the final blot was probed with a β-actin antibody.

showed that neither BRCA1 wild-type, nor C61G, foci localisation is altered by LMB (Nelson and Holt, 2010). Figure 4.6b shows the nuclear and cytoplasm fractions of LMB- treated MEFs (5 µM for 6 hours). GAPDH and Histone 4 show the separation of cytoplasm and nucleus and β-actin is used as the loading control. Due to the unclear nature of the western blot no determination can be made to determine if LMB does affect the localisation of Brca1 or Brca1 C61G protein. This result needs to be repeated further with an antibody that is more specific when used in western blot.

4.7 Degradation of Brca1 and Brca1 C61G protein

It is debated as to whether the degradation of BRCA1 C61G is quicker (Brzovic *et al*., 1998; Brzovic *et al*., 2001a; Choudhury *et al*., 2004; Wang *et al*., 2014b) than wild-type BRCA1 or the same (Campbell *et al*., 2001; Lu *et al*., 2007; Nelson and Holt, 2010). To assess the degradation of Brca1 C61G, MEFs that were homozygote for either *Brca1* wild-type or *Brca1* C61G only were either mock treated (0 hour) or treated with Cycloheximide (CHX, 100 µM) for 2, 4, 6 or 8 hours (Figure 4.7a). Cycloheximide inhibits protein synthesis without affecting RNA production (Young *et al*., 1963). CtIP was used as a known protein that shows degradation in the 8 hour time period of CHX treatment, regardless of *BRCA1* mutation status (Yu *et al*., 2006). β-actin is used as a loading control.

The CHX time course (Figure 5.7a) is not clear enough to determine if there is a quantifiable or relevant change in the degradation of Brca1 protein between the genotypes of the MEFs. Therefore, this experiment should be repeated with multiple Brca1 antibodies and a time point before drawing any conclusions. BRCA1 has also been reported to be degraded by the proteasome (Blagosklonny *et al*., 1999; Brodie and Henderson, 2010; Choudhury *et al*., 2004; Hammond-Martel *et al*., 2010; Hayami *et al*., 2005; Lu *et al*., 2007; Stebbing *et al*., 2015;

Wang *et al*., 2014b; Zhang *et al*., 2012) after being ubiquitinated by other E3 ubiquitin ligases (not autoubiquitination) (Choudhury *et al*., 2004; Lu *et al*., 2007; Lu *et al*., 2012; Wang *et al*., 2014b; Zhang *et al*., 2012). The proteasomal degradation can be blocked by the use of the proteasomal inhibitor MG132 (Rock *et al*., 1994). Figure 4.7b shows a time course spanning 8 hours of DMSO (D) or MG132 treated MEFs with either wild-type or C61G Brca1 protein. Cyclin A is known to accumulate in cells after MG132 treatment (Geley *et al*., 2001). Whilst a small change in Brca1 protein could be said to be seen in figure 5.7b, the GH118 Brca1 antibody does not allow for an accurate or clearly determinable result between genotypes. This experiment should also be repeated with a different Brca1-spefic antibody.

4.8 Ionising radiation-induced foci formation in *Brca1* C61G cells

Figures 4.8-12 show 7 different cell lines that have varying genotypes summarised in table 4.1. This section will also refer to NIH3T3s which are a common mouse cell line that can be

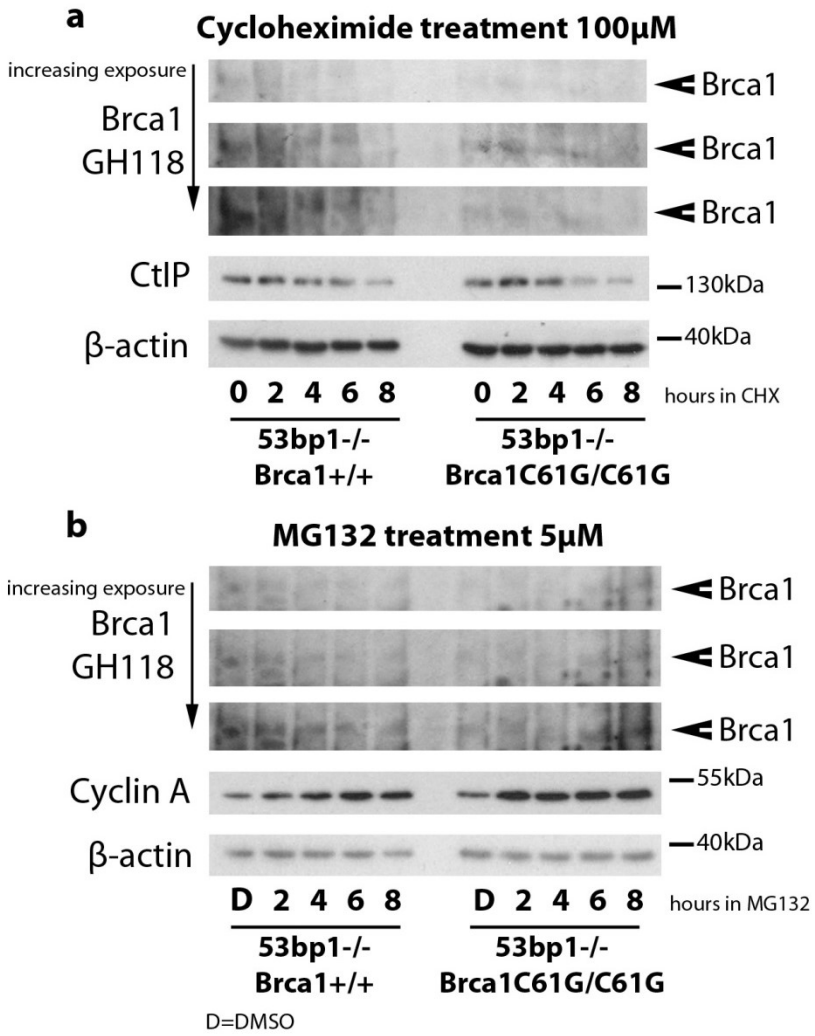

Figure 4.7 – Exploring Brca1 protein degradation using Cycloheximide and MG132
[a] shows a western blot of whole cell extract MEF samples untreated (0) or treated with 100 µM Cycloheximide (CHX) for 2, 4, 6 or 8 hours. The molecular weights are predicted using Prestained PageRuler protein ladder and shown on the right of the blot. The band predicted to be the Brca1 are shown using arrows (right). The genotype of the samples is depicted below. The first three letterboxes show 3 exposures of a single blot probed with mouse Brca1 GH118 antibody. The fourth letterbox shows a blot probed with a CtIP antibody and the final blot was probed with a β-actin antibody. [b] shows a western blot of whole cell extract MEF samples treated with DMSO (D) for 8 hours or treated with 5 µM MG132 for 2, 4, 6 or 8 hours. The molecular weights are predicted using Prestained PageRuler protein ladder and shown on the right of the blot. The band predicted to be the Brca1 are shown using arrows (right). The genotype of the samples is depicted below. The first three letterboxes show 3 exposures of a single blot probed with mouse Brca1 GH118 antibody. The fourth letterbox shows a blot probed with a Cyclin A antibody and the final blot was probed with a β-actin antibody.

used as an epithelial seeding layer for other cells (such as stem cells or primary cells) but is also used as a wild-type mouse cell line. The *53bp1* wild-type *Brca1* exon 11-deleted MEFs were published by Cao *et al* (Cao *et al*., 2009) and their *53bp1*-null counterparts were published by Ward *et al* (Ward *et al*., 2003b).

4.8.1 53bp1 ionising radiation-induced foci

The *53bp1*$^{-/-}$*Brca1*$^{C61G/C61G}$ mice are viable with the removal of *53bp1* (Section 4.3) and this is likely to be due to the removal of the homologous recombination (HR) block caused by 53bp1 (Bouwman *et al*., 2010; Bunting *et al*., 2010; Bunting *et al*., 2012; Cao *et al*., 2009) (Section 1.5.3). The *53bp1*-null mutation does not produce any full-length 53bp1 protein (Figure 4.4a) and therefore it cannot form ionising radiation-induced foci (IRIF) (Ward *et al*., 2003b). Figure 4.8 shows immunofluorescent stained untreated cells stained for DNA (Hoechst), 53BP1 and the DNA damage marker, γH2AX. As discussed previously (Section 1.4.1), 53BP1 binds to DNA ends and can be used as a marker for DSBs.

This figure shows that the cells with two copies of the *53bp1*-null mutation do not produce 53bp1 foci spontaneously unlike cells with a wild-type copy of *53bp1*. Figure 4.9 shows cells stained as the previous figure (Figure 4.8), but the cells were treated with 5 Gray of ionising radiation (IR) 1 hour before fixation (Schultz *et al*., 2000). As shown in this figure, IR causes an increase in γH2AX foci in all cell lines and an increase of 53bp1-γH2AX co-localising foci in cell lines that have a wild-type copy of *53bp1* as expected (Schultz *et al*., 2000; Ward *et al*., 2003a). This confirms that the *53bp1*-null mutation does not produce 53bp1 IRIF.

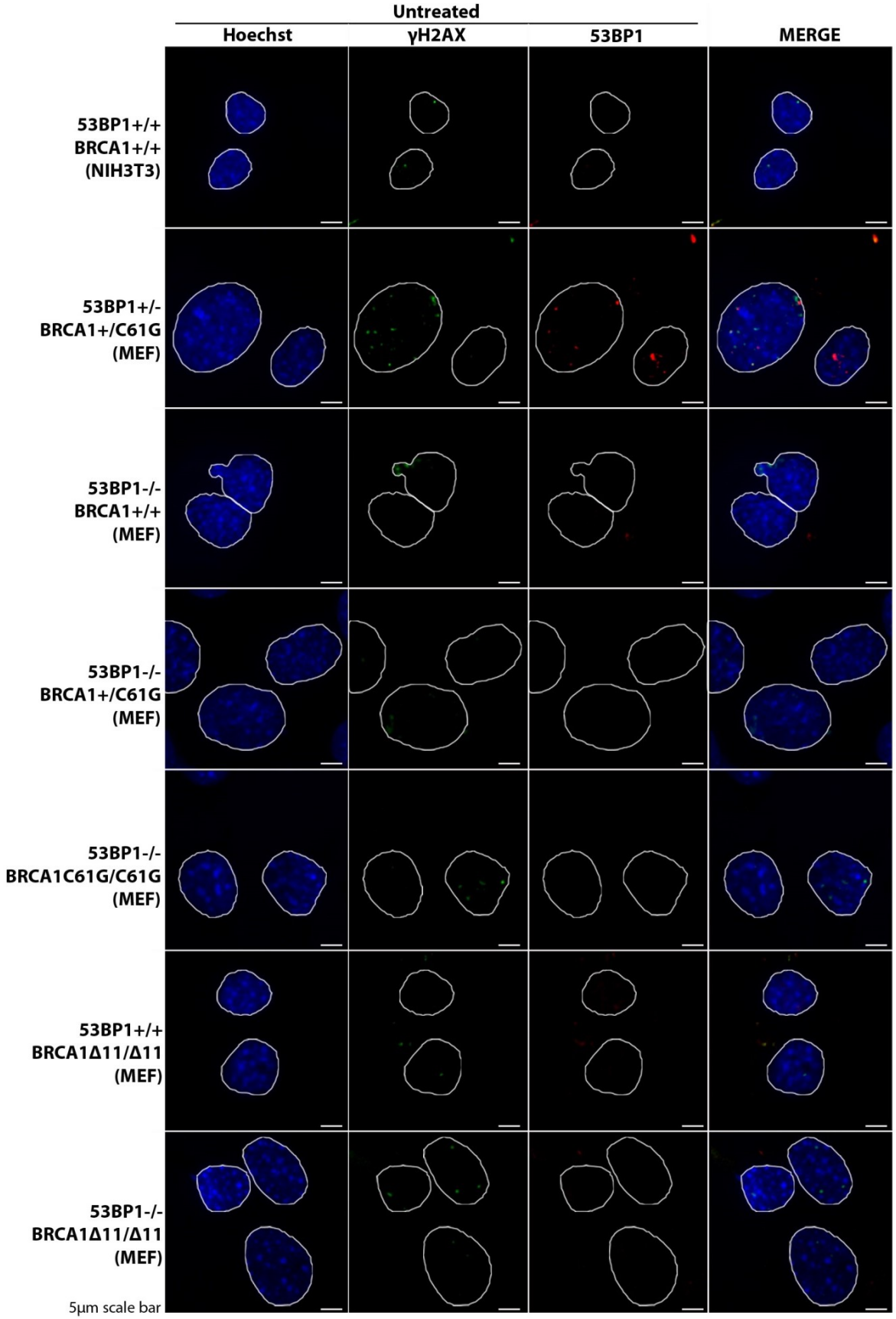

Figure 4.8 – 53bp1 and γH2AX immunofluorescent foci in untreated cells

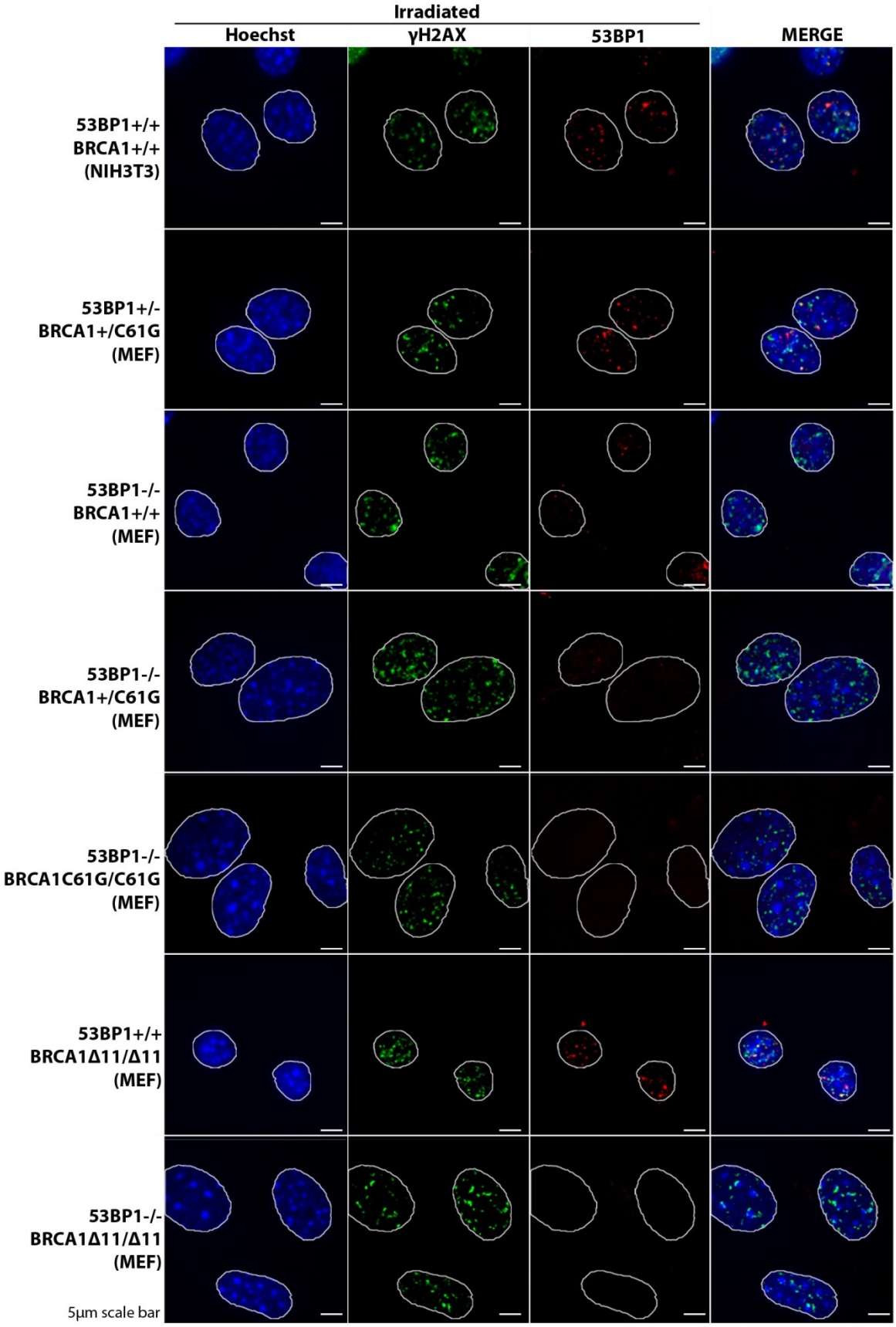

Figure 4.9 – 53bp1 and γH2AX immunofluorescent foci in IR-treated cells

Figure 4.8 – 53bp1 and γH2AX immunofluorescent foci in untreated cells
This figure shows a panel of images of untreated cells stained to show the nucleus (Hoechst-blue), γH2AX (green) and 53BP1 (red). Further details of the immunofluorescent staining protocol is discussed in section 2.4.7. The genotype of the cells is stated on the left of the row and the final images on the row (far right) are a merged image of all stains (MERGE). White lines outline the nucleus of the cells. Scale bar is 5 µm.

Figure 4.9 – 53bp1 and γH2AX immunofluorescent foci in IR-treated cells
This figure shows a panel of images of cells after 1 hour of exposure to 5 Gray of ionising radiation and stained to show the nucleus (Hoechst-blue), γH2AX (green) and 53BP1 (red). Further details of the immunofluorescent staining protocol is discussed in section 2.4.7. The genotype of the cells is stated on the left of the row and the final images on the row (far right) are a merged image of all stains (MERGE). White lines outline the nucleus of the cells. Scale bar is 5 µm.

4.8.2 Brca1 ionising radiation-induced foci

BRCA1 produces foci when cells are treated with IR (Li and Yu, 2013; Scully *et al*., 1997a; Wei *et al*., 2008) although, unlike 53bp1, BRCA1 IRIF are not just representative of DSB ends as BRCA1 may also form at other sites of DNA damage or stress (Au and Henderson, 2007) (Section 1.4.2). However, the majority of DNA damage caused by IR is DSBs and the BRCA1 foci that co-localise with γH2AX are likely to be DSBs (Paull *et al*., 2000). Cells were not treated or treated with 5 Gray of IR and fixed after 1 hour, a time suggested to be when BRCA1 is localised to orchestrate HR (Paull *et al*., 2000; Wei *et al*., 2008), and stained for DNA (Hoechst), Brca1 (GH118) and γH2AX. Figure 4.10 shows untreated cells that have a background level of γH2AX staining and a few Brca1 foci, showing spontaneous DNA damage and non-IR-induced Brca1 and γH2AX foci. Figure 4.11 shows cells treated with IR have a higher level of γH2AX foci (as seen in figure 4.9) and a large induction of Brca1-γH2AX co-localising foci in cells with a wild-type copy of *Brca1*. However, $53bp1^{-/-}Brca1^{C61G/C61G}$ cells show very few Brca1-γH2AX co-localising foci suggesting Brca1 C61G does not form as many foci as wild-type Brca1. To quantify this further, 100 IR-treated cells from 3 separate experiments were examined and Brca1-γH2AX co-localising foci were counted (Figure

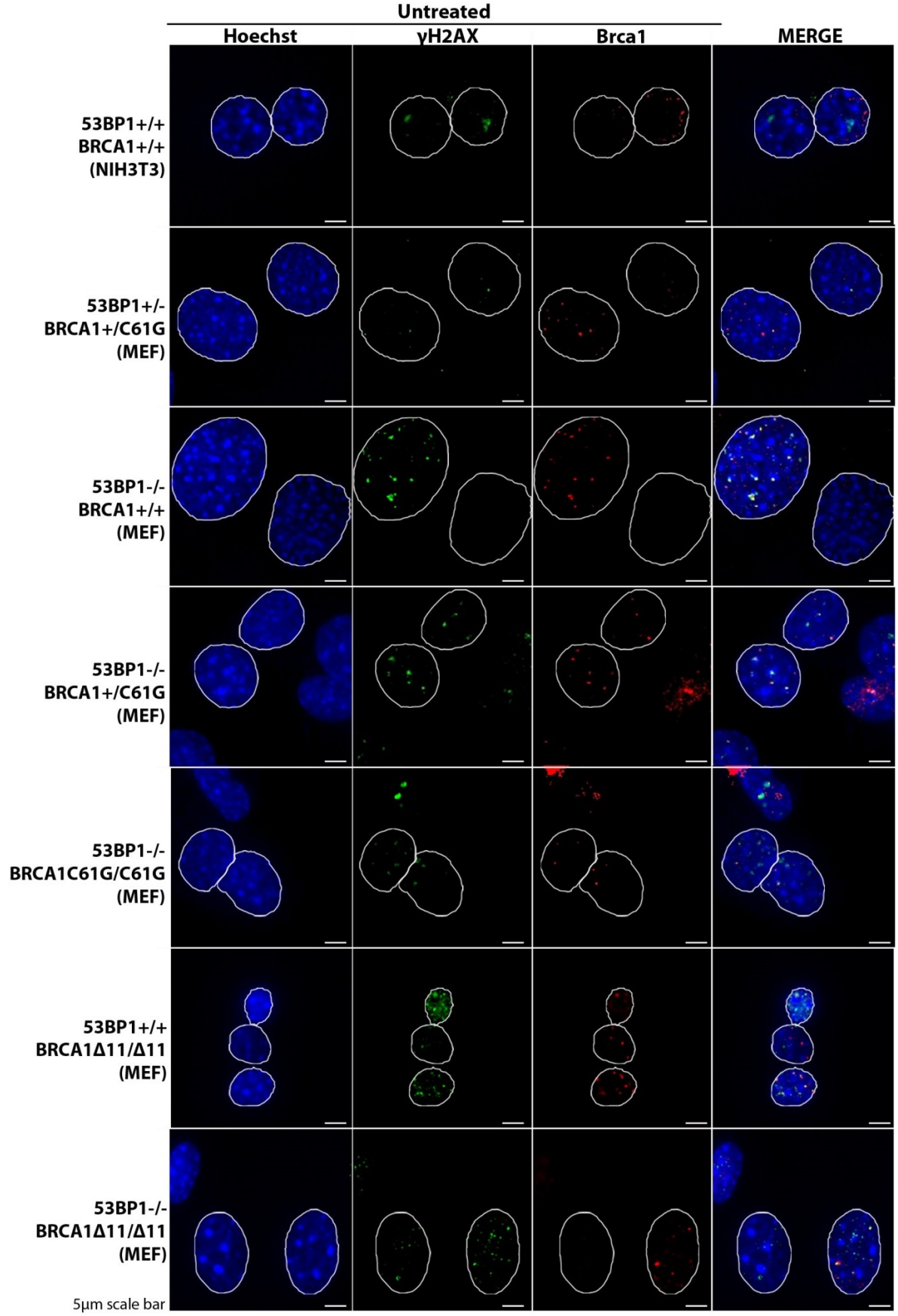

Figure 4.10 – Brca1 and γH2AX immunofluorescent foci in untreated cells

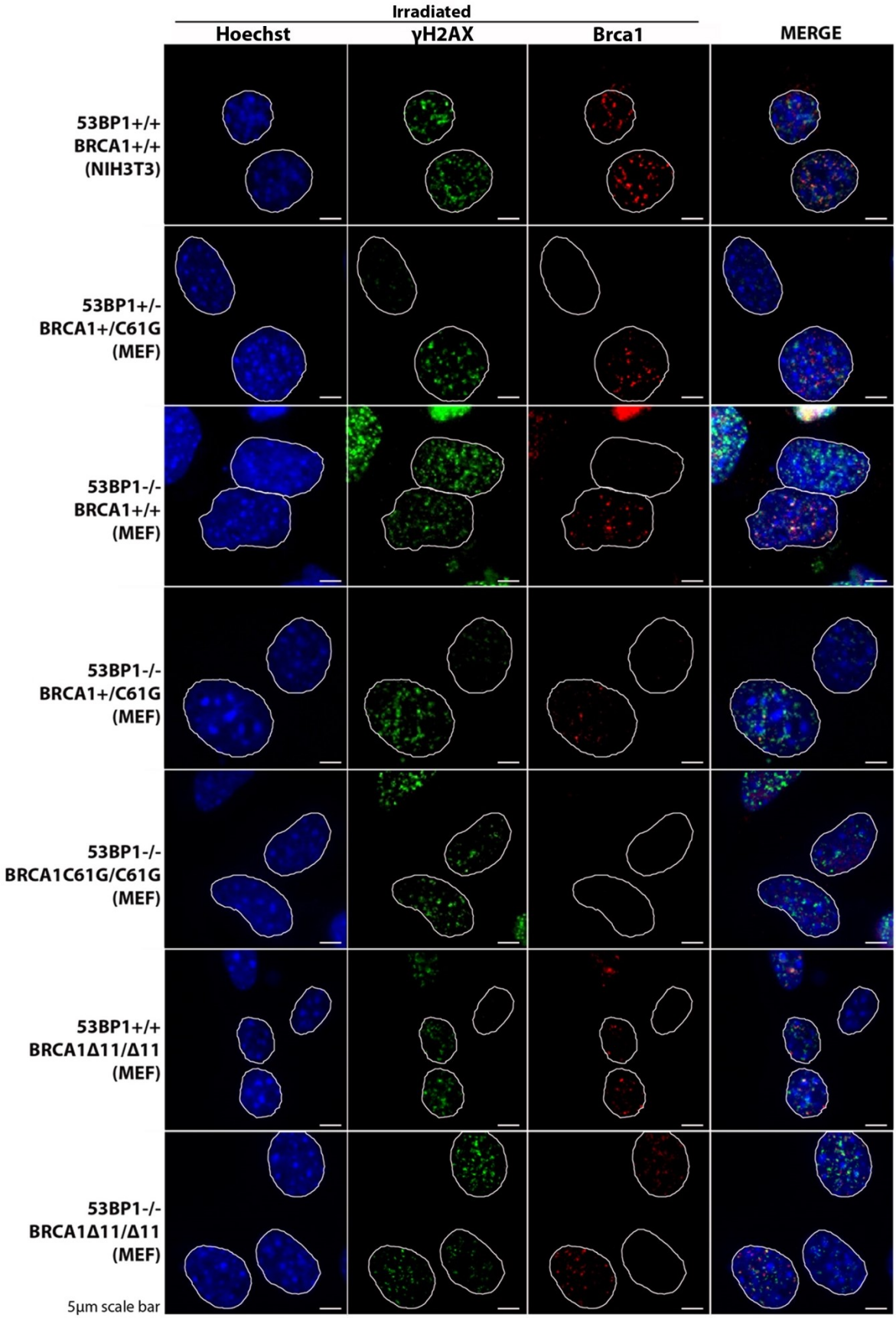

Figure 4.11 – Brca1 and γH2AX immunofluorescent foci in IR-treated cells

Figure 4.10- Brca1 and γH2AX immunofluorescent foci in untreated cells
This figure shows a panel of images of untreated cells stained to show the nucleus (Hoechst-blue), γH2AX (green) and Brca1 (red). Further details of the immunofluorescent staining protocol are discussed in section 2.4.7. The genotype of the cells is stated on the left of the row and the final images on the row (far right) are a merged image of all stains (MERGE). White lines outline the nucleus of the cells. Scale bar is 5 µm.

Figure 4.11- Brca1 and γH2AX immunofluorescent foci in IR-treated cells
This figure shows a panel of images of cells after 1 hour of exposure to 5 Gray of ionising radiation and stained to show the nucleus (Hoechst-blue), γH2AX (green) and Brca1 (red). Further details of the immunofluorescent staining protocol are discussed in section 2.4.7. The genotype of the cells is stated on the left of the row and the final images on the row (far right) are a merged image of all stains (MERGE). White lines outline the nucleus of the cells. Scale bar is 5 µm.

4.12b,c). Brca1-γH2AX co-localising foci were also counted in 100 cells in the untreated cells in two of these experiments (Figure 4.12a). Untreated cells contain sites of DNA damage (shown by γH2AX foci) because the cells naturally incur spontaneous DNA damage through normal cellular activities. In the untreated cells, there was a significant increase in the number of Brca1-γH2AX co-localising foci in *53bp1*$^{-/-}$*Brca1*$^{+/+}$ MEFs compared *53bp1*$^{+/-}$ *Brca1*$^{+/C61G}$ MEFs. This could be predicted since the removal of 53bp1 is known to increase the amount of DSBs that are repaired through HR (Bouwman *et al*., 2010; Bunting *et al*., 2010; Bunting *et al*., 2012; Cao *et al*., 2009) so there would be more sites of DNA damage (γH2AX) that co-localise with Brca1 foci. The removal of wild-type Brca1 has been suggested to allow NHEJ to progress at sites of DSBs (Bunting et al., 2010) and therefore the decreased number of Brca1-γH2AX co-localising foci in the *53bp1*$^{-/-}$*Brca1*$^{+/C61G}$ and *53bp1*$^{-/-}$*Brca1*$^{C61G/C61G}$ (although not significantly for the latter) may be a result of this. Although it is also possible that the reduction seen in the MEFs with one or two copies of *Brca1* C61G (with or without wild-type *53bp1*) are due to the C61G mutation altering the ability of the protein to localise to DNA damage.

There were significantly fewer cells with more than 5 co-localising Brca1-γH2AX foci in the *53bp1*$^{-/-}$*Brca1*$^{C61G/C61G}$ MEFs suggesting that Brca1 C61G protein is dramatically less efficient at localising to DSBs (Figure 4.12b). The C61G mutation in *BRCA1* causes a structural change which could alter its interaction with proteins that causes the reduction in localisation of Brca1 to IRIF. As discussed, the C61G mutation has been shown to alter the binding between BRCA1 and BARD1, and this interaction, at least partially, is responsible for BRCA1 localisation to DSBs (Greenberg *et al*., 2006; Li and Yu, 2013; Wei *et al*., 2008).

When looking at the number of cells with either 1, 2, 3, 4, 5 or no Brca1-γH2AX foci (Figure 4.12c), we see that there are significantly fewer cells with 4 or 5 Brca1 C61G-γH2AX foci compared to cells with a wild-type Brca1. This alongside the presence of Brca1 C61G-γH2AX foci in the untreated cells suggested that Brca1 foci can still form and the reduction of Brca1 C61G protein (Figures 4.3-7) could partially be the cause of the reduced foci. It may be that fewer Brca1 C61G molecules are localising to each DSBs and this low level of protein is not detected or visible within the range of sensitivity of this IF antibody (GH118) or this microscopy method.

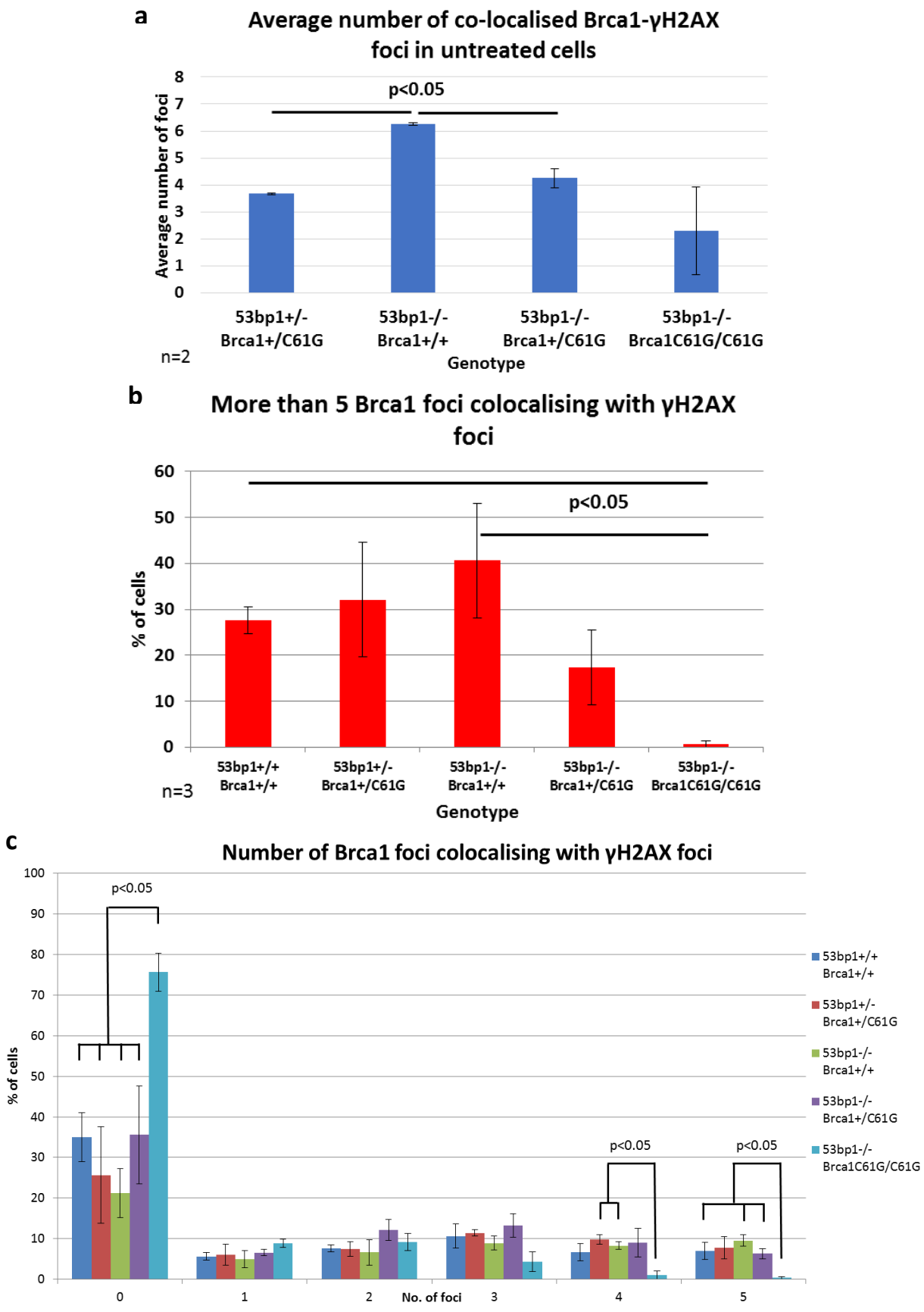

Figure 4.12 – Counts of Ionising-radiation-induced Brca1 foci

Figure 4.12 – Counts of Ionising-radiation-induced Brca1 foci
[a] shows a bar chart of the average number of co-localised γH2AX and Brca1 foci in untreated MEFs. These results are from two separate experiments each with 100 cells. Error bars present standard error. [b] shows a bar chart of the average percentage of cells with more than 5 Brca1 foci that co-localise with γH2AX foci of 100 cells from three separate experiments. All cells were treated with 5 Gray of ionising radiation and fixed after 1 hour. The genotypes of the cells are as stated below. The error bars represent standard error and the asterisks (*) show which results are significantly different with a p value of less than 0.05 after a t-test (Type 2 two-tailed student t-test). [c] shows a bar chart of the average percentage of cells with each number of Brca1 foci that co-localise with γH2AX foci from three separate experiments. All cells were treated with 5 Gray of ionising radiation and fixed after 1 hour. The genotypes of the cells are as stated in the key. The error bars represent standard error and the asterisks (*) show which results are significantly different with a p value of less than 0.05 after a t-test (Type 2 two-tailed student t-test). Further details of the immunofluorescent staining protocol is discussed in section 2.4.7.

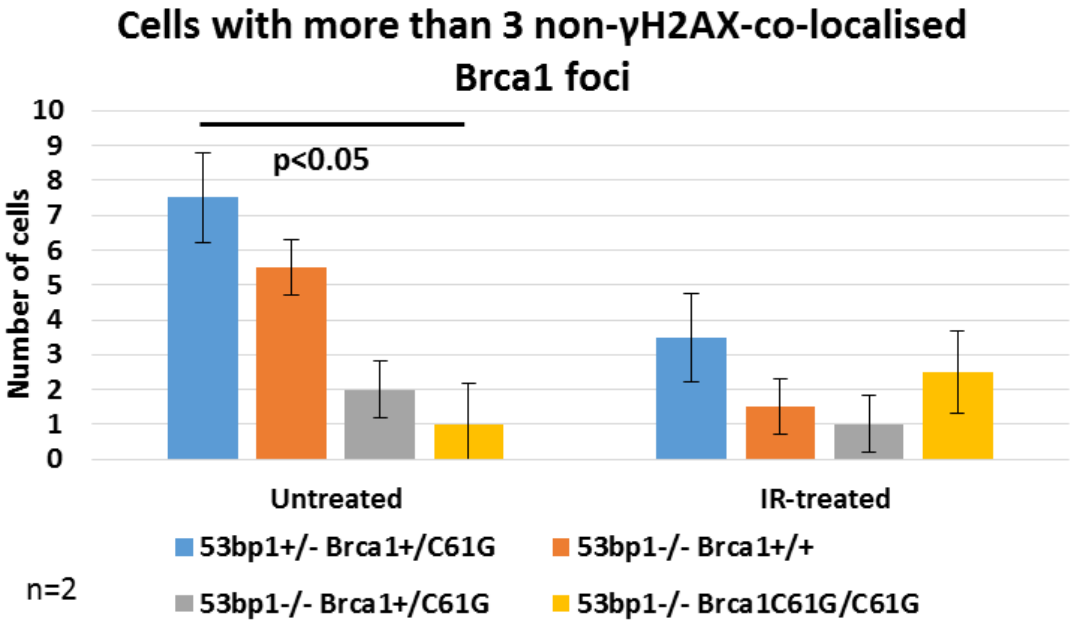

Figure 4.13 – Number of cells with more than three Brca1 foci that do not co-localise with γH2AX foci
This figure shows a bar chart of the number of cells with more than three Brca1 foci that do not co-localise with γH2AX foci. These are the results from two separate experiments and the error bars represent standard error. Cells were either untreated or treated with 5 Gray of ionising radiation and fixed after an hour. The cells genotypes is indicated in the key below the image.

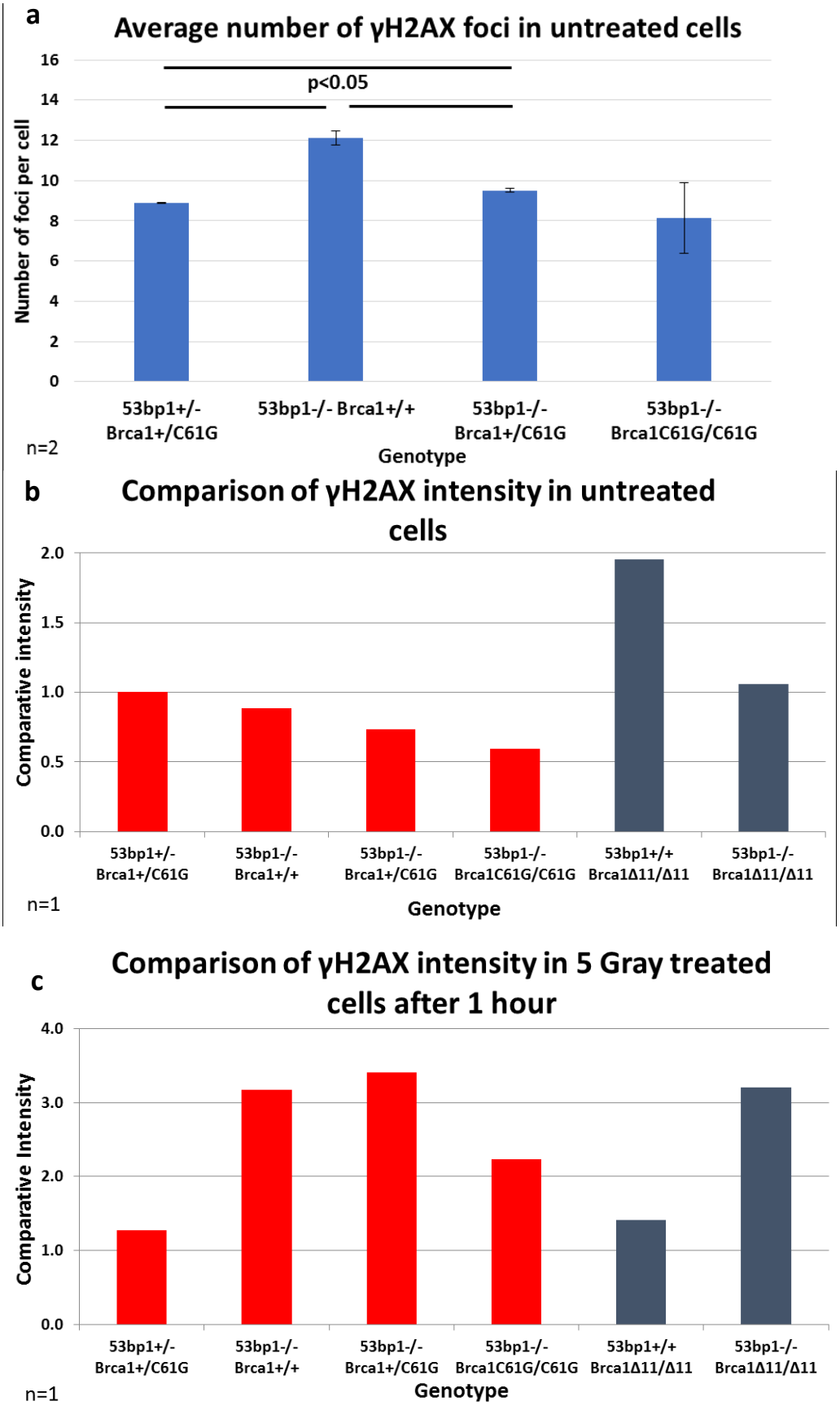

Figure 4.14 – Levels of γH2AX foci in untreated and IR-treated cells

Figure 4.14 – Levels of γH2AX foci in untreated and IR-treated cells
[a] shows a bar chart of the average number of γH2AX foci in two separate experiments each with 100 cells. The genotypes are stated below and the error bars shows standard error. The lines refer to the genotypes between which there is a significant difference (a p value of less than 0.05) determined by a t-test (Type 2 two-tailed student t-test). [b] shows a bar chart of the average intensity of γH2AX stain in untreated MEFs of the genotypes indicated. [c] shows a bar chart of the average intensity of γH2AX stain of cells an hour after being treated with 5 Gray of IR. [b,c] These results are from n=1. The red bars are the Brca1 C61G MEFs and the blue bars are the Brca1 Δ11 MEFs.

Figure 4.12b also shows an increase in Brca1-γH2AX co-localising foci in *53bp1*$^{-/-}$*Brca1*$^{+/+}$ MEFs. Since the 53BP1 antagonises BRCA1 action in orchestrating HR (Bouwman *et al*., 2010; Bunting *et al*., 2010; Bunting *et al*., 2012; Cao *et al*., 2009), this increase in Brca1-γH2AX foci could show that more DSBs are being repaired via HR than NHEJ. This increase in HR is seen in the literature (Bouwman *et al*., 2010; Bunting *et al*., 2010; Bunting *et al*., 2012; Cao *et al*., 2009).

The *Brca1* exon 11-deletion allele does not form full-length Brca1 protein (Figure 4.3b) but produces an approximately 92 kDa protein (Huber *et al*., 2001). Although this protein is described to be a predominantly cytoplasmic protein (Qin *et al*., 2011; Thakur *et al*., 1997), in figure 4.11 it is clear that it does form Brca1-γH2AX foci in response to DSBs as reported in Hubert *et al* (Huber *et al*., 2001). The Brca1 GH118 antibody epitope maps to the C-terminus of Brca1 and this localisation suggests the C-terminus of the Brca1 Δ11 protein is still structurally recognisable by this antibody. This does bring into question the functional nature of Brca1 Δ11 as discussed in the introduction and its use as a Brca1-deficient control.

As previously stated, BRCA1 can form foci that do not represent DNA damage and do no co-localise with γH2AX (Au and Henderson, 2007). To see if the *Brca1* C61G mutation alters these foci, cells from the previously described experiment (n=2, 100 cells from each

experiment) were also counted for the number of Brca1 foci that do not co-localise with γH2AX (Figure 4.13). In the untreated condition, there was a decrease in number of cell with more than three Brca1 foci that do not co-localise with γH2AX in cells without a wild-type *53bp1* and a further decrease in cells with one or two copies of *Brca1* C61G (Figure 4.13). Whilst there is a difference between the number of cells with more than three non-γH2AX co-localising Brca1 foci in these MEFs, it is difficult to say what this means without further investigation into the function behind these Brca1 foci. It can be said that the reduction in these foci is not necessarily caused by the *Brca1* C61G mutation because the *53bp1*$^{+/-}$ *Brca1*$^{+/C61G}$ MEFs have a *Brca1* C61G allele, and has the greatest number of cells with more than three Brca1 non-co-localising foci. It could be speculated that the function behind these Brca1 foci is not affected by the *Brca1* C61G mutation, or is only affected in a *53bp1*-null background.

Due the removal or mutation of two tumour suppressing genes (*53bp1* and *Brca1*), it is important to see if there is an increased level of γH2AX foci in these cells and this represents the level of unrepaired DNA damage in these cells. Cells were either untreated or treated with 5 Gray IR and fixed after 1 hour and stained with for with γH2AX antibody. Figure 4.14a shows the average number of γH2AX foci in each cell of the various genotypes from two experiments each with 100 cells counted. This shows that the number of γH2AX foci in cells without a wild-type copy of *53bp1* is significantly increased. This agrees with previous literature that the removal of *53bp1* causes genome instability (Ward et al., 2003b). This increase is partially alleviated in *53bp1*$^{-/-}$*Brca1*$^{+/C61G}$ MEFs, perhaps due to the reduction in wild-type Brca1 leading to more error-free repair in these cells. The *53bp1*$^{-/-}$*Brca1*$^{C61G/C61G}$ MEFs do appear to have a decrease in γH2AX foci compared to the *53bp1*$^{-/-}$*Brca1*$^{+/C61G}$ MEFs,

but the error bars on the results of these two experiments (n=2) are too great for this to be determined. If this were to be confirmed, this would indicated that the increase in unresolved DNA damage caused by the removal of *53bp1* can be compensated for by the mutation of *Brca1*.

When cells are treated with IR, the DNA damage is greatly increased at the γH2AX stain can appear as foci or as pan staining due to the large number of foci. Due to this, the nuclei of cells can be measured for the intensity of γH2AX stain and compared to an average background level of stain to determine the degree of increase in intensity representing the increase in DNA damage. Figure 4.14b shows the measure of γH2AX intensity in the untreated *Brca1* C61G MEFs and the *Brca1* Δ11 MEFs and figure 4.14c shows the γH2AX intensity in the corresponding IR-treated MEFs. The *Brca1* Δ11 MEFs shows the expected phenotype which is that there is more unresolved DNA damage (γH2AX intensity), in cells with wild-type *53bp1* than without *53bp1*. Figure 4.14b shows that there is a small decrease in γH2AX intensity in cells lacking wild-type *53bp1* and again with one or two *Brca1* C61G alleles. This does not completely correlate with the γH2AX foci count in figure 4.14a in that the $53bp1^{+/-}Brca1^{+/C61G}$ MEFs show less DNA damage than cells without *53bp1*. Due to this and this data being of 100 cells in a single experiment, before any conclusions can be made this could need to be repeated multiple times. Figure 4.14c has the same caveat of needing to be repeated. This figure does show that there is more unresolved DNA damage 1 hour after IR in $53bp1^{-/-}Brca1^{\Delta 11/\Delta 11}$ MEFs than those with *53bp1*, which would agree with 53bp1 being needed for the speedy NHEJ repair. The $53bp1^{-/-}Brca1^{+/+}$ MEFs do show an increase in γH2AX intensity compared to the $53bp1^{+/-}Brca1^{+/C61G}$ MEFs which may be for the same reason. The presence of two *Brca1* C61G mutations appears to alleviate some of the DNA

damage in *53bp1*-null cells, but with the *53bp1*$^{-/-}$*Brca1*$^{+/C61G}$ MEFs having increased levels of γH2AX intensity and the lack of repeats, no conclusions can be formed.

4.9 Discussion

This chapter has shown that the *Brca1* C61G homozygote embryonic lethality can be rescued by the genetic deletion of *53bp1*. The rescuing of the embryonic lethality suggests that the C61G missense mutation causes Brca1 protein to be altered so that it can no longer remove the 53bp1-dependent block in HR, despite the mutation being a single amino acid substitution.

Previous research has suggested that the C61G mutation causes dramatic effects to Brca1 N-terminal structure that can cause the BRCA1 RING domain to become less stable, inactive as an E3 ubiquitin enzyme and be less able to bind to BARD1 (Brzovic *et al*., 1998; Brzovic *et al*., 2001a; Brzovic *et al*., 2003; Choudhury *et al*., 2004; Hashizume *et al*., 2001; Joukov *et al*., 2001; Mallery *et al*., 2002; Morris and Solomon, 2004; Nelson and Holt, 2010; Ruffner *et al*., 2001; Wang *et al*., 2014b; Wu *et al*., 1996). These alterations can change the localisation and degradation of Brca1 protein. The data in this chapter supports that when Brca1 C61G is expressed at endogenous levels, there is less Brca1 C61G protein compared to wild-type Brca1 protein (Figure 4.4), and it is less detectable at sites of DNA damage than Brca1 wild-type protein (Figure 4.12b,c).

The reduction in Brca1 protein in the nucleus (Figure 4.4) and the dramatic reduction of Brca1 C61G-γH2AX foci after IR (Figure 4.12) in the homozygote *Brca1* C61G mice, may cause HR defects and genomic instability that could lead to embryonic lethality. However, this data has shown Brca1 C61G protein and foci are not completely abolished, presenting the

question of whether these DSBs are repaired via HR. These results could suggest that the C61 residue is important for Brca1-dependent DSB repair once it reaches DSBs, perhaps through the maintenance of the N-terminal heterodimer structure with Bard1 or its importance in E3 ubiquitin ligase activity.

It has been reported, and is shown in figure 4.11, that Brca1 Δ11-deleted protein can localise to DSBs and that it may have function as it mimics a naturally occurring isoform of Brca1 (Au and Henderson, 2007; Huber *et al*., 2001). The *Brca1* Δ11-deleted cells also have a milder phenotype compared to *Brca1*-null cells (Section 1.5.3) which suggests that the Brca1 Δ11 protein may be able to compensate for the loss of full-length Brca1. Since codon 61 is in the Exon 11-deleted isoforms, it likely to affect all N-terminal functions of *Brca1* and the *Brca1* C61G mutation may reduce the protein levels of multiple Brca1 isoforms. The *Brca1 C61G* allele may cause a more severe phenotype than *Brca1* Δ11-deleted MEFs that is more like a *Brca1*-null phenotype.

The effect on cytoplasmic and nuclear Brca1 C61G protein levels and its localisation does suggest that the C61G mutation cannot be seen as a mutation that only affects the N-terminal functions of *Brca1* nor as a separation-of-function mutation. Therefore, these MEFs cannot be used to support a function of the E3 ubiquitin ligase activity of Brca1. However, these cells have shown that this *Brca1* N-terminal patient mutation, that does not appear as severe in sequence alteration as a truncating mutation, can have large effects on the Brca1 protein and its regulation.

Chapter 5 – Changes in cellular functions due to the *Brca1* C61G mutation.

5.1 Introduction

In humans, the C61G mutation in a *BRCA1* allele correlates to an increased risk of a person developing breast and ovarian cancer which is more likely to become a cancer that is difficult to treat (Section 1.2.1). This is the driving force behind exploring the effects of this specific mutation to tumourigenesis and cellular responses to chemotherapeutic agents. Many of the chemotherapeutic agents aim to cause large amounts of DNA damage that require BRCA1-dependent homologous recombination (HR) to repair, which is erroneous in *BRCA1*-mutated tumours. This leads to an overwhelming amount of unrepaired DNA damage, causing the cell to die through an inability to divide correctly (mitotic catastrophe) or through apoptosis (programmed cell death).

It has been shown that *BRCA1*-mutated tumours or *BRCA1*-mutated cancer cell lines are sensitive to specific double-strand break (DSB)-inducing agents, such as platinum agents (Cass *et al*., 2003; Tassone *et al*., 2003; Tassone *et al*., 2009) and poly (ADP)-ribose polymerase (PARP) inhibitors (PARPi) (Farmer *et al*., 2005; Fong *et al*., 2009; Turner *et al*., 2008).

BRCA1-mutated cells are sensitive to PARP inhibitors because they take advantage of synthetic lethality (Farmer *et al*., 2005; Fong *et al*., 2009; Lord *et al*., 2008). This is when blockage of several pathways of DNA damage repair causes lethality due to unrepaired DNA lesions. PARP inhibitors block the repair of ssDNA breaks (SSBs) (Gradwohl *et al*., 1990; Ménissier-de Murcia *et al*., 1989; Strom *et al*., 2011) which are converted into DSBs during

replication and are repaired through BRCA1-dependent HR (Liu *et al*., 2008; Satoh and Lindahl, 1992). Therefore when you treat *BRCA1*-mutated tumours with PARP inhibitors, SSBs are not repaired and in replication they become DSBs that cannot be repaired by HR due to the absence of BRCA1. This leaves the naturally occurring DSBs and the PARP inhibitor-induced DSBs (from SSBs) to be repaired through error-prone DSB repair pathways such as non-homologous end-joining (NHEJ). This leads to an overwhelming amount of DNA damage or errors and mutations in the DNA, which can be too many to repair or too damaging for the cell to survive and the cell will undergo apoptosis or mitotic catastrophe.

Platinum agents, such as Cisplatin (Pascoe and Roberts, 1974; Royer-Pokora *et al*., 1981) and Mitomycin C (MMC) (Iyer and Szybalski, 1963), cause DNA crosslinks (or interstrand crosslinks; ICL) that are repaired by the FANC/HR pathway. *BRCA1* mutated cancer cells are sensitive to these agents because mutated BRCA1 is not able to function and repair is impaired (Bhattacharyya *et al*., 2000; Bouwman *et al*., 2010; Bunting *et al*., 2012; Garcia-Higuera *et al*., 2001; Long *et al*., 2014; Sawyer *et al*., 2015). Although it has been shown that the removal of *53bp1* from *Brca1* mutated cells can restore HR (Bouwman *et al*., 2010; Bunting *et al*., 2010; Cao *et al*., 2009), it has also been shown that this does not rescue DNA crosslink repair (Bunting *et al*., 2012), suggesting BRCA1 has a 53bp1-independent role in DNA crosslink repair.

BRCA1 mutated cells can become resistance to platinum-based agents (Fong *et al*., 2010; Rottenberg *et al*., 2008; Taniguchi *et al*., 2003) and in some studies this has been shown to be due to secondary *BRCA1* reversion mutations (Norquist *et al*., 2011; Swisher *et al*., 2008) or wild-type BRCA1 allele overexpression (Husain *et al*., 1998; Johnson *et al*., 2013)

hypothesized to allow functional HR. *BRCA1* mutated cells have also been shown to become insensitive to PARPi's (Rottenberg *et al*., 2008) and in some studies PARPi resistance correlates with resistance to platinum-based drugs (Fong *et al*., 2010; Johnson *et al*., 2013; Norquist *et al*., 2011). Jaspers *et al*, and Oplustilova *et al*, show that the reduction in 53BP1 protein (via shRNA targeting) or mutation in *53BP1*, reduces the sensitivity of *BRCA1* mutated cells to PARPi's (Jaspers *et al*., 2013; Oplustilova *et al*., 2012). Both papers suggest that it is the restoration of HR (shown by Rad51 foci in Jaspers *et al*) that causes this resistance to PARPi treatment (Jaspers *et al*., 2013; Oplustilova *et al*., 2012). In agreement with these papers, Johnson *et al* showed in some ovarian carcinomas that BRCA1 overexpression alongside a reduction in 53BP1 protein confers resistance to platinum-based drugs and PARPi's (Johnson *et al*., 2013).

The development of drug resistance in *BRCA1* mutated cells and the resistance caused by the removal of 53BP1 protein, highlights the need to study how these drugs cause sensitivity in *BRCA1* mutated cells and how 53BP1 can alter these cells' sensitivity to each agent.

It is widely thought that the loss of the wild-type allele of BRCA1 in people who carry a *BRCA1* mutation is the first step in tumourigenesis, but there is more evidence that this may not be the case. Some studies have shown that BRCA1 roles in DNA repair may be impaired by the loss of one BRCA1 allele, called haploinsufficiency (Cousineau and Belmaaza, 2007; Cressman *et al*., 1999b; Ernestos *et al*., 2010; Zhang *et al*., 1998). If *BRCA1* mutations do cause haploinsufficiency, then it is perhaps necessary to look at the processes that happen before a *BRCA1* mutation carrier develops cancer. This chapter will use both heterozygote

and homozygote *Brca1* C61G cells to ascertain if this mutation causes haploinsufficiency in the cells response to DNA-damaging agents in the absence of *53bp1*.

This chapter will also look at the response of *53bp1*$^{-/-}$*Brca1*$^{+/C61G}$ *and 53bp1*$^{-/-}$*Brca1*$^{C61G/C61G}$ cells to DNA-damaging agents that create DSBs in different ways. This will help isolate which Brca1 DNA damage repair roles are independent of 53bp1.

Since the removal of *53bp1* has rescued the embryonic lethality of homozygote *Brca1* C61G mice (Section 4.3), this chapter will also look at whether HR is functional in these mouse embryonic fibroblasts (MEFs) by looking at the formation of Rad51 foci after IR. It will also examine the response of the FANC and HR pathways after MMC in *53bp1*$^{-/-}$*Brca1*$^{C61G/C61G}$ cells, by looking at the formation of FANCD2 foci and Rad51 foci.

5.2 Brca1 C61G sensitivity to DNA-damaging agents

To further investigate if the removal of *53bp1* from *Brca1* C61G mutant mice would also restore DSB repair, the previously described MEFs (Section 4.3) were treated with a range of doses of different DNA-damaging agents and the survival of these cells was measured in a clonogenic survival assay (Section 2.4.8). *Brca1* Δ11 (exon 11-deleted) MEFs, (with or without *53bp1*) were also subjected to the same experiment as a comparison, however, they cannot be directly compared as they have been spontaneously immortalised, unlike the *Large T antigen* immortalised *Brca1* C61G MEFs (Table 4.1).

It is important to note that *53bp1*$^{+/-}$*Brca1*$^{+/C61G}$ MEFs are used to compare with the results of the *53bp1*-null homozygote MEF lines (which have either wild-type *Brca1* alleles, or are heterozygote or homozygote for the *Brca1* C61G mutation), as they possess a single wild-type copy of the *53bp1* and *Brca1* allele and one mutated allele. The literature suggests that

the removal of one copy of wild-type *53bp1* does not cause any sensitivity to DNA-damaging agents (Ward *et al*., 2003b). As for the *Brca1* C61G allele, the *53bp1*-null *Brca1* C61G heterozygote cell line can be used to test for a heterozygote or a haploinsufficient phenotype.

5.2.1 Ionising Radiation

Ionising radiation (IR) produces many types of DNA damage (Painter, 1974) but gamma radiation predominantly causes DSBs (Yamamoto *et al*., 1985). BRCA1 is well known to play multiple roles in the repair of DSBs (Section 1.4.1) and the C61G mutation is thought to alter BRCA1's role in DSB repair (Drost *et al*., 2011; Li and Yu, 2013; Nelson and Holt, 2010) (this is contested by Fan *et al*, (Fan *et al*., 2001b)). The removal of *53bp1* from *Brca1* mutated mice rescues embryonic lethality and the HR repair defect (Bouwman *et al*., 2010; Bunting *et al*., 2010; Bunting *et al*., 2012; Cao *et al*., 2009).

BRCA1 is needed for efficient NHEJ (Bau *et al*., 2004; Bau *et al*., 2006; Coupier *et al*., 2004; Lee *et al*., 2000; Wang *et al*., 2006; Zhong *et al*., 2002b; Zhuang *et al*., 2006) through aiding micro-homology annealing (Zhong *et al*., 2002b) and precise end-joining (Wang *et al*., 2006; Zhuang *et al*., 2006). BRCA1 also has a role in the localisation of NBS1 (Kitagawa *et al*., 2004) and ATM (Wang *et al*., 2006) which is important for NHEJ.

MEFs without a wild-type *53bp1* allele are known to be sensitive to IR because *53bp1* is important for the promotion of NHEJ (Ward *et al*., 2003b) to repair DSBs. As expected, $53bp1^{-/-}Brca1^{+/+}$ and $53bp1^{-/-}Brca1^{+/C61G}$ MEFs show significantly ($p<0.05$) reduced survival after treatment with 3, 5 or 8 Gray of IR (Figure 5.1a) compared to $53bp1^{+/-}Brca1^{+/C61G}$ cells. Cells with two copies of *Brca1* C61G were significantly more sensitive to IR than cells with

one wild-type copy of *Brca1* and one C61G mutated copy of *Brca1* after 3 or 5 Gray of IR, suggesting that the C61G mutation does alter the ability of Brca1 to respond to IR-induced DNA damage, despite the lack of the 53bp1-block on HR. This

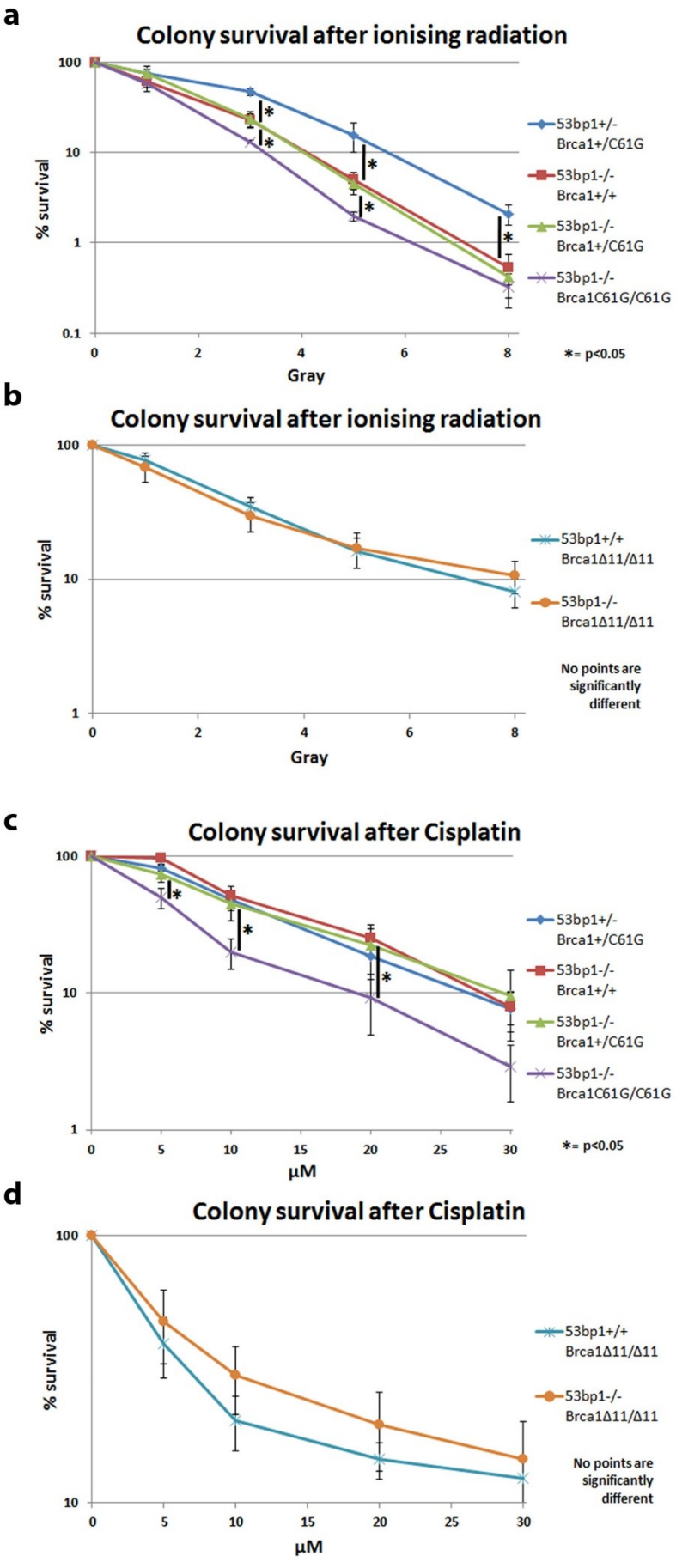
a
Colony survival after ionising radiation
% survival
Gray
53bp1+/- Brca1+/C61G
53bp1-/- Brca1+/+
53bp1-/- Brca1+/C61G
53bp1-/- Brca1C61G/C61G
*= p<0.05
b
Colony survival after ionising radiation
% survival
Gray
53bp1+/+ Brca1Δ11/Δ11
53bp1-/- Brca1Δ11/Δ11
No points are significantly different
c
Colony survival after Cisplatin
% survival
μM
53bp1+/- Brca1+/C61G
53bp1-/- Brca1+/+
53bp1-/- Brca1+/C61G
53bp1-/- Brca1C61G/C61G
*= p<0.05
d
Colony survival after Cisplatin
% survival
μM
53bp1+/+ Brca1Δ11/Δ11
53bp1-/- Brca1Δ11/Δ11
No points are significantly different

Figure 5.1 – Colony survival assays of MEFs after treatment with ionising radiation or Cisplatin
*[a] and [b] are colony survival assay results showing the survival of MEFs after treatment with varying doses of ionising radiation (IR) (0, 1, 3, 5 or 8 Gray) and [c] and [d] are colony survival assay results showing the survival of MEFs after treatment with varying doses of Cisplatin (0, 5μM, 10μM, 20μM and 30μM). The key on the left refers to the point shape and colour that depict each genotype. * represent points that are significantly different from each other (shown by black line) with a p value of <0.05 from a t-test. Error bars show standard error. Results are the average 3 or more separate experiments, each with 3 or more replicates.*

increased sensitivity may not be due to faulty HR but because of BRCA1's role in NHEJ. Both the homozygote *Brca1* Δ11 MEFs, with or without 53bp1 wild-type allele, were equally sensitive to IR (Figure 5.1b) despite of the literature showing that the removal of *53bp1* from the homozygote *Brca1* Δ11 MEFs rescues the sensitivity of DSB-inducing agents (Bouwman *et al*., 2010; Bunting *et al*., 2010).

5.2.2 DNA crosslinking agents

Cisplatin is a DNA crosslinking agent (Pascoe and Roberts, 1974) and BRCA1 has a role in DNA crosslink repair (Bhattacharyya *et al*., 2000; Bouwman *et al*., 2010; Bunting *et al*., 2012; Garcia-Higuera *et al*., 2001; Sawyer *et al*., 2015). It has been shown that *Brca1*-defective cells are sensitive to DNA crosslinks (Bhattacharyya *et al*., 2000; Bouwman *et al*., 2010; Bunting *et al*., 2012; Garcia-Higuera *et al*., 2001; Sawyer *et al*., 2015) and removal of *53bp1* from $Brca1^{\Delta 11/\Delta 11}$ cells, does not rescue this phenotype (Bunting *et al*., 2012). Although a rescue of Cisplatin sensitivity was seen in $53bp1^{-/-}Brca1^{\Delta 5\text{-}13/\Delta 5\text{-}13}$ cells (Bouwman *et al*., 2010).

In alignment with the literature (Mohni *et al*., 2015), figure 5.1c shows there is no difference in sensitivity to Cisplatin in cells without a wild-type copy of *53bp1* and those with ($53bp1^{+/-}Brca1^{+/C61G}$ and $53bp1^{-/-}Brca1^{+/C61G}$), suggesting 53bp1 does not play a role in DNA crosslink repair. Cells with two copies of *Brca1* C61G do show significant ($p<0.05$) sensitivity to

Cisplatin (with doses of 5, 10 or 20μM, suggesting that the C61G mutation does impair the role Brca1 has in DNA crosslink repair. *Brca1* Δ11 MEFs are reported (Bunting *et al*., 2012) to be sensitive to DNA crosslinking agents with or without *53bp1* and figure 5.1d agrees with this finding. Figures 5.1c and d, both show that the removal of *53bp1* does not alter the sensitivity in *Brca1*-mutated cells, suggesting that Brca1's role in DNA crosslink repair is independent of 53bp1.

5.2.3 Topoisomerase inhibitor

Topoisomerase enzymes relieve the stress of overwound DNA by inducing DNA breaks, allowing the DNA to unwind, and then the break is repaired (Poccia *et al*., 1978). Topoisomerase I relieves DNA stress by causing a SSB in the DNA which allows the tension to resolve and then reanneals the break (Liu and Wang, 1979). Camptothecin (CPT) is a topoisomerase I inhibitor which allows topoisomerase I to cause a SSB but does not allow it to anneal (Hsiang *et al*., 1985). It also does not allow topoisomerase I to release the DNA causing a bound complex of CPT, DNA and topoisomerase I (Hsiang *et al*., 1985). In the presence of CPT, topoisomerase I is covalently bound to the 3' end of the SSB that it has created which leave the protein-DNA complex that needs to be cleaved to be resolved (Hsiang *et al*., 1985). CPT is therefore a poison. If these protein-DNA complexes and the involved SSB remain unrepaired, they are converted into DSBs during DNA replication (Liu *et al*., 2008; Satoh and Lindahl, 1992).

Cells with two copies of *Brca1* C61G show significantly ($p<0.05$) reduced survival after CPT treatment (20, 40 or 80μM) than cells with one or two copies of wild-type *Brca1* (Figure 5.2a). This suggests Brca1 has a role in resolving the DNA damage after treatment with CPT.

Cells with one wild-type copy of *53bp1* and one *Brca1* C61G allele appear to be more sensitive to CPT than cells

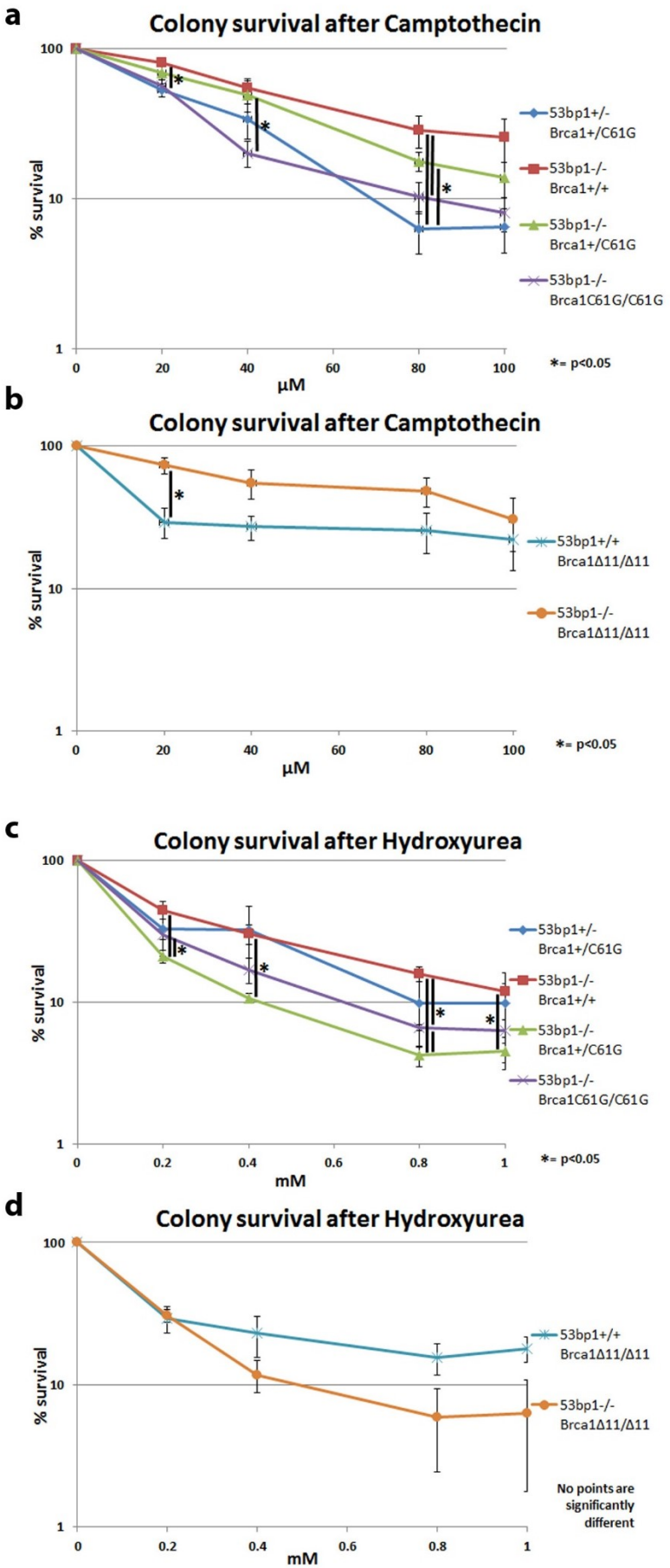
a
Colony survival after Camptothecin
100
10
1
% survival
0
20
40
60
80
100
µM
*
*
*
53bp1+/-
Brca1+/C61G
53bp1-/-
Brca1+/+
53bp1-/-
Brca1+/C61G
53bp1-/-
Brca1C61G/C61G
*= p<0.05
b
Colony survival after Camptothecin
100
10
1
% survival
0
20
40
60
80
100
µM
*
53bp1+/+
Brca1Δ11/Δ11
53bp1-/-
Brca1Δ11/Δ11
*= p<0.05
c
Colony survival after Hydroxyurea
100
10
1
% survival
0
0.2
0.4
0.6
0.8
1
mM
*
*
*
*
53bp1+/-
Brca1+/C61G
53bp1-/-
Brca1+/+
53bp1-/-
Brca1+/C61G
53bp1-/-
Brca1C61G/C61G
*= p<0.05
d
Colony survival after Hydroxyurea
100
10
1
% survival
0
0.2
0.4
0.6
0.8
1
mM
53bp1+/+
Brca1Δ11/Δ11
53bp1-/-
Brca1Δ11/Δ11
No points are
significantly
different

Figure 5.2 – Colony survival assays of MEFs after treatment with Camptothecin or Hydroxyurea
*[a] and [b] are colony survival assay results showing the survival of MEFs after 16 hours of treatment with varying doses of Camptothecin (0, 20μM, 40μM, 80μM and 100μM) and [c] and [d] are colony survival assay results showing the survival of MEFs after 16 hours of treatment with varying doses of Hydroxyurea (0, 0.2mM, 0.4mM, 0.8mM and 1mM). The key on the left refers to the point shape and colour that depict each genotype. * represent points that are significantly difference from each other (shown by black line) with a p value of <0.05 from a t-test. Error bars show standard error. Results are the average 3 or more separate experiments, each with 3 or more replicates.*

without *53bp1* (significantly for doses 20 and 80μM), suggesting 53bp1 hinders the repair of CPT lesions (Figure 5.2a). Previous papers have showed that the removal of 53bp1 (in a wild-type Brca1 cell) can render cells resistant to CPT (Nakamura *et al*., 2006). But other papers have shown that 53bp1 depletion in the U20S cell line to sensitize cells to CPT (Yoo *et al*., 2005). *Brca1* Δ11 cells without *53bp1* are not significantly sensitive to CPT treatment as seen in Bunting *et al* (Bunting *et al*., 2010), but when they do have 53bp1 protein ($53bp1^{+/+}Brca1^{\Delta11/\Delta11}$) they are comparatively more sensitive (Figure 5.2b). Statistical analysis using a t-test showed that only at 20μM did CPT cause a significant difference in sensitivity in the *Brca1* Δ11 MEFs, despite the cell survival difference seen between $53bp1^{+/+}Brca1^{\Delta11/\Delta11}$ and $53bp1^{-/-}Brca1^{\Delta11/\Delta11}$ MEFs at higher doses of CPT. This agrees with the result that 53bp1 has a role in antagonising the repair of CPT-induced DNA damage.

5.2.4 DNA replication stress-inducing agents

Replication stress can be induced when the ribonucleotide reductase enzyme (RNR) is inhibited and nucleotides are not available for replication to continue (Levenson and Hamlin, 1993). This leads to replication fork stalling which, after a period of time, leads to replication forks collapsing into DSBs (Saintigny *et al*., 2001). Hydroxyurea (HU) is a RNR inhibitor (Sinha and Snustad, 1972) which temporarily stalls replication forks that can be restarted if HU is

removed, or become DSBs if HU is present for an extended period of time, such as 16 hours (Saintigny *et al*., 2001).

53bp1-null cells containing one or two copies of *Brca1* C61G show a reduced cell survival after a 16 hour treatment of HU (*53bp1*$^{-/-}$*Brca1*$^{+/C61G}$- all doses;*53bp1*$^{-/-}$*Brca1*$^{C61G/C61G}$- 0.8mM only) (Figure 5.2c) compared to cells with only wild-type *Brca1*. *53bp1*$^{+/-}$*Brca1*$^{+/C61G}$ cells shows a variable intermediate phenotype and *53bp1*$^{-/-}$*Brca1*$^{+/C61G}$ cells are significantly more sensitive to HU than cells with two copies of *Brca1* C61G at doses 0.2 and 0.8mM. This may suggest that a single copy of *Brca1* C61G does alter the resolution of HU-induced DSBs which is enhanced by the removal of *53bp1*. Supporting this, the removal of *53bp1* has been shown to sensitise cells to HU (Tripathi *et al*., 2007). However, this does not help explain why cells with no wild- type *53bp1* and two copies of *Brca1* C61G are not as sensitive as *53bp1*$^{-/-}$ *Brca1*$^{+/C61G}$ cells. This could be further supported by the use of other replication stress-inducing agents, to look for similar results. *Brca1* Δ11 cells show greater sensitivity to HU when *53bp1* is removed in figure 5.2d, which agrees with figure 5.2c that the lack of *53bp1* does make *Brca1*-mutated cells more sensitive to HU-induced DNA damage.

5.2.5 PARP inhibitors

PARPi's target poly (ADP)-ribose polymerase (PARP) enzyme which is important for the creation of PAR chains at sites of single-strand breaks (Altmeyer *et al*., 2009). These chains lead to the correct recruitment of repair proteins to ensure the single-strand breaks are repaired (Gradwohl *et al*., 1990; Ménissier-de Murcia *et al*., 1989; Strom *et al*., 2011); otherwise single-strand breaks will become a double-strand break during replication (Liu *et*

al., 2008; Satoh and Lindahl, 1992). PARPi's have been used to overburden *BRCA1* and *BRCA2*-mutated cancer cells with DSBs which they cannot repair because of the BRCA defect,

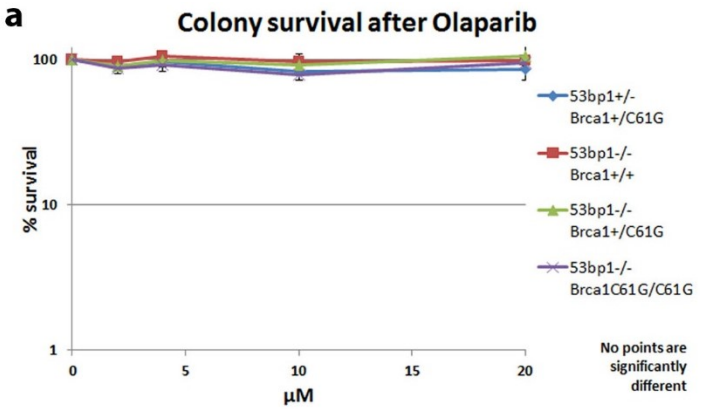
a
Colony survival after Olaparib
100
10
1
% survival
0
5
10
15
20
µM
53bp1+/-
Brca1+/C61G
53bp1-/-
Brca1+/+
53bp1-/-
Brca1+/C61G
53bp1-/-
Brca1C61G/C61G
No points are
significantly
different

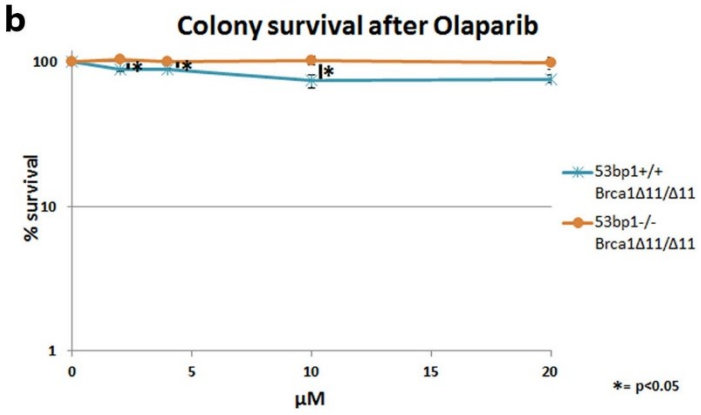
b
Colony survival after Olaparib
100
10
1
% survival
0
5
10
15
20
µM
*
*
*
53bp1+/+
Brca1Δ11/Δ11
53bp1-/-
Brca1Δ11/Δ11
*= p<0.05

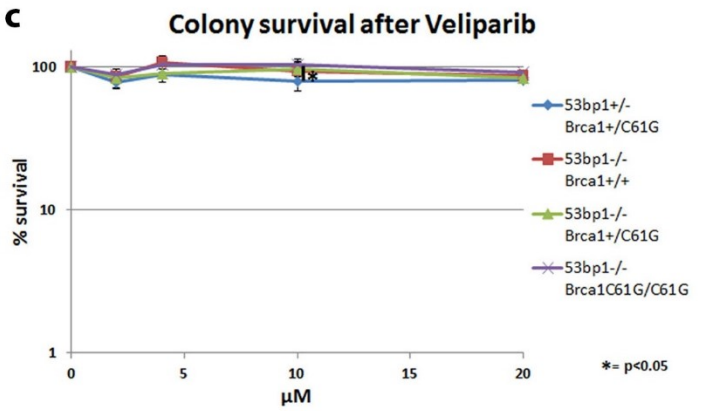
c
Colony survival after Veliparib
100
10
1
% survival
0
5
10
15
20
µM
*
53bp1+/-
Brca1+/C61G
53bp1-/-
Brca1+/+
53bp1-/-
Brca1+/C61G
53bp1-/-
Brca1C61G/C61G
*= p<0.05

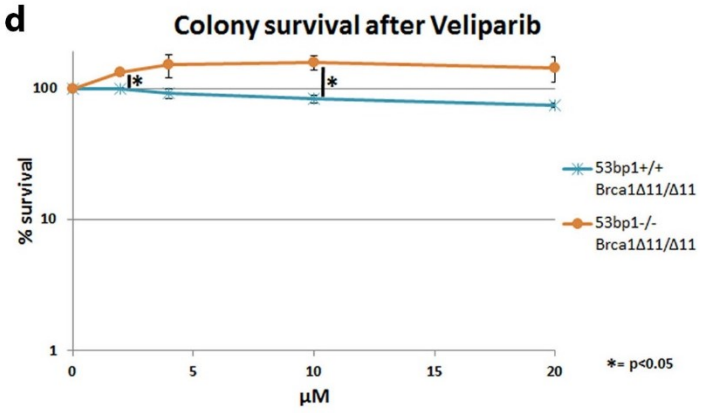
d
Colony survival after Veliparib
100
10
1
% survival
0
5
10
15
20
µM
*
*
53bp1+/+
Brca1Δ11/Δ11
53bp1-/-
Brca1Δ11/Δ11
*= p<0.05

Figure 5.3 – Colony survival assays of MEFs after treatment with Olaparib or Veliparib
*[a] and [b] are colony survival assay results showing the survival of MEFs after 2 hours of treatment with varying doses of Olaparib (0, 2μM, 4μM, 10μM and 20μM) and [c] and [d] are colony survival assay results showing the survival of MEFs after 2 hours of treatment with varying doses of Veliparib (0, 2μM, 4μM, 10μM and 20μM). The key on the left refers to the point shape and colour that depict each genotype. * represent points that are significantly different from each other (shown by black line) with a p value of <0.05 from a t-test. Error bars show standard error. Results are the average 3 or more separate experiments, each with 3 or more replicates.*

therefore cells die (through apoptosis or mitotic catastrophe) (Bryant *et al*., 2005; Farmer *et al*., 2005). Olaparib and Veliparib are both PARPi's but they have slightly different results in the lesion that is created on the DNA (Murai *et al*., 2012). Both Olaparib and Veliparib inhibit PARP which hinders single-strand break repair, but they have the potential to stabilise the PARPi/PARP/DNA complex (Murai *et al*., 2012). Veliparib creates a weaker DNA/PARP complex than Olaparib, and falls off the DNA readily (Murai *et al*., 2012), leaving the single-strand break unrepaired. Olaparib does not disassociated with the DNA/PARP complex easily. This action by Olaparib creates a lesion on the DNA that needs to be removed before the DNA damage can be repaired, making Olaparib a poison. Any single-strand break that is not repaired is converted to a DSB during replication. Due to the difference in Olaparib and Veliparib potency, more Veliparib is needed to produce the same PAR reduction than Olaparib (Murai *et al*., 2012).

Cells with functional HR DSB repair are not sensitive to PARPi's as when the SSBs are converted into DSBs they are repaired efficiently. If the cell is HR-defective (such as a homozygote *Brca1* mutation) than the DSBs created in replication will be repaired by a less error-free repair pathways (i.e. NHEJ) which will lead to unrepaired DNA or mutated DNA. In cells that have a wild-type copy of *Brca1* and *53bp1* (*53bp1*$^{+/-}$*Brca1*$^{+/C61G}$ MEFs), HR repair will not be defective and therefore will not be sensitive to PARPi's.

Previous papers (Bunting *et al*., 2010; Bunting *et al*., 2012) have reported that *53bp1* removal from *Brca1*-mutated cells renders resistance to PARPi, and 53bp1 loss is seen in some PARPi resistance *Brca1*-mutated mouse tumours (Jaspers *et al*., 2013; Johnson *et al*., 2013).

Figure 5.3a shows that there is no significant reduction in cell survival after Olaparib treatment between MEFs carrying one or two copies of the *Brca1* C61G allele and MEFs with only wild-type *Brca1*. *Brca1* C61G homozygote MEFs that have intact *53bp1* are needed to determine if the *Brca1* C61G does cause sensitivity to PARP inhibitors. From this experiment it cannot be said if the removal of *53bp1* plays a role in PARP sensitivity in *Brca1* C61G-mutated cells. Neither the $53bp1^{-/-}Brca1^{\Delta11/\Delta11}$ MEFs, nor the $53bp1^{+/+}Brca1^{\Delta11/\Delta11}$ cells show any sensitivity to Olaparib, despite there being a statistically significant difference in colony number after treatment. Bunting *et al* (Bunting *et al*., 2010), showed that *Brca1* Δ11 homozygote cells were sensitive to the PARPi Ku58948, and that the removal of *53bp1* alleles from homozygote *Brca1* Δ11 MEFs reduced this sensitivity. Figure 5.3b does not show an increase sensitivity in $53bp1^{+/+}Brca1^{\Delta11/\Delta11}$ MEFs to Olaparib which does not replicate the sensitivity to PARPi using these MEFs in Bunting *et al* (Bunting *et al*., 2010).

Figure 5.3c shows no difference in sensitivity between $53bp1^{-/-}Brca1^{C61G/C61G}$ cells and $53bp1^{+/-}Brca1^{+/C61G}$ cells after Veliparib treatment. The only significantly different data point ($p<0.05$) between these cells is at 10μM of Veliparib but this small difference is unlikely to convey any functional significance between the genotypes. *Brca1* Δ11 cells with *53bp1* also lack sensitivity to Veliparib but cells without *53bp1* appear to have a small growth advantage (due to their being more growth than untreated cells) (Figure 5.3d). Although there are

significant data points, this data is unlikely to be functionally relevant and would need to be repeated with various clones of each genotype and several PARP inhibitors with similar properties as Veliparib, before it can be said to show a functional growth advantage.

Brca1 Δ11 homozygote MEFs show no sensitivity to Olaparib and Veliparib despite Bunting *et al* papers (Bunting *et al*., 2010; Bunting *et al*., 2012) showing *Brca1* Δ11 MEFs are sensitive to the PARP inhibitor Ku58948 and this sensitivity can be rescued by the removal of *53bp1*. One reason for this difference may be that Ku58948 have slightly different activities to Olaparib and Veliparib. Another reason could be that the *Brca1* Δ11 MEFs have acquired unknown mutations during culture that have altered their sensitivity to PARP inhibitors. This could be determined by using multiple early passage clones from the cell line or a MEF line from a genetically identical embryo.

Unfortunately the results in this section cannot determine if *Brca1* C61G does cause sensitivity to PARP inhibitors as there isn't a *53bp1* wild-type *Brca1* C61G homozygote control MEF line. It is important to note that the PARPi's were confirmed to be active because other members of the lab were using the stocks at the same time and getting positive sensitivity data. These results have also not been able to replicate previous PARP sensitivity seen in the *Brca1* Δ11 homozygote cells. Therefore more experiments using multiple clones and *53bp1*-reconsituted *Brca1* C61G homozygote MEFs are needed to investigate the role of *53bp1* removal on *Brca1* C61G MEFs.

5.3 IR-induced Rad51 foci and HR

As discussed in the introduction (Section 1.4.1), Rad51 localises to the sites of resected DNA that is coated in pRPA, where it displaces the RPA and directly connects with the single-

stranded DNA (Sung and Robberson, 1995). Rad51 polymers provide a filament that can find regions of homology on a sister chromatid to use as a template for the replication across the

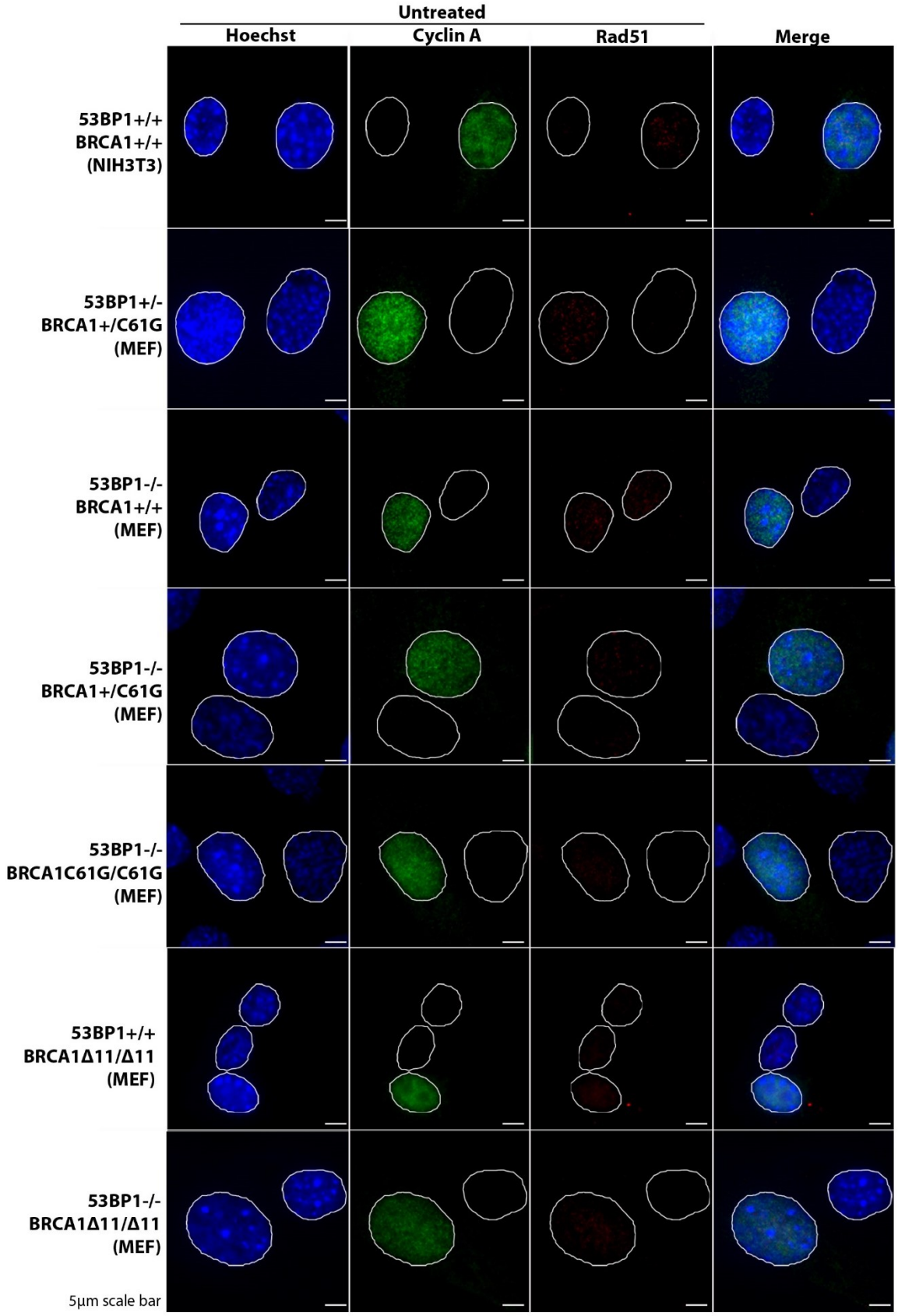

Figure 5.4 – Untreated MEFs stained for Rad51 foci

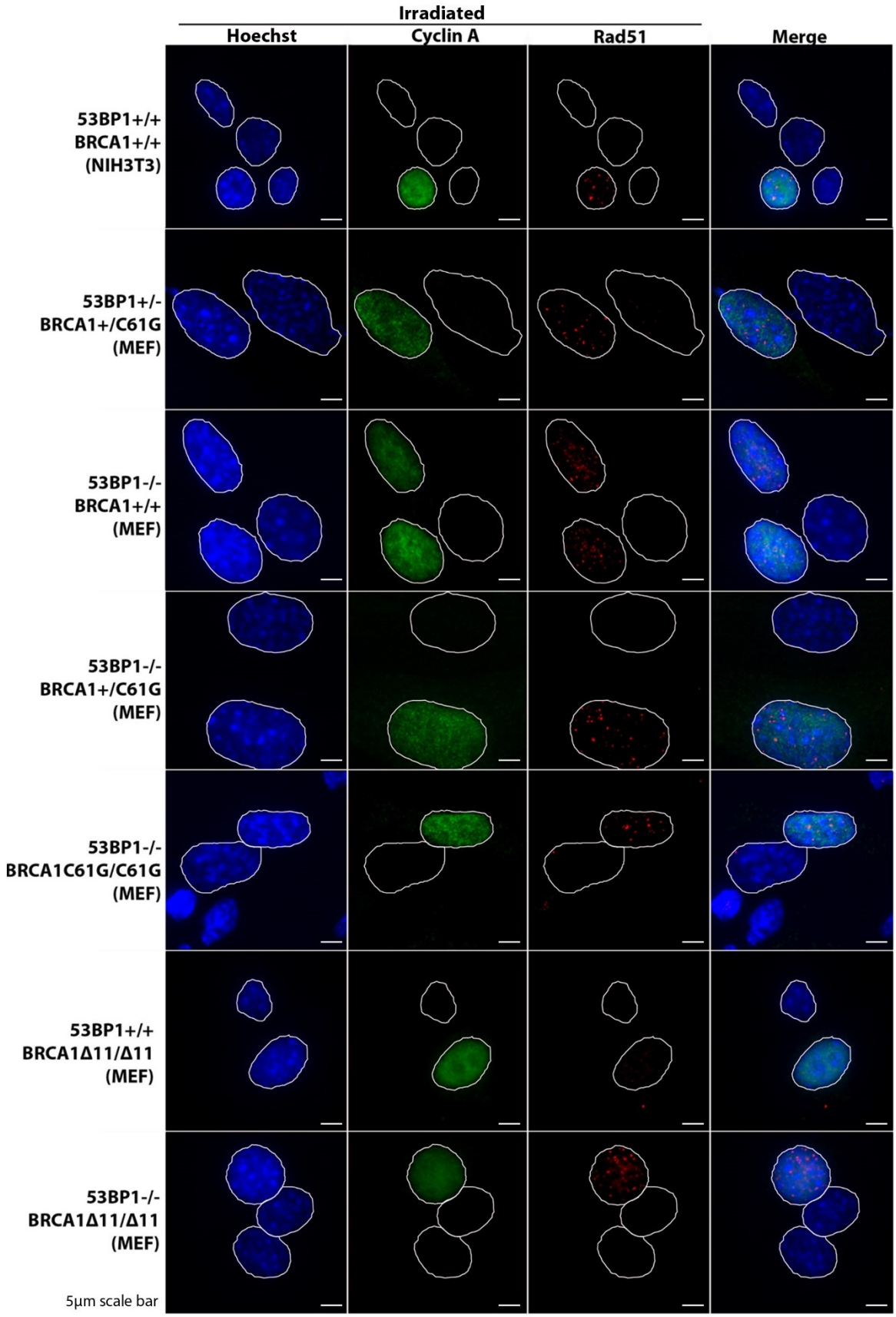

Figure 5.5 – Ionising radiation treated MEFs stained for Rad51 foci

Figure 5.4 – Untreated MEFs stained for Rad51 foci
This figure shows a panel of images of untreated cells stained to show the nucleus (Hoechst-blue), Cyclin A (green) and Rad51 foci (red). The genotype of the MEFs are stated on the left of the row and the final images on the row (far right) are a merged image of all stains (MERGE). White lines outline the nucleus of the cells. Scale bar is 5µm.

Figure 5.5 – Ionising radiation treated MEFs stained for Rad51 foci
This figure shows a panel of images of cells treated with 5 Gray of ionising radiation and fixed 4 hours post-IR. They were then stained to show the nucleus (Hoechst-blue), Cyclin A (green) and Rad51 foci (red). The genotype of the MEFs are stated on the left of the row and the final images on the row (far right) are a merged image of all stains (MERGE). White lines outline the nucleus of the cells. Scale bar is 5µm.

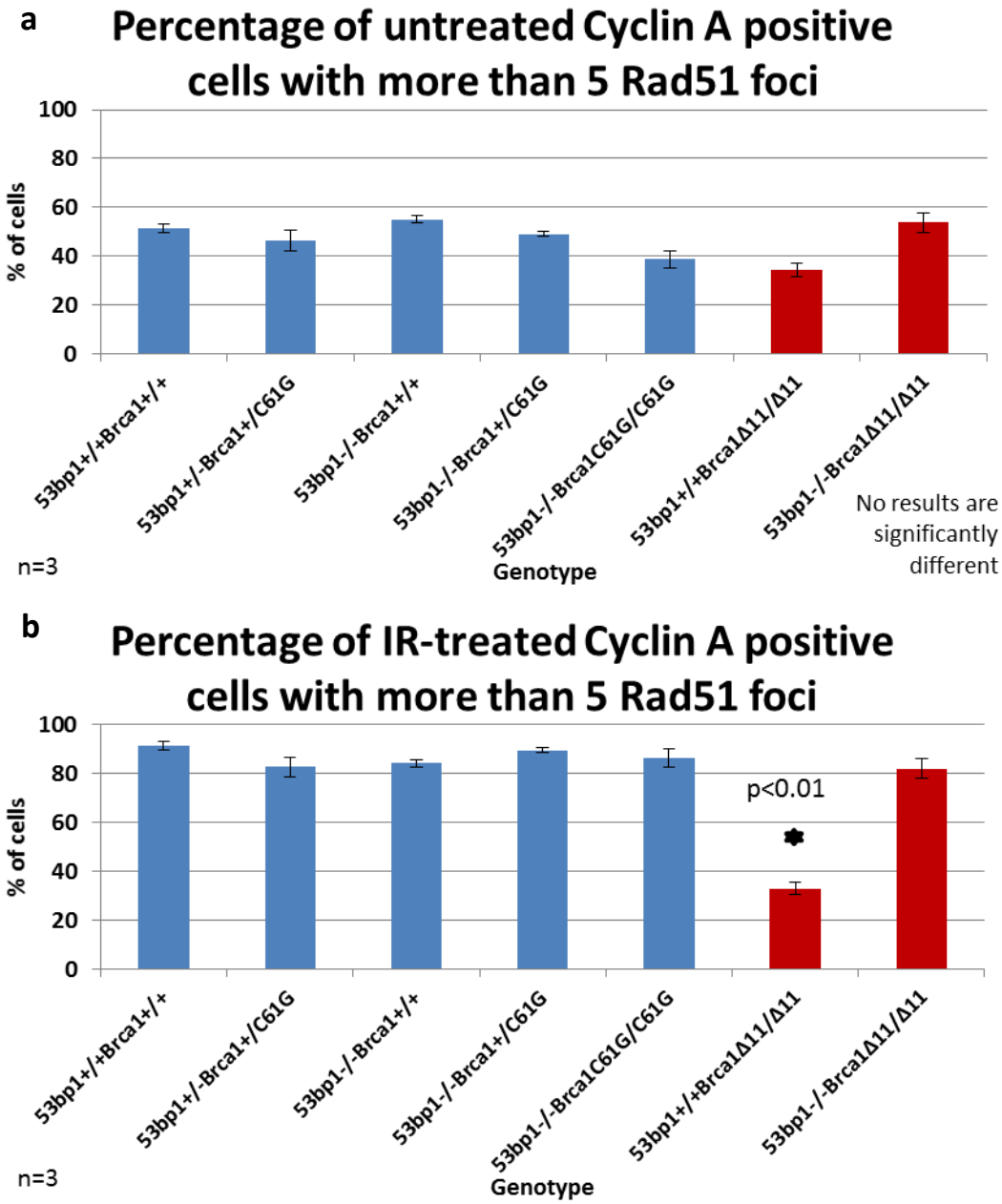

Figure 5.6 – Foci count of Rad51 foci in Cyclin A positive untreated and IR-treated cells
[a] shows the percentage of cells with more than 5 Rad51 foci in Cyclin A positive cells in untreated cells. [b] shows the percentage of cells with more than 5 Rad51 foci in Cyclin A positive cells 4 hour after being treated with ionising radiation. These percentages are from 3 separate experiments in which 100 cells of each condition were analysed. The error bars represent standard error and the asterisks (*) show which data points are significantly different from each other with a p value of less than 0.01 after a t-test (type 2 two-tailed student t-test).

resected DNA (Saleh-Gohari and Helleday, 2004; Sung, 1994). This is a pinnacle step making this type of DSB repair predominantly error-free (Saleh-Gohari and Helleday, 2004). The use of a sister chromatid as a template means cells must be in S or G2 phase to perform HR (Saleh-Gohari and Helleday, 2004).

Rad51 is used as a marker to show that HR is induced and Rad51 foci formation is defective in many HR protein-mutated cells (Bhattacharyya *et al*., 2000; Digweed *et al*., 2002; Godthelp *et al*., 2002; O'Regan *et al*., 2001; Yuan *et al*., 1999). It is important to note that although Rad51 is downstream of proteins that are important for HR, it is not the final step. Rad51 foci do not indicate successful ligation of the DSB DNA strands or if the DSB repair was error-free. Figures 5.4 and 5.5 are of MEFs that were either untreated or exposed to 5 Gray of IR, and fixed after 4 hours. The cells were permeablised (See methods section 2.4.7) and stained for Cyclin A (green), Rad51 (red) and DNA (Hoechst-blue). Cells that positively stain for Cyclin A are in S or G2 phase of the cell cycle (Carbonaro-Hall *et al*., 1993), where HR is possible due to the presence of a sister chromatid. The untreated MEFs (Figure 5.4) show a low level of Rad51 foci in Cyclin A-positive cells. There is a dramatic increase of bright Rad51 foci in Cyclin A-positive cells in MEFs treated with IR (Figure 5.5). To quantify this further, the Rad51 foci in 100 Cyclin A-positive cells of each IR treated condition were counted from three separate experiments.

Figure 5.6a shows there is no significant difference between genotypes in the number of Cyclin A positive cells with more than 5 Rad51 foci. This is likely due to there being no defect of Rad51 foci in cells with the low level of spontaneous DNA damage caused by any of the Brca1 mutations. Figure 5.6b shows that there was no significant difference in the number of

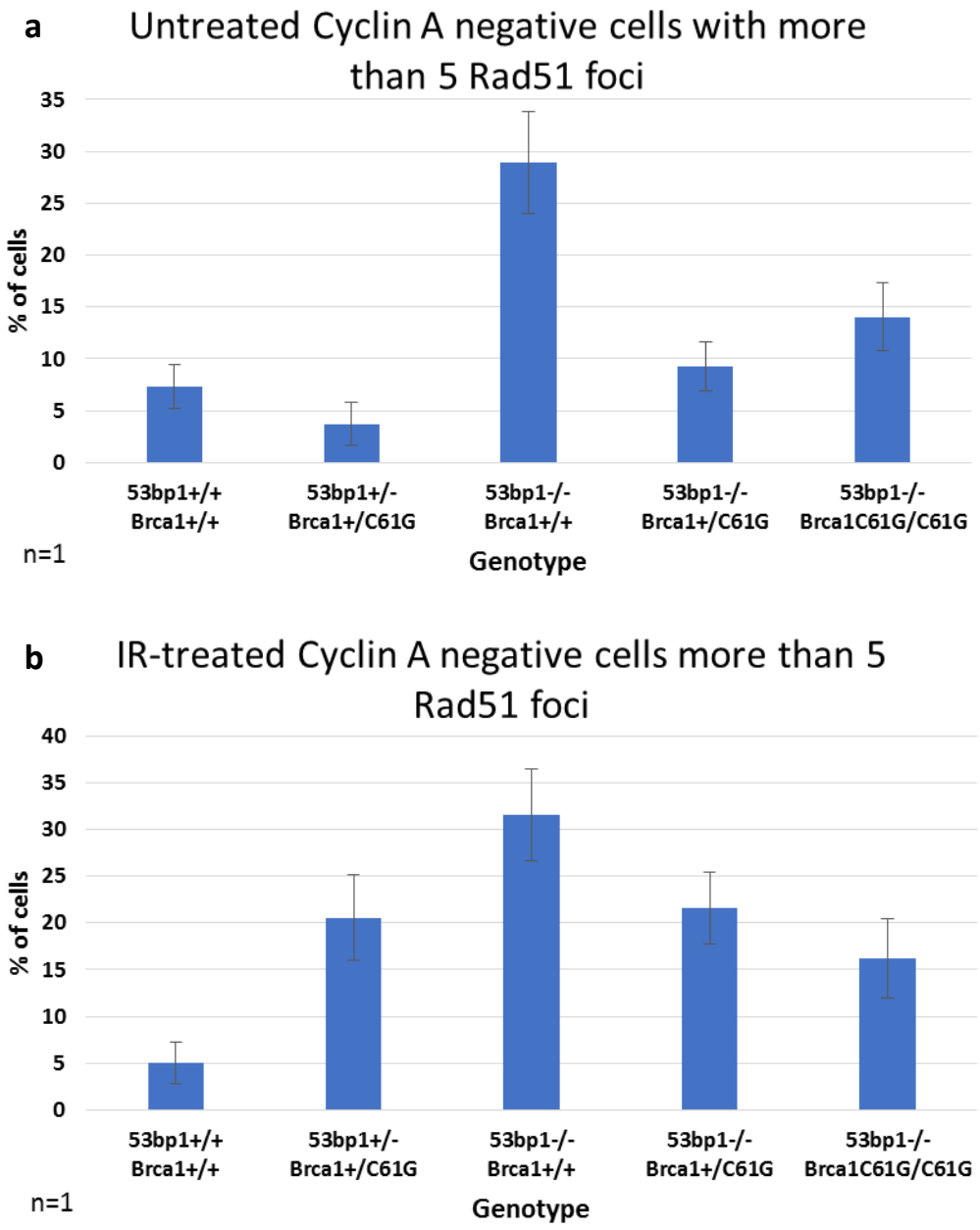

Figure 5.7 – Foci count of Rad51 foci in Cyclin A negative untreated and IR-treated cells
[a] shows the percentage of cells with more than 5 Rad51 foci in Cyclin A negative cells in untreated cells. [b] shows the percentage of cells with more than 5 Rad51 foci in Cyclin A positive cells 4 hours after being treated with ionising radiation. These are results from a single experiment and the error bars show standard deviation.

foci in MEFs with one or two copies of *Brca1* C61G. The lack of *53bp1* does appear to affect the number of Rad51 foci. *53bp1*$^{+/+}$*Brca1*$^{\Delta 11/\Delta 11}$ MEFs show a significant decrease ($p<0.01$) in the levels of Rad51 foci but the removal of *53bp1* (*53bp1*$^{-/-}$*Brca1*$^{\Delta 11/\Delta 11}$) increases the number of Rad51 foci, which agrees with the previous paper (Bouwman *et al*., 2010) . This rescue suggests that the removal of *53bp1* in *Brca1* Δ11 mutated cells restores the ability of HR to progress to form Rad51 foci because *53bp1* is absent as an antagonist to DSB end resection. The similar level of Rad51 foci in *53bp1*$^{-/-}$*Brca1*$^{C61G/C61G}$ cells to *53bp1*$^{+/-}$*Brca1*$^{+/C61G}$ cells would suggest that HR is functional up to the point of Rad51 foci production in these cells. Drost *et al* (Drost *et al*., 2011), use a HR assay to show that the *Brca1* C61G mutation does reduce the levels of HR, but the *Brca1* C61G mutated tumour cells produced Rad51 foci unlike the *Brca1*-null tumour cells. This brings into question whether the C61G mutation is important for the presence of Rad51 foci, as the tumour cells will have acquired unknown mutations. Unfortunately wild-type *53bp1 Brca1* C61G homozygote cells could not be cultured to examine the Rad51 foci in these cells (neither through isolation of *53bp1*$^{+/+}$*Brca1*$^{C61G/C61G}$ MEFs nor the re-introduction of *53bp1* cDNA).

HR should be only possible in S/G2 phase because cells need a copy of the gene, a sister chromatid, to complete repair and as a result of this, HR is cell cycle controlled. It is possible to see some Rad51 foci in G1 cells due to microhomology repair and/or other functions of Rad51 that cause the formation of foci. Figure 5.7a shows that in untreated Cyclin A negative cells, indicative of G1, there are more cells with more than 5 Rad51 foci in *53bp1*$^{-/-}$ cells than those with a copy of wild-type *Brca1*. This could be an indicator that the removal of *53bp1* increases the ability of HR to be induced in G1. Cells with one or two copies of *Brca1* C61G allele show a reduction in the percentage of cells with more than 5 Rad51 foci compared to

53bp1$^{-/-}$*Brca1*$^{+/+}$ cells. It has been suggested that the mutation of *Brca1* in *53bp1*-null cells can lead to a partial restoration of NHEJ due to the lack of control of DSB repair choice pathway (Bunting et al., 2010). This could be the reason for this difference between the genotypes. Figure 5.7b shows cells in G1 after being treated with 5 Gray of IR that have been counted for the number of Rad51 foci. Again, there is an increase of cells with more than 5 Rad51 foci in *53bp1*$^{-/-}$*Brca1*$^{+/+}$ cells and a reduction with one or two copies of *Brca1* C61G. This is likely to be for the same reasons as the differences in Rad51 foci between genotypes in the untreated MEFs. However, the increase level of cells with more than 5 Rad51 foci in *53bp1*$^{+/-}$*Brca1*$^{+/C61G}$ MEFs could indicate a heterozygote phenotype of a reduced control of DSB repair pathway due to the single mutations in *53bp1* and *Brca1*. Figure 5.7 is based on n=1 data and therefore cannot be tested to see if the differences are significantly different. Therefore the experiment in this figure will need to be repeated for a conclusive result.

As discussed, Rad51 foci do not represent the final completion step of HR and figure 5.1a shows that *Brca1* C61G does cause 53bp1-independent IR sensitivity, which together suggests that the *Brca1* C61G mutation does have a 53bp1-independent role in the repair of DSBs, despite there being no defect in Rad51 foci formation.

5.4 Heterochromatin and BRCA1

BRCA1 is involved in regulating chromatin structure which can be disrupted by *BRCA1*-mutations (Ye *et al*., 2001; Zhu *et al*., 2011). It has been reported to be responsible for both condensation (Zhu *et al*., 2011) and the unfolding of DNA (Ye *et al*., 2001). Condensed regions of chromatin (heterochromatin centres) can be seen using a DNA stain (Hoechst) which are visible in the nuclei of murine cells. *Brca1* loss in mice has shown to reduce the

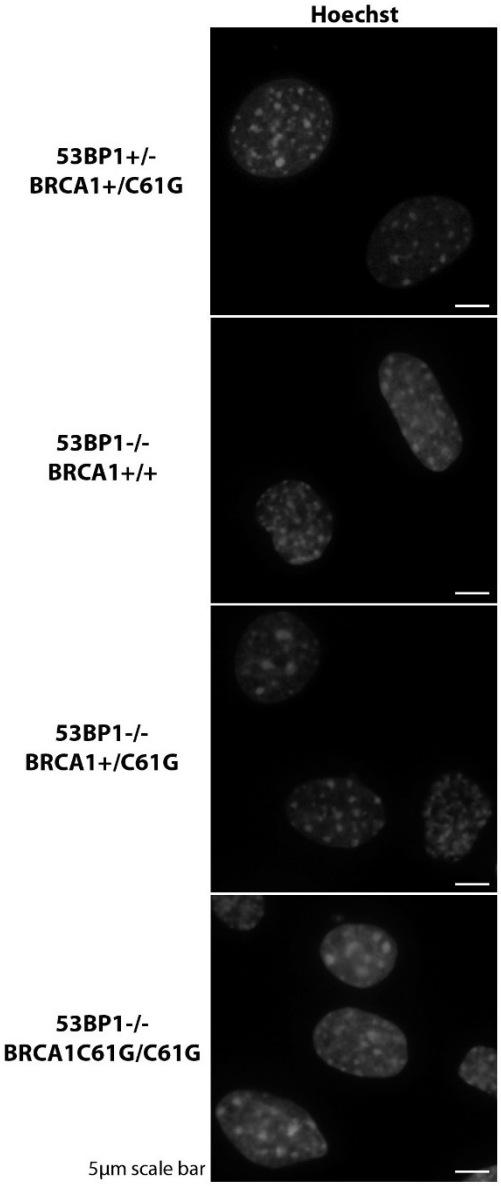

Figure 5.8 – Heterochromatin centres in nuclei
This figure shows untreated MEFs stained with Hoechst. The lighter grey regions show the heterochromatin centres and the darker grey regions in the nucleus represent the less dense chromatin. This is a representative image from 100 cells from a single experiment. Scale bar is 5µm.

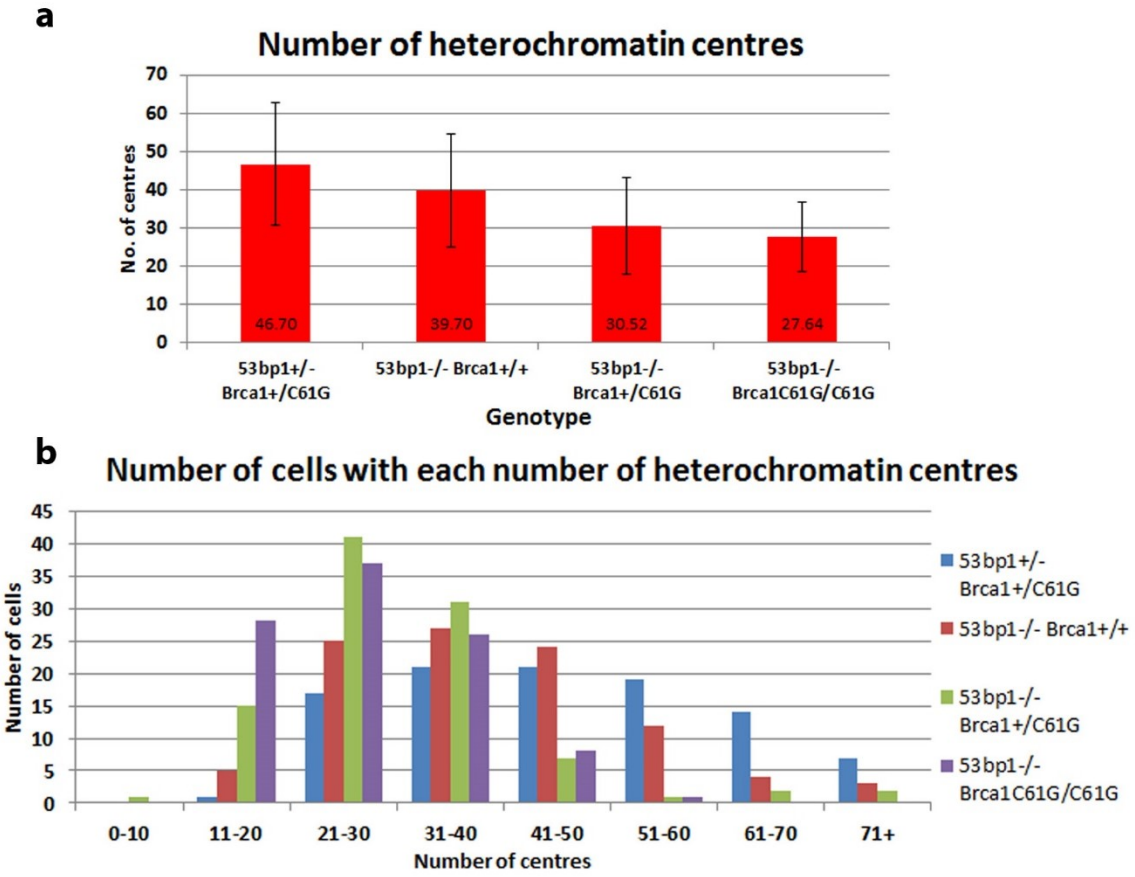

Figure 5.9 – Heterochromatin centre number alterations

[a] shows the average number of heterochromatin centres per cell in MEFs. [b] shows the number of cells with each number of foci in the indicated range. Error bars show the standard deviation. These results were determined through staining the DNA (Hoechst) of untreated MEFs and counting 100 cells from a single experiment.

level of condensation of satellite regions in chromatin resulting in a reduction in heterochromatin centres (Zhu *et al*., 2011). This alteration in condensed regions can alter the regulation and transcription of genes and, in turn, this can cause dramatic effects to the regulation of cellular processes. Zhu *et al*, showed that the deregulation of satellite DNA by the loss of *Brca1* was sufficient to produce Brca1 tumour suppressor-associated defects such as genome instability (Zhu *et al*., 2011). Ye *et al*, show that Brca1 is needed for de-condensation of specific regions of DNA (Ye *et al*., 2001), suggesting that Brca1's function in chromatin organisation may be specific to the region of DNA involved. Figure 5.8 shows MEFs fixed and stained with Hoechst to show the heterochromatin centres and the nucleus of the cells. 100 cells from this single experiment were analysed for the number of heterochromatin centres and these preliminary results are shown in figure 5.9. Figure 5.9a shows the average number of heterochromatin centres per cell in the nucleus for each genotype. Figure 5.9b shows the number of cells containing the number of heterochromatin centres within the stated range. Figure 5.9a shows fewer heterochromatin centres per cell in cells without *53bp1* and with one or two copies of *Brca1* C61G. Figure 5.9b shows that there are more cells within the 11-20, and 21-30 heterochromatin centres per cell range in the MEFs that have one or two copies of *Brca1* C61G and lack *53bp1*. These results could suggest that removal of one or two copies of *Brca1* C61G further reduces the number of heterochromatin centres. This preliminary data could suggest that Brca1 have a role in heterochromatin centre number and that Brca1's role is disrupted by the C61G mutation.

These results are from 100 cells of each condition from a single experiment and therefore would need to be repeated before any conclusions could be made. Also, this data interpretation is difficult as these images were not taken using a confocal microscope, and

therefore the identification of heterochromatin centres throughout the cells is not as precise as on images from a confocal microscope. This could be improved by identification of heterochromatin through an antibody that is more specific to heterochromatin than Hoechst, such as HP1. This experiment would be improved by using a confocal microscope and co-staining with a heterochromatin marker.

5.5 DNA crosslink repair FANCD2 and Rad51 foci

As discussed in the introduction, BRCA1 has been shown to have an HR-independent role in DNA crosslink repair (Bunting *et al*., 2012; Long *et al*., 2014) (Section 1.4.1), which results in cells carrying a mutated *Brca1* allele being sensitive to MMC and Cisplatin (Bhattacharyya *et al*., 2000; Bouwman *et al*., 2010; Bunting *et al*., 2012; Garcia-Higuera *et al*., 2001; Sawyer *et al*., 2015) even after the removal of *53bp1* (Bunting *et al*., 2012) (although Bouwman *et al*, did not see this (Bouwman *et al*., 2010)). BRCA1 is known to be essential for the localisation of ubiquitinated FANCD2 (Bunting *et al*., 2012; Castella *et al*., 2015; Garcia-Higuera *et al*., 2001; Long *et al*., 2014; Vandenberg *et al*., 2003; Yeo *et al*., 2014; Zhang *et al*., 2010) and Rad51 (Bhattacharyya *et al*., 2000; Long *et al*., 2014; Sawyer *et al*., 2015) to sites of DNA crosslinks and DSBs, although BRCA1, Rad51 and FANCD2 do colocalise in the nuclear foci in S phase without cells being treated with DNA-damaging agents (Hussain *et al*., 2004; Long *et al*., 2014; Taniguchi *et al*., 2002).

MMC (Iyer and Szybalski, 1963) and Cisplatin (Pascoe and Roberts, 1974) are both DNA crosslinking agents, but Cisplatin induces intrastrand crosslinks in the DNA at a higher level than interstrand crosslinks (Royer-Pokora *et al*., 1981). Despite this difference MMC and Cisplatin are both used when looking at DNA crosslink repair.

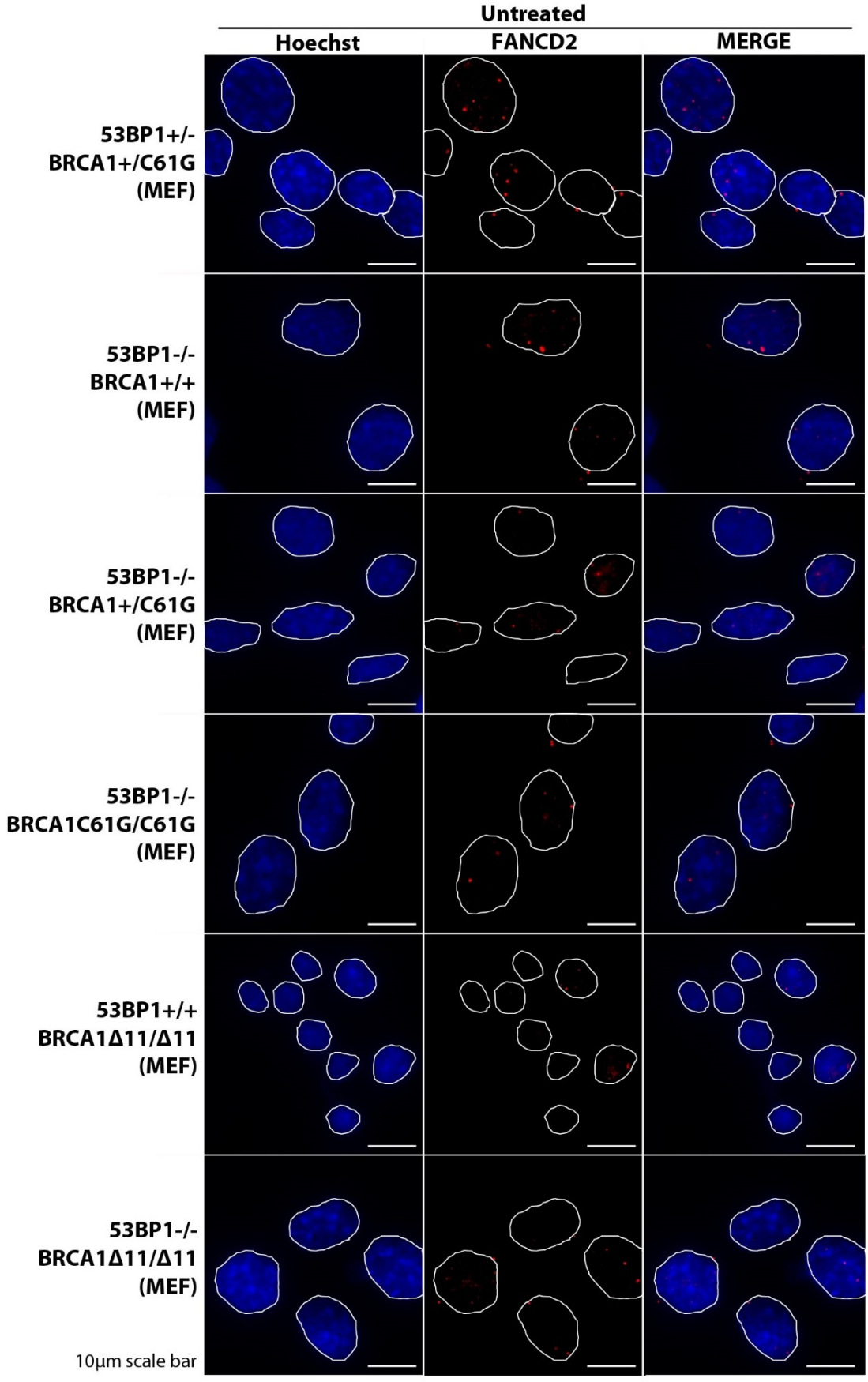

Figure 5.10 – Untreated MEFs stained for FANCD2 foci

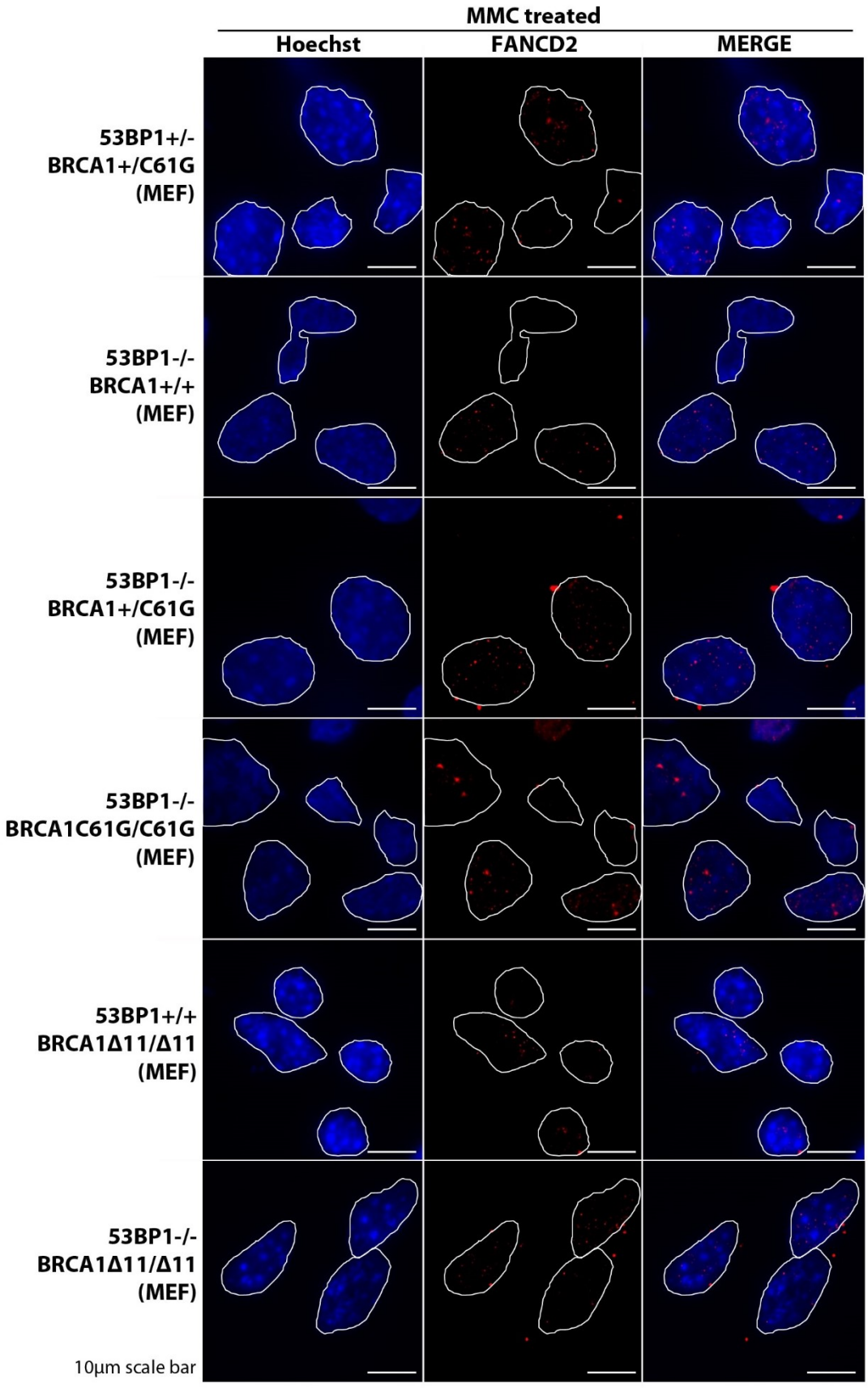

Figure 5.11 – Mitomycin C treated MEFs stained for FANCD2 foci

Figure 5.10 – Untreated MEFs stained for FANCD2 foci

This figure shows a panel of images of untreated cells stained to show the nucleus (Hoechst-blue) and FANCD2 foci (red). The genotype of the MEFs are stated on the left of the row and the final images on the row (far right) are a merged image of all stains (MERGE). White lines outline the nucleus of the cells. Scale bar is 10µm.

Figure 5.11 – Mitomycin C treated MEFs stained for FANCD2 foci

This figure shows a panel of images of cells treated with 250ng/µl of mitomycin C for 24 hours. They were then fixed and stained to show the nucleus (Hoechst-blue) and FANCD2 foci (red). The genotype of the MEFs are stated on the left of the row and the final images on the row (far right) are a merged image of all stains (MERGE). White lines outline the nucleus of the cells. Scale bar is 10µm.

Figure 5.1d shows an equal amount of sensitivity to Cisplatin with or without *53bp1*, in *Brca1*$^{\Delta 11/\Delta 11}$ cells as previously shown in Bunting *et al* (Bunting *et al*., 2012). Figure 5.1c showed that cells without *53bp1* and two copies of the *Brca1* C61G allele, are also sensitive to Cisplatin. To investigate this sensitivity further, cells were treated with MMC (250ng/µl) for 24 hours, and the FANCD2 foci were counted.

In untreated MEFs, there were FANCD2 foci in cells from every genotype (Figure 5.10) and when treated with MMC the number of foci greatly increased (Figure 5.11). The average number of cells with more than 10 FANCD2 foci in untreated and MMC treated cells is displayed in figure 5.12. These averages are from 100 cells counted in each genotype in three separate experiments. There is no significant difference between genotypes in the number of cells with more than 10 FANCD2 foci in untreated MEFs (Figure 5.12a), suggesting that none of the *Brca1* mutations or the lack of *53bp1* causes a defect in spontaneously induced ICL repair, although the levels of damage may be too small to quantify a difference. The *53bp1*$^{+/+}$*Brca1*$^{\Delta 11/\Delta 11}$ cells show a reduced number of cells with more than 10 FANCD2 foci (Figure 5.12b) as seen in Bunting *et al* (Bunting *et al*., 2012), but the removal of *53bp1* shows an increase in this number. This is interesting as in Bunting *et al* (Bunting *et al*., 2012),

they show a small decrease (not significant) in FANCD2 foci in *53bp1*$^{-/-}$*Brca1*$^{\Delta 11/\Delta 11}$ cells compared to *Brca1* Δ11 cells with *53bp1*, but figure 5.12b shows the opposite. It should also be noted that although the Cisplatin sensitivity between these two genotypes is not

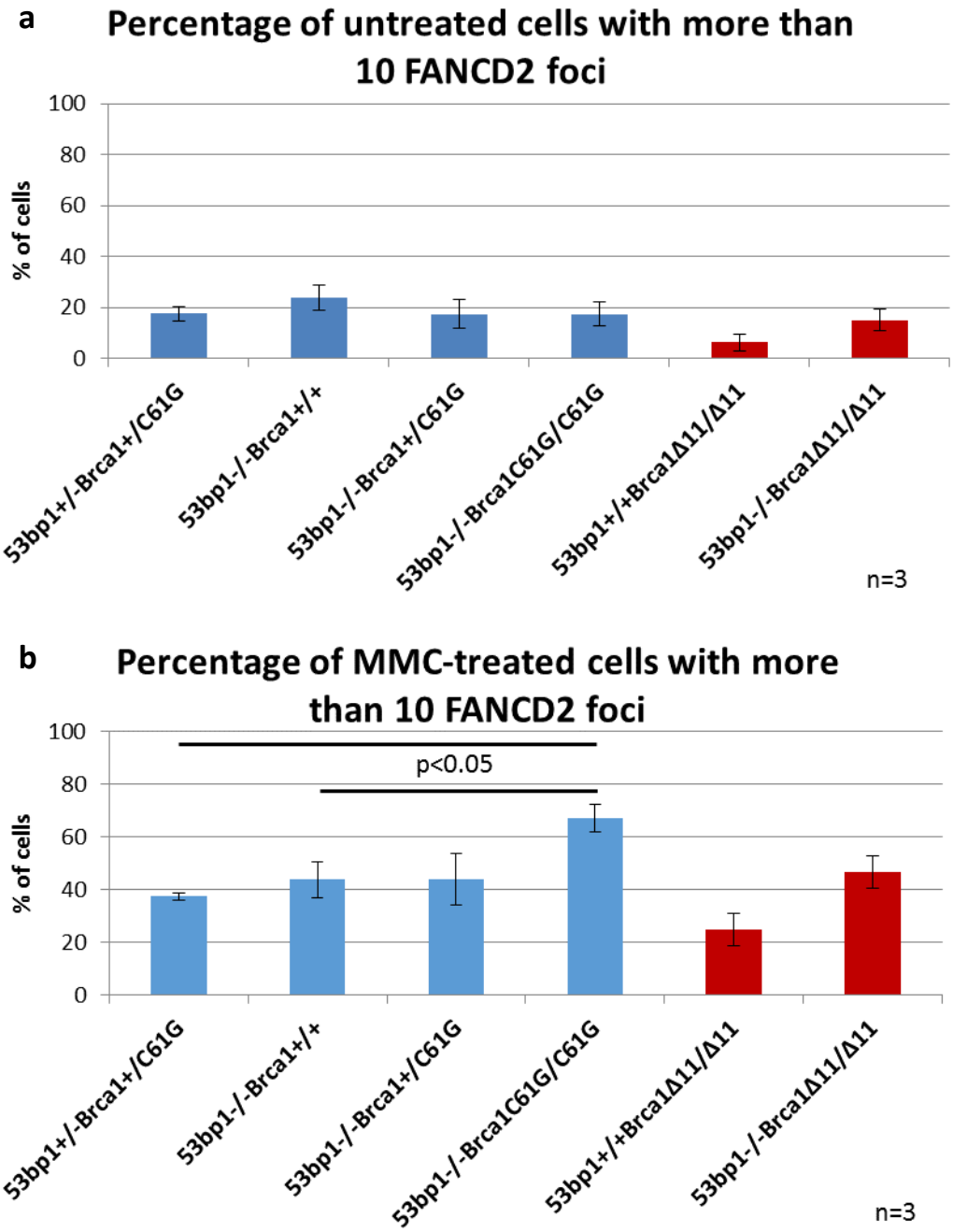

Figure 5.12 – Foci count of FANCD2 foci in untreated and MMC treated MEFs
[a] shows the percentage of cells with more than 10 FANCD2 foci in untreated cells. [b] shows the percentage of cells with more than 10 FANCD2 foci after being treated with 250ng/µl of mitomycin C (MMC) for 24 hours. These percentages are from 3 separate experiments in

which 100 cells of each condition were analysed. The error bars represent standard error and the significant p values from a t-test are indicated (type 2, two-tailed student t-test).

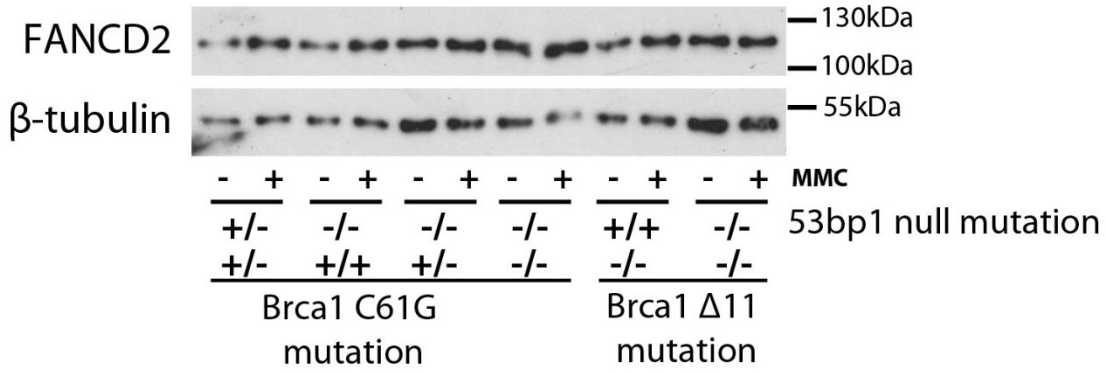

Figure 5.13 – FANCD2 protein levels after MMC treatment in MEFs
This figure shows the western blot depicting the protein levels of FANCD2 and β-tubulin in the MEFs with or without 24 hours of mitomycin C treatment (250ng/µl).

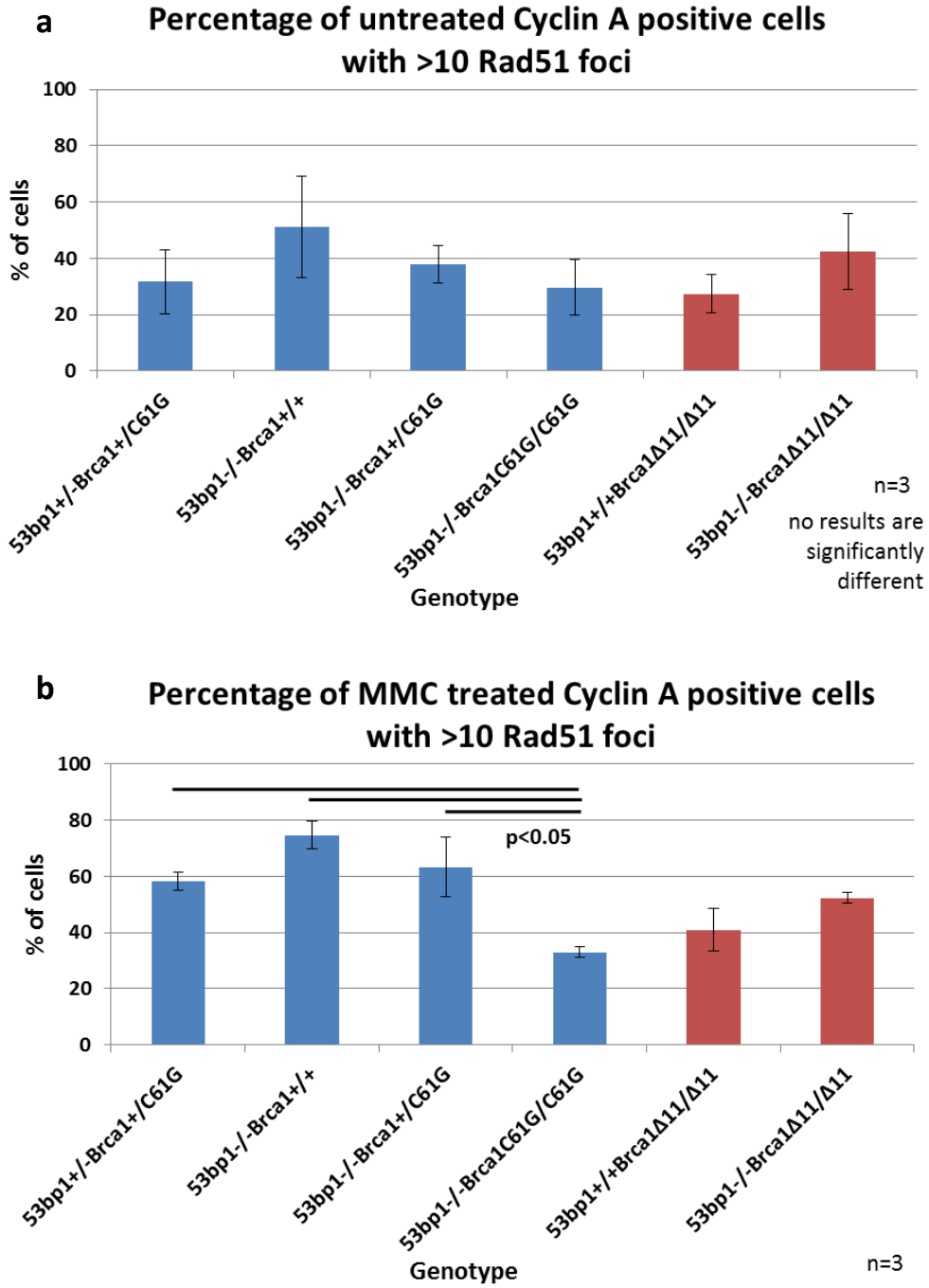

Figure 5.14 – Foci count of Rad51 foci in Cyclin A positive untreated and MMC treated MEFs

[a] shows the percentage of cells with more than 10 Rad51 foci in untreated Cyclin A positive cells. [b] shows the percentage of Cyclin A positive cells with more than 10 FANCD2 foci after being treated with 250ng/µl of mitomycin C (MMC) for 24 hours. These percentages are from 3 separate experiments in which 100 cells of each condition were analysed. The error bars represent standard error and the significant p values from a t-test are indicated (type 2, two-tailed student t-test).

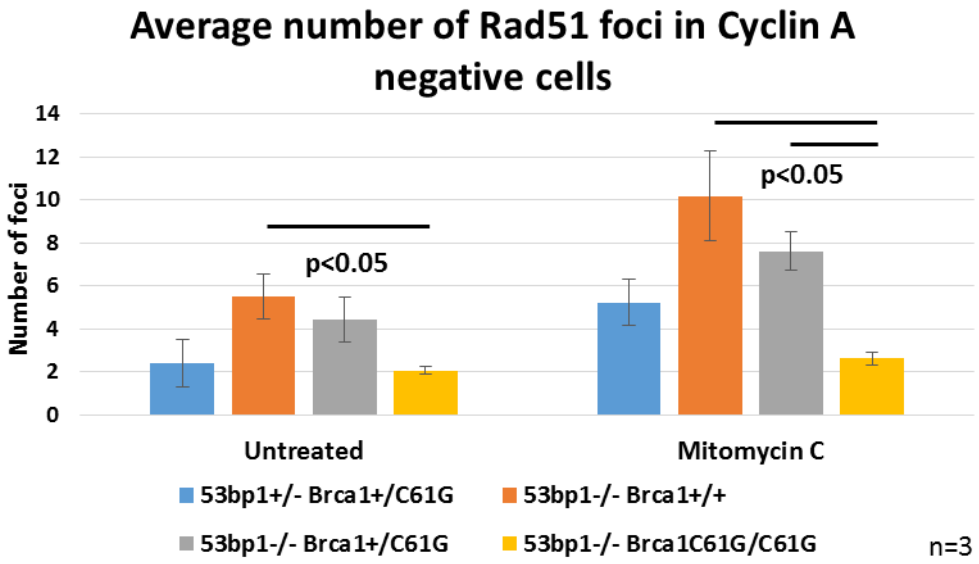

Figure 5.15 – Foci count of Rad51 foci in Cyclin A negative untreated and MMC treated MEFs

This figure shows the average number of Rad51 foci untreated and mitomycin C (MMC) treated Cyclin A negative cells. Treated cells were treated with 250ng/µl of MMC for 24 hours. These percentages are from 3 separate experiments. The error bars represent standard error and the significant p values from a t-test are indicated (type 2, two-tailed student t-test).

significantly different, figure 5.1d does show a small improvement in survival in *53bp1*$^{-/-}$ *Brca1*$^{\Delta 11/\Delta 11}$ cells. The removal of both wild-type copies of *53bp1* does not cause a significant change in the amount of FANCD2 foci (Figure 5.12a) produced after MMC treatment compared to *53bp1*$^{+/-}$*Brca1*$^{+/C61G}$ MEFs. The presence of two copies of the *Brca1* C61G allele does significantly increase (p>0.05) the number of FANCD2 foci after MMC. This almost 2-fold increase has not been reported before with a *BRCA1* mutation. This result could indicate there is reduced repair and clearance of FANCD2 foci. If this is true, then this may indicate a blockage in the DNA crosslink repair response pathway. The increase in FANCD2 foci may be due to an increase in FANCD2 protein levels allowing more sites of DNA damage to have sufficient protein to be visible using immunofluorescence.

Figure 5.13 shows that the levels of FANCD2 are similar across the genotypes suggesting no correlation between *BRCA1* genotype and FANCD2 protein levels. The increase in protein band width in the MMC treated samples is likely to be due to the modified FANCD2 protein that has not resolved into a separate band in this experiment. The amount of ubiquitinated-FANCD2 is known not to be affected by *BRCA1* mutation (Bunting *et al*., 2012; Long *et al*., 2014; Vandenberg *et al*., 2003).

Rad51 foci were counted in 100 cells, from 3 separate experiments, to see if DNA crosslink repair was continuing after the localisation of FANCD2 foci (Figure 5.14). Figure 5.16 shows

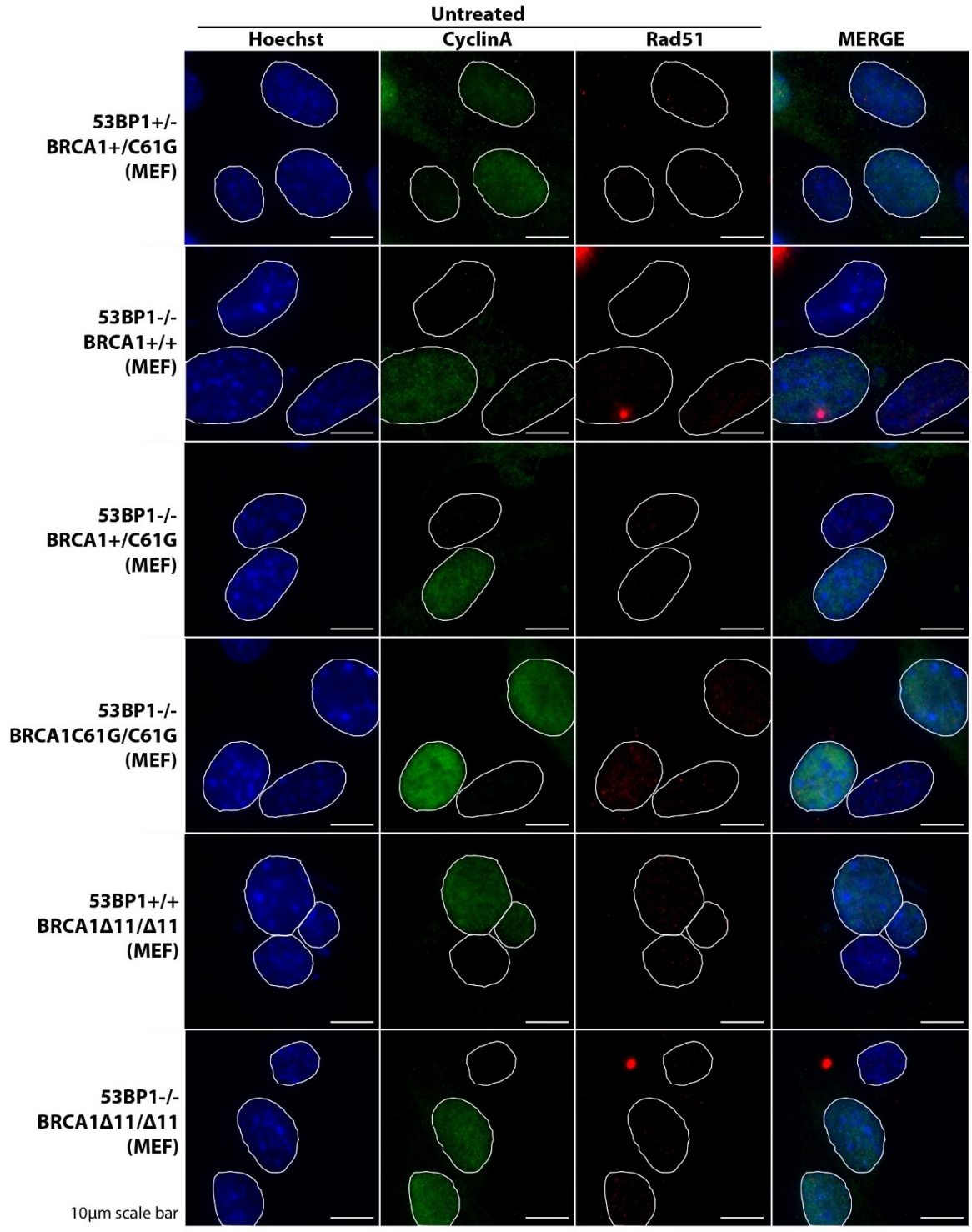

Figure 5.16 – Untreated MEFs stained for Rad51 foci

This figure shows a panel of images of untreated cells stained to show the nucleus (Hoechst-blue), Cyclin A (green) and Rad51 foci (red). The genotype of the MEFs are stated on the left of the row and the final images on the row (far right) are a merged image of all stains (MERGE). White lines outline the nucleus of the cells. Scale bar is 10µm.

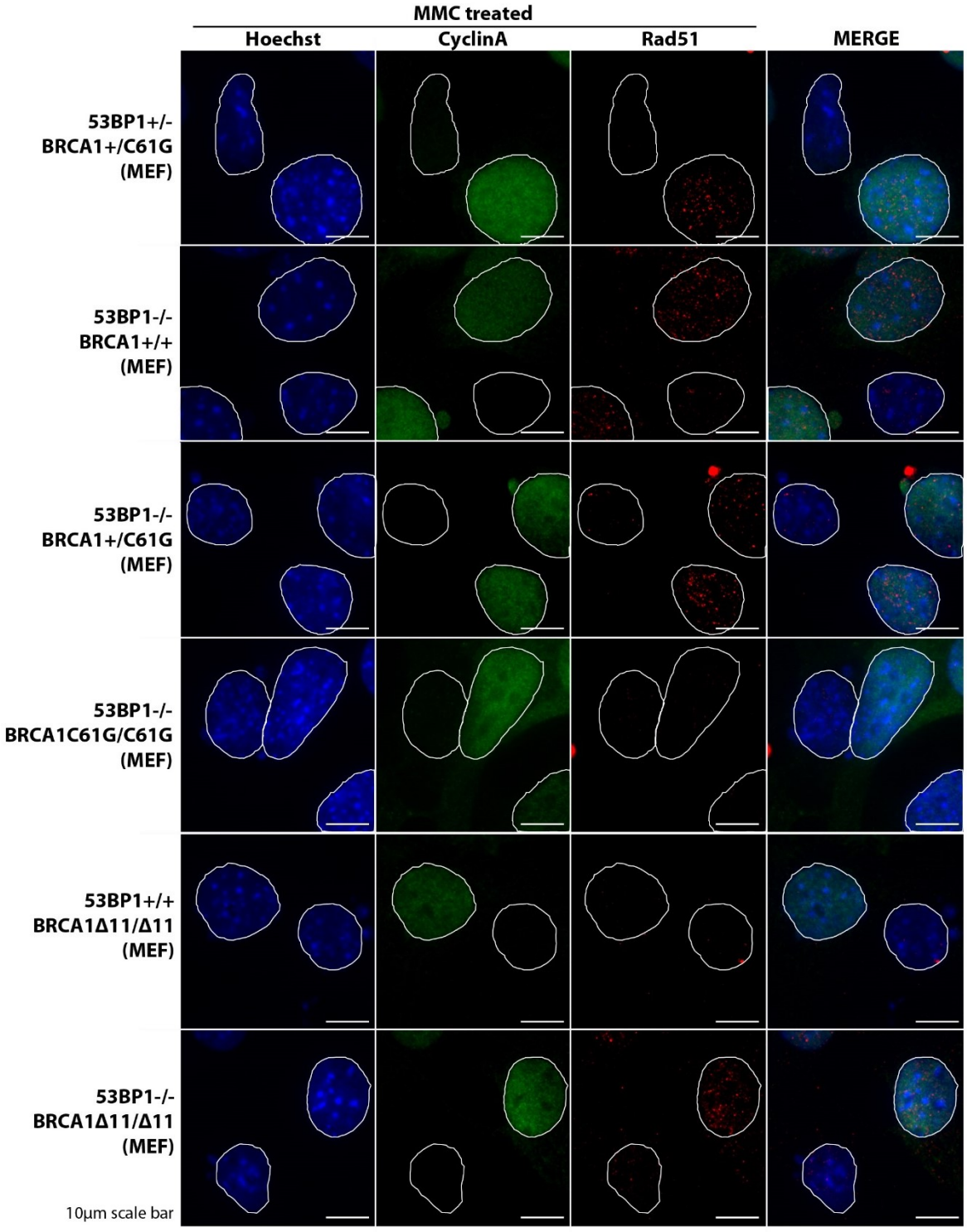

Figure 5.17 – Mitomycin C treated MEFs stained for Rad51 foci

This figure shows a panel of images of cells treated with 250ng/µl of mitomycin C for 24 hours. They were then fixed and stained to show the nucleus (Hoechst-blue), Cyclin A (green) and Rad51 foci (red). The genotype of the MEFs are stated on the left of the row and the final images on the row (far right) are a merged image of all stains (MERGE). White lines outline the nucleus of the cells. Scale bar is 10µm.

untreated cells and figure 5.17 shows MMC treated cells (24 hours 250ng/µl) stained with Cyclin A, Rad51 foci and Hoerchst (DNA). It is clear that the number of Rad51 foci do increase in cells upon treatment with MMC in Cyclin A-positive (S/G2 phase) cells, compared to untreated cells. Figure 5.14 are the percentage of untreated and MMC-treated cells from this experiment that have more than 10 Rad51 foci in S/G2 (Cyclin A positive cells). Whilst the untreated (Figure 5.14a) and MMC-treated (Figure 5.14b) MEFs shows the same relationship of Rad51 foci between genotypes (more/less in the same genotypes when compared), these results are not significantly different. In figure 5.14b, *53bp1* wild-type and *53bp1*-null *Brca1* Δ11 MEFs show a similar percentage of cells with more than 10 Rad51 foci, although slightly lower percentage is seen in the cells with *53bp1*. This is in agreement with *53bp1* removal failing to rescue the DNA crosslink sensitivity seen in *Brca1* Δ11 MEFs. The removal of *53bp1* from *Brca1*-mutated cells does restore the Rad51 foci after IR (Figure 5.6) suggesting HR is induced (Bouwman *et al*., 2010; Bunting *et al*., 2010; Cao *et al*., 2009). DNA crosslink repair uses the HR pathway for the final stages of repair (Bunting *et al*., 2012; Hinz *et al*., 2007; Knipscheer *et al*., 2009; Long *et al*., 2014) and the NHEJ pathway is antagonised through FA signalling to promote this use of HR (Adamo *et al*., 2010; Lundberg *et al*., 2001; Pace *et al*., 2010). This idea is consistent with BRCA1 having a 53bp1-independent role in DNA crosslink repair and the removal of *53bp1* having little effect on HR repair of DNA crosslinks (Bunting *et al*., 2012; Mohni *et al*., 2015). In contrast, the removal of wild-type *53bp1* from MEFs does appear to cause a small increase in Rad51 foci (Figure 5.14b) albeit not significant, suggesting there may be a role of 53bp1 in antagonising Rad51 foci formation after MMC.

Two copies of *Brca1* C61G have half the average number of cells with more than 10 Rad51 foci as cells with one or more copy of wild-type *Brca1* (Figure 5.14b). Considering that the number of Rad51 foci in *53bp1*$^{-/-}$*Brca1*$^{C61G/C61G}$ MEFs is comparable to *Brca1* wild-type MEFs after IR (Figure 5.6), it is interesting that there is a reduction after MMC treatment. Since the HR pathway has shown to be functional to the production of Rad51 foci in these MEFs after IR, this result suggests that the lack of Rad51 foci after MMC is due to a block on DNA crosslink repair that occurs before the HR pathway is used for the DNA repair.

As discussed in section 5.3, Rad51 foci in Cyclin A negative cells can indicate that the DNA repair is not as controlled due to the mutation of *Brca1* and *53bp1*. This experiment quantified the actual number of Rad51 foci, unlike the IR-Rad51 experiment looked for more than 5 foci. As in the results after IR (Figure 5.7), there is an increase in Rad51 foci in *53bp1*$^{-/-}$ *Brca1*$^{+/+}$ and the same intermediate effect in *Brca1* C61G heterozygote MEFs. Although MMC-induced ICLs do require parts of HR to repair their DNA, the DNA is repaired in G1 and therefore the Rad51 foci in the G1 cells in this experiment are likely to be due to any spontaneous DNA damage or the resulting DNA damage due to abnormal ICL repair followed by mitosis. Due to this, it is most likely a confirmation of the abnormal DSB repair control in G1 and not necessarily to do with these mutations causing effects on the FANC pathway in the G1 phase of the cell cycle.

The decrease in Rad51 foci with the increase in FANCD2 foci seen in *53bp1*$^{-/-}$*Brca1*$^{C61G/C61G}$ MEFs, together could suggest that these MEFs have faulty FANCD2 foci disassembly which causes DNA crosslink repair to be blocked before Rad51 foci can be produce. This would show that *Brca1* C61G alters the role Brca1 in FANCD2 disassembly, not in recruitment or

localisation of foci. This is not the case with the *Brca1* Δ11 mutation suggesting that these mutations have different effects on the role of Brca1 in DNA crosslink repair.

5.6 Discussion

This chapter has highlighted the roles of 53bp1 and Brca1 that are dependent-on and independent-of each other in response to DNA damage and cellular control.

53BP1 has well studied roles in NHEJ and in the prevention of DSB end resection which is antagonised by BRCA1, but it also has roles in chromosome and telomere stability that are independent of BRCA1. This chapter has also shown a Brca1-independent role for 53bp1 in the repair of DNA damage after CPT and HU that would be interesting to study further.

This thesis has agreed with the literature that the removal of *53bp1* from homozygote *Brca1*-mutated mice does rescue embryonic lethality, and in cells, the lack of *53bp1* restores the formation of Rad51 foci after IR. However, the *Brca1* C61G mutation appears to render cells sensitive to IR despite the presence of Rad51 foci. The IR sensitivity alongside the 53bp1-independent sensitivity seen after CPT, HU and Cisplatin, suggest Brca1 has other roles in DNA repair that does not involve the removal of 53bp1 from DSB sites.

Since IR causes multiple types of DNA damage, the sensitivity seen may be due to the same lesion-removal defect that causes sensitivity to other DNA-damaging agents. BRCA1 has been reported, alongside CtIP and the MRN complex, to be involved in Topoisomerase II-induced DNA/protein lesions (Aparicio *et al*., 2016). BRCA1 has a role in the removal of CMG protein complex from sites of DNA crosslinks before a DSB is created (Long *et al*., 2014) (Figure 5.18). *BRCA1* mutated cells have previously shown a lack of FANCD2 foci after treated with DNA crosslinking agents, suggesting BRCA1 has a role in FANCD2 foci formation

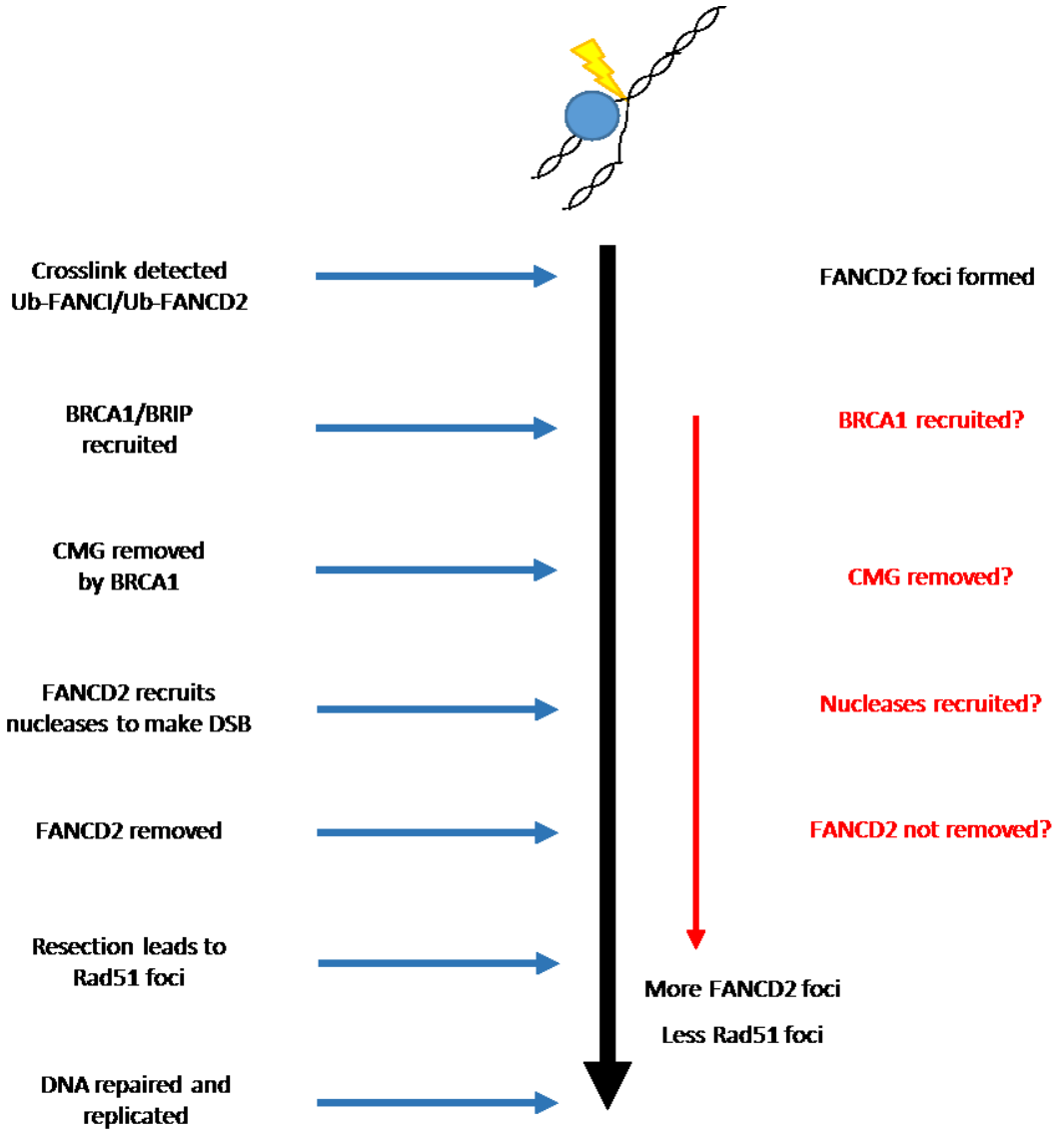

Figure 5.18 – Model of BRCA1 function in the DNA crosslink/FANC repair pathway
This figure shows simplified points in the DNA crosslink repair pathway (blue arrows) alongside the evidence shown in this thesis and possibly defects caused by the Brca1 C61G mutation (red arrows).

therefore explaining the DNA crosslink sensitivity seen in *BRCA1*-mutated cells (Bouwman *et al*., 2010; Bunting *et al*., 2012; Garcia-Higuera *et al*., 2001; Vandenberg *et al*., 2003; Zhang *et al*., 2010). FANCD2 then localises nucleases that create a DSB and this is repaired through HR, which includes the formation of Rad51 foci. In this chapter, the data shows that *53bp1*$^{-/-}$ *Brca1*$^{C61G/C61G}$ mutated cells have increased levels of FANCD2 foci, which has not been shown before, and reduced levels of Rad51 foci (Figure 5.18). This does not support a role for BRCA1 that is upstream of FANCD2 localisation to foci, and one speculation is that Brca1 may be involved in the disassembly of FANCD2 foci. Since we do not currently have the data to pin-point the step at which Brca1 affects the repair. Figure 5.18 shows a model of ICL repair and Brca1's role in this pathway, alongside the possible steps that are faulty to cause the phenotype described in this chapter. This data does support a role of BRCA1 in DNA crosslink repair that is independent of its role in HR and independent of 53bp1, since there is a reduction in Rad51 foci after MMC but not after IR. This is also concurs with the homozygote *Brca1* C61G cell sensitivity seen after Cisplatin treatment.

Many of the 53bp1-independent Brca1 phenotypes described in this chapter may lead to the DNA damage sensitivity of *Brca1* C61G homozygote cells. It has been discussed that the IR sensitivity in cells that produce IR-induced Rad51 foci indicative of active HR, may suggest that *Brca1* C61G homozygote cells do not repair DNA damage in an error-free manner. It has been suggested that both NHEJ and HR are possible after the removal of *53bp1* and wild-type *Brca1* (Bouwman *et al*., 2010; Bunting *et al*., 2010), but this does not mean that the repair in these cells is precise. This reduced control over HR (error-free) and NHEJ (error-prone) at a DSB is shown in untreated MEFs (Figure 5.7 and 5.15). It may be that the repair

leaves errors that could involve sister chromatid exchanges leading to loss of heterozygosity or mutation in genes that cause DNA-damaging agent sensitivity.

Another phenotype that may cause DNA damage sensitivity and genome instability described in the *Brca1* C61G homozygote cells is the relaxation of the chromatin leading to less heterochromatin centres (Figure 5.8). This can lead to the activation of genes and transcriptional regulators that alter the global cell response to DNA damage. It has been suggested that this alone can promote tumourigenesis (Zhu *et al*., 2011).

The literature is contradictory as to whether a single mutated allele of *BRCA1* can cause cellular defects that promote tumourigenesis without the loss of heterozygosity (LOH). Many studies have looked at whether DNA damage repair is altered in patient samples from *BRCA1* mutation carriers with or without cancer and individuals without an inherited *BRCA1* mutation, and the results have been divided. Whilst several papers suggest there is no difference in DNA damage repair in *BRCA1* mutation carrier cells compared to wild-type cells (Baeyens *et al*., 2002; Baeyens *et al*., 2004; Baria *et al*., 2001; Nieuwenhuis *et al*., 2002; Rothfuss *et al*., 2000), other studies have shown that DNA damage repair is altered in *BRCA1* mutation carrier cells (Barwell *et al*., 2007; Buchholz *et al*., 2002; Ernestos *et al*., 2010; Foray *et al*., 1999; Kote-Jarai *et al*., 2006; Speit *et al*., 2000; Speit and Trenz, 2004) and this could indicate a problem with DNA repair before the LOH. Febrer *et al* suggests that DNA repair is affected by a loss of a wild-type *BRCA1* allele but this repair defect is only seen in M phase of the cell cycle (Febrer *et al*., 2008). Whilst Trenz *et al* have conflicting results on whether DNA repair is fully functional depending on which method is used (Trenz *et al*., 2003a; Trenz *et al*., 2002; Trenz *et al*., 2003b). Rothfuss *et al* showed no significant difference between *BRCA1*-

mutation carriers and non-carriers for DSB repair, using the Comet assay, but showed that *BRCA1* mutation carrier cells had abnormal microtubule rate suggesting that some BRCA1 functions may be affected by the loss of one allele of *BRCA1* (Rothfuss *et al*., 2000). The number of patient samples is relatively low in these studies and human samples have the disadvantage of having a variety of naturally occurring unknown mutations. Therefore, studies have used cell lines to look at *BRCA1* heterozygosity or haploinsufficiency.

There is research that describes a dosage affect caused by a lack of BRCA1 that affects the DDR (Baldeyron *et al*., 2002; Cousineau and Belmaaza, 2007; Snouwaert *et al*., 1999; You *et al*., 2004; Zhang *et al*., 1998). You *et al*, showed that the C61G mutation caused a reduction in cell growth in the MCF10A cell line, despite with the presence of wild-type BRCA1 (You *et al*., 2004). This also invites the question of whether mutated BRCA1 protein can cause detrimental effects to a cell in a dominant-negative manner, which has been shown in multiple studies (Fan *et al*., 2001b; Sylvain *et al*., 2002; Zhang *et al*., 1998). Although Moynahan *et al* has suggested that the expression levels in studies using cell lines to investigate haploinsufficiency and dominant-negative *BRCA1* mutation, is not physiologically sufficient to rescue these defects but the correction of a genomic *BRCA1* allele does rescue the seen defects (Moynahan *et al*., 2001a).

However, Brown *et al* shows that mice with a truncating *Brca1* mutation are radiosensitive and have altered mammary development (Brown *et al*., 2002), Jeng *et al* shows heterozygote *Brca1* Δ11 mice develop spontaneous tumours that do not show LOH (Jeng *et al*., 2007), and Cressman *et al* show that *p53* mutated mice have a higher rate of mammary tumour development when they have a single allele of *Brca1* mutated (Cressman *et al*.,

1999b). These two mouse studies are not affected by the non-physiological expression levels Moynahan *et al* describes (Moynahan *et al*., 2001a), and show that a single *Brca1* mutation can lead to cellular defects.

When examining the *53bp1*$^{-/-}$*Brca1*$^{+/C61G}$ MEFs responses to DNA-damaging agents, it appears that in certain cases cells heterozygote for the *Brca1* C61G mutation display a different phenotype from the *53bp1*$^{-/-}$*Brca1*$^{+/+}$ MEFs. *53bp1*$^{-/-}$*Brca1*$^{+/C61G}$ cells show an identical phenotype to cells that are homozygote for *Brca1* C61G in their sensitivity to HU. *53bp1*$^{-/-}$*Brca1*$^{+/C61G}$ cells show an intermediate phenotype between *53bp1*$^{-/-}$*Brca1*$^{+/+}$ cells and *53bp1*$^{-/-}$*Brca1*$^{C61G/C61G}$ cells in their sensitivity to CPT, their number of Rad51 foci in G1 MEFs (after IR or MMC) and in their number of heterochromatin centres. These results suggest that wild-type Brca1 levels are important for specific roles of Brca1 and that there may be a haploinsufficiency seen in *Brca1* C61G heterozygote cells. Considering the contradictory data on whether the loss of a single *BRCA1* allele can produce changes to cellular processes discussed in section 5.1, these results agree that haploinsufficiency can cause defects in DNA repair and that only some of Brca1's roles are affected by the one *Brca1* wild-type allele. This knowledge could influence the way in which *BRCA1* mutation carriers are viewed in terms of tumour development, as loss of heterozygosity may not be the driving force behind initial tumourigenesis.

Several phenotypes in the *53bp1*-null *Brca1* C61G homozygote cells are not reproduced in the *53bp1*-null *Brca1* Δ11 homozygote cells: such as the response to Olaparib, the growth advantage to Veliparib, the lack of sensitivity to CPT and IR, the change in number of MMC-induced FANCD2 foci and the restoration in Rad51 foci after MMC. These would suggest that

the two *Brca1* mutations have altered responses to the same DNA-damaging agents, due to the effect of each mutation on the Brca1 protein. Brca1 Δ11 is similar to naturally-occurring Brca1 isoforms, and produces an approximately 92 kDa protein (Figure 4.4) which localises to DSBs (Figure 4.11), whereas Brca1 C61G is not as effectively recruited to DSBs (Figure 4.11 and 12) and is reduced in the nucleus compared to cells with wild-type Brca1 protein (Figure 4.5). This suggests that the Brca1 Δ11 could still have function from the unperturbed RING and BRCT domains and therefore may not be comparable to *Brca1*-null mutations. The *Brca1* C61G mutation appears to be a more dramatic mutation in its phenotype, despite the relatively small change to the DNA sequence, compared to the *Brca1* Δ11 mutation.

The results in this chapter also could affect the way in which we think about the treatment of *Brca1* patients in several ways. Firstly, the removal of *53bp1* does alter *Brca1* mutated cells response to PARPi's and therefore 53BP1 expression status could provide a biomarker for how *BRCA1*-mutated cells will react to drug therapy. Secondly, *BRCA1* mutations do cause haploinsufficiency which leads to tumour development, and therefore there may be interventions (drug or otherwise) that are not already used, that could prevent or delay tumour development. Finally, the MEFs have provided a way of looking at the phenotypes causes by a specific *BRCA1* patient mutation, and this has shown that a genetically small mutation has had dramatic effects on the entire protein. Therefore, more information is needed on how mutations affect the entire protein to predict the effect on the function of BRCA1 protein and understand the tumours that develop from said mutation.

Chapter 6 – *53bp1*$^{-/-}$*Brca1*$^{C61G/C61G}$ mice phenotypes

6.1 Introduction

Brca1 mouse models (as discussed in section 1.5) have provided a whole organism in which to study phenotypes that are produced when *Brca1* is mutated. Some mouse models produce an increased tumour risk phenotype similar to human *BRCA1* mutation carriers (Jeng *et al*., 2007), but not all phenotypes are replicated, i.e. tissue in which the cancer develops. Mouse models do not always replicate human disease, but the scientific knowledge that is gained by genetically manipulating a mammal far outweigh the disadvantages of the discrepancies.

Many of the *Brca1* mutant mice models are homozygote in genotype and most are embryonic lethal. There have been no reported cases of a homozygote *BRCA1* mutation genotype in humans (only compound heterozygotes) suggesting that they are embryonic lethal in humans like in the mouse models. There are mutation in other genes (such as *p53* or *53bp1*) that show a rescue of the embryonic lethality caused by the homozygote *Brca1* mutation. Although this double mutant condition has never been reported in humans, both *p53* and *53bp1* are known to be mutated in breast cancers and the cells from the double mutant mice may replicate the specific conditions in these cancer cells. Reduced 53bp1 expression in breast cancer, and specifically in triple-negative breast cancers, is known to correlate with reduced survival (Bouwman *et al*., 2010). With this in mind, the phenotypes seen in *53bp1*$^{-/-}$*Brca1*$^{C61G/C61G}$ mice may provide more information about the functional roles of 53bp1 and the *Brca1* C61G allele, than they are to provide insight into the development of breast cancer in *BRCA1* mutation carriers.

As discussed in the introduction chapter (Section 1.5), the majority of *Brca1* mutated mice have an increased rate of tumourigenesis (Tables 6.1 and 6.2) (Bachelier *et al*., 2003; Berton *et al*., 2003; Cao *et al*., 2003; Cao *et al*., 2006; Chodankar *et al*., 2005; Cressman *et al*., 1999a; Cressman *et al*., 1999b; Drost *et al*., 2011; Kim *et al*., 2004; Liu *et al*., 2007a; Ludwig *et al*., 2001; McCarthy *et al*., 2007; Shakya *et al*., 2008; Shakya *et al*., 2011; Xu *et al*., 1999a; Xu *et al*., 2001c). Some papers that describe an increased rate of tumour development, are in mice that have a conditional tissue-specific mutation in *Brca1* (Table 6.2), such as *K14*-expressing epithelial cells, to overcome the embryonic lethality of a homozygote *Brca1* mutation (Berton *et al*., 2003; Chodankar *et al*., 2005; Drost *et al*., 2011; Liu *et al*., 2007a; McCarthy *et al*., 2007). These mice can help understanding how the loss of wild-type Brca1 protein can cause tumourigenesis in that particular tissue. The embryonic lethality of the *Brca1* Δ11 homozygote mutation can be rescued by mutating one or two *p53* alleles (Cao *et al*., 2003; Xu *et al*., 1999a; Xu *et al*., 2001c) or both *Chk2* alleles (Cao *et al*., 2006), adult mice of these genotypes show an increased rate of tumour formation compared to mice with a wild-type *Brca1* allele (Table 6.1). Some *Brca1* mutant mice which carry a missense mutation, do not show embryonic lethality; such as mice with the *Brca1* S1598F (Shakya *et al*., 2011), I26A (Shakya *et al*., 2011) or the S971A (Kim *et al*., 2004) mutation. But only the S971 and S1598F *Brca1* mutation show increased tumour incidence (Table 6.1). *Brca1*$^{F/C61G}$*;p53*$^{F/F}$ *K14-Cre* tissue-specific mutation mouse model suggests that the presence of a C61G mutated Brca1 protein causes tumourigenesis above the rate of *Brca1*-null mice (both of a *p53*-null background in epithelial cells) suggesting a wild-type Brca1 N-terminus is important for tumour suppression. However, the lack of tumour development in the *Brca1* N-terminal I26A mutated mice (Shakya *et al*., 2011), does suggest that the N-terminus of Brca1 may not be

Table 6.1 – Table of homozygote Brca1 mice with increased rates of tumourigenesis (non-embryonic lethal Brca1 mutations or rescued by the removal of p53 or Chk2)

Reference	Genotype	Tumour incidence	Tissue type
(Cressman *et al*., 1999a)	*Brca1$^{aa223\text{-}763/aa223\text{-}763}$;p53$^{-/-}$* (only 3 mice)	All three mice had lymphomas, one also had hemangiosarcoma. Tumours developed between 10-12 weeks	Lymphomas, organ was not specified
(Xu *et al*., 2001c)	*Brca1$^{\Delta11/\Delta11}$;trp53 $^{+/-}$* or $^{-/-}$	*Brca1$^{-/-}$p53$^{+/-}$* produced tumours within 6-12 months, no wild-type comparison	Mammary tumours
(Ludwig *et al*., 2001)	*Brca1$^{tr/tr}$*, truncation of Brca1 at aa924	*Brca1$^{tr/tr}$* mice developed tumours (76/89; 85%). Control mice develop tumours (2/27; 26%) at an older age	Mediastinal, nodal lymphomas, angiosarcomas, spindle cell retroperitoneal sarcomas, breast, lung, liver, uterus, kidney, colon, and other, including ovarian teratoma
(Cao *et al*., 2003)	*Brca1$^{\Delta11/\Delta11}$;p53$^{+/-}$*	Male mice developed lymphoma (30%) before 7 months. Female developed mammary tumours from 6-12 months	Mostly mammary tumours in females, other mice developed tumours in the bone brain liver, lung, thymus and spleen
(Bachelier *et al*., 2003)	*Brca1$^{\Delta11/\Delta11}$;p53$^{+/-}$* or *p53$^{-/-}$*	*Brca1$^{\Delta11/\Delta11}$;p53$^{+/-}$* mice developed T cell thymic lymphomas (18/66; 27%) within 12-28 weeks whilst *p53$^{+/-}$* mice did not develop any tumours in the same time frame. 7 *Brca1$^{\Delta11/\Delta11}$* mice were not embryonic lethal and survived over 1 year without any lymphoma incidence. Two of the female *Brca1$^{\Delta11/\Delta11}$* mice developed mammary tumours	Thymus and mammary tumours
(Kim *et al*., 2004)	*Brca1$^{S971A/S971A}$*	6 of the mice showed mammary hyperplasia, and 7 out of 8 females has uteri abnormalities Three of the mice has lost their ovaries to uncontrolled growth. When mice were irradiated, *Brca1$^{S971A/S971A}$* mice started to develop tumours after 3 months and at 1 year 80% of mice has tumours compared to 15% in control mice	Mammary gland hyperplasia and uteri and ovaries with polyps and show abnormal structures. Irradiated mice developed mostly lymphomas but also 3 mammary tumours, one colon tumour and one uterus tumour
(Cao *et al*., 2006)	*Brca1$^{\Delta11/\Delta11}$;Chk2$^{-/-}$*	72% of *Brca1$^{\Delta11/\Delta11}$;Chk2$^{-/-}$* mice had mammary tumours at 16 months (16/22). The average age of incidence was 12 months	Mostly mammary, ovarian with some liver and thymus, unlike *p53$^{-/-}$* mice
(Shakya *et al*., 2011)	*Brca1$^{I26A/\Delta2}$* or *Brca1$^{S1598F/S1598F}$*	*Brca1$^{I26A/I26A}$* or *$^{I26A/-}$* mice showed same level of tumours as control mice (18.6% with older age of incidence). S1598F showed similar levels of tumours to truncating Brca1 (68.1%; 49/72)	Paper did not state where non-tissue-targeted tumours occurred

Table 6.2 – Table of conditionally expressed homozygote Brca1 mice with increased rates of tumourigenesis

Reference	Genotype	Tumour incidence	Tissue type
(Xu *et al*., 1999a)	*Brca1*$^{\Delta 11/\Delta 11}$ or *Brca1*$^{Ko22/Ko22}$ with *MMTV-Cre* or *Wap-Cre* expression	3 out of 10 *Brca1*$^{Ko22/\Delta 11}$ *MMTV-Cre* mice developed tumours and 2 out of 13 *Brca1*$^{Ko22/\Delta 11}$ *Wap-Cre* mice developed tumours	All tumours were mammary tumours
(Berton *et al*., 2003)	*Brca1*$^{\Delta 11/\Delta 11}$ *K5-Cre* expression	Tumours developed after 1 year and by 88 weeks in 72% (13/18) in *Brca1*$^{\Delta 11/-}$ *K5-Cre* mice. This was significantly higher than *Brca1*$^{+/-}$ and *K5 Brca1*$^{\Delta 11/+}$ and *Brca1*$^{\Delta 11/+}$ mice. Less than 5% of controls developed tumours by 88 weeks	Majority of tumours were of the inner ear canal or oral epithelium. Others tumours developed in the skin or vagina, two were sarcoma of the gastrointestinal tract and one was a diffused lymphoma
(Chodankar *et al*., 2005)	*Brca1*$^{\Delta 11/\Delta 11}$ *Fshr-Cre* expression	*Brca1*$^{\Delta 11/\Delta 11}$ *Fshr-Cre* mice developed one ovary solid tumour and several kidney cysts. Mice showed atypical ovaries but had not developed into tumours. No tumours were found in control mice	Ovary and kidney tumours
(Liu *et al*., 2007a)	*Brca1*$^{\Delta 11/\Delta 11}$ *K14-Cre* expression	*Brca1*$^{\Delta 11/\Delta 11}$ *K14-Cre* mice developed spontaneous tumours. Mammary tumours were only found in *Brca1*$^{\Delta 11/\Delta 11}$ *K14-Cre* when *p53* was also mutated	High grade mammary tumours developed in mice with a *Brca1* mutation, which is similar to human *BRCA1*-mutated tumours
(McCarthy *et al*., 2007)	*Brca1*$^{\Delta 22\text{-}24/\Delta 22\text{-}24}$ *BLG-Cre* expression	*Brca1*$^{\Delta 22\text{-}24/\Delta 22\text{-}24}$ *BLG-Cre* mice developed tumours at a rate of 12% (5/43) with a latency of 12-15 months, which is increased compared to *Brca1*$^{+/\Delta 22\text{-}24}$ *BLG-Cre* mice. 64% of *Brca1*$^{\Delta 22\text{-}24/\Delta 22\text{-}24}$*;p53*$^{+/-}$ *BLG-Cre* mice developed mammary tumours (25/39) within 6-46 weeks (all but one by 31 weeks)	Mammary tumours were the most common to develop but some mice had tumours in the surrounding tissues and salivary glands
(Shakya *et al*., 2008)	*Brca1*$^{\Delta 2/\Delta 2}$ *Wap-Cre* expression	*Brca1*$^{+/\Delta 2}$ mice remained tumour free throughout the study. 35 tumours were found in 31 of the 33 *Brca1*$^{\Delta 2/\Delta 2}$ mice	Mammary tumours
(Drost *et al*., 2011)	*Brca1*$^{F/C61G}$*;p53*$^{F/F}$ *K14-Cre* expression	More tumours (particularly mammary) developed in *Brca1*$^{F/C61G}$*;p53*$^{F/F}$ *K14-Cre* mice than *Brca1*$^{F/F}$*;p53*$^{F/F}$ *K14-Cre* mice. Tumour latency in Brc*a1*$^{F/C61G}$*;p53*$^{F/F}$ *K14-Cre* mice was of 197 days and in *Brca1*$^{F/F}$*;p53*$^{F/F}$ *K14-Cre* mice it was 236 days. Difference between mammary tumours is not significant (p=0.056), only when skin tumours were taken into account. Less skin tumours in C61G than B1-null. and B1-null more often carried both skin and mammary tumours	Mammary and skin tumours formed. More *Brca1*$^{F/F}$*;p53*$^{F/F}$ *K14-Cre* mice developed both skin and mammary tumours than mice with a C61G mutation

needed for tumour suppression. It is important to note that because the presence of Brca1 C61G protein increased tumour develop compared to *Brca1*-null mice (Drost *et al*., 2011), suggesting that the *Brca1* C61G mutation may lead to a protein that causes a dominant-negative phenotype that affects tumour suppression, and that the I26A mutation affects the ubiquitin ligase activity of the Brca1:Bard1 heterodimer but not the Brca1:Bard1 heterodimer binding, unlike the C61G mutation (Brzovic *et al*., 2003). These differences in N-terminal *Brca1* mutations makes it clear that the understanding of the role of the N-terminal stability and catalytic function, separately, is important for assessing what role the N-terminus of Brca1 may play in tumour suppression.

Despite *53bp1* and *Brca1* mutant mice showing an increased rate of tumour development, $53bp1^{-/-}Brca1^{\Delta 11/\Delta 11}$ mice (Bunting *et al*., 2010) did not show any increased tumour formation higher than $53bp1^{-/-}$ mice (Ward *et al*., 2003a), unlike the *p53* mutation rescued $Brca1^{\Delta 11/\Delta 11}$ mice that did develop tumours at a higher rate than *p53* mutated mice (Bachelier *et al*., 2003; Xu *et al*., 1999a; Xu *et al*., 2001c). This could be because with 53bp1 present *Brca1*-mutated cells are being repaired through error-prone methods because HR is not functional (Bunting *et al*., 2010). On top of this, the *p53* mutation is likely to allow some cells to pass through cell cycle checkpoints despite DNA damage and this on its own can lead to genomic instability ($p53^{+/-}$ mice develop tumours (Donehower *et al*., 1992)) (Kuerbitz *et al*., 1992). Without 53bp1 in the *Brca1* Δ11 homozygote cells, the error-free DSB repair pathway of HR can occur and Brca1 Δ11 mutated protein still functions as a tumour suppressor.

The types of tumours that the *Brca1*-mutated mice produce are varied in their tissue type. The *Brca1* Δ11 homozygote mice that have been rescued by the removal of *p53* or *Chk2* (Cao

et al., 2003; Cao *et al*., 2006; Xu *et al*., 1999a; Xu *et al*., 2001c) produce *Brca1*-associated mammary tumours and the mice that have a tissue-specific *Brca1* mutation (Drost *et al*., 2011; Liu *et al*., 2007a; McCarthy *et al*., 2007) and the mice with S971A *Brca1* mutation (which does not cause embryonic lethality) show spontaneous development of mammary tumours (Kim *et al*., 2004). Liu *et al* show that the epithelial conditional *Brca1* Δ11 mutation causes mammary tumour development and these tumours are mostly high grade which is similar to what is found in human *BRCA1*-mutated tumours (Liu *et al*., 2007a).

Several other mouse models with biallelic *Brca1* mutations show an increased rate of lymphoma development (Bachelier *et al*., 2003; Cressman *et al*., 1999a; Ludwig *et al*., 2001). The lymphomas produced in these mice are mostly T-cell in origin (Bachelier *et al*., 2003), but some nodal lymphomas are B-cell in origin (Ludwig *et al*., 2001). Jeng *et al* examined heterozygote *Brca1* Δ11 mutant mice which showed that 70% of mice developed tumours and of those tumours 50% were lymphomas (2 were mammary tumours) (Jeng *et al*., 2007). The irradiation of these mice showed a switch to the majority of tumours being ovarian tumours (Jeng *et al*., 2007). Kim *et al* and Cao *et al* described that mice developed tumours due to the lack of Brca1 after exposure to a DNA-damaging agent such as IR (Kim *et al*., 2009b) or MNAN (Methyl-n-amyl nitrosamine) (Cao *et al*., 2007) and these tumours were found in multiple tissues and included mammary tumours and thymic lymphomas. Other mice with DDR associated protein mutations such as in *p53* (Dudgeon *et al*., 2014), *ATM* (Xu *et al*., 1996) and *RNF8* (Li *et al*., 2010), also show a higher rate of lymphoma development.

Approximately 8% of *53bp1*$^{-/-}$ mice develop CD4+ CD8+ T cell lymphomas within 4-7 months (Ward *et al*., 2003b). It is suggested that these mice develop more lymphomas because

53bp1 has a role in V(D)J recombination, which uses NHEJ to insert variation into the T-cell receptor which is important for immune responses (Difilippantonio *et al*., 2008). The dysregulation of NHEJ in these cells leads to reduced immune system function because of the lack of specific immunoglobulins (Ig's) that are created using long-range NHEJ for which 53bp1 is needed to be efficient (Difilippantonio *et al*., 2008). The lack of 53bp1 in lymphocytes also means the DSBs created to induce variation are now repaired in other ways which causes genome instability and is predicted to be why lymphocytes become lymphomas in these mice (Ward *et al*., 2003b).

In the discussed mouse models, the location or region in which *Brca1* gene has been mutated does not appear to correlate to the tissue type in which the cancer will develop (excluding tissue-specific conditional mutations), therefore it is difficult to predict what (if any) tumours will develop from specific *Brca1* mutations. The variation in tissue in which tumorigenesis occurs also poses the question whether Brca1 has specific tumour suppressing roles in these tissues, or whether these cells are particularly sensitive to DNA repair protein mutations.

Mutations in DNA repair genes can cause male-specific sterility in mice (Section 1.5.4) (Fernandez-Capetillo *et al*., 2003; Kopanja *et al*., 2011; Li *et al*., 2010; Lou *et al*., 2006; Lu *et al*., 2010; Santos *et al*., 2010; Simhadri *et al*., 2014) due to impaired DNA repair (Cressman *et al*., 1999a; Kopanja *et al*., 2011; Lou *et al*., 2006; Santos *et al*., 2010; Schaetzlein *et al*., 2013; Xu *et al*., 2003; Xu *et al*., 1996) or a lack of meiotic chromosome crossing over (Boateng *et al*., 2013; Xu *et al*., 2003) or XY body control during meiosis (Adamo *et al*., 2008; Fernandez-Capetillo *et al*., 2003; Santos *et al*., 2010). *Brca1*-mutated mice that are not embryonic lethal

have shown infertility in male mice (Figure 1.8) (Cressman *et al*., 1999a; Ludwig *et al*., 2001; Shakya *et al*., 2011) but have also shown no infertility in either sex (Kim *et al*., 2004; Kim *et al*., 2006; Kim *et al*., 2009b) (Figure 1.8). After the embryonic lethality was rescued in homozygote *Brca1*-mutated mice using mutation in *p53* (Xu *et al*., 2003), *Chk2* (Cao *et al*., 2006) or *53bp1* (Bunting *et al*., 2012), the resulting double homozygote mutant male mice were infertile and had smaller testes than mice with a wild-type copy of *Brca1*. The ability of the *Brca1* mutation to cause male-specific infertility or not, may lead to more information about the functional roles of Brca1 in meiosis and the regions of Brca1 that are needed for these functions.

This chapter focuses on the phenotypes of the $53bp1^{-/-}Brca1^{C61G/C61G}$ mice and compares them to their littermates and phenotypes seen in previous *Brca1* mutant mouse models.

6.2 Rescue of embryonic lethality and Mendelian ratio

As discussed in section 4.3, the *53bp1*-null mice (Ward *et al*., 2003b) and the *Brca1* C61G heterozygote mice (Drost *et al*., 2011) were bred together to produce the $53bp1^{-/-}$ $Brca1^{C61G/C61G}$ mice, suggesting that the removal of 53bp1 from these mice has rescued the embryonic lethality caused by having two *Brca1* C61G alleles. The $53bp1^{-/-}Brca1^{\Delta11/\Delta11}$ mice were shown to be viable, unlike $Brca1^{\Delta11/\Delta11}$ mice (Xu *et al*., 1999a), and were born at the expected Mendelian ratio, showing a full recovery of embryonic development (Bouwman *et al*., 2010; Bunting *et al*., 2010; Bunting *et al*., 2012). Figure 6.1a and table 6.3 show the number of mice born to multiple parental crosses (both parents were $53bp1^{-/-}Brca1^{+/C61G}$) and the expected Mendelian ratio and expected numbers of offspring. The $53bp1^{-/-}$ $Brca1^{C61G/C61G}$ mice were born at a ratio of 0.192 which is not significantly different from the

expected ratio of 0.25 and therefore no defect was seen in the number of living *53bp1*$^{-/-}$ *Brca1*$^{C61G/C61G}$ mice.

Table 6.3 – Expected Mendelian ratio and actual ratio of the genotypes of mice born from 53bp1*$^{-/-}$*Brca1*$^{+/C61G}$ *parental cross (none of the actual genotype ratios are significantly different from the expected ratios)

	Numbers		Ratios	
	Expected	Actual	Expected	Actual
***53bp1*$^{-/-}$*Brca1*$^{+/+}$**	53.25	58	0.25	0.272
***53bp1*$^{-/-}$*Brca1*$^{+/C61G}$**	106.5	114	0.5	0.535
***53bp1*$^{-/-}$*Brca1*$^{C61G/C61G}$**	53.25	41	0.25	0.192

Table 6.4 shows the number of male and female *53bp1*$^{-/-}$*Brca1*$^{C61G/C61G}$ mice born from all *53bp1*$^{-/-}$*Brca1*$^{+/C61G}$ parental crosses. Males and females were born at a 0.483 and 0.517 ratio, which is not significantly different from the expected ratio of 0.5 for both genders, suggesting that there is no gender bias in the birth rate of *53bp1*$^{-/-}$*Brca1*$^{C61G/C61G}$ mice.

Table 6.4 – Expected ratio and actual ratio of the gender of mice born from 53bp1*$^{-/-}$ *Brca1*$^{+/C61G}$ *parental cross

	Numbers		Ratios	
	Expected	Actual	Expected	Actual
Males	103.5	100	0.5	0.483
Females	103.5	107	0.5	0.517

These results suggest that the lack of 53bp1 in the homozygote *Brca1* C61G mice has rescued the embryonic lethality of the mice to produce expected numbers of genotype and gender of *53bp1*$^{-/-}$*Brca1*$^{C61G/C61G}$ mice.

Figure 6.1b shows the general survival (the number of mice that died from general unknown causes, i.e. not tumours) of *53bp1*$^{-/-}$*Brca1*$^{+/+}$, *53bp1*$^{-/-}$*Brca1*$^{+/C61G}$ and *53bp1*$^{-/-}$*Brca1*$^{C61G/C61G}$ mice. *53bp1*$^{-/-}$ mice have an increase in the number of non-tumour-related morbidity compared to *53bp1*$^{+/-}$ mice due to being partially immunocompromised (Ward *et al*., 2003b).

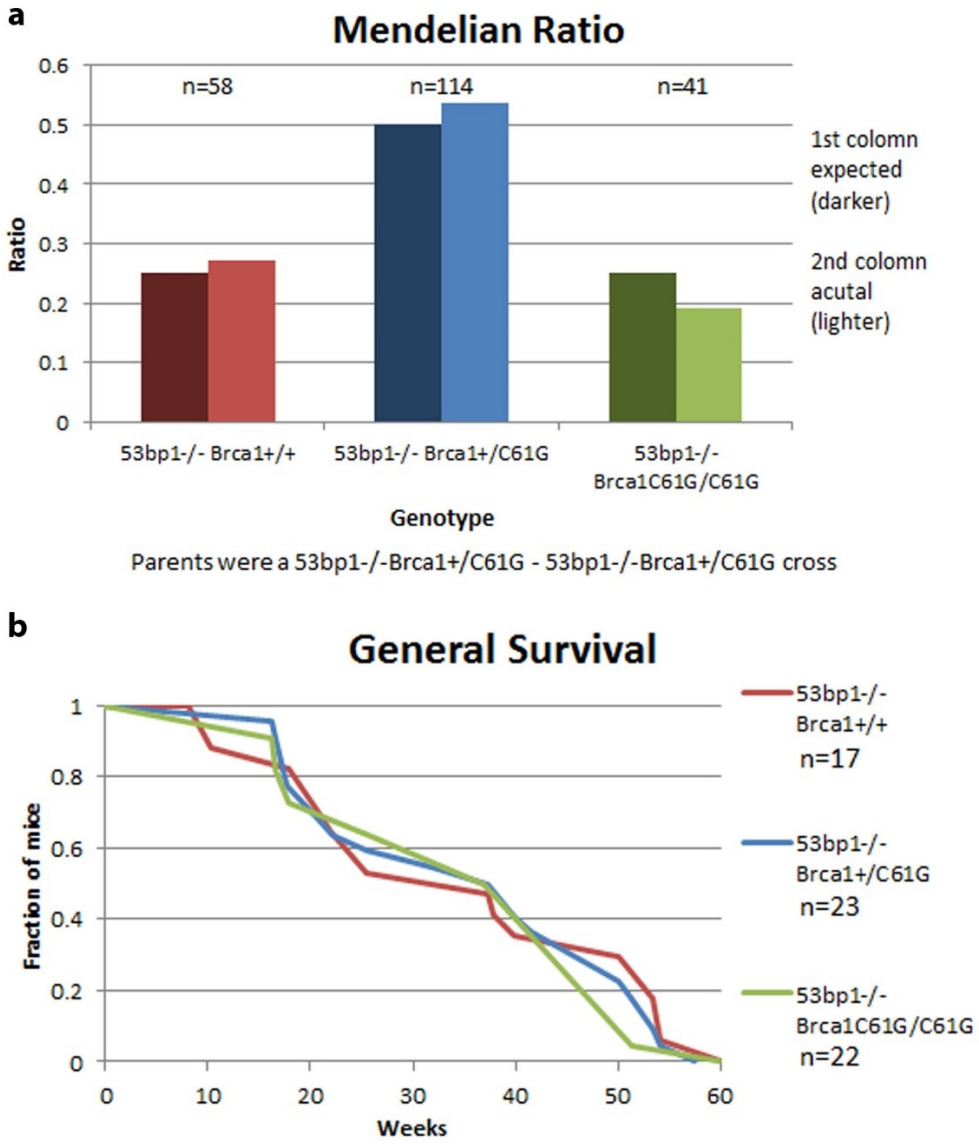

Figure 6.1 – Mendelian Ratio and general survival of 53bp1$^{-/-}$Brca1$^{C61G/C61G}$ mice
[a] shows the Mendelian ratios of each genotype that were produced from parental crosses of two 53bp1$^{-/-}$Brca1$^{+/C61G}$ mice. The darker coloured bars represent the expected Mendelian ratio for each genotype from this cross, and the lighter coloured bars are the actual ratios of each genotype observed from this cross. The number of mice of each genotype from the 34 litters from 14 breeding pairs, is shown as 'n=…'. [b] shows the general survival of the mice from each genotype across 60 weeks. The decent of the line is the fraction of mice from each genotype that were culled due to signs of morbidity that did not have tumours upon necropsy and their age at death. The maximum survival is stated as 1, and is equal to the number of mice in that genotype (n=…).

Figure 6.1b shows that the rate of survival of these mice, is equivalent between the genotypes showing that the loss of one or both wild-type copies of *Brca1* with the *53bp1*-null background does not cause more non-tumour-related deaths than in *53bp1*$^{-/-}$*Brca1*$^{+/+}$ mice. This suggests that this phenotype is specific to *53bp1* loss and is not exasperated by the *Brca1* C61G mutation.

6.3 Phenotypes of the *53bp1*$^{-/-}$*Brca1*$^{C61G/C61G}$ mice

6.3.1 Testes and male sterility

As discussed in 6.1, some *Brca1* mutated mice have shown male-specific infertility (Cao *et al*., 2006; Cressman *et al*., 1999a; Ludwig *et al*., 2001; Shakya *et al*., 2011; Xu *et al*., 2003) so all possible breeding crosses using the *53bp1*$^{-/-}$*Brca1*$^{C61G/C61G}$ mice were tested (Figure 6.2a). From these breeding crosses, all crosses that involved a male *53bp1*$^{-/-}$*Brca1*$^{C61G/C61G}$ mouse did not produce offspring (grey arrows in figure 6.2a). The females of these crosses did produce a vaginal plug suggesting that the infertility was not due to a behavioural change but due to a defect in the sperm of the *53bp1*$^{-/-}$*Brca1*$^{C61G/C61G}$ mice (firing blanks).

On dissection of male mice, the testes of *53bp1*$^{-/-}$*Brca1*$^{C61G/C61G}$ mice were found to be significantly smaller than their littermates (Figure 6.2b,c). This was also noted in other *Brca1*-mutated male mice (Cressman *et al*., 1999a; Shakya *et al*., 2011) and shown to be due to a failure in the pachytene stage of prophase (Cressman *et al*., 1999a; Shakya *et al*., 2011; Xu *et al*., 2003). Xu *et al* showed that the DSB repair and meiosis crossover was faulty in cells with two *Brca1* Δ11 alleles and this could be the reason for the failure of correct meiosis in spermatocytes (Xu *et al*., 2003). Without further investigation into the exact point of

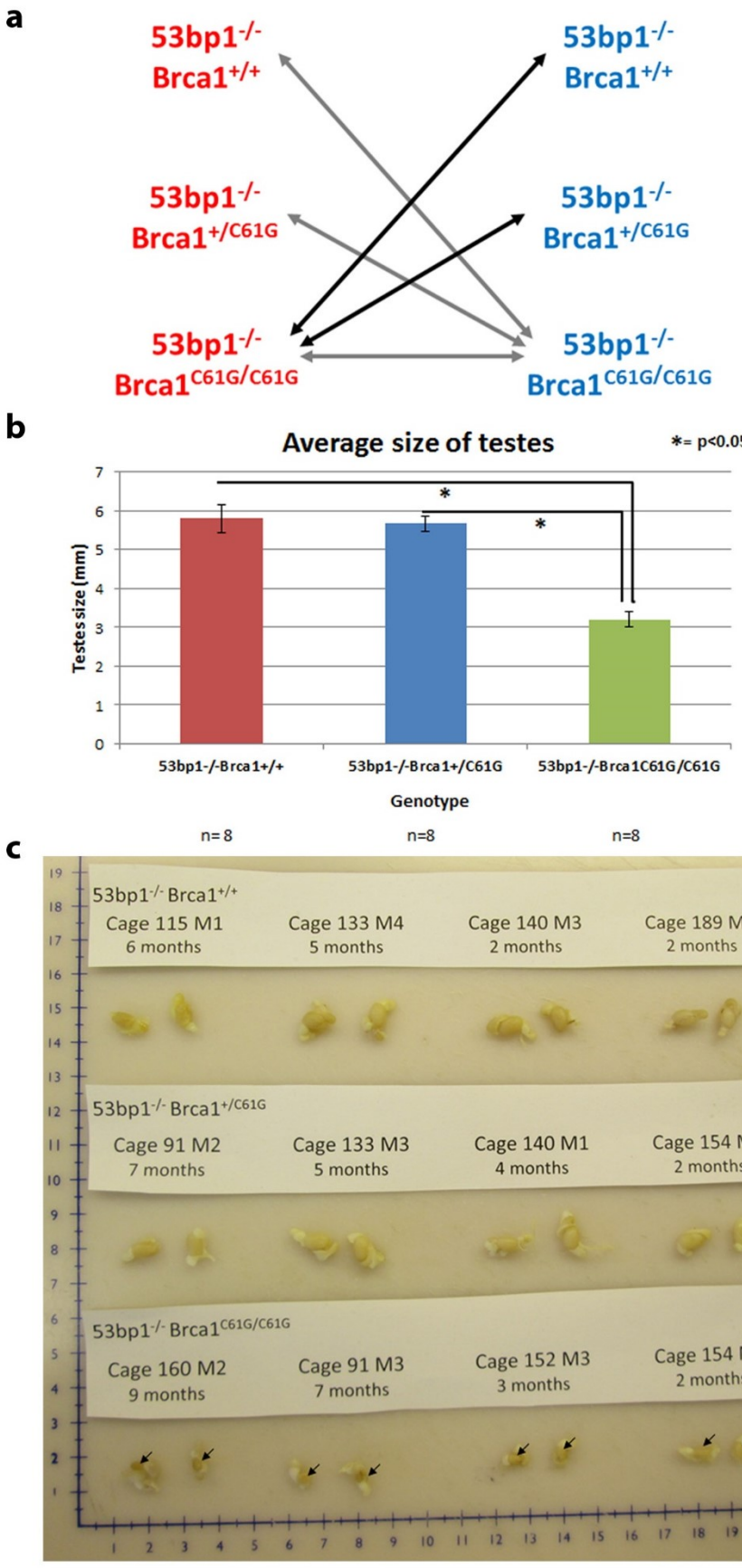
a
53bp1-/- Brca1+/+
53bp1-/- Brca1+/+
53bp1-/- Brca1+/C61G
53bp1-/- Brca1+/C61G
53bp1-/- Brca1C61G/C61G
53bp1-/- Brca1C61G/C61G
b
Average size of testes
*= p<0.05
Testes size (mm)
0
1
2
3
4
5
6
7
*
*
53bp1-/-Brca1+/+
53bp1-/-Brca1+/C61G
53bp1-/-Brca1C61G/C61G
Genotype
n= 8
n=8
n=8
c
53bp1-/- Brca1+/+
Cage 115 M1
6 months
Cage 133 M4
5 months
Cage 140 M3
2 months
Cage 189 M1
2 months
53bp1-/- Brca1+/C61G
Cage 91 M2
7 months
Cage 133 M3
5 months
Cage 140 M1
4 months
Cage 154 M1
2 months
53bp1-/- Brca1C61G/C61G
Cage 160 M2
9 months
Cage 91 M3
7 months
Cage 152 M3
3 months
Cage 154 M2
2 months

Figure 6.2 – Male sterility and testes size of 53bp1$^{-/-}$Brca1$^{C61G/C61G}$ mice
*[a] shows the genotypes of the breeding pair combinations that were tested using either the male (blue) or female (red) 53bp1$^{-/-}$Brca1$^{C61G/C61G}$ mice. The black arrows show the breeding crosses that produced live offspring and the grey arrows show the breeding crosses that did not produce offspring. At least three of each genotype pairings were tested. [b] shows the average size (mm) of testes from 8 males of each genotype. * represent points that are significantly different from each other (shown by black line) with a p value of <0.05 from a t-test. Error bars show standard error. [c] shows 4 sets of testes and seminiferous tubules from a range of ages (some littermates) of each genotype. The arrows indicate the smaller testes from the 53bp1$^{-/-}$Brca1$^{C61G/C61G}$ mice. Ruler bars are in centimetres.*

abnormality in the *53bp1$^{-/-}$Brca1$^{C61G/C61G}$* spermatogenesis, it is not clear if the *Brca1* C61G mutation causes the same defect in meiosis as previous *Brca1* mutated mice.

6.3.2 Weight

Some of the *Brca1* mutated mice have been smaller than littermates with a wild-type copy of *Brca1* (Table 6.5) (Cao *et al*., 2003; Cao *et al*., 2006; Kim *et al*., 2009b; Shakya *et al*., 2011), but other papers did not notice any difference in body weight (Bunting *et al*., 2012; Kim *et al*., 2004; Kim *et al*., 2006). Figure 6.3a shows there is a small but not significant decrease in average body weight of *53bp1$^{-/-}$Brca1$^{C61G/C61G}$* compared to mice with a wild-type *Brca1* allele (24.26g compared to 25.32g and 26.19g). Figure 6.3b shows the weight of mice and the age at which they were weighed, this also shows that many of the *53bp1$^{-/-}$Brca1$^{C61G/C61G}$* mice are smaller than the majority of mice from the other genotypes, although there are outliers. Shakya *et al* noted a 5-10% body weight decrease in mice with the *Brca1* I26A mutation (although not statistically significant) (Shakya *et al*., 2011), and other groups have reported an age-related decrease in weight mice carrying *Brca1* mutations (Cao *et al*., 2003; Kim *et al*., 2009b). Considering this, it may be that the weight decrease is not large enough to be significantly different with this number of mice and weight in general appears to be variable.

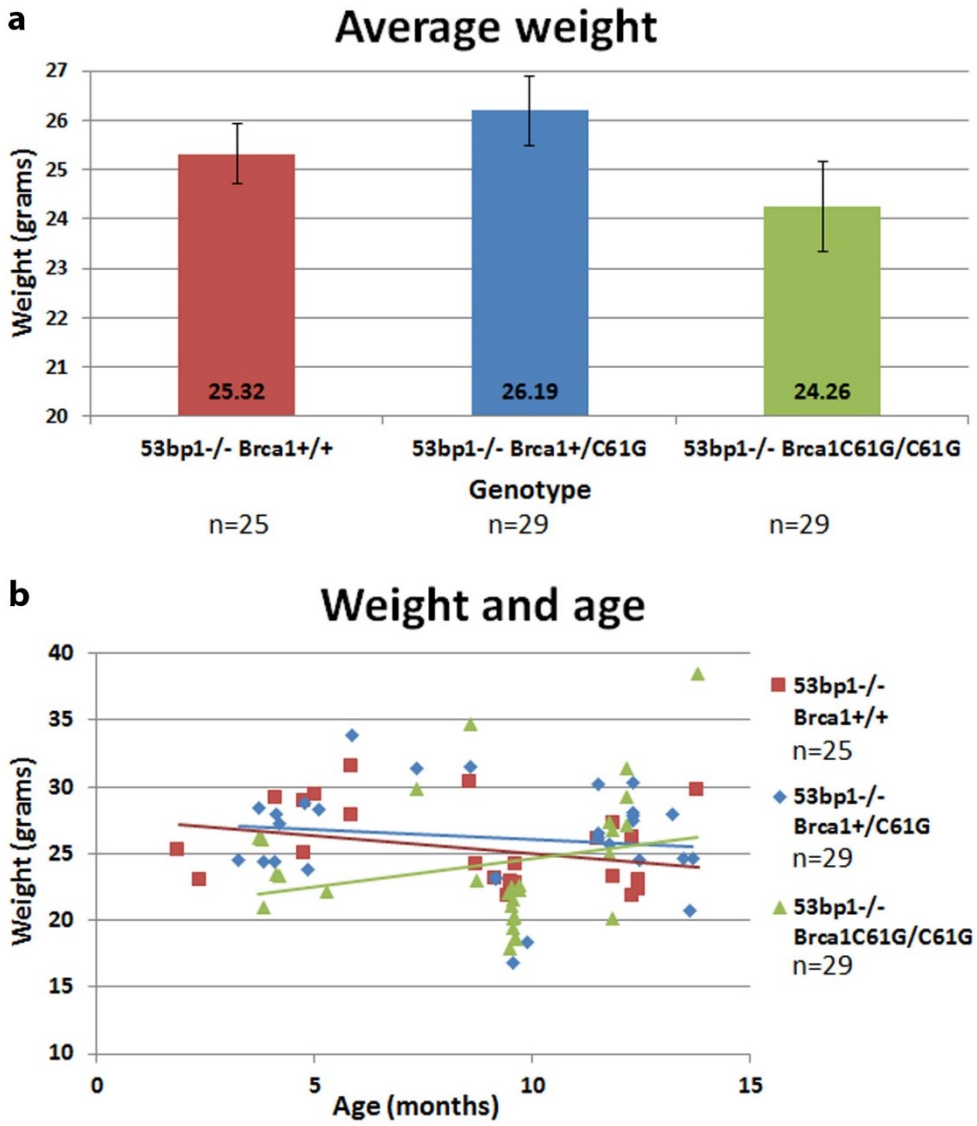

Figure 6.3 – Average weight of 53bp1$^{-/-}$Brca1$^{C61G/C61G}$ mice
[a] shows the average weight of mice from each genotype. Error bars show standard error. None of these weight are significantly different from each other. [b] shows the weights and ages of mice from each genotype. Lines indicate the average weight for the age of the mice. The number of mice in each genotype is shown as 'n=…'.

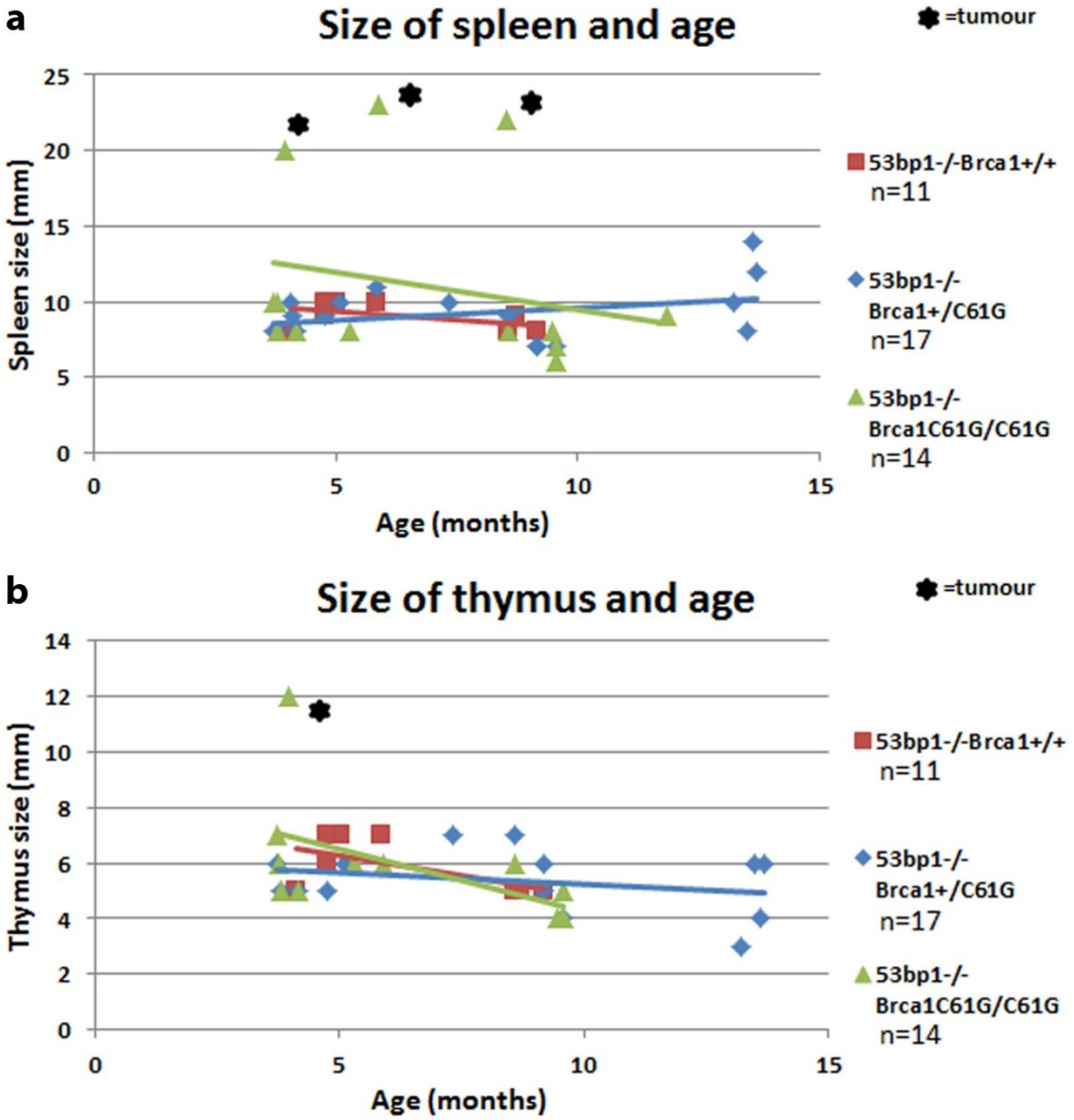

Figure 6.4 – Size of spleen and thymus, and age of 53bp1$^{-/-}$Brca1$^{C61G/C61G}$ mice

This figure shows the [a] size (mm) of spleen and b] the size (mm) of thymuses and relative age of mice of indicated genotypes. The number of mice in each genotype is shown as 'n=…'. Stars indicate a spleen or thymus that was determined to contain a tumour. Lines indicate the average size for spleens or thymuses against the age of the mice.

Table 6.5 – Table of Brca1 mice with an altered weight phenotype or normal weight

Reference	Genotype	Weight status
(Cao *et al*., 2003)	*Brca1$^{\Delta 11/\Delta 11}$;p53$^{+/-}$*	Mice developed age-related weight loss over 64 weeks and the difference between *Brca1$^{\Delta 11/\Delta 11}$;p53$^{+/-}$* and *p53$^{+/-}$* became greater with time
(Cao *et al*., 2006)	*Brca1$^{\Delta 11/\Delta 11}$;Chk2$^{-/-}$*	*Brca1$^{\Delta 11/\Delta 11}$;Chk2$^{-/-}$* mice weight 85% of control mice at 6 months and 10% of the mice showed further reduced weight with age
(Kim *et al*., 2009b)	*Brca1$^{S1152A/S1152A}$*	*Brca1$^{S1152A/S1152A}$* mice had a similar body weight to control mice up to 6 months. After this time body weight decreased in *Brca1* mutant mice whilst the weight of control mice increased and these were significantly different
(Shakya *et al*., 2011)	*Brca1$^{I26A/I26A}$*	*Brca1$^{I26A/I26A}$* mice showed a 5-10% body weight decrease compared to mice with wild-type *Brca1*
(Kim *et al*., 2004)	*Brca1$^{S971A/S971A}$*	phenotypically normal
(Kim *et al*., 2006)	*Brca1$^{FL/FL}$* (Full-length Brca1 only)	phenotypically normal
(Shakya *et al*., 2011)	*Brca1$^{S1598F/S1598F}$*	phenotypically normal
(Bunting *et al*., 2012)	*Brca1$^{\Delta 11/\Delta 11}$;53bp1$^{-/-}$*	phenotypically normal

6.3.3 Spleen and thymus size

The spleen and thymus was isolated and measured from all dissected mice to ensure any enlarged organs could be identified as tumourigenic. This is because previous papers *Brca1*-mutated mice papers showing an increased risk of lymphomas (Bachelier *et al*., 2003; Cao *et al*., 2007; Cressman *et al*., 1999a; Kim *et al*., 2006; Ludwig *et al*., 2001). Figure 6.4 shows the size of the spleen (Figure 6.4a) and thymus (Figure 6.4b) of dissected mice and the age at which they were dissected. This shows that apart from the organs in which a tumour had developed (marked by an asterisk), there was no difference in the sizes of organs between the three genotypes of mice.

6.4 Tumour development

6.4.1 Tumour incidence rate and organ origin

53bp1$^{-/-}$*Brca1*$^{C61G/C61G}$ mice and their littermates were watched to see if they would develop tumours at a higher rate if they lacked a wild-type *Brca1*. Figure 6.5 is a Kaplein Meyer graph showing the rate at which mice from each genotype were found to have a tumour upon dissection (culled due to signs of morbidity). When an abnormal organ was found (wrong shape/size/texture etc) it was photographed and fixed as stated in Chapter 2.5.5. The organs that were determined to be cancerous are shown in Appendices figures III and IV, alongside the diagnosis (from pathologist at HistoloGix), and genotype and age of relevant mouse. Although these results are not significantly different between the genotypes due to low numbers (Table 6.6), it is clear that the *53bp1*$^{-/-}$*Brca1*$^{+/+}$ mice did not develop tumours in the same time frame that the mice with one copy of *Brca1* C61G develop half the rate of tumours as the mice that are homozygote for *Brca1* C61G. These observations need to be replicated with larger numbers of mice over a longer period of time, but as preliminary data this suggests that the C61G mutation in *Brca1* does cause an increased rate of tumour incidence in mice lacking *53bp1*. It also could suggest that one copy of *Brca1* C61G is enough to increase risk of tumourigenesis in mice in a similar manner to *BRCA1* mutation carriers having an increased risk of breast and ovarian cancer.

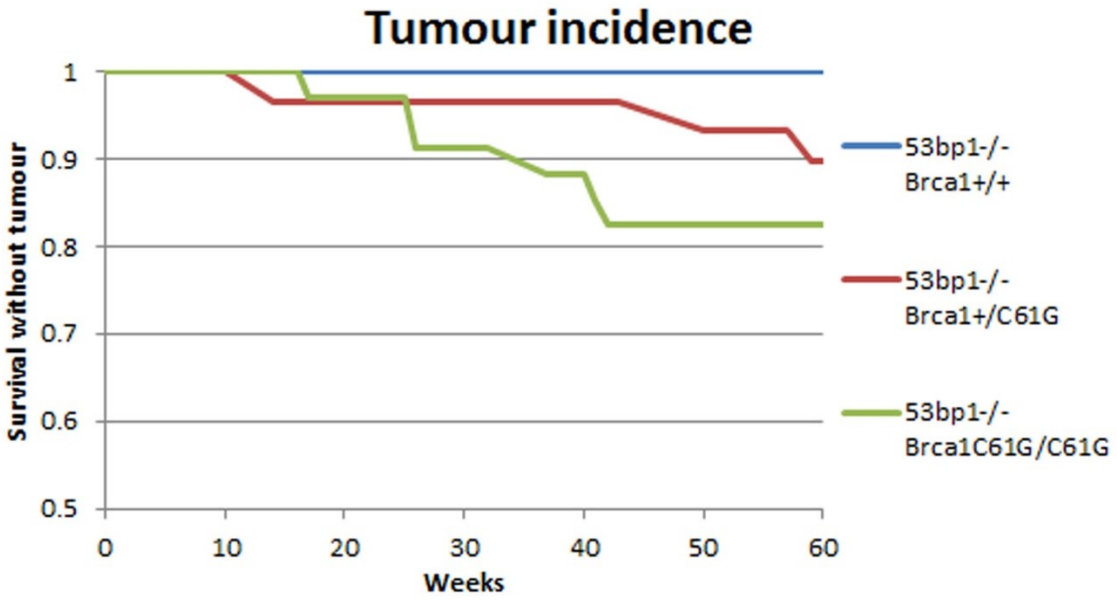

Figure 6.5 – Tumour incidence in 53bp1$^{-/-}$Brca1$^{C61G/C61G}$ mice
This figure shows the fraction of mice from each genotype that were found to have developed a tumour within all the dissected mice that were culled across 60 weeks. Tumours were determined from H&E staining and diagnosed by the pathologist at HistoloGix (Section 2.5.6).

Table 6.6 – Incidence of tumours in dissected mice

	n=	Incidence
53bp1$^{-/-}$Brca1$^{+/+}$	25	0
53bp1$^{-/-}$Brca1$^{+/C61G}$	29	3
53bp1$^{-/-}$Brca1$^{C61G/C61G}$	34	6

Table 6.7 – Tumour incidence in tissue/organ from each genotype

	Spleen	Intestine	Liver	Thymus
53bp1$^{-/-}$Brca1$^{+/+}$	0	0	0	0
53bp1$^{-/-}$Brca1$^{+/C61G}$	1	1	1	1
53bp1$^{-/-}$Brca1$^{C61G/C61G}$	3	1	0	3

Although the *53bp1$^{-/-}$* mice are known to have an increased rate of lymphoma development (Ward *et al*., 2003b), it is likely that the outbreeding or the short time span (60 weeks) is the reason behind the lack of tumour incidence in the *53bp1$^{-/-}$Brca1$^{+/+}$* mice.

The tissue in which the tumours develop is also of interest as it is still not completely clear why *BRCA1* mutations cause predominantly breast and ovarian cancer in humans. Previous

mouse models have shown a range of tissue types to develop tumours due to a *Brca1* mutation, and a substantial number of these mice tumours are lymphomas (Bachelier *et al*., 2003; Cao *et al*., 2003; Cressman *et al*., 1999a; Ludwig *et al*., 2001) or mammary tumours (Cao *et al*., 2003; Cao *et al*., 2006; Kim *et al*., 2004; Xu *et al*., 1999a; Xu *et al*., 2001c). Table 6.7 lists the tissues in which tumours were found in the mice in table 6.6 and in which different genotypes they occurred (some mice had tumours in multiple organs). Of the 11 tumours that were found, 4 were from *53bp1*$^{-/-}$*Brca1*$^{+/C61G}$ mice; the spleen and liver tumours were found in one mouse, and the thymus and intestine tumours were found in different mice. The 7 tumours from *53bp1*$^{-/-}$*Brca1*$^{C61G/C61G}$ mice were found in 6 mice; they consisted of three spleen tumours, 3 thymus tumours and an intestinal tumour (one spleen and one thymus tumour was found in the same mouse). There was one incidence of a mouse with suspected mammary tumours on both left and right side inguinal mammary glands but these tumours have not been assessed further to confirm cancer as of this time (data not included).

6.4.2 Tumour histology

To confirm the presence of cancer in the suspected tumours that were isolated from all mice, the tumours mentioned in table 6.6 and other organs that were abnormal (ovaries with cysts) were sent to HistoloGix Ltd, for blocking, sectioning and H&E stained (Section 2.5.6). The results confirmed which of the specimens were cancerous through the density of cells and types of cell that were found (Figure 6.6i and ii). The histology confirmed that all but two tumours are malignant lymphomas. The *53bp1*$^{-/-}$*Brca1*$^{+/C61G}$ mouse with both a spleen and liver tumours were diagnosed to be a histocytic sarcoma and haemangiosarcoma, respectively. Most of the histology images (Figure 6.6i and ii) showed a range of abnormal

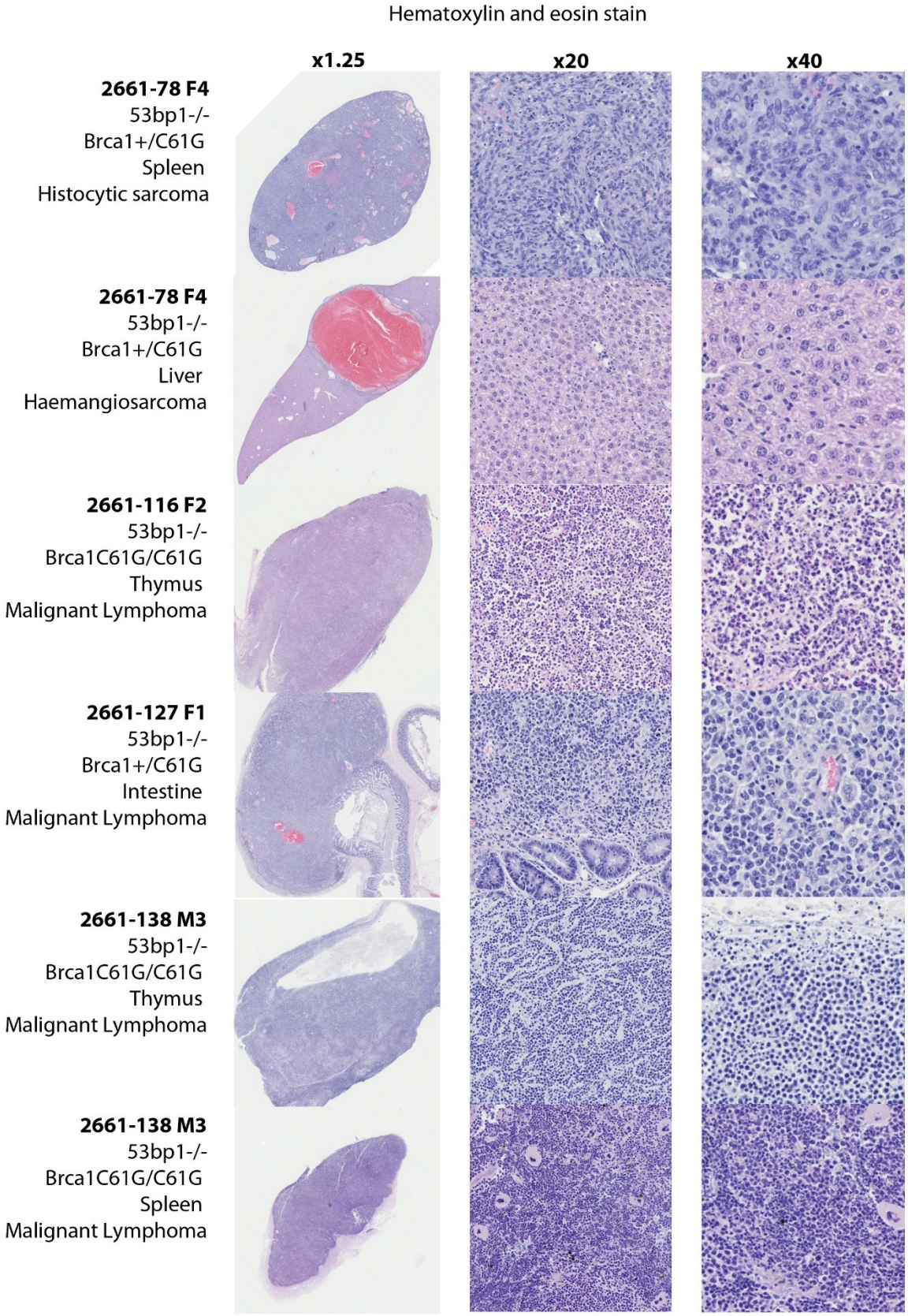

Figure 6.6i – Histological images of tumours from Appendices figures III and IV

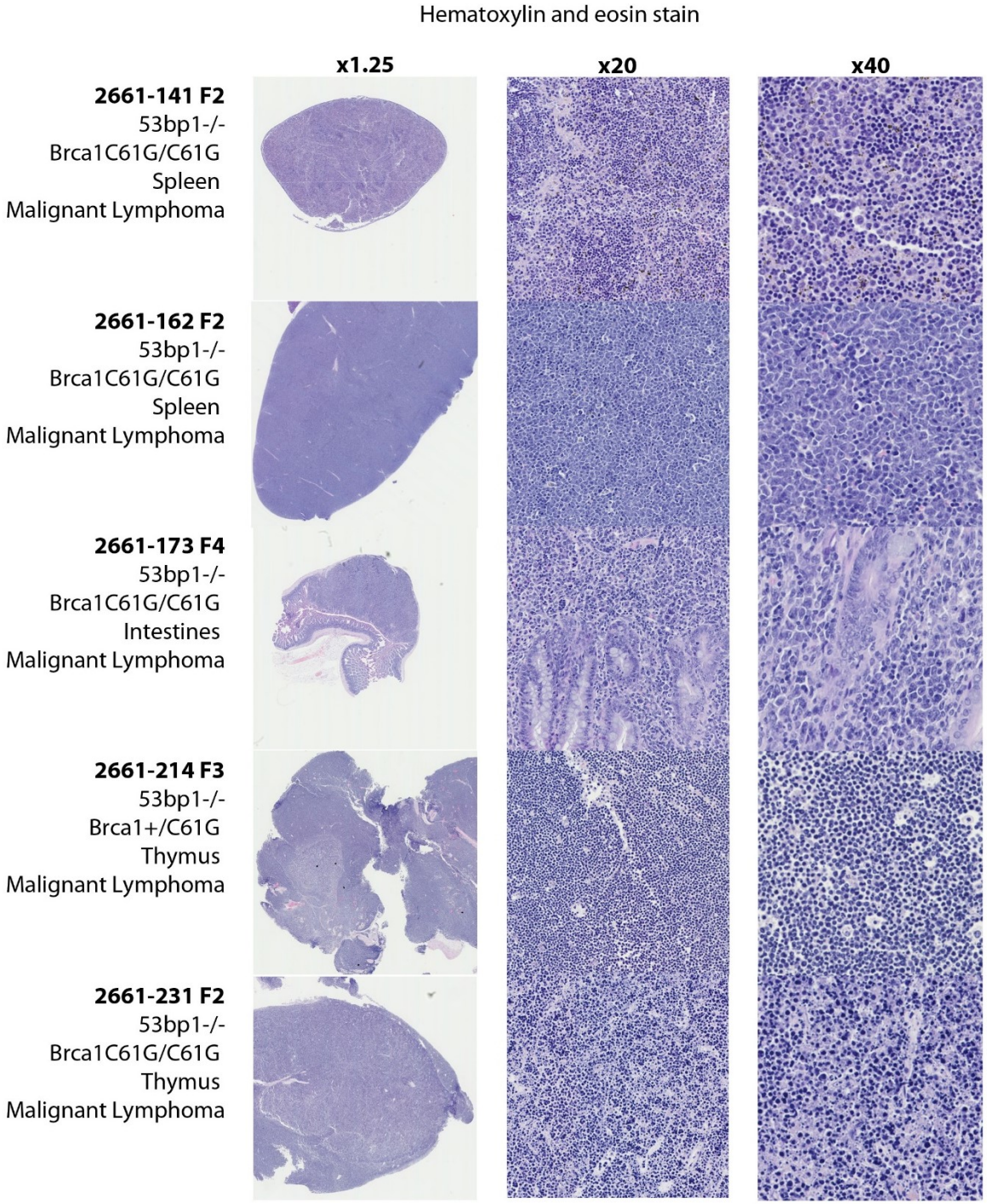

Figure 6.6ii – Histological images of tumours from Appendices figures III and IV continued

Figure 6.6i and ii – Histological images of tumours from Appendices figures III and IV
This figure shows the histological staining using H&E (Methods section 2.5.6) of tumours from Appendices figures I and II. Mice are identified using their cage number and gender number. Genotypes and tumour diagnosis is indicated on the left. The diagnosis was determined by the pathologist, David Fairley, at HistoloGix from original slides and images. Magnification of images by HistoloGix Ltd is as above column (x1.25, x20 or x40).

cells showing signs of enlarged nuclei, reduced cytoplasmic fractions, malformed nuclei and some samples showed Reed-Sternberg cells (large cells with multiple nuclei) that are associated with lymphoma. Although the abnormal cells are enough to diagnose that these tumours are lymphomas, without further histological staining, the particular type of lymphoma cannot be diagnosed.

The origin of the lymphomas could be tested by staining with either CD4 to mark T cell-lineage and B220 to mark B cell-lineage. Other markers could be used to find the point in T or B-cell development the tumour originated; such as IgM and IgD for correctly matured B cells and CD3 and CD45R for correctly matured T cells. This could help to show if the tumour is produced from the genomic instability created by the DSBs formed in V(D)J recombination.

6.5 Discussion

This chapter has shown that the removal of *53bp1* from the $Brca1^{C61G/C61G}$ mice does rescue the developmental defect caused by the *Brca1* mutation because $53bp1^{-/-}Brca1^{C61G/C61G}$ mice are born at expected Mendelian ratio. The lack of developmental defects suggests that the 53bp1-Brca1 interplay is the cause behind the defect in development. Figure 6.1b shows that the *Brca1* genotype does not influence the general survival of $53bp1^{-/-}$ mice suggesting that the *Brca1* C61G mutation does not affect the immune deficiency that causes spontaneous mouse death from unknown reasons.

The $53bp1^{-/-}Brca1^{C61G/C61G}$ mice provide new evidence for two Brca1 roles that are disrupted by the C61G mutation; male fertility and tumour suppression.

$53bp1^{-/-}Brca1^{C61G/C61G}$ mice have male-specific infertility, and this is not a trait associated with *53bp1* deficiency (Ward *et al*., 2003b) but with mice lacking wild-type *Brca1*. Other

Brca1 mutated mice that show male-specific infertility carry either a truncating *Brca1* mutation (Ludwig *et al*., 2001), the N-terminal missense mutation I26A (Shakya *et al*., 2011), the amino acid deletions Δ223-763 (Cressman *et al*., 1999a), the removal of exon 11 (alongside removal of a wild-type p53 allele) (Cao *et al*., 2006; Xu *et al*., 2003) or a Exon 2 deletion (stated to be a protein null-mutation, and alongside the removal of 53bp1) in *Brca1* (Bunting *et al*., 2012; Ludwig *et al*., 1997). Not all *Brca1* mutations cause male sterility; $Brca1^{S1152A/S1152A}$ (Kim *et al*., 2009b), $Brca1^{S971A/S971A}$ (Kim *et al*., 2004) or mice with only full-length *Brca1* (no Δ11 isoform) (Kim *et al*., 2006) do not confer any sterility in male or female mice. These results alongside our findings, could suggest that the N-terminal RING domain and the C-terminal BRCT domains of Brca1 are required for male fertility. The ubiquitin ligase function of Brca1 may also be required since the Δ223-763 mutation does remove some of the N-terminal region known to be needed for BRCA1 autoubiquitination (Chen *et al*., 2002), and the I26A mutant is a Brca1 E3 ubiquitin ligase activity-targeting mutation (Brzovic *et al*., 2003). The *Brca1* C61G mutation protein levels are reduced compared to wild-type Brca1 protein (Figure 4.5) so the male infertility seen in these mice may be due to the reduced levels of the entire Brca1 protein and therefore may not provide evidence for N-terminal function of Brca1 in meiosis. But since there is remaining C61G mutated protein, which lacks ubiquitin ligase activity (Figure 3.6), it is possible that this may contribute to the male sterility, however levels of Brca1 in meiotic cells would need to be investigated. Whether the $53bp1^{-/-}Brca1^{C61G/C61G}$ male infertility is due to Brca1's role in the crossover regulation, or sex chromosome inactivation, would require further investigation. The male sterility in $53bp1^{-/-}$ $Brca1^{C61G/C61G}$ mice which is not seen in littermates suggests this is an example of a 53bp1-

independent role for Brca1 and a role in which one wild-type allele of *Brca1* is sufficient for normal function.

The increase in tumour development in *53bp1*$^{-/-}$ mice with one or two copies of *Brca1* C61G suggests that the removal of 53bp1 does not rescue the Brca1 tumour suppressing function that is disrupted by this mutation. It is interesting that the *53bp1*$^{-/-}$*Brca1*$^{\Delta 11/\Delta 11}$ mice do not show any increased tumour development over 53bp1-null mice (Bunting *et al*., 2010), suggesting that there is a difference in the tumour suppressing properties of the *Brca1* C61G and Δ11 mutated protein. The fact that heterozygotes do produce tumours at a higher rate than *53bp1*$^{-/-}$*Brca1*$^{+/+}$ mice is suggestive of a 53bp1-independent tumour suppressing role for Brca1 with the *Brca1* C61G mutation causing haploinsufficiency. The reduced protein seen in mice with one or two copies of *Brca1* C61G (Section 4.5) suggest that the C61G mutation reduced the amount of Brca1 protein, therefore it is not possible to say that the N-terminus of Brca1 is important for tumour suppression. It would be interesting to look at the *Brca1* allele status and protein status in the tumours from the *53bp1*$^{-/-}$*Brca1*$^{+/C61G}$ mice to see if LOH has occurred, or if the protein is reduced compared to normal tissues in that mouse. This would give more idea of the influence of Brca1 protein levels and the role of LOH in tumour development in these mice.

The majority of tumours found in the mice with a *Brca1* C61G mutation were lymphomas, which is similar to other *Brca1* mutated mice (Bachelier *et al*., 2003; Cao *et al*., 2007; Cressman *et al*., 1999a; Jeng *et al*., 2007; Ludwig *et al*., 2001), and *53bp1*$^{-/-}$ mice (Ward *et al*., 2003b). It would be interesting to stain the lymphomas to see if they are B or T-cell in origin since the *Brca1* mutant mice are known to produce a mix of B and T cell lymphomas

(Bachelier *et al*., 2003; Jeng *et al*., 2007; Ludwig *et al*., 2001), but the *53bp1*$^{-/-}$ mice produce exclusively T cell lymphomas (Ward *et al*., 2003b). This information would be able to shed light on whether the *Brca1* C61G mutation was important for a Brca1 role in lymphocyte genome maintenance or if the *53bp1*$^{-/-}$ phenotype is exacerbated by a *Brca1* mutation.

One avenue would be to see which lymphocyte development stage that the tumour originated from as, if it is the dysregulation of the TCR, CSR and V(D)J recombination which happens in maturing B and T-cells, this may give more insight into the role that 53bp1 and Brca1 play in DNA repair in these processes.

In a recent paper, Vasanthakumar *et al* created mice that possessed two copies of *Brca1* Δ11 allele conditionally expressed in haematopoietic cells (Vasanthakumar *et al*., 2016). These mice developed bone marrow failure from 1 month and 6 had developed haematopoietic malignancies by 190 days (4 lymphomas, 1 acute myeloid leukaemia and 1 erythroleukemia) and cells from these malignancies showed chromosomal instability and a sensitivity to mitomycin C, a DNA crosslinking-agent (Vasanthakumar *et al*., 2016). They also presented evidence that suggested that cells in the peripheral blood originated from the bone marrow malignancies and they infiltrated organs (Vasanthakumar *et al*., 2016). This could suggest that lymphoma development in the organs may originate from a bone marrow malignancy. Brca1 has been shown to be important in the maintenance of haematopoietic stem cells populations (Bai *et al*., 2013) and some myeloid leukaemias show a reduced expression of Brca1 (Deutsch *et al*., 2003; Scardocci *et al*., 2006). This data may suggest that *Brca1* has a role in haematopoietic cell genome stability and therefore, it may be interesting to

investigate bone marrow changes in the *53bp1*$^{-/-}$*Brca1*$^{C61G/C61G}$ mice to look for a mechanism behind the development of lymphomas in these mice.

It is interesting that the same level of lymphoma development is not seen in human patients carrying a *BRCA1* mutation (Chen *et al*., 2013; Friedenson, 2007; Kadouri *et al*., 2007; Kim *et al*., 2014; Shen *et al*., 2006; Shih *et al*., 2000; Yossepowitch *et al*., 2003), although there are two cases, each of an individual *BRCA1* mutation carrier patient that developed a B-cell lymphoma (Kim *et al*., 2015; Shen *et al*., 2000). This may highlight the unknown and unexplained differences between human diseases and the mouse model of the corresponding disease.

The rescue of developmental defects seen in *Brca1* C61G homozygote mice by the removal of *53bp1* suggests that any other phenotypes in the mice are indicative of Brca1 roles that are affected by the C61G mutation but roles in which 53bp1 does not play a part, i.e tumour suppression or meiosis.

Chapter 7 – Discussion

7.1 Evaluation of data

7.1.1 Novel data

This thesis has discussed the gap in the literature for investigation into N-terminal *BRCA1* patient mutations expressed at endogenous levels in cells created by genome editing (not in genomically unstable tumour cells), and this gap is largely due to the embryonic lethality of *Brca1* homozygote mutations. The research described here shows the creation of a MEF cell line and starts to investigate Brca1 C61G protein and its effects.

The novel findings in this thesis are:-

- A comparison of *in vitro* E3 ubiquitin ligase activity using mouse and human Brca1:Bard1 RING domain heterodimer showing that they are equivalent in their ability to make polyubiquitin chains (Chapter 3.5).
- There is a role for Bard1 in Brca1:Bard1 heterodimer E3 ubiquitin ligase activity in mouse that is not associated with the stability of the heterodimer and that the arginine residue 93 is important for this Bard1 function (Chapter 3.7). This confirms the role of the corresponding human BARD1 R99 residue that have been described Ruth Densham from the Morris lab, but not yet published.
- The removal of *53bp1* from homozygote *Brca1* C61G mice does rescue embryonic lethality but *53bp1*$^{-/-}$*Brca1*$^{C61G/C61G}$ cells are still significantly more sensitive to IR than cells with only wild-type *Brca1*, despite HR being functional to the point of normal Rad51 foci levels (Chapter 5 and 6) (previous papers suggest the lack of HR DSB repair may be the cause of embryonic lethality (Bouwman *et al*., 2010; Bunting *et al*.,

2010)). This is different from the literature as the *53bp1*$^{-/-}$*Brca1*$^{\Delta 11/\Delta 11}$ cells show a wild-type level of cell survival after IR-treatment (Figure S1 in Bunting *et al*, 2010) compared to the reduced cell survival seen in *p53*$^{-/-}$*Brca1*$^{\Delta 11/\Delta 11}$ cells (Bunting *et al*., 2010).

- Two copies of *Brca1* C61G causes an increase in FANCD2 foci and a reduction of Rad51 foci after MMC treatment (Chapter 5.5) compared cell with wild-type *Brca1*. The literature has previously shown that a reduction in wild-type Brca1 has led to a decrease in FANCD2 foci (Bunting *et al*., 2012; Garcia-Higuera *et al*., 2001; Vandenberg *et al*., 2003; Zhang *et al*., 2010) and a decrease in cells with Rad51 foci after MMC (Bunting *et al*., 2012).
- *53bp1*$^{-/-}$ mice with one or two copies of *Brca1* C61G do have an increased rate of tumour development (Chapter 6.4). This is not the case with *53bp1*$^{-/-}$*Brca1*$^{\Delta 11/\Delta 11}$ mice that do not show an increase incidence of tumours compared to mice with a wild-type copy of *Brca1* (Bunting *et al*., 2010).

7.1.2 Caveats of the data

Data presented here has various caveats which need to be taken into consideration before making firm conclusions and adding the data here to the literature. Firstly, there are control cells which would have made this data stronger, such as cells with wild-type *53bp1* and homozygote *Brca1* C61G mutation. These cells would have provided a control to look at the effects of the *Brca1* C61G mutation without any background phenotypes from the lack of *53bp1*. However, *Brca1* C61G mice are embryonic lethal and attempts to produce a cell line through the addition of *53bp1* cDNA through transfection or electroporation caused cell death.

The *Brca1* Δ11 cell lines do not replicate the published data despite using the stated protocols (Bunting *et al*., 2010; Bunting *et al*., 2012). This was particularly evident in looking at FANCD2 foci and the cells reactions to DNA-damaging drugs and IR (Chapter 5). The NIH3T3 cells line was also used as a wild-type control cell line, but also has caveats as it is designed to be a senescent mono-layer cell line for the growth of primary cells. When using NIH3T3 cells as a control for the comparison of 53bp1 and Brca1 protein, it became evident that they produced a higher amount of 53bp1 protein than expected and very little Brca1 protein, despite being 'wild-type' cells. This makes NIH3T3 unreliable as the protein status (perhaps genomic status) for these important proteins is not clear and is likely not to replicate wild-type conditions. If the *Brca1* Δ11 cells and the NIH3T3 cells are not reproducing expected conditions, then comparisons using these cells need to be confirmed using alternative controls.

53bp1$^{+/-}$*Brca1*$^{+/C61G}$ cells are used throughout this these as control for comparison but it is important to consider that they are heterozygote for both *Brca1* and *53bp1*. Ward *et al* reported that one copy of *53bp1* is sufficient for normal 53bp1 roles, and therefore they should behave as wild-type cells in respect to *53bp1* phenotypes (Ward *et al*., 2003b). This is not the same with *Brca1* mutations as a single mutated allele gives increased risk in cancer development in human and mice (Clark *et al*., 2012; Cressman *et al*., 1999b), and cellular functions are altered with a single mutated *Brca1* allele which has been shown in the literature (Barwell *et al*., 2007; Buchholz *et al*., 2002; Ernestos *et al*., 2010; Febrer *et al*., 2008; Foray *et al*., 1999; Kote-Jarai *et al*., 2006; Rothfuss *et al*., 2000; Speit *et al*., 2000; Speit and Trenz, 2004) and in this thesis (Chapter 7.2.4). This thesis does compare *53bp1*-null background cells with wild-type *Brca1* and heterozygote and homozygote *Brca1* C61G cells

to look the effect of a single *Brca1* C61G mutation. This data could be repeated with a wild-type control MEF line, however, since a *Brca1*$^{C61G/C61G}$ cell would not be produced (Drost *et al*., 2011), the data would still have the caveat of a *53bp1*-null background. It would be interesting to use a *Brca1*$^{+/C61G}$ and wild-type cell line to look further at the roles of a heterozygote *Brca1* C61G mutation.

The whole-cell protein extract (WCE) western blots in this thesis produced variable data when using the GH118 anti-Brca1 antibody. However when the cytoplasm and nuclear fractions of MEFs were used as separate western blot samples or this antibody (GH118) was used for IRIF, the results were consistent between repeats. This data does allow more information on the localisation of Brca1 protein than the measurement of Brca1 protein in a WCE. Before publishing or taking firm conclusions from the WCE western blots, other Brca1-specific antibodies should be used to repeat this experiment.

Finally, the tumour data here is preliminary and could not be statistically analysed due to the small sample size. There were delays in acquiring home office licences for this tumour watch which reduced the number of results available for analysis at this time. This delay also caused a reduction in the length of time mice were part of the tumour watch which I believe has not allowed enough time for these outbred *53bp1*-null mice to produce tumours (like previous papers have shown (Ward *et al*., 2003b)). Despite this, the data in this thesis does shown more tumour incidence in mice with one or two copies of *Brca1* C61G allele than those with only wild-type *Brca1*.

The cell cycle can greatly influence the way cells respond to DNA-damaging agents, and although the *Brca1* C61G MEF cells divide at a similar rate (tissue culture passaging), further

experiments into the presence of cell cycle checkpoint should be investigated. An attempt to look at the G2/M checkpoint was made using PI stain across time points after IR, but the control cells (*53bp1*$^{+/-}$*Brca1*$^{+/C61G}$) showed abnormalities (an unidentified population of cells) which made incomparable to the experimental MEFs. Therefore other controls, such as wild-type cells, and an alternative *53bp1*$^{+/-}$*Brca1*$^{+/C61G}$ MEF cell line should be used to assess the cell cycle checkpoints in *53bp1*$^{-/-}$*Brca1*$^{C61G/C61G}$ MEFs.

7.2 Discussion of the results

7.2.1 Brca1 C61G protein

As discussed in the introduction, the literature suggests that further investigation is needed into the structural consequences of N-terminal pathogenic mutations, particularly into the whether the BRCA1 C61G protein is stable or instable as the literature is divided (Chapter 1.3.3). The *Brca1* C61G missense mutation has been shown here to affect the entire Brca1 protein levels in cells, its degradation potential and its localisation to IRIF (Chapter 5). This suggests that a missense mutation can cause protein-wide defects and that individual mutations should be studied to be able to predict which residues would produce this effect. Unfortunately the tumour incidence and cell-based data in this thesis does not provide information about the N-terminal function of Brca1 because the C61G mutation affect is not specific to the N-terminal region of Brca1 as it affects the stability of the whole protein. Although the *Brca1* C61G mutation does affect the E3 ubiquitin ligase activity of the Brca1:Bard1 heterodimer *in vitro* (Chapter 3), it cannot be said that the phenotypes described here are specifically due to a defect in Brca1 ubiquitin ligase activity due to the reduction in Brca1 C61G protein.

7.2.2 *Brca1* C61G in DNA repair and genome stability

The embryonic lethality of *Brca1* mutant homozygote mice is suggested to be due to overwhelming DNA damage and errors, that makes normal embryonic develop unsustainable. The removal of *53bp1* from *Brca1* mutant cells has previously been shown to rescue *Brca1* mutant phenotypes, specifically *Brca1* Δ11 phenotypes (Chapter 1.5.5) (Bouwman *et al*., 2010; Bunting *et al*., 2010; Cao *et al*., 2009) and this is due to DSB repair being functional in Brca1 mutated cells that lack 53bp1. The presence of *53bp1*$^{-/-}$ *Brca1*$^{C61G/C61G}$ mice and MEFs shows that the absence of *53bp1* does rescue the embryonic lethality of a homozygote *Brca1* C61G mutation. This agrees with the literature that the *53bp1* and *Brca1* are antagonistic in their roles of promoting either DSB repair pathway and the mutation of both *53bp1* and *Brca1* alleles leads to normal development of mice through the same alleviation of DNA damage (Bouwman *et al*., 2010; Bunting *et al*., 2010).

According to their research, *53bp1*$^{-/-}$*Brca1*$^{\Delta 11/\Delta 11}$ cells show normal cell survival after IR-treatment and similar levels of cells with Rad51 foci formation comparable to wild-type cells (Bunting *et al*., 2010). Here, it is shown that *53bp1*$^{-/-}$*Brca1*$^{C61G/C61G}$ cells have a similar number of cells with Rad51 foci formation after IR compared to cells with a wild-type copy of *Brca1.* But, we have also shown *53bp1*$^{-/-}$*Brca1*$^{C61G/C61G}$ cells have a significantly reduced cell survival after IR treatment compared to cells with a wild-type copy of *Brca1* (Chapter 5). Since it appears that HR is functional beyond the DSB repair pathway choice, there are two possible theories as to why these cells are sensitive to IR. Firstly, HR is functional and the sensitivity is caused by Brca1 being defective for its role in NHEJ, or secondly, there are defects in HR after the presence of Rad51 foci that are affected by the *Brca1* C61G mutation, but not the *Brca1* Δ11 mutation (Bunting *et al*., 2010). BRCA1's role in NHEJ appears to be in

aiding Ku80 stability at DSB DNA ends providing an error-free method of DSB repair in G1 phase of the cell cycle (Dohrn *et al*., 2012; Jiang *et al*., 2013a; Wei *et al*., 2008). Since IR-induced breaks throughout the cell cycle, it could be that BRCA1 C61G protein causes erroneous repair in G1 and this leads to the reduced survival of *53bp1*$^{-/-}$*Brca1*$^{C61G/C61G}$ MEFs after IR. It is also interesting to note that the reported Ku80 binding site is competitive with BARD1, the RING domain, and this is mutated in the *53bp1*$^{-/-}$*Brca1*$^{C61G/C61G}$ MEFs but the Brca1 Δ11 isoform that is present in *53bp1*$^{-/-}$*Brca1*$^{\Delta 11/\Delta 11}$ cells would have a wild-type RING domain (Jiang *et al*., 2013a; Wei *et al*., 2008). This could be further investigated by looking at the DNA sequences of DNA repaired in these cells through HR and NHEJ in G1 and G2 phase of the cell cycle, to see if these are being repaired by these repair pathways and if the repair is error-free.

The literature describes BRCA1's role in DNA crosslink repair to be *53bp1*-independent role (Bunting *et al*., 2012) and therefore is would be predicted that *53bp1*$^{-/-}$*Brca1*$^{C61G/C61G}$ MEFs would be sensitive to DNA crosslinking agents, such as Cisplatin and MMC. Long *et al* report that BRCA1 is essential for the removal of the CMG helicase from DNA crosslinks to allow FANCD2 and nuclease localisation (Long *et al*., 2014). The *53bp1*$^{-/-}$*Brca1*$^{C61G/C61G}$ MEFs are Cisplatin sensitive as were the *53bp1*$^{-/-}$*Brca1*$^{\Delta 11/\Delta 11}$ cells (Bunting *et al*., 2012). However, *53bp1*$^{-/-}$*Brca1*$^{C61G/C61G}$ MEFs have an increased level of FANCD2 foci after MMC which is the opposite of what has been reported in *53bp1*$^{-/-}$*Brca1*$^{\Delta 11/\Delta 11}$ cells (Bunting *et al*., 2012) and other Brca1-depleted cells (Bouwman *et al*., 2010; Garcia-Higuera *et al*., 2001; Vandenberg *et al*., 2003; Zhang *et al*., 2010). Since the Brca1 C61G protein appears to reduce protein levels but not eradicate the protein, it could be that the increase in FANCD2 foci after MMC in *53bp1*$^{-/-}$*Brca1*$^{C61G/C61G}$ MEFs is the dominant effect of C61G mutated *Brca1* that stops the

removal of FANCD2 from DNA crosslink sites, and different *Brca1* mutations may not produce this effect. However, it is also possible that BRCA1 C61G is functional for FANCD2 recruitment but it cannot remove CMG which is a step needed for FANCD2 foci removal (Long *et al*., 2014). Long *et al*, blocked the DNA polymerase (using Aphidicolin) which delayed CMG unloading from ICL replication forks, and this did not disrupt the localisation of BRCA1, FANCD2 and Rad51 (Long *et al*., 2014), suggesting that BRCA1's recruitment of FANCD2 and Rad51 to site of ICL repair is independent of BRCA1's role in CMG unloading. FANCD2 recruitment was also shown to be prior to CMG removal (Long *et al*., 2014) despite its role in creating DNA incisions which is downstream of CMG unloading (Knipscheer *et al*., 2009), suggesting CMG unloading may delay the role of FANCD2 in incision formation and, consequently, its dispersion from sites of ICL as we have seen in *53bp1*$^{-/-}$*Brca1*$^{C61G/C61G}$ MEFs. Long *et al*, also reported that the BRCT domains were required for BRCA1 recruitment to ICL's and that the BRCA1:BARD1 heterodimer was essential for CMG unloading (Long *et al*., 2014). This suggests that BRCA1 RING domain is needed for the CMG unloading, but may be independent of the BRCT domains roles in localisation and recruitment of FANCD2, and therefore Brca1 C61G can be functional for FANCD recruitment but not be able to unload the CMG helicase causing defects in DNA crosslink repair.

This does agree with the literature in that Brca1 has a 53bp1-independent role in DNA crosslink repair (Bunting *et al*., 2012), but is novel in its effect on FANCD2 foci. Further investigation could identify if CMG or BRCA1 also have prolonged localisation to DNA crosslinks to help unpick the mechanism behind this phenotype.

CPT and HU both produce DNA/protein lesions as part of the DNA damage they exert and HR is used as part of the method of repairing these lesions. The *53bp1*$^{-/-}$*Brca1*$^{C61G/C61G}$ cells showed significant sensitivity to CPT compared to *53bp1*$^{-/-}$*Brca1*$^{+/+}$ MEFs, however, the *53bp1*$^{+/-}$*Brca1*$^{+/C61G}$ cells were similar in sensitivity to cells with *53bp1*$^{-/-}$*Brca1*$^{C61G/C61G}$ cells suggesting another control (a fully wild-type control) is needed to confirm this finding. The *53bp1*$^{-/-}$*Brca1*$^{C61G/C61G}$ cells did show some sensitivity (only one data point is significant due to large standard errors) to HU compared to *53bp1*$^{-/-}$*Brca1*$^{+/+}$ MEFs. However, *53bp1*$^{-/-}$ *Brca1*$^{+/C61G}$ cells showed a significantly greater sensitivity on all data point compared to *53bp1*$^{-/-}$*Brca1*$^{+/+}$ MEFs and the control *53bp1*$^{+/-}$*Brca1*$^{+/C61G}$ cells were variable in their sensitivity. If the sensitivity of *53bp1*$^{-/-}$*Brca1*$^{+/+}$ MEFs to CPT and HU were to be confirmed through further experiments, then this would merit further investigation into whether Brca1 C61G influences the repair of DNA/protein lesions. Especially as a recent paper described a role for BRCA1 in DNA adducts created after Topoisomerase II inhibitors (Aparicio *et al*., 2016).

Defects in DNA repair lead to the accumulation of DNA errors and unresolved DNA damage, continuing to cells that are genomically unstable. Despite the normal development of *53bp1*$^{-/-}$*Brca1*$^{C61G/C61G}$ mice, *53bp1*$^{-/-}$*Brca1*$^{C61G/C61G}$ cells are sensitive to multiple DNA-damaging agents suggesting that DNA repair is erroneous. *53bp1*$^{-/-}$*Brca1*$^{C61G/C61G}$ mice also show a higher incidence of tumour development (Chapter 6) which is an indicator of genome instability and typical of mice with a genetic DNA repair defect.

7.2.3 *Brca1* C61G and male-specific Infertility

The male-specific infertility in *53bp1*$^{-/-}$*Brca1*$^{C61G/C61G}$ mice (Chapter 6) does agree with other *Brca1* mutant mouse models that show a similar phenotype (Introduction section 1.5.4), that *Brca1* is specifically important for male spermatogenesis. This role is not seen in mice with *53bp1* mutations (Ward *et al*., 2003b), but is also seen in male *53bp1*$^{-/-}$*Brca1*$^{-/-}$ mice (Bunting *et al*., 2012). Brca1 has been shown to have roles in meiosis that include DSB repair enabling chromatid crossover events (Cressman *et al*., 1999a; Shakya *et al*., 2011; Xu *et al*., 2003) and a role in inactivating unsynapsed chromosomes and the XY body (Adamo *et al*., 2008; Ganesan *et al*., 2002; Turner *et al*., 2004; Turner *et al*., 2005; Xu *et al*., 2003). Collectively this suggests that it is a *53bp1*-independent *Brca1* role that causes male-specific infertility in the *53bp1*$^{-/-}$*Brca1*$^{C61G/C61G}$ mice.

7.2.4 *Brca1* C61G heterozygote effects

Several of the results in this thesis suggests that a heterozygote *Brca1* C61G mutation is adequate to produce cellular defects. *53bp1*$^{-/-}$*Brca1*$^{+/C61G}$ MEFs show the following heterozygote phenotypes: decrease in Brca1 C61G protein levels, reduced Brca1 IRIF in Brca1 heterozygote cells and the tumour incidence in *53bp1*$^{-/-}$*Brca1*$^{+/C61G}$ mice. The decrease in Brca1 protein levels in the cell and in the nucleus and cytoplasm in heterozygote *Brca1* C61G cells (with or without *53bp1*) (Chapter 4) has the potential to produce haploinsufficient phenotypes. There are less Brca1 IRIF in *53bp1*$^{+/-}$*Brca1*$^{+/C61G}$ cells compared to *53bp1*$^{-/-}$ *Brca1*$^{+/+}$ cells (Chapter 4) and this is likely to be due to the reduction of Brca1 C61G protein compared to cells with two wild-type *Brca1* alleles. This reduction in Brca1 IRIF also has the potential to produce haploinsufficient phenotype due to a lack of Brca1 localising for its roles in DNA repair. This thesis has also shown that mice with one or more copy of *Brca1* C61G in

a *53bp1*-null background do have an increased rate of tumour development (Chapter 6). This, again, is likely to be due to the *Brca1* C61G mutation causes a reduction in Brca1 protein (Chapter 4) and the C61G mutated Brca1 protein that is present in the cells altering genome stability in the *53bp1*-null background. This thesis does not investigate whether the tumours that arose in the *53bp1*$^{-/-}$*Brca1*$^{+/C61G}$ mice have lost the wild-type allele of *Brca1* or whether the *Brca1* C61G allele causes haploinsufficiency or a dominant-negative phenotype in maintaining genome instability in a *53bp1*-null background. It would be interesting to add *53bp1*$^{+/+}$*Brca1*$^{+/C61G}$ and *53bp1*$^{+/-}$*Brca1*$^{+/C61G}$ mice to the tumour watch programme to assess whether they also show a higher rate of tumour development and to look at whether these tumours show loss of heterozygosity of *Brca1*.

7.2.5 *Brca1* Δ11 and *Brca1* C61G phenotypes

The *Brca1* C61G mutation causes a reduction in Brca1 protein suggesting the defect is protein-wide (Chapter 4) and not a specific defect to the N-terminus of the Brca1 protein. Brca1 Δ11 mimics a known BRCA1 isoform that lacks exon 11 and therefore Brca1 Δ11 protein does produce a protein product and it has been shown that it can localise to IRIF (Huber *et al*., 2001). This thesis shows that these two *Brca1* mutations (*Brca1* C61G and *Brca1* Δ11) display different phenotypes in a *53bp1*-null background. *53bp1*-null homozygote *Brca1* Δ11 cells are not sensitive to IR or CPT (Chapter 5), and show reduced a normal level of FANCD2 foci after MMC (Chapter 5), unlike *53bp1*-null homozygote *Brca1* C61G cells which are sensitive to IR and CPT and show an increase in FANCD2 levels after MMC (Chapter 5). *53bp1*$^{-/-}$*Brca1*$^{C61G/C61G}$ cells also show a decrease in Rad51 foci after MMC and increased tumour development in mice, unlike *53bp1*$^{-/-}$*Brca1*$^{\Delta 11/\Delta 11}$ counterparts (Chapter 5 and 6). Bunting *et al* showed that the *53bp1*$^{-/-}$*Brca1*$^{\Delta 11/\Delta 11}$ mice were fertile, but *53bp1*$^{-/-}$

Brca1$^{\varphi/\varphi}$ male mice (ϕ – Exon 2 is deleted) were infertile like the *53bp1*$^{-/-}$*Brca1*$^{C61G/C61G}$ mice presented in this thesis (Bunting *et al*., 2012).

It is possible to speculate from these results that the *Brca1* Δ11 mutation does not affect the role that Brca1 has in IR and CPT sensitivity that is altered by the *Brca1* C61G mutation, and perhaps this is due to Brca1 Δ11 having intact RING and BRCT domains. The remaining Brca1 C61G protein could have a dominant-negative phenotype on DNA damage which cannot be rescued by the removal of 53bp1 protein, and the Brca1 Δ11 protein may behave as the Δ11 isoform and the protein does not cause defects from its presence. The fact that the *Brca1* Δ2 deletion (Bunting *et al*., 2012), which removes all Brca1 protein, causes male sterility like the Brca1 C61G protein suggests that it is the inability of Brca1 to function that causes the male-specific infertility. The Brca1 Δ11 does not cause infertility (Bunting *et al*., 2012) and therefore it is likely that the Brca1 Δ11 does have some ability to function. Other *Brca1* mouse models that have either a BRCT or RING domain disrupting mutation show male sterility suggesting both the C-terminus and N-terminus is important for *Brca1*'s role in male meiosis (Figure 1.11).

Considering this, the attributed phenotypes in the literature using Brca1 Δ11 alleles may not reflect a truly defective Brca1. The *Brca1* C61G mutation investigated here is not a clearly defective Brca1 as there is remaining Brca1 C61G protein and it may cause dominant-negative phenotypes. Therefore it is important to clarify what a mutation does to the protein in an *in vitro* and *in vivo* manner since the effects may be diverse. Using a patient mutation, such as C61G, does create clinically relevant research, and highlight the need for more basic research to understand pathogenic human *BRCA1* mutations.

7.2.6 Clinical implications

Since *BRCA1* C61G is a patient mutation, the data here has the potential to provide information that aids how *BRCA1* C61G carriers are seen clinically. Firstly, this thesis shows that reduction of Brca1 C61G protein compare to wild-type Brca1 protein therefore the cells may show phenotypes that relate to the entire protein not just N-terminus-involving functions. It is also important that these MEFs have been genomically manipulated and Brca1 C61G is expressed at endogenous levels, making the phenotypes clinically relevant in comparison to data from overexpressed *BRCA1* C61G cDNA. Data from this thesis could also provide information for cancers that have reduced BRCA1 expression or sporadic N-terminal *BRCA1* gene mutations.

The MEFs and mice were only possible to study due to the absence of *53bp1* rescuing the embryonic lethality of *Brca1* C61G homozygote mice. This means the majority of data in this thesis is in a *53bp1*-null background which is not replicative of human patients. However, Bouwman *et al* show that reduced 53BP1 expression has a correlation to poorer survival outcome of patients with breast cancer (and triple-negative breast cancer) (Bouwman *et al*., 2010), suggesting 53bp1 reduction could be used as a biomarker for harder-to-treat breast cancers. Therefore the data from the *53bp1*$^{-/-}$*Brca1*$^{C61G/C61G}$ cells may provide insight into these tumours.

This thesis shows *53bp1*$^{-/-}$*Brca1*$^{C61G/C61G}$ cells are sensitive to IR, CPT, HU and Cisplatin (Chapter 5). The sensitivity to these agents suggests *Brca1* C61G influences Brca1's role in DNA crosslink repair and, potentially, NHEJ or DSB repair involving DNA lesions. Therefore *53BP1*-negative, *BRCA1*-mutated cancer cells should be sensitive to chemotherapies that

cause DNA damage similar to these agents. However, it is likely that these cells are highly genomically unstable and may become resistant to therapies.

The *Brca1* heterozygote phenotypes described in this thesis could show that *Brca1* does not need to be fully absent to cause phenotypes that promote genome instability. A single *Brca1* C61G allele causes a reduction in Brca1 protein (Chapter 4) and the remaining mutated protein could potentially cause dominant-negative effects on Brca1 roles, such as in collapsed replication fork repair (Chapter 5). This is more acutely seen in the development of tumours in mice with one copy of *Brca1* C61G that are *53bp1*-null (Chapter 6). If these tumours are produced due to a single *Brca1* allele mutation in a genomically unstable (*53bp1*-null) background, then it brings into question whether loss of *BRCA1* heterozygosity is needed for cancer development in *BRCA1* mutation carrier. It may be that mutations in other genes that lead to genomic instability, such as *53bp1* or *p53*, could be the first step to tumour development in heterozygote *BRCA1* C61G cells. This is supported by the presence of *BRCA1* mutation carrier tumour cells maintaining their wild-type *BRCA1* allele (Clark *et al*., 2012; Neuhausen and Marshall, 1994; Smith *et al*., 1992; Wei *et al*., 2005).

7.3 Future experiments

Experiments that could be done to further this experiment can be broadly characterised into three groups: those that strengthen the current data explored in this thesis, those that explore the effects of *Brca1* C61G in DNA repair and further mouse experiments to provide more information on tumour development.

Red writing indicates the potential methods that could be used to for each experiment.

7.3.1 Key experiments

- Addition controls are needed to strengthen current data: *53bp1*$^{-/-}$*Brca1*$^{-/-}$ control would investigate any haploinsufficiency and possible dominant-negative phenotypes from *Brca1* C61G (genome editing), *53bp1*$^{+/+}$*Brca1*$^{C61G/C61G}$ cells would provide evidence of the phenotype *Brca1* C61G causes without the *53bp1*-null background or cancer cell line disadvantages (lentivirus/retrovirus insertion of conditional *53bp1* expression vector), *p53*$^{+/-}$*Brca1*$^{C61G/C61G}$ would aid in determining what *Brca1* C61G phenotypes are compounded by the removal of 53bp1, and wild-type MEFs would provide a strong control for all experiments (MEF immortalisation from mouse breeding).
- An alternative antibody to GH118 is needed to confirm and strength current data that suggests Brca1 C61G causes protein-wide defects; suggested experiments to compliment are the whole cell extract repeats, degradation and localisation studies (western blotting, drug treatments).
- *In vivo* protein analysis would allow confirmation of the predicted effects on the Brca1:Bard1 heterodimer due to the *Brca1* C61G mutation: immunoprecipitations using tagged Bard1 to look at binding with Brca1 C61G (IP and western blot, Bard DNA vector expression).
- Cell cycle is essential for assessing how a cell controls the method and timing of DNA repair and this would eliminate any compounding defects, such as genomic instability, that could be caused by cell cycle defects: cell cycle profiling of untreated and irradiated MEFs (PI stain, phosphorylation Histone 3 stain, FACs) and mitosis for chromosome errors and mitotic catastrophe (metaphase spreads, Nocodazole treatment, immunofluorescent microscopy during mitosis).

7.3.2 Exploring Brca1 C61G in DNA repair

- NHEJ/HR levels could reveal the DSB repair pathway balance in cells that lack 53bp1 and wild-type Brca1, and this could be used to assess the level of errors in DNA repair: look at the DSB repair pathway balance in *53bp1*$^{-/-}$*Brca1*$^{C61G/C61G}$ MEFs (traffic light system) and investigate whether repair is erroneous (DNA repair assay and breakpoint sequence analysis).
- Investigation into DNA crosslink repair in cells with Brca1 C61G could help to decipher the mechanisms in which Brca1 is involved into ICL repair: look at Brca1/FANCD2 foci to establish co-localisation (immunofluorescent labelling and microscopy), look for other proteins (e.g. associated nucleases) to look for other defects in the DNA crosslink pathway (immunofluorescent labelling and microscopy), and use timecourse experiments to look at the outcomes of DNA crosslink repair (immunofluorescent labelling and microscopy).
- The specific effects of Brca1 C61G reduced ubiquitin ligase activity in DNA repair is not fully understood and studying this further will provide information about the specific roles of Brca1 ubiquitin ligase activity in maintaining genome stability:

ubiquitin levels at sites of DSB repair that are affects by the *Brca1* C61G mutation such as DNA crosslink repair and HR after IR (immunofluorescent labelling and microscopy).

7.3.3 Further mouse experiments

- A longer and more comprehensive tumour watch would confirm the increase of tumour development in mice with one or two copies of *Brca1* C61G and assessing mice that are heterozygote for *Brca1* C61G would correlate with human *BRCA1* mutation carrier cancer incidence: continue tumour watch adding *53bp1*$^{+/-}$*Brca1*$^{+/C61G}$ mice and *53bp1*$^{+/+}$*Brca1*$^{+/C61G}$ mice, analyse tumours for the type of lymphoma and other tumours (e.g. breast cancers) (histopathology of tumours), look at the Brca1 allele status in the tumours from *53bp1*$^{-/-}$*Brca1*$^{+/C61G}$ mice for loss of heterozygosity (DNA sequencing and/or chromosome analysis).
- Adding *p53/Brca1* mutant mice to the genotypes in the tumour watch is likely to accelerate the tumour development caused by *Brca1* C61G and would provide more information into whether the tissues we see the tumours in are driven by *Brca1*, *53bp1* or *p53* mutation: created *p53*$^{+/-}$ and *p53*$^{-/-}$ *Brca1* C61G homozygote mice to look at the development of tumours and the specific tissues that they develop in (mouse dissection and histopathology).

Appendices

Figure 1 – BRCA1 gene gain and loss tree

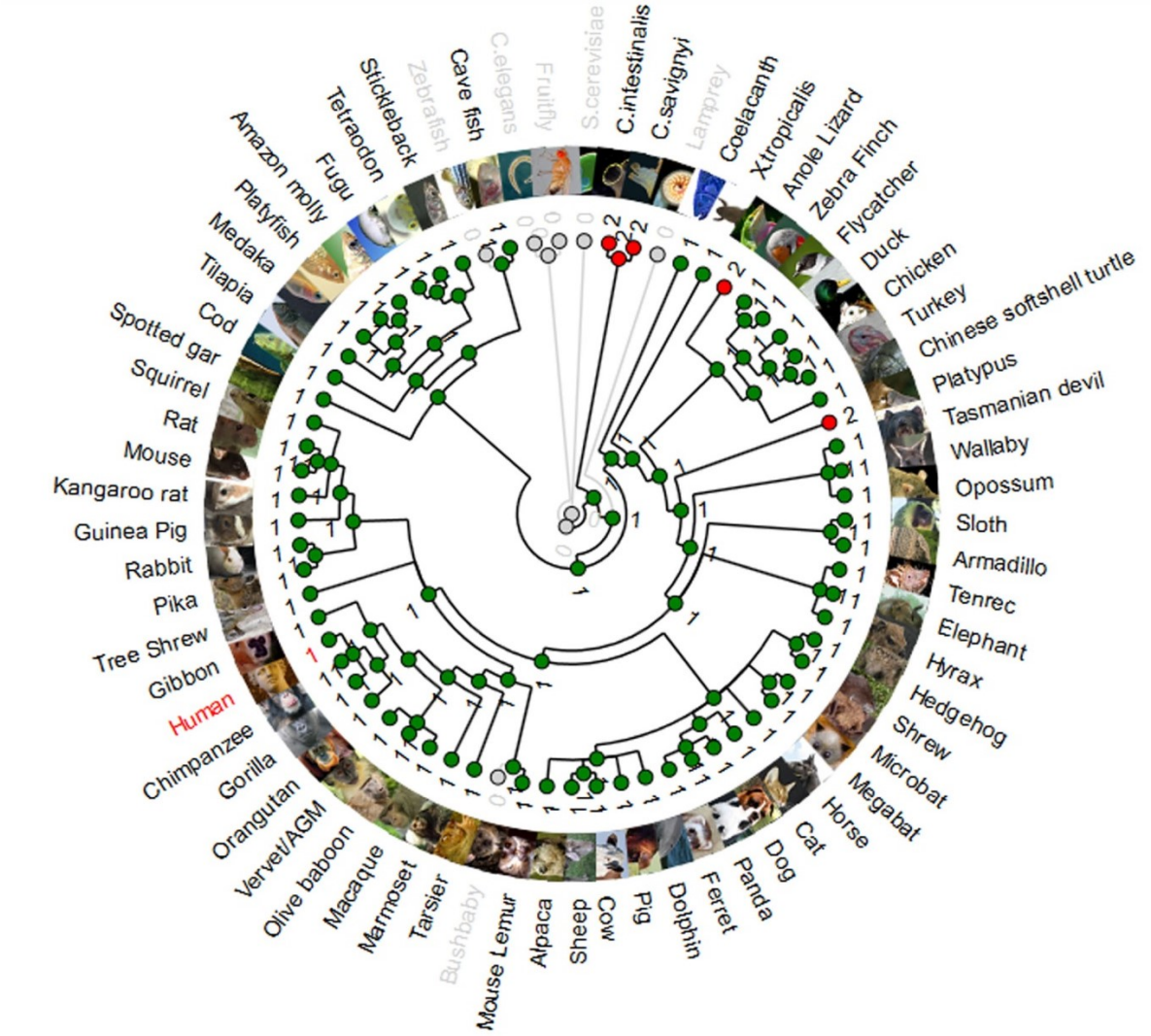

This ENSEMBL orthologue tree shows the gains and losses of BRCA1 orthologues in species and estimate time of divergence from the most recent ancestors. Grey dots show an absence of a BRCA1 orthologue. Green dots show the presence of one BRCA1 orthologue and red dots show the presence of two BRCA1 orthologues. Length of branches show estimated length of time of divergence.
http://www.ensembl.org/Homo_sapiens/Gene/SpeciesTree?db=core;g=ENSG00000012048;r=17:43044295-43125483 Accessed 25/08/2015

Figure 2 – BARD1 gene gain and loss tree

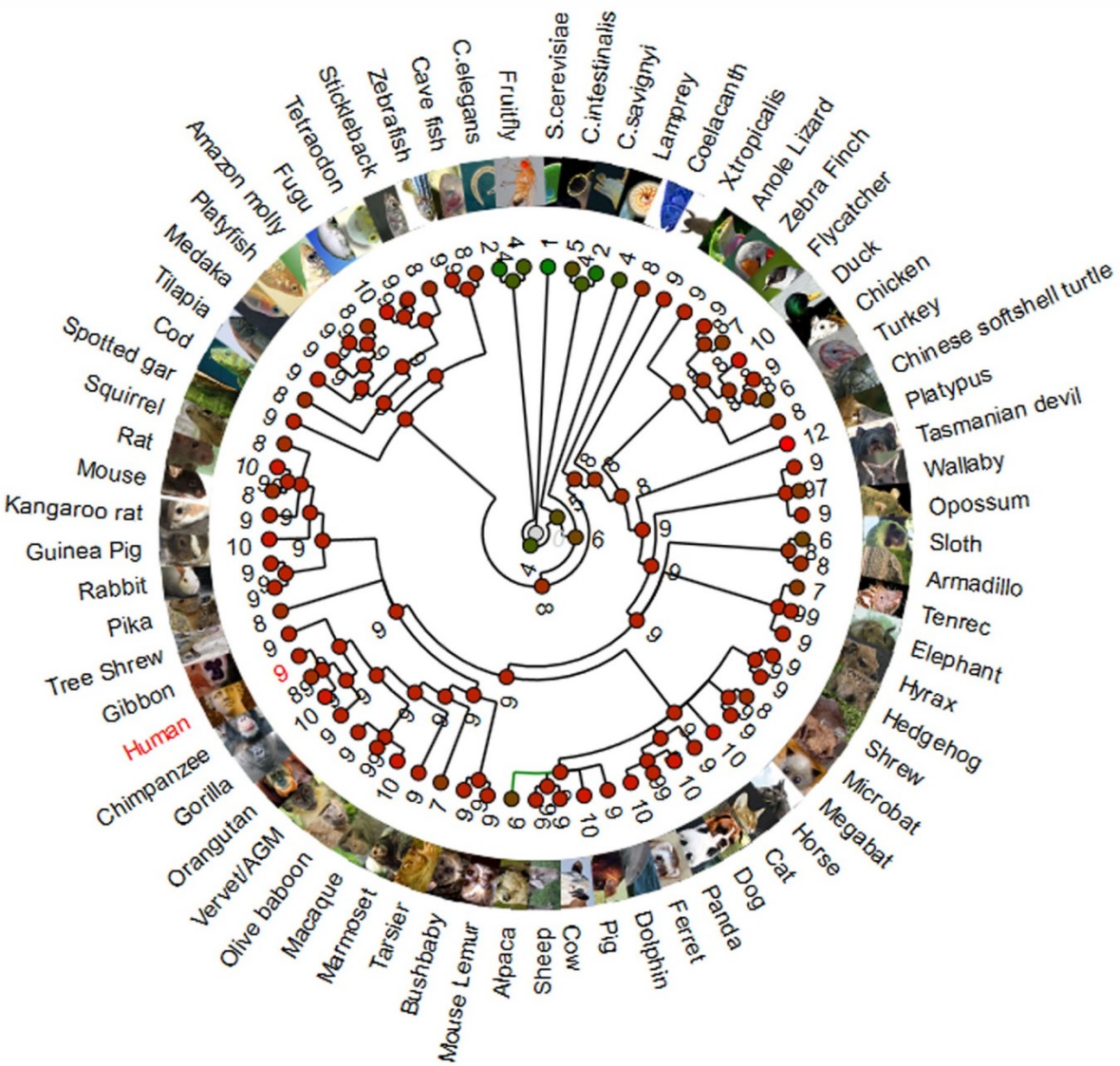

This ENSEMBL orthologue tree shows the gains and losses of BARD1 genes in species and estimate time of divergence from the most recent ancestors. Grey dots show an absence of a BARD1 orthologue. Green dots show the presence of one to five BARD1 orthologue and red dots show the presence of 6 or more BARD1 orthologues. Length of branches show estimated length of time of divergence.
http://www.ensembl.org/Homo_sapiens/Gene/SpeciesTree?db=core;g=ENSG00000138376;r=2:214725646-214809711 Accessed 25/08/2015

Figure 3 – Images of tumours/organs from 53bp1$^{-/-}$Brca1$^{+/C61G}$ and 53bp1$^{-/-}$Brca1$^{C61G/C61G}$ mice

Cage 2661-78 Female 4 - 53bp1-/-Brca1+/C61G (59 weeks, 414 days)

Tumour 1 - Enlarged spleen with tumour- Histiocytic sarcoma

Tumour 2 - Red lump in liver lobe- Haemangiosarcoma

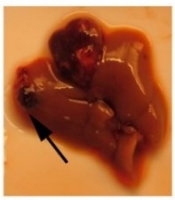

Cage 2661-116 Female 2 - 53bp1-/-Brca1C61G/C61G (41 weeks, 288 days)

Tumour 1 - Enlarged thymus (no image)- Malignant Thymic Lymphoma

Cage 2661-127 Female 1 - 53bp1-/-Brca1+/C61G (50 weeks, 350 days)

Tumour 1 - Tumour on intestines - Malignant Lymphoma

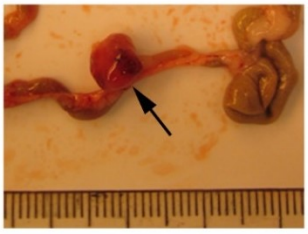

Cage 2661-138 Male 3 - 53bp1-/-Brca1C61G/C61G (17 weeks, 120 days)

Tumour 1 - Enlarged thymus - Malignant Thymic Lymphoma

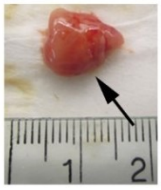

Tumour 2 - Enlarged Spleen- Malignant Lymphoma

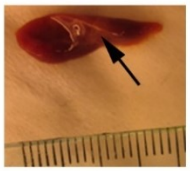

Figure 4 – Images of tumours/organs from 53bp1$^{-/-}$Brca1$^{+/C61G}$ and 53bp1$^{-/-}$Brca1$^{C61G/C61G}$ mice continued

Cage 2661-141 Female 2 - 53bp1-/-Brca1C61G/C61G (37 weeks, 259 days)
Tumour 1 - Enlarged Spleen- Malignant Lymphoma

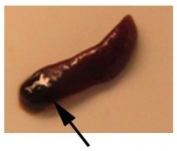

Cage 2661-162 Female 2 - 53bp1-/-Brca1C61G/C61G (26 weeks, 179 days)
Tumour 1 - Enlarged spleen - Malignant Lymphoma

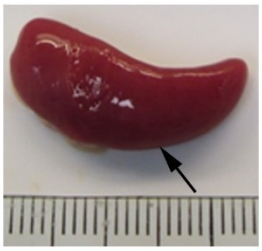

Cage 2661-173 Female 4 - 53bp1-/-Brca1C61G/C61G (42 weeks, 292 days)
Tumour 1 - Tumour on intestines - Malignant Lymphoma

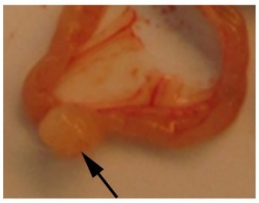

Cage 2661-214 Female 3 - 53bp1-/-Brca1+/C61G (14 weeks, 99 days)
Tumour 1 - Enlarged thymus and chest cavity tumours - Malignant Thymic Lymphoma

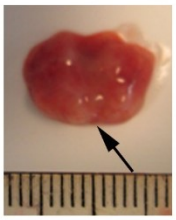

Cage 2661-231 Female 2 - 53bp1-/-Brca1C61G/C61G (26 weeks, 178 days)

Tumour 1 - Enlarged thymus and chest cavity tumours - Malignant Thymic Lymphoma

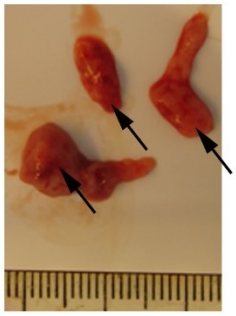

Figures 3 and 4 – Images of tumours/organs from 53bp1$^{-/-}$Brca1$^{+/C61G}$ and 53bp1$^{-/-}$ Brca1$^{C61G/C61G}$ mice

This figure identifies the mice that had developed a tumour upon dissection and shows the organ/tumour. Two mice had two tumours; remaining mice had a single tumour. The genotype and age of the mice are as indicated. Tumour diagnosis was determined after histological analysis.

References

Acharya, N., Johnson, R.E., Prakash, S., et al. (2006) Complex formation with Rev1 enhances the proficiency of Saccharomyces cerevisiae DNA polymerase zeta for mismatch extension and for extension opposite from DNA lesions. **Molecular and cellular biology,** 26 (24): 9555-9563.

Adamo, A., Collis, S.J., Adelman, C.A., et al. (2010) Preventing nonhomologous end joining suppresses DNA repair defects of Fanconi anemia. **Molecular cell,** 39 (1): 25-35.

Adamo, A., Montemauri, P., Silva, N., et al. (2008) BRC-1 acts in the inter-sister pathway of meiotic double-strand break repair. **EMBO reports,** 9 (3): 287-292.

Aiub, C.A., Mazzei, J.L., Pinto, L.F., et al. (2004) Participation of BER and NER pathways in the repair of DNA lesions induced at low N-nitrosodiethylamine concentrations. **Toxicology Letters,** 154 (1-2): 133-142.

Aiyar, S.E., Sun, J.L., Blair, A.L., et al. (2004) Attentuation of estrogen receptor alpha-mediated transcription through estrogen-stimulated recruitment of a negative elongation factor. **Genes and Development,** 18 (17): 2134-2146.

Alter, B.P., Greene, M.H., Velazquez, I., et al. (2003) Cancer in Fanconi anemia. **Blood,** 101 (5): 2072.

Altmeyer, M., Messner, S., Hassa, P.O., et al. (2009) Molecular mechanism of poly(ADP-ribosyl)ation by PARP1 and identification of lysine residues as ADP-ribose acceptor sites. **Nucleic acids research,** 37 (11): 3723-3738.

Andrews, H.N., Mullan, P.B., McWilliams, S., et al. (2002) BRCA1 regulates the interferon gamma-mediated apoptotic response. **Journal of Biological Chemistry,** 277 (29): 26225-26232.

Aparicio, T., Baer, R., Gottesman, M., et al. (2016) MRN, CtIP, and BRCA1 mediate repair of topoisomerase II-DNA adducts. **Journal of cellular biochemistry,** 212 (4): 399-408.

Au, W.W.Y. and Henderson, B.R. (2007) Identification of sequences that target BRCA1 to nuclear foci following alkylative DNA damage. **Cellular signalling,** 19 (9): 1879-1892.

Aymard, F., Bugler, B., Schmidt, C.K., et al. (2014) Transcriptionally active chromatin recruits homologous recombination at DNA double-strand breaks. **Nature Structure and Molecular Biology,** 21 (4): 366-374.

Bachelier, R., Xu, X., Wang, X., et al. (2003) Normal lymphocyte development and thymic lymphoma formation in Brca1 exon-11-deficient mice. **Oncogene,** 22 (4): 528-537.

Bae, I., Rih, J.K., Kim, H.J., et al. (2005) BRCA1 regulates gene expression for orderly mitotic progression. **Cell Cycle,** 4 (11): 1641-1666.

Baeyens, A., Thierens, H., Claes, K., et al. (2004) Chromosomal radiosensitivity in BRCA1 and BRCA2 mutation carriers. **International Journal of Radiation Biology,** 80 (10): 745-756.

Baeyens, A., Thierens, H., Claes, K., et al. (2002) Chromosomal radiosensitivity in breast cancer patients with a known or putative genetic predisposition. **British Journal of Cancer,** 87 (12): 1379-1385.

Bai, L., Shi, G., Zhang, X., et al. (2013) Transgenic expression of BRCA1 disturbs hematopoietic stem and progenitor cells quiescence and function. **Experimental cell research,** 319 (17): 2739-2746.

Baldeyron, C., Jacquemin, E., Smith, J., et al. (2002) A single mutated BRCA1 allele leads to impaired fidelity of double strand break end-joining. **Oncogene,** 21 (9): 1401-1410.

Barber, L.J. and Boulton, S.J. (2006) BRCA1 ubiquitylation of CtIP: Just the tIP of the iceberg? **DNA repair,** 5 (12): 1499-1504.

Baria, K., Warren, C., Roberts, S.A., et al. (2001) Correspondence re: A. Rothfuss et al., Induced micronucleus frequencies in peripheral blood lymphocytes as a screening test for carriers of a BRCA1 mutation in breast cancer families. Cancer Res., 60: 390–394, 2000. **Cancer research,** 61 (15): 5948-5949.

Barwell, J., Pangon, L., Georgious, A., et al. (2007) Lymphocyte radiosensitivity in BRCA1 and BRCA2 mutation carriers and implications for breast cancer susceptibility. **International Journal of Cancer,** 121 (7): 1631-1636.

Bau, D.T., Fu, Y.P., Chen, S.T., et al. (2004) Breast cancer risk and the DNA double-strand break end-joining capacity of nonhomologous end-joining genes are affected by BRCA1. **Cancer research,** 64 (14): 5013-5019.

Bau, D.T., Mau, Y.C. and Shen, C.Y. (2006) The role of BRCA1 in non-homologous end-joining. **Cancer letters,** 240 (1): 1-8.

Bekker-Jensen, S., Danielsen, J.R., Fugger, K., et al. (2010) HERC2 coordinates ubiquitin-dependent assembly of DNA repair factors on damaged chromosomes. **Nature cell biology,** 12 (1): 80-86.

Bellani, M.A., Boateng, K.A., McLeod, D.,., et al. (2010) The expression profile of the major mouse SPO11 isoforms indicates that SPO11beta introduces double strand breaks and suggests that SPO11alpha has an additional role in prophase in both spermatocytes and oocytes. **Molecular and cellular biology,** 30 (18): 4391-4403.

Berkovich, E., Monnat, R.J.,Jr and Kastan, M.B. (2007) Roles of ATM and NBS1 in chromatin structure modulation and DNA double-strand break repair. **Nature cell biology,** 9 (6): 683-690.

Berndsen, C.E. and Wolberger, C. (2014) New insights into ubiquitin E3 ligase mechanism. **Nature Structure and Molecular Biology,** 21 (4): 301-307.

Berton, T.R., Matsumoto, T., Page, A., et al. (2003) Tumor formation in mice with conditional inactivation of Brca1 in epithelial tissues. **Oncogene,** 22 (35): 5415-5426.

Bhattacharyya, A., Ear, U.S., Koller, B.H., et al. (2000) The Breast Cancer Susceptibility Gene BRCA1 Is required for subnuclear assembly of Rad51 and survival following treatment with the DNA cross-linking agent Cisplatin. **Journal of Biological Chemistry,** 275 (31): 23899-23903.

Biasini, M., Bienert, S., Waterhouse, A., et al. (2014) SWISS-MODEL: modelling protein tertiary and quaternary structure using evolutionary information. **Nucleic acids research,** 42 (W1): W252-W258.

Blagosklonny, M.V., An, W.G., Melillo, G., et al. (1999) Regulation of BRCA1 by protein degradation. **Oncogene,** 18 (47): 6460-6468.

Boateng, K.A., Bellani, M.A., Gregoretti, I.V., et al. (2013) Homologous pairing preceding SPO11-mediated double-strand breaks in mice. **Developmental cell,** 24 (2): 196-205.

Bochar, D.A., Wang, L., Beniya, H., et al. (2000) BRCA1 is associated with a human SWI/SNF-related complex: linking chromatin remodeling to breast cancer. **Cell,** 102 (2): 257-265.

Boddy, M.N., Gaillard, P.L., McDonald, W.H., et al. (2001) Mus81-Eme1 Are Essential Components of a Holliday Junction Resolvase. **Cell,** 107 (4): 537-548.

Boersma, V., Moatti, N., Sequera-Bayona, S., et al. (2015) MAD2L2 controls DNA repair at telomeres and DNA breaks by inhibitig 5' end resection. **Nature,** 521 (7553): 537-540.

Botuyan, M.V., Lee, J., Ward, I.M., et al. (2006) Structural Basis for the Methylation State-Specific Recognition of Histone H4-K20 by 53BP1 and Crb2 in DNA Repair. **Cell,** 127 (7): 1361-1373.

Boulton, S.J., Martin, J.S., Polanowska, J., et al. (2004) BRCA1/BARD1 orthologues required for DNA repair in Caenorhabditis elegans. **Current Biology,** 14 (1): 33-39.

Bouwman, P., Aly, A., Escandell, J.M., et al. (2010) 53BP1 loss rescues BRCA1 deficiency and is associated with triple-negative and BRCA-mutated breast cancers. **Nat Struct Mol Biol,** 17 (6): 688-695.

Brodie, K.M. and Henderson, B.R. (2010) Differential modulation of BRCA1 and BARD1 nuclear localisation and foci assembly by DNA damage. **Cellular signalling,** 22 (2): 291-302.

Brodie, S.G., Xu, X., Qiao, W., et al. (2001) Multiple genetic changes are associated with mammary tumorigenesis in Brca1 conditional knockout mice. **Oncogene,** 20 (51): 7514-7523.

Brown, M.A., Nicolai, H., Howe, K., et al. (2002) Expression of a truncated Brca1 protein delays lactational mammary development in transgenic mice. **Transgenic Research,** 11 (5): 467-478.

Bryant, H.E., Schultz, N., Thomas, H.D., et al. (2005) Specific killing of BRCA2-deficient tumours with inhibitors of poly(ADP-ribose) polymerase. **Nature,** 434 (7035): 913-917.

Brzovic, P.S., Keeffe, J.R., Nishikawa, H., et al. (2003) Binding and recognition in the assembly of an active BRCA1/BARD1 ubiquitin-ligase complex. **Proceedings of the National Academy of Sciences,** 100 (10): 5646-5651.

Brzovic, P.S., Meza, J.E., King, M., et al. (2001a) BRCA1 RING domain cancer-predisposing mutations: Structural consequences and effects on protein-protein interactions. **Journal of Biological Chemistry,** 276 (44): 41399-41406.

Brzovic, P.S., Meza, J., King, M., et al. (1998) The cancer-predisposing mutation C61G disrupts homodimer formation in the NH2-terminal BRCA1 RING finger domain. **Journal of Biological Chemistry,** 273 (14): 7795-7799.

Brzovic, P.S., Rajagopal, P., Hoyt, D.W., et al. (2001b) Structure of a BRCA1-BARD1 heterodimeric RING-RING complex. **Nat Struct Mol Biol,** 8 (10): 833-837.

Buchholz, T.A., Wu, X., Hussain, A., et al. (2002) Evidence of haplotype insufficiency in human cells containing a germline mutation in BRCA1 or BRCA2. **International Journal of Cancer,** 97 (5): 557-561.

Buckley, N.E., Hosey, A.M., Gorski, J.J., et al. (2007) BRCA1 regulates IFN-gamma signalling through a mechanism involving the type I INFs. **Molecular Cancer Research,** 5 (3): 261-270.

Buis, J., Stoneham, T., Spehalski, E., et al. (2012) Mre11 regulates CtIP-dependent double-strand break repair by interaction with CDK2. **Nat Struct Mol Biol,** 19 (2): 246-252.

Bunting, S., Callén, E., Kozak, M., et al. (2012) BRCA1 functions independently of Homologous Recombination in DNA Interstrand Crosslink Repair. **Molecular cell,** 46 (2): 125-135.

Bunting, S.F., Callen, E., Wong, N., et al. (2010) 53BP1 inhibits Homologous Recombination in Brca1-deficient cells by blocking resection of DNA breaks. **Cell,** 141 (2): 243-254.

Burma, S., Chen, B.P., Murphy, M., et al. (2001) ATM Phosphorylates Histone H2AX in Response to DNA Double-strand Breaks. **Journal of Biological Chemistry,** 276 (45): 42462-42467.

Butler, L.R., Densham, R.M., Jia, J., et al. (2012) The proteasomal de-ubiquitinating enzyme POH1 promotes the double-strand DNA break response. **The EMBO journal,** advance online publication.

Callen, E., Di Virgilio, M., Kruklak, M.J., et al. (2013) 53BP1 mediates productive and mutagenic DNA repair through distinct phosphoprotein interactions. **Cell,** 153 (6): 1266-1280.

Calvo, V. and Beato, M. (2011) BRCA1 counteracts progesterone action by ubiquitination leading to progesterone receptor degradation and epigenetic silencing of target promoters. **Cancer research,** 71 (9): 3422-3431.

Camacho, C., Coulouris, G., Avagyan, V., et al. (2009) BLAST+: architecture and applications. **BMC bioinformatics,** 10 421.

Campbell, M., Aprelikova, O.N., van der Meer, R., et al. (2001) Construction and characterization of recombinant adenoviruses expressing human BRCA1 or murine Brca1 genes. **Cancer gene therapy,** 8 (3): 231.

Cantor, S., Drapkin, R., Zhang, F., et al. (2004) The BRCA1-associated protein BACH1 is a DNA helicase targeted by clinically relevant interacting mutations. **Proc.Natl.Acad.Sci.U.S.A.,** 101 (8): 2357-2362.

Cantor, S.B. and Andreassen, P.R. (2006) Assessing the link between BACH1 and BRCA1 in the FA pathway. **Cell Cycle,** 5 (2): 164-167.

Cantor, S.B., Bell, D.W., Ganesan, S., et al. (2001) BACH1, a novel helicase-like protein, interacts directly with BRCA1 and contributes to its DNA repair function. **Cell,** 105 (1): 149-160.

Cao, L., Kim, S., Xiao, C., et al. (2006) ATM-Chk2-p53 activation prevents tumorigenesis at an expense of organ homeostasis upon Brca1 deficiency. **The EMBO journal,** 25 (10): 2167-2177.

Cao, L., Li, W., Kim, S., et al. (2003) Senescence, aging, and malignant transformation mediated by p53 in mice lacking the Brca1 full-length isoform. **Genes & development,** 17 (2): 201-213.

Cao, L., Xu, X., Cao, L.L., et al. (2007) Absence of full-length Brca1 sensitizes mice to oxidative stress and carcinogen-induced tumorigenesis in the esophagus and forestomach. **Carcinogenesis,** 28 (7): 1401-1407.

Cao, L., Xu, X., Bunting, S.F., et al. (2009) A selective requirement for 53BP1 in the biological response to genomic instability induced by Brca1 deficiency. **Molecular cell,** 35 (4): 534-541.

Carbonaro-Hall, D., Williams, R., Wu, L., et al. (1993) G1 expression and multistage dynamics of cyclin A in human osteosarcoma cells. **Oncogene,** 8 (6): 1649-1659.

Cass, I., Baldwin, R.L., Varkey, T., et al. (2003) Improved survival in women with BRCA-associated ovarian carcinoma. **Cancer,** 97 (9): 2187-2195.

Castella, M., Jacquemont, C., Thompson, E.L., et al. (2015) FANCI regulates recruitment of the FA core complex at sites of DNA damage independently of FANCD2. **PLoS genetics,** 11 (10): e1005563.

Chabalier, C., Lamare, C., Racca, C., et al. (2006) BRCA1 Downregulation Leads to Premature Inactivation of Spindle Checkpoint and Confers Paclitaxel Resistance. **Cell Cycle,** 5 (9): 1001-1007.

Chandler, J., Hohenstein, P., Swing, D.A., et al. (2001) Human BRCA1 gene rescues the embryonic lethality of Brca1 mutant mice. **Genesis (New York, N.Y.: 2000),** 29 (2): 72-77.

Chang, S., Biswas, K., Martin, B.K., et al. (2009) Expression of human BRCA1 variants in mouse ES cells allows functinoal analysis of BRCA1 mutations. **Journal of Clinical Investigation,** 119 (10): 3160-3171.

Chapman, J.R., Barral, P., Vannier, J.B., et al. (2013) RIF1 is essential for 53BP1-dependent nonhomologous end joining and suppression of DNA double-strand break resection. **Molecular cell,** 49 (5): 858-871.

Chapman, J.R., Sossick, A.J., Boulton, S.J., et al. (2012) BRCA1-associated exclusion of 53BP1 from DNA damage sites underlies temporal control of DNA repair. **Journal of cell science,** 125 (15): 3529-3534.

Chen, A., Kleiman, F.E., Manley, J.L., et al. (2002) Autoubiquitination of the BRCA1·BARD1 RING ubiquitin ligase. **Journal of Biological Chemistry,** 277 (24): 22085-22092.

Chen, G.C., Guan, L.S., Yu, J.H., et al. (2001) Rb-associated protein 46 (RbAp46) inhibits transcriptional transactivation mediated by BRCA1. **Biochemical and biophysical research communications,** 284 (2): 507-514.

Chen, L., Nievera, C.J., Lee, A.Y., et al. (2008) Cell Cycle-dependent Complex Formation of BRCA1·CtIP·MRN Is Important for DNA Double-strand Break Repair. **Journal of Biological Chemistry,** 283 (12): 7713-7720.

Chen, Y., Chen, C.F., Riley, D.J., et al. (1995) Aberrant subcellular localization of BRCA1 in breast cancer. **Science,** 270 (5237): 789-791.

Chen, Y., Zheng, T., Lan, Q., et al. (2013) Polymorphisms in DNA repair patwhays genes, body mass index, and risk of non-Hodgkin lymphoma. **American Journal of Hematology,** 88 (7): 606-611.

Chen, Y., Farmer, A.A., Chen, C., et al. (1996) BRCA1 is a 220-kDa nuclear phosphoprotein that is expressed and phosphorylated in a cell cycle-dependent manner. **Cancer research,** 56 (14): 3168-3172.

Chen, Z., Arciero, C.A., Wang, C., et al. (2006) BRCC36 is essential for ionizing radiation-induced BRCA1 phosphorylation and nuclear foci formation. **Cancer Research,** 66 (10): 5039-5046.

Chen, Z. and Pickart, C.M. (1990) A 25-kilodalton ubiquitin carrier protein (E2) catalyzes multi-ubiquitin chain synthesis via lysine 48 of ubiquitin. **Journal of Biological Chemistry,** 265 (35): 21835-21842.

Chiba, N. and Parvin, J.D. (2001) Redistribution of BRCA1 among four different protein complexes following replication blockage. **Journal of Biological Chemistry,** 276 (42): 38549-38554.

Chodankar, R., Kwang, S., Sangiorgi, F., et al. (2005) Cell-nonautonomous induction of ovarian and uterine serous cystadenomas in mice lacking a functional Brca1 in ovarian granulosa cells. **Current biology,** 15 (6): 561-565.

Choi, J.D., Park, M.A. and Lee, J.S. (2012) Suppression and recovery of BRCA1-mediated transcription by HP1γ via modulation of promoter occupancy. **Nucleic acids research,** 40 (22): 11321-11338.

Choudhury, A.D., Xu, H. and Baer, R. (2004) Ubiquitination and proteasomal degradation of the BRCA1 tumor suppressor is regulated during cell cycle progression. **Journal of Biological Chemistry,** 279 (32): 33909-33918.

Ciccia, A., McDonald, N. and West, S.C. (2008) Structural and functional relationships of the XPF/MUS81 family of proteins. **Annual Review of Biochemistry,** 77 259-287.

Clark, S.L., Rodriguez, A.M., Snyder, R.R., et al. (2012) Structure-Function of the tumours suppressor BRCA1. **Computational and Structural Biotechnology Journal,** 1 (1):.

Cohn, M.A. and D'Andrea, A.D. (2008) Chromatin recruitment of DNA repair proteins: lessons from the fanconi anemia and double-strand break repair pathways. **Molecular cell,** 32 (3): 306-312.

Cohn, M.A., Kee, Y., Haas, W., et al. (2009) UAF1 is a subunit of multiple deubiquitinating enzyme complexes. **The Journal of biological chemistry,** 284 (8): 5343-5351.

Cohn, M.A., Kowal, P., Yang, K., et al. (2007) A UAF1-containing multisubunit protein complex regulates the Fanconi anemia pathway. **Molecular cell,** 28 (5): 786-797.

Cole, A.R., Lewis, L.P. and Walden, H. (2010) The structure of the catalytic subunit FANCL of the Fanconi anemia core complex. **Nature structural & molecular biology,** 17 (3): 294-298.

Coleman, K.A. and Greenberg, R.A. (2011) The BRCA1-RAP80 complex regulates DNA repair mechanism utilization by restricting end resection. **The Journal of biological chemistry,** 286 (15): 13669-13680.

Collis, S.J., Ciccia, A., Deans, A.J., et al. (2008) FANCM and FAAP24 function in ATR-mediated checkpoint signalling independently of the Fanconi anemia core complex. **Molecular Cell,** 32 (3): 313-324.

Cortez, D., Wang, Y., Qin, J., et al. (1999) Requirement of ATM-dependent phosphorylation of brca1 in the DNA damage response to double-strand breaks. **Science,** 286 (5442): 1162-1166.

Cotta-Ramusino, C., McDonald, E.R.,3rd, Hurov, K., et al. (2011) A DNA damage response screen identifies RHINO, a 9-1-1 and TopBP1 interacting protein required for ATR signaling. **Science (New York, N.Y.),** 332 (6035): 1313-1317.

Coupier, I., Baldeyron, C., Rousseau, A., et al. (2004) Fidelity of DNA double-strand break repair in heterozygous cell lines harbouring BRCA1 missense mutations. **Oncogene,** 23 (4): 914-919.

Cousineau, I. and Belmaaza, A. (2007) BRCA1 haploinsufficiency, but not heterozygosity fror a BRCA1-truncating mutation, deregulates homologous recombination. **Cell Cycle,** 6 (8): 962-971.

Cressman, V.L., Backlund, D.C., Avrutskaya, A.V., et al. (1999a) Growth retardation, DNA repair defects, and lack of spermatogenesis in BRCA1-deficient mice. **Molecular and cellular biology,** 19 (10): 7061-7075.

Cressman, V.L., Backlund, D.C., Hicks, E.M., et al. (1999b) Mammary tumor formation in p53- and BRCA1-deficient mice. **Cell growth & differentiation,** 10 (1): 1-10.

Croke, M., Neumann, M.A., Grotsky, D.A., et al. (2013) Differences in 53BP1 and BRCA1 regulation between cycling and non-cycling cells. **Cell Cycle,** 12 (23): 3629-3639.

Crossan, G.P. and Patel, K.J. (2012) The Fanconi anaemia pathway orchestrates incisions at sites of crosslinked DNA. **The Journal of pathology,** 226 (2): 326-337.

Cunningham, F., Amode, M.R., Barrell, D., et al. (2015) Ensembl 2015. **Nucleic acids research,** 43 (D1): D662-D669.

Dan, J., Liu, Y., Liu, N., et al. (2014) Rif1 maintains telomere length homeostasis of ESCs by mediating heterochromatin silencing. **Developmental Cell,** 29 (1): 7-19.

De Brakeleers, S., De Greve, J., Desmedt, C., et al. (2016) Frequent incidence of BARD1-truncating mutations in germline DNA from triple-negative breast cancer patients. **Clinical genetics,** 89 (3): 336-340.

de Murcia, J.M., Niedergang, C., Trucco, C., et al. (1997) Requirement of poly(ADP-ribose) polymerase in recovery from DNA damage in mice and in cells. **Proc.Natl.Acad.Sci.U.S.A.,** 94 (14): 7303-7307.

de Winter, J.P., Leveille, F., van Berkel, C.G., et al. (2000a) Isolation of a cDNA representing the Fanconi anemia complementation group E gene. **American Journal of Human Genetics,** 67 (5): 1306-1308.

de Winter, J.P., Rooimans, M.A., van Der Weel, L., et al. (2000b) The Fanconi anaemia gene FANCF encodes a novel protein with homology to ROM. **Nature Genetics,** 24 (1): 15-16.

de Winter, J.P., Waisfisz, Q., Rooimans, M.A., et al. (1998) The Fanconi anaemia group G gene FANCG is identical with XRCC9. **Nature Genetics,** 20 (3): 281-283.

Dendouga, N., Gao, H., Moechars, D., et al. (2005) Disruption of murine Mus81 increases genomic instability and DNA damage sensitivity but does not promote tumorigenesis. **Molecular and cellular biology,** 25 (17): 7569-7579.

Deutsch, E., Jarrousse, S., Buet, D., et al. (2003) Down-regulation of BRCA1 in BCR-ABL-expressing hematopoietic cells. **Blood,** 101 (11): 4583-4588.

Di Paolo, A., Racca, C., Calsou, P., et al. (2014) Loss of BRCA1 impairs centromeric cohesion and triggers chromosomal instability. **FASEB Journal,** 28 (12): 5250-5261.

Difilippantonio, S., Gapud, E., Wong, N., et al. (2008) 53BP1 facilitates long-range DNA end-joining during V(D)J recombination. **Nature,** 456 (77221): 529-533.

Digweed, M., Rothe, S., Demuth, I., et al. (2002) Attenuation of the formation of DNA-repair foci containing RAD51 in Fanconi anaemia. **Carcinogenesis,** 23 (7): 1121-1126.

Dodd, R.B., Allen, M.D., Brown, S.E., et al. (2004) Solution structure of the Kaposi's Sarcoma-associated Herpesvirus K3 N-terminal domain reveals a novel E2-binding C4HC3-type RING domain. **Journal of Biological Chemistry,** 279 (51): 53840-53847.

Dohrn, L., Salles, D., Siehler, S.Y., et al. (2012) BRCA1-mediated repression of mutagenic end-joining of DNA double-strand breaks requires complex formation with BACH1. **The Biochemical journal,** 441 (3): 919-926.

Doil, C., Mailand, N., Bekker-Jensen, S., et al. (2009) RNF168 Binds and Amplifies Ubiquitin Conjugates on Damaged Chromosomes to Allow Accumulation of Repair Proteins. **Cell,** 136 (3): 435-446.

Donehower, L.A., Harvey, M., Slagle, B.L., et al. (1992) Mice deficient for p53 are developmentally normal but susceptible to spontaneous tumours. **Nature,** 356 (6366): 215-221.

Dong, Y., Hakimi, M., Chen, X., et al. (2003) Regulation of BRCC, a Holoenzyme Complex Containing BRCA1 and BRCA2, by a Signalosome-like Subunit and Its Role in DNA Repair. **Molecular cell,** 12 (5): 1087-1099.

Draga, M., Madgett, E.B., Vandenberg, C.J., et al. (2015) BRCA1 is required for maintenance of phospho-Chk1 and G2/M arrest during DNA crosslink repair in DT40 cells. **Molecular and cellular biology,** .

Drost, R., Bouwman, P., Rottenberg, S., et al. (2011) BRCA1 RING function is essential for tumor suppression but dispensable for therapy resistance. **Cancer Cell,** 20 (6): 797-809.

Drouet, J., Frit, P., Delteil, C., et al. (2006) Interplay between Ku, Artemis, and the DNA-dependent protein kinase catalytic subunit at DNA ends. **The Journal of biological chemistry,** 281 (38): 27784-27793.

Dudgeon, C., Chan, C., Kang, W., et al. (2014) The evolution of thymic lymphomas in p53 knockout mice. **Genes and Development,** 28 (23): 2643-2620.

Erdile, L.F., Heyer, W.D., Kolodner, R., et al. (1991) Characterization of a cDNA encoding the 70-kDa single-stranded DNA-binding subunit of human replication protein A and the role of the protein in DNA replication. **Journal of Biological Chemistry,** 266 (18): 12090-12098.

Ernestos, B., Nikolaos, P., Koulis, G., et al. (2010) Increased chromosomal radiosensitivity in women carrying BRCA1/BRCA2 mutations assessed with the G2 assay. **International Journal of Radiation Oncology Biology Physics,** 76 (4): 1199-1205.

Escribano-Diaz, C., Orthwein, A., Fradet-Turcotte, A., et al. (2013) A cell cycle-dependent regulatory circuit composed of 53BP1-RIF1 and BRCA1-CtIP controls DNA repair pathway choice. **Molecular cell,** 49 (5): 872-883.

Evans, M.D., Saparbaev, M. and Cooke, M.S. (2010) DNA repair and the origins of urinary oxidized 2'-deoxyribonucleosides. **Mutagenesis,** 25 (5): 433-442.

Fabbro, M., Savage, K., Hobson, K., et al. (2004a) BRCA1-BARD1 complexes are required for p53Ser-15 phosphorylation and a G1/S arrest following ionizing radiation-induced DNA damage. **The Journal of biological chemistry,** 279 (30): 31251-31258.

Fabbro, M., Rodriguez, J.A., Baer, R., et al. (2002) BARD1 induces BRCA1 intranuclear foci formation by increasing RING-dependent BRCA1 nuclear import and inhibiting BRCA1 nuclear export. **Journal of Biological Chemistry,** 277 (24): 21315-21324.

Fabbro, M., Schuechner, S., Au, W.W.Y., et al. (2004b) BARD1 regulates BRCA1 apoptotic function by a mechanism involving nuclear retention. **Experimental cell research,** 298 (2): 661-673.

Fan, S., Ma, Y.X., Wang, C., et al. (2001a) Role of direct interaction in BRCA1 inhibition of estrogen receptor activity. **Oncogene,** 20 (1): 77-87.

Fan, S., Yuan, R., Ma, Y.X., et al. (2001b) Mutant BRCA1 genes antagonize phenotype of wild-type BRCA1. **Oncogene,** 20 (57): 8215-8235.

Fan, W., Jin, S., Tong, T., et al. (2002) BRCA1 regulates GADD45 through its interaction with the OCT-1 and CAAT motifs. **Journal of Biological Chemistry,** 277 (10): 8061-8067.

Fanconi, G. (1964) Hypothesis of chromosomal translocation as a genetic interpretation of Fanconi's familial contitutional panmyelopathy. **Helv. Paediatr. Acta.,** 19 29-33.

Farmer, H., McCabe, N., Lord, C.J., et al. (2005) Targeting the DNA repair defect in BRCA mutant cells as a therapeutic strategy. **Nature,** 434 (7035): 917-921.

Fau, S.Y., Fau, B.A. and Chen, P.L. (2003) NFBD1, a novel nuclear protein with signature motifs of FHA and BRCT, and an internal 41-amino acid repeat sequence, is an early participant in DNA damage response. **The Journal of biological chemistry,** 278 (8): 6323-6329.

Febrer, E., Mestres, M., Rosa Caballín, M., et al. (2008) Mitotic delay in lymphocytes from BRCA1 heterozygotes unable to reduce the radiation-induced chromosomal damage. **DNA Repair,** 7 (11): 1907-1911.

Feng, L., Fong, K.W., Wang, J., et al. (2013) RIF1 counteracts BRCA1-mediated end resection during DNA repair. **Journal of Biological Chemistry,** 288 (16): 11134-11143.

Feng, L., Huang, J. and Chen, J. (2009) MERIT40 facilitates BRCA1 localization and DNA damage repair. **Genes & development,** 23 (6): 719-728.

Fernandez-Capetillo, O., Mahadevaiah, S.K., Celeste, A., et al. (2003) H2AX is required for chromatin remodeling and inactivation of sex chromosomes in male mouse meiosis. **Developmental Cell,** 4 (4): 497-508.

Filipponi, D., Muller, J., Emelyanov, A., et al. (2013) Wip1 controls global heterochromatin silencing via ATM/BRCA1-dependent DNA methylation. **Cancer Cell,** 24 (4): 528-541.

Fong, P.C., Yap, T.A., Boss, D.S., et al. (2010) Poly(ADP)-ribose polymerase inhibition: frequent durable responses in BRCA carrier ovarian cancer correlating with platinum-free interval. **Journal of clinical oncology,** 28 (15): 2512-2519.

Fong, P.C., Boss, D.S., Yap, T.A., et al. (2009) Inhibition of ooly(ADP-ribose) polymerase in tumors from BRCA mutation carriers. **N Engl J Med,** 361 (2): 123-134.

Foray, N., Randrianarison, V., Marot, D., et al. (1999) Gamma-rays-induced death of human cells carrying mutations of BRCA1 or BRCA2. **Oncogene,** 18 (51): 7334-7342.

Fradet-Turcotte, A., Canny, M.D., Escribano-Diaz, C., et al. (2013) 53BP1 is a reader of the DNA-damage-induced H2A Lys 15 ubiquitin mark. **Nature,** 499 (7456): 50-54.

Fridlich, R., Annamalai, D., Roy, R., et al. (2015) BRCA1 and BRCA2 protect against oxidative DNA damage converted into double-strand breaks during DNA replication. **DNA Repair,** 30 11-20.

Friedenson, B. (2007) The BRCA1/2 pathway prevents hematologic cancers in addition to breast and ovarian cancers. **BMC cancer,** 7 (152):.

Friedman, L.S., Thistlethwaite, F.C., Petel, K.J., et al. (1998) Thymic Lymphomas in Mice with a Truncating Mutation in Brca2. **Cancer research,** 58 (7): 1338-1343.

Furuta, S., Wang, J.M., Wei, S., et al. (2006) Removal of BRCA1/CtIP/ZBRK1 repressor complex on ANG1 promoter leads to accelerated mammary tumour growth contributed by prominent vasculature. **Cancer Cell,** 10 (1): 13-24.

Galanty, Y., Belotserkovskaya, R., Coates, J., et al. (2009) Mammalian SUMO E3-ligases PIAS1 and PIAS4 promote responses to DNA double-strand breaks. **Nature,** 462 (7275): 935-939.

Ganesan, S., Silver, D.P., Greenberg, R.A., et al. (2002) BRCA1 supports XIST RNA concentration on the inactive X chromosome. **Cell,** 111 (3): 393-405.

Garcia-Higuera, I., Taniguchi, T., Ganesan, S., et al. (2001) Interaction of the Fanconi Anemia proteins and BRCA1 in a common pathway. **Molecular cell,** 7 (2): 249-262.

Gardini, A., Baillat, D., Cesaroni, M., et al. (2014) Genome-wide analysis reveals a role for BRCA1 and PALB2 in transcriptional co-activation. **EMBO,** 33 (8): 890-905.

Garner, E. and Smogorzewska, A. (2011) Ubiquitylation and the Fanconi anemia pathway. **FEBS letters,** 585 (18): 2853-2860.

Gatti, M., Pinato, S., Maspero, E., et al. (2012) A novel ubiquitin mark at the N-terminal tail of histone H2As targeted by RNF168 ubiquitin ligase. **Cell Cycle,** 11 (13): 2538-2544.

Geley, S., Kramer, E., Gieffers, C., et al. (2001) Anaphase-promoting complex/cyclosome–dependent proteolysis of human cyclin A starts at the beginning of mitosis and is not subject to the spindle assembly checkpoint. **The Journal of cell biology,** 153 (1): 137-148.

Godthelp, B.C., Artwert, F., Joenje, H., et al. (2002) Impaired DNA damage-induced nuclear Rad51 foci formation uniquely characterizes Fanconi anemia group D1. **Oncogene,** 21 (32): 5002-5005.

Gong, C., Fujino, K., Monteiro, L.J., et al. (2015) FOXA1 repression is associated with loss of BRCA1 and increased promoter methylation and chromatin silencing in breast cancer. **Oncogene,** 34 (39): 5012-5024.

Gonzalez-Hormazabal, P., Reyes, J.M., Blanco, R., et al. (2012) The BARD1 Cys557Ser variant and risk of familial breast cancer in South-American population. **Molecular Biology Reports,** 39 (8): 8091-8098.

Gorski, B., Byrski, T., Huzarski, T., et al. (2000) Founder mutations in the BRCA1 gene in Polish families with breast-ovarian cancer. **American Journal of Human Genetics,** 66 (6): 1963-1968.

Gorski, J.J., Savage, K.I., Mulligan, J.M., et al. (2011) Profiling of the BRCA1 transcriptome through microarray and ChIP-chip analysis. **Nucleic Acids Research,** 39 (22): 9536-9548.

Gottlieb, T.M. and Jackson, S.P. (1993) The DNA-dependent protein kinase: requirement for DNA ends and association with Ku antigen. **Cell,** 72 (1): 131-142.

Gowen, L.C., Johnson, B.L., Latour, A.M., et al. (1996) Brca1 deficiency results in early embryonic lethality characterized by neuroepithelial abnormalities. **Nature genetics,** 12 (2): 191-194.

Gradwohl, G., De Murcia, J.M., Molinete, M., et al. (1990) The second zinc-finger domain of poly(ADP-ribose) polymerase determines specificity for single-stranded breaks in DNA. **Proceedings of the National Academy of Sciences of the United States of America,** 87 (8): 2990-2994.

Grantham, R. (1974) Amino acid difference formula to help explain protein evolution. **Science,** 185 (4154): 862-864.

Greenberg, R.A., Sobhian, B., Pathania, S., et al. (2006) Multifactorial contributions to an acute DNA damage response by BRCA1/BARD1-containing complexes. **Genes & development,** 20 (1): 34-46.

Gu, Y., Seidl, K.J., Rathbun, G.A., et al. (1997) Growth retardation and leaky SCID phenotype of Ku70-deficient mice. **Immunity,** 7 (5): 653-665.

Gudas, J.M., Li, T., Nguyen, H., et al. (1996) Cell cycle regulation of BRCA1 messenger RNA in human breast epithelial cells. **Cell growth & differentiation : the molecular biology journal of the American Association for Cancer Research,** 7 (6): 717-723.

Gudmundsdottir, K., Lord, C.J., Witt, E., et al. (2004) DSS1 is required for RAD51 focus formation and genomic stability in mammalian cells. **EMBO reports,** 5 (10): 989-993.

Guex, N. and Peitsch, M.C. (1997) SWISS-MODEL and the Swiss-PdbViewer: an environment for comparative protein modeling. **Electrophoresis,** 18 (15): 2714-2723.

Haas, A.L. and Siepmann, T.J. (1997) Pathways of ubiquitin conjugation. **The FASEB Journal,** 11 (14): 1257-1268.

Hakem, R., de la Pompa, J.L., Elia, A., et al. (1997) Partial rescue of Brca1 (5-6) early embryonic lethality by p53 or p21 null mutation. **Nature genetics,** 16 (3): 298-302.

Hakem, R., de la Pompa, J.L., Sirard, C., et al. (1996) The tumor suppressor gene Brca1 is required for embryonic cellular proliferation in the mouse. **Cell,** 85 (7): 1009-1023.

Hammarsten, O. and Chu, G. (1998) DNA-dependent protein kinase: DNA binding and activation in the absence of Ku. **Proceedings of the National Academy of Sciences of the United States of America,** 95 (2): 525-530.

Hammond-Martel, I., Pak, H., Yu, H., et al. (2010) PI 3 Kinase related kinases-independent proteolysis of BRCA1 regulates Rad51 recruitment during genotoxic stress in human cells. **PLoS ONE,** 5 (11): 14027.

Hanada, K., Budzowska, M., Davies, S.L., et al. (2007) The structure-specific endonuclease Mus81 contributes to replication restart by generating double-strand DNA breaks. **Nat Struct Mol Biol,** 14 (11): 1096-1104.

Hara, K., Hashimoto, H., Murakumo, Y., et al. (2010) Crystal structure of human REV7 in complex with a human REV3 fragment and structural implication of the interaction between DNA polymerase zeta and REV1. **The Journal of biological chemistry,** 285 (16): 12299-12307.

Harkin, D.P., Bean, J.M., Miklos, D., et al. (1999) Induction of GADD45 and JNK/SAPK-dependent apoptosis following inducible expression of BRCA1. **Cell,** 97 (5): 575-586.

Harte, M.T., Gorski, J.J., Savage, K.I., et al. (2014) NF-κB is a critical mediator of BRCA1-induced chemoresistance. **Oncogene,** 33 (6): 713-723.

Harte, M.T., O'Brien, G.J., Ryan, N.M., et al. (2010) BRD7, a subunit of SWI/SNF complexes, binds directly to BRCA1 and regulates BRCA1-dependent transcription. **Cancer research,** 70 (6): 2538-2547.

Hartman, A.R. and Ford, J.M. (2002) BRCA1 induces DNA damage recognition factors and enhances nucleotide excision repair. **Nature genetics,** 32 (1): 180-184.

Hashizume, R., Fukuda, M., Maeda, I., et al. (2001) The RING heterodimer BRCA1-BARD1 is a ubiquitin ligase inactivated by a breast cancer-derived mutation. **The Journal of biological chemistry,** 276 (18): 14537-14540.

Hatchi, E., Skourti-Stathaki, K., Ventz, S., et al. (2015) BRCA1 recruitment to transcriptional pause sites is required for R-loop-driven DNA damage repair. **Molecular Cell,** 57 (4): 636-647.

Hayami, R., Sato, K., Wu, W., et al. (2005) Down-regulation of BRCA1-BARD1 ubiquitin ligase by CDK2. **Cancer research,** 65 (1): 6-10.

Hershko, A., Heller, H., Elias, S., et al. (1983) Components of ubiquitin-protein ligase system. Resolution, affinity purification, and role in protein breakdown. **Journal of Biological Chemistry,** 258 (13): 8206-8214.

Hill, S.J., Rolland, T., Adelmant, G., et al. (2014) Systematic screening reveals a role for BRCA1 in the response to transcription-associated DNA damage. **Genes and Development,** 28 (17): 1957-1975.

Hinz, J.M., Nham, P.B., Urbin, S.S., et al. (2007) Disparate contributions of the Fanconi anemia pathway and homologous recombination in preventing spontaneous mutagenesis. **Nucleic acids research,** 35 (11): 3733-3740.

Hodge, C.D., Ismail, I.H., Edwards, R.A., et al. (2016) RNF8 E3 ubiquitin ligase stimulates Ubc13 E2 conjugating activity that is essential for DNA double-strand break signaling and BRCA1 tumour suppressor recruitment. **Journal of Biological Chemistry,** M116.715698-in press.

Hofmann, R.M. and Pickart, C.M. (1999) Noncanonical MMS2-encoded ubiquitin-conjugating enzyme functions in assembly of novel polyubiquitin chains for DNA repair. **Cell,** 96 (5): 645-653.

Hohenstein, P., Kielman, M.F., Breukel, C., et al. (2001) A targeted mouse Brca1 mutation removing the last BRCT repeat results in apoptosis and embryonic lethality at the headfold stage. **Oncogene,** 20 (20): 2544-2550.

Holloway, J.K., Booth, J., Edelmann, W., et al. (2008) MUS81 generates a subset of MLH1-MLH3-independent crossovers in mammalian meiosis. **PLoS genetics,** 4 (9):.

Hosey, A.M., Gorski, J.J., Murray, M.M., et al. (2007) Molecular basis for estrogen receptor alpha deficiency in BRCA1-linked breast cancer. **J.Natl.Cancer Inst.,** 99 (22): 1683-1694.

Howlett, N.G., Taniguchi, T., Olson, S., et al. (2002) Biallelic inactivation of BRCA2 in Fanconi anemia. **Science (New York, N.Y.),** 297 (5581): 606-609.

Hsiang, Y.H., Hertzberg, R., Hecht, S., et al. (1985) Camptothecin induces protein-linked DNA breaks via mammalian DNA topoisomerase I. **The Journal of biological chemistry,** 260 (27): 14873-14878.

Hsu, L.C. and White, R.L. (1998) BRCA1 is associated with the centrosome during mitosis. **Proc.Natl.Acad.Sci.U.S.A.,** 95 (22): 12983-12988.

Huang, J., Huen, M.S., Kim, H., et al. (2009) RAD18 transmits DNA damage signalling to elicit homologous recombination repair. **Nature cell biology,** 11 (5): 592-603.

Huber, L.J., Yang, T.W., Sarkisian, C.J., et al. (2001) Impaired DNA damage response in cells expressing an exon 11-deleted murine Brca1 variant that localizes to nuclear foci. **Molecular and cellular biology,** 21 (12): 4005-4015.

Huen, M.S.Y., Grant, R., Manke, I., et al. (2007) RNF8 Transduces the DNA-Damage Signal via Histone Ubiquitylation and Checkpoint Protein Assembly. **Cell,** 131 (5): 901-914.

Humphrey, J.S., Salim, A., Erdos, M.R., et al. (1997) Human BRCA1 inhibites growth in yeast: potential use in diagnostic testing. **Proc.Natl.Acad.Sci.U.S.A.,** 94 (11): 5820-5825.

Husain, A., He, G., Venkatraman, E.S., et al. (1998) BRCA1 up-regulation is associated with repair-mediated resistance to cis-diamminedichloroplatinum(II). **Cancer research,** 58 (6): 1120-1123.

Hussain, S., Wilson, J.B., Medhurst, A.L., et al. (2004) Direct interaction of FANCD2 with BRCA2 in DNA damage response pathways. **Human molecular genetics,** 13 (12): 1241-1248.

Iliakis, G., Wang, H., Perrault, A.R., et al. (2004) Mechanisms of DNA double strand break repair and chromosome aberration formation. **Cytogenetic and Genome Research,** 104 (1-4): 14-20.

Iliakis, G., Wang, Y., Guan, J., et al. (2003) DNA damage checkpoint control in cells exposed to ionizing radiation. **Oncogene,** 22 (37): 5834-5847.

Ismail, I.H., Gagne, J.P., Genois, M.M., et al. (2015) The RNF138 E3 ligase displaces Ku to promote DNA end resection and regulate DNA repair pathway choice. **Nature cell biology,** 17 (11): 1446-1457.

Iyer, V.N. and Szybalski, W. (1963) A molecular mechanism of Mitomycin action: Linking of complementary DNA strands. **Proceedings of the National Academy of Sciences of the United States of America,** 50 355-362.

Jaspers, J.E., Kersbergen, A., Boon, U., et al. (2013) Loss of 53BP1 causes PARP inhibitor resistance in Brca1-mutated mouse mammary tumors. **Cancer Discovery,** 3 (1): 68-81.

Jeng, Y.M., Cai-Ng, S., Li, A., et al. (2007) Brca1 heterozygous mice have shortened life span and are prone to ovarian tumorigenesis with haploinsufficiency upon ionizing irradiation. **Oncogene,** 26 (42): 6160-6166.

Ji, G., Yan, L., Lui, W., et al. (2013) Polymorphisms in double-strand breaks repair genes are associated with impaired fertility in Chinese population. **Reproduction,** 145 (5): 463-470.

Jiang, G., Plo, I., Wang, T., et al. (2013a) BRCA1-Ku80 Protein Interaction Enhances End-joining Fidelity of Chromosomal Double-strand Breaks in the G1 Phase of the Cell Cycle. **Journal of Biological Chemistry,** 288 (13): 8966-8976.

Jiang, N., Shen, Y., Fei, X., et al. (2013b) Valosin-containing protein regulates the protasome-mediated degradation of DNA-PKcs in glioma cells. **Cell death and disease,** 30 (4): e647.

Jin, S., Gao, H., Mazzacurati, L., et al. (2009) BRCA1 interaction of centrosomal protein Nlp is required for successful mitotic progression. **Journal of Biological Chemistry,** 284 (34): 22970-22977.

Johnson, N., Johnson, S.F., Yao, W., et al. (2013) Stabilization of mutant BRCA1 protein confers PARP inhibitor and platinum resistance. **Proceedings of the National Academy of Sciences of the United States of America,** 110 (42): 17041-17046.

Jones, R.M. and Petermann, E. (2012) **Replication fork dynamics and the DNA damage response.** , Biochemical Journal.

Joughin, B.A., Tidor, B. and Yaffe, M.B. (2005) A computational method for the anaysis and prediction of protein: phosphopeptide-binding sites. **Protein science,** 14 (1): 131-139.

Joukov, V., Groen, A.C., Prokhorova, T., et al. (2006) The BRCA1/BARD1 heterodimer modulates ran-dependent mitotic spindle assembly. **Cell,** 127 (3): 539-552.

Joukov, V., Chen, J., Fox, E.A., et al. (2001) Functional communication between endogenous BRCA1 and its partner, BARD1, during Xenopus laevis development. **Proceedings of the National Academy of Sciences,** 98 (21): 12078-12083.

Kadouri, L., Hubert, A., Rotenberg, Y., et al. (2007) Cancer risks in carriers of the BRCA1/2 Ashkenazi founder mutations. **Journal of Medical Genetics,** 44 (7): 467-471.

Kakarougkas, A., Ismail, A., Klement, K., et al. (2013a) Opposing roles for 53BP1 during homologous recombination. **Nucleic acids research,** 41 (21): 9719-9731.

Kakarougkas, A., Ismail, A., Katsuki, Y., et al. (2013b) Co-operation of BRCA1 and POH1 relieves the barriers posed by 53BP1 and RAP80 to resection. **Nucleic acids research,** 41 (22): 10298-10311.

Karppinen, S.M., Erkko, H., Reini, K., et al. (2006) Identification of a common polymorphism in the TopBP1 gene associated with hereditary susceptibility to breast and ovarian cancer. **European journal of cancer,** 42 (15): 2647-2652.

Kawai, H., Li, H., Chun, P., et al. (2002) Direct interaction between BRCA1 and the estrogen receptor regulates vascular endothelial growth factor (VEGF) transcription and secretion in breast cancer cells. **Oncogene,** 21 (50): 7730-7739.

Kennedy, R.D., Gorski, J.J., Quinn, J.E., et al. (2005) BRCA1 and c-Myc associate to transcriptionally repress psoriasin, a DNA damage-inducible gene. **Cancer research,** 65 (22): 10265-10272.

Kim, H., Huang, J. and Chen, J. (2007a) CCDC98 is a BRCA1-BRCT domain-binding protein involved in the DNA damage response. **Nature structural & molecular biology,** 14 (8): 710-715.

Kim, H.N., Kim, N.Y., Yu, L., et al. (2014) Polymorphisms in DNA repair genes and MDR1 and the risk for non-Hodgkin lymphoma. **International Journal of Molecular Science,** 15 (4): 6703-6716.

Kim, H.S., Lee, S.W., Choi, Y.J., et al. (2015) Novel germline mutation of BRCA1 gene in a 56-year-old woman with breast cancer, ovarian cancer, and Diffuse Large B-cell lymphoma. **Cancer Research and Treatment,** 47 (3): 534-438.

Kim, H., Chen, J. and Yu, X. (2007b) Ubiquitin-binding protein RAP80 mediates BRCA1-dependent DNA damage response. **Science,** 316 (5828): 1202-1205.

Kim, J.M., Kee, Y., Gurtan, A., et al. (2008) Cell cycle-dependent chromatin loading of the Fanconi anemia core complex by FANCM/FAAP24. **Blood,** 111 (10): 5215-5222.

Kim, J.M., Parmar, K., Huang, M., et al. (2009a) Inactivation of murine Usp1 results in genomic instability and a Fanconi anemia phenotype. **Developmental cell,** 16 (2): 314-320.

Kim, J., McAvoy, S.A., Smith, D.I., et al. (2005) Human TopBP1 Ensures Genome Integrity during Normal S Phase. **Molecular and cellular biology,** 25 (24): 10907-10915.

Kim, S.S., Cao, L., Baek, H.J., et al. (2009b) Impaired skin and mammary gland development and increased gamma-irradiation-induced tumorigenesis in mice carrying a mutation of S1152-ATM phosphorylation site in Brca1. **Cancer research,** 69 (24): 9291-9300.

Kim, S.S., Cao, L., Li, C., et al. (2004) Uterus hyperplasia and increased carcinogen-induced tumorigenesis in mice carrying a targeted mutation of the Chk2 phosphorylation site in Brca1. **Molecular and cellular biology,** 24 (21): 9498-9507.

Kim, S.S., Cao, L., Lim, S.C., et al. (2006) Hyperplasia and spontaneous tumor development in the gynecologic system in mice lacking the BRCA1-Delta11 isoform. **Molecular and cellular biology,** 26 (18): 6983-6992.

Kitagawa, R., Bakkenist, C.J., McKinnon, P.J., et al. (2004) Phosphorylation of SMC1 is a critical downstream event in the ATM-NBS1-BRCA1 pathway. **Genes & development,** 18 (12): 1423-1438.

Kleiman, F.E., Wu-Baer, F., Fonseca, D., et al. (2005) BRCA1/BARD1 inhibition of mRNA 3' processing involves targeted degradation of RNA polymerase II. **Genes and Development,** 19 (10): 1227-1237.

Klein Douwel, D., Boonen, R.A., Long, D.T., et al. (2014) XPF-ERCC1 acts in unhooking DNA interstrand crosslinks in cooperation with FANCD2 and FANCP/SLX4. **Molecular Cell,** 54 (3): 460-471.

Klonowska, K., Ratajska, M., Czubak, K., et al. (2015) Analysis of large mutations in BARD1 in patients with breast and/or ovarian cancer: the Polish population as an example. **Science Reports,** 5 10424.

Knipscheer, P., Raschle, M., Smogorzewska, A., et al. (2009) The Fanconi anemia pathway promotes replication-dependent DNA interstrand cross-link repair. **Science,** 326 (5960): 1698-1701.

Kocylowski, M.K., Rey, A.J., Stewart, G.S., et al. (2015) Ubiquitin-H2AX fusions render 53BP1 recruitment to DNA damage sites independent of RNF8 or RNF168. **Cell Cycle,** 14 (11): 1748-1758.

Koonin, E.V., Altschul, S.F. and Bork, P. (1996) BRCA1 protein products... Functional motifs... **Nature Genetics,** 13 (3): 266-268.

Kopanja, D., Roy, N., Stoyanova, T., et al. (2011) Cul4A is essential for spermatogenesis and male fertility. **Developmental Biology,** 352 (2): 278-287.

Kostyrko, K., Bosshard, S., Urban, Z., et al. (2015) A role for homologous recombinattion proteins in cell cycle regulation. **Cell Cycle,** 14 (17): 2853-2861.

Kote-Jarai, Z., Salmon, A., Mengitsu, T., et al. (2006) Increased level of chromosomal damage after irradiation of lymphocytes from BRCA1 mutation carriers. **British Journal ofCancer,** 94 (2): 308-310.

Kuerbitz, S.J., Plunkett, B.S., Walsh, W.V., et al. (1992) Wild-type p53 is a cell cycle checkpoint determinant following irradiation. **Proceedings of the National Academy of Sciences of the United States of America,** 89 (16): 7491-7495.

Kumaraswamy, E. and Shiekhattar, R. (2007) Activation of BRCA1/BRCA2-associated helicase BACH1 is required for timely progression through S phase. **Molecular and cellular biology,** 27 (19): 6733-6741.

Kuo, C.Y., Li, X., Stark, J.M., et al. (2016) RNF4 regulates DNA double-strand break repair in a cell cycle-dependent manner. **Cell Cycle,** 15 (6): 787-798.

Kysela, B., Chovanec, M. and Jeggo, P.A. (2005) Phosphorylation of linker histones by DNA-dependent protein kinase is required for DNA ligase IV-dependent ligation in the presence of histone H1. **Proceedings of the National Academy of Sciences of the United States of America,** 102 (6): 1877-1882.

Lane, T.F., Lin, C., Brown, M.A., et al. (2000) Gene replacement with the human BRCA1 locus: tissue specific expression and rescue of embryonic lethality in mice. **Oncogene,** 19 (36): 4085-4090.

Larson, J.S., Tonkinson, J.L. and Lai, M.T. (1997) A BRCA1 mutant alters G2-M cell cycle control in human mammary epithelial cells. **Cancer research,** 57 (16): 3351-3355.

Lavin, M.F. (2007) ATM and the Mre11 complex combine to recognize and signal DNA double-strand breaks. **Oncogene,** 26 (56): 7749-7758.

Le Page, F., Randrianarison, V., Marot, D., et al. (2000) BRCA1 and BRCA2 are necessary for the transcription-coupled repair of the oxidative 8-oxoguanine lesion in human cells. **Cancer research,** 60 (19): 5548-5552.

Lee, J.S., Collins, K.M., Brown, A.L., et al. (2000) hCds1-mediated phosphorylation of BRCA1 regulates the DNA damage response. **Nature,** 404 (6774): 201-204.

Lee, K.J., Saha, J., Sun, J., et al. (2016) Phosphorylation of Ku dictates DNA double-strand break (DSB) repair pathway choice in S phase. **Nucleic acids research,** 44 (4): 1732-1745.

Lee, M.S., Green, R., Marsillac, S.M., et al. (2010) Comprehensive analysis of missense variations in the BRCT domain of BRCA1 by structural and functional assays. **Cancer research,** 70 (12): 4880-4890.

Lee, S.A., Roques, C., Magwood, A.C., et al. (2009) Recovery of deficient homologous recombination in Brca2-depleted mouse cells by wild-type Rad51 expression. **DNA repair,** 8 (2): 170-181.

Levenson, V. and Hamlin, J.L. (1993) A general protocol for evaluating the specific effects of DNA replication inhibitors. **Nucleic acids research,** 21 (17): 3997-3404.

Levitus, M., Rooimans, M.A., Steltenpool, J., et al. (2004) Heterogeneity in Fanconi anemia: evidence for 2 new genetic subtypes. **Blood,** 103 (7): 2498-2503.

Levitus, M., Waisfisz, Q., Godthelp, B.C., et al. (2005) The DNA helicase BRIP1 is defective in Fanconi anemia complementation group J. **Nature Genetics,** 37 (9): 934-935.

Li, H., Lee, T.H. and Avraham, H. (2002) A novel tricomplex of BRCA1, Nmi, and c-Myc inhibits c-Myc-induced human telmerase reverse transcriptase gene (hTERT) promoter activity in breast cancer. **Journal of Biological Chemistry,** 277 (23): 20965-20973.

Li, L., Halaby, M., Hakem, A., et al. (2010) Rnf8 deficiency impairs class switch recombination, spermatogenesis, and genomic integrity and predisposes for cancer. **The Journal of experimental medicine,** 207 (5): 983-997.

Li, M. and Yu, X. (2013) Function of BRCA1 in the DNA damage response is mediated by ADP-ribosylation. **Cancer Cell,** 23 (5): 693-704.

Li, S., Chen, P.L., Subramanian, T., et al. (1999) Binding of CtIP to the BRCT repeats of BRCA1 involved in the transcription regulation of p21 is disrupted upon DNA damage. **Journal of Biological Chemistry,** 274 (16): 11334-11338.

Liang, L., Deng, L., Nguyen, S.C., et al. (2008) Human DNA ligases I and III, but not ligase IV, are required for microhomology-mediated end joining of DNA double-strand breaks. **Nucleic acids research,** 36 (10): 3297-3310.

Litman, R., Peng, M., Jin, Z., et al. (2005) BACH1 is critical for homologous recombination and appears to be the Fanconi anemia gene product FANCJ. **Cancer cell,** 8 (3): 255-265.

Liu, C.Y., Flesken-Nikitin, A., Li, S., et al. (1996) Inactivation of the mouse Brca1 gene leads to failure in the morphogenesis of the egg cylinder in early postimplantation development. **Genes & development,** 10 (14): 1835-1843.

Liu, H., Zhang, H., Sun, X., et al. (2013) A cross-sectional study of associations between nonsynonymous mutations of the BARD1 gene and breast cancer in Han Chinese women. **Asia Pacific Journal of Public Health,** 25 (4): 8S-14S.

Liu, L.F. and Wang, J.C. (1979) Interaction between DNA and Escherichia coli DNA topoisomerase I. Formation of complexes between the protein and superhelical and nonsuperhelical duplex DNAs. **The Journal of biological chemistry,** 254 (21): 11082-11088.

Liu, W., Zong, W., Wu, G., et al. (2010) Turnover of BRCA1 involves in radiation-induced apoptosis. **PLoS ONE,** 5 (12): 14484.

Liu, X., Shi, Y., Guan, R., et al. (2008) Potentiation of temozolomide cytotoxicity by poly(ADP)ribose polymerase inhibitor ABT-888 requires a conversion of single-stranded DNA damages to double-stranded DNA breaks. **Molecular cancer research,** 6 (10): 1621-1629.

Liu, X., Holstege, H., van der Gulden, H., et al. (2007a) Somatic loss of BRCA1 and p53 in mice induces mammary tumors with features of human BRCA1-mutated basal-like breast cancer. **Proceedings of the National Academy of Sciences,** 104 (29): 12111-12116.

Liu, Z., Wu, J. and Yu, X. (2007b) CCDC98 targets BRCA1 to DNA damage sites. **Nat Struct Mol Biol,** 14 (8): 716-720.

Lo Ten Foe, J.R., Rooimans, M.A., Bosnoyan-Collins, L., et al. (1996) Expression cloning of a cDNA for the major Fanconi anaemia gene, FAA. **Nature Genetics,** 14 (3): 320-323.

London, T.B., Barber, L.J., Mosedale, G., et al. (2008) FANCJ is a structure-specific DNA helicase associated with the maintenance of genome G/C tracts. **Journal of Biological Chemistry,** 282 (52): 36132-36139.

Long, D.T., Raschle, M., Joukov, V., et al. (2011) Mechanism of RAD51-dependent DNA interstrand cross-link repair. **Science,** 333 (6038): 84-87.

Long, D., Joukov, V., Budzowska, M., et al. (2014) BRCA1 promotes unloading of the CMG helicase from a stalled DNA replication fork. **Molecular cell,** 56 (1): 174-185.

Lord, C.J., McDonald, S., Swift, S., et al. (2008) A high-throughput RNA interference screen for DNA repair determinants of PARP inhibitor sensitivity. **DNA repair,** 7 (12): 2010-2019.

Lou, Z., Minter-Dykhouse, K., Franco, S., et al. (2006) MDC1 maintains genomic stability by participating in the amplification of ATM-dependent DNA damage signals. **Molecular Cell,** 21 (2): 187-200.

Lu, L.Y., Wu, J., Ye, L., et al. (2010) RNF8-dependent histone modifications regulate nucleosome removal during spermatogenesis. **Developmental cell,** 18 (3): 371-384.

Lu, Y., Amleh, A., Sun, J., et al. (2007) Ubiquitination and proteasome-mediated degradation of BRCA1 and BARD1 during steroidogenesis in human ovarian granulosa cells. **Molecular Endocrinology,** 21 (3): 651-663.

Lu, Y., Li, J., Cheng, D., et al. (2012) The F-box protein FBXO44 mediates BRCA1 ubiquitination and degradation. **Journal of Biological Chemistry,** 287 (49): 41014-41022.

Ludwig, T., Chapman, D.L., Papaioannou, V.E., et al. (1997) Targeted mutations of breast cancer susceptibility gene homologs in mice: lethal phenotypes of Brca1, Brca2, Brca1/Brca2, Brca1/p53, and Brca2/p53 nullizygous embryos. **Genes & development,** 11 (10): 1226-1241.

Ludwig, T., Fisher, P., Ganesan, S., et al. (2001) Tumorigenesis in mice carrying a truncating Brca1 mutation. **Genes & development,** 15 (10): 1188-1193.

Lukas, C., Melander, F., Stucki, M., et al. (2004) Mdc1 couples DNA double-strand break recognition by Nbs1 with its H2AX-dependent chromatin retention. **The EMBO journal,** 23 (13): 2674-2683.

Lundberg, R., Mavinakere, M. and Campbell, C. (2001) Deficient DNA end joining activity in extracts from fanconi anemia fibroblasts. **The Journal of biological chemistry,** 276 (12): 9543-9549.

MacLachlan, T.K., Takimoto, R. and El-Deiry, W.S. (2002) BRCA1 directs a selective p53-dependent transcriptional response towards growth arrest and DNA repair targets. **Molecular and cellular biology,** 22 (12): 4280-4292.

Mailand, N., Bekker-Jensen, S., Faustrup, H., et al. (2007) RNF8 Ubiquitylates Histones at DNA Double-Strand Breaks and Promotes Assembly of Repair Proteins. **Cell,** 131 (5): 887-900.

Mak, T.W., Hakem, A., McPherson, J.P., et al. (2000) Brca1 required for T cell lineage development but not TCR loci rearrangement. **Nature immunology,** 1 (1): 77-82.

Mallery, D.L., Vandenberg, C.J. and Hiom, K. (2002) Activation of the E3 ligase function of the BRCA1/BARD1 complex by polyubiquitin chains. **The EMBO journal,** 21 (24): 6755-6762.

Manke, I.A., Lowery, D.M., Nhuyen, A., et al. (2003) BRCT repeats as phosphopeptide-binding modules involved in protein targeting. **Science,** 302 (5645): 636-639.

Martin, R.W., Orelli, B.J., Yamazoe, M., et al. (2007) RAD51 up-regulation bypasses BRCA1 function and is a common feature of BRCA1-deficient breast tumors. **Cancer research,** 67 (20): 9658-9665.

Matthew, C.G. (2006) Fanconi anaemia genes and susceptibility to cancer. **Oncogene,** 25 (43): 5875-5884.

Mattiroli, F., Vissers, J.H., van Dijk, W.J., et al. (2012) RNF168 ubiquitinates K13-15 on H2A/H2AX to drive DNA damage signaling. **Cell,** 150 (6): 1182-1195.

McCarthy, A., Savage, K., Gabriel, A., et al. (2007) A mouse model of basal-like breast carcinoma with metaplastic elements. **The Journal of pathology,** 211 (4): 389-398.

McPherson, J.P., Lemmers, B., Chahwan, R., et al. (2004) Involvement of mammalian Mus81 in genome integrity and tumor suppression. **Science,** 304 (5678): 1822-1826.

McWilliam, H., Li, W., Uludag, M., et al. (2013) Analysis Tool Web Services from the EMBL-EBI. **Nucleic acids research,** 41 (W1): W597-W600.

Meerang, M., Ritz, D., Paliwal, S., et al. (2011) The ubiquitin-selective segregase VCP/p97 orchestrates the response to DNA double-strand breaks. **Nature cell biology,** 13 (11): 1376-1382.

Meetei, A.R., de Winter, J.P., Medhurst, A.L., et al. (2003) A novel ubiquitin ligase is deficient in Fanconi anemia. **Nature Genetics,** 35 (2): 165-170.

Meetei, A.R., Levitus, M., Xue, Y., et al. (2004) X-linked inheritance of Fanconi anemia complementation group B. **Nature Genetics,** 36 (11): 1219-1224.

Meetei, A.R., Medhurst, A.L., Ling, C., et al. (2005) A human ortholog of archaeal DNA repair protein Hef is defective in Fanconi anemia complementation group M. **Nature Genetics,** 37 (9): 958-963.

Ménissier-de Murcia, J., Molinete, M., Gradwohl, G., et al. (1989) Zinc-binding domain of poly(ADP-ribose)polymerase participates in the recognition of single strand breaks on DNA. **Journal of Molecular Biology,** 210 (1): 229-233.

Metzger, M.B., Pruneda, J.N., Klevit, R.E., et al. (2014) RING-type E3 ligases: master manipulators of E2 ubiquitin-conjugating enzymes and ubiquitination. **Biochimica et Biophysica Acta,** 1843 (1): 47-60.

Miki, Y., Swensen, J., Shattuck-Eidens, D., et al. (1994) A strong candidate for the breast and ovarian cancer susceptibility gene BRCA1. **Science,** 266 (5182): 66-71.

Min, J., Allali-Hassani, A., Nady, N., et al. (2007) L3MBTL1 recognition of mono- and dimethylated histones. **Nat Struct Mol Biol,** 14 (12): 1229-1230.

Mohni, K.N., Thompson, P.S., Luzwick, J.W., et al. (2015) A synthetic lethal screen identifies DNA repair pathways that sensitize cancer cells to combined ATR inhibition and Cisplatin treatments. **PloS one,** 10 (5): e0125482.

Monterio, A.N., August, A. and Hanafusa, H. (1996) Evidence for a transcriptional activation function of BRCA1 C-terminal region. **Proc.Natl.Acad.Sci.U.S.A.,** 93 (24): 13595-13599.

Morales, J.C., Xia, Z., Lu, T., et al. (2003) Role for the BRCA1 C-terminal Repeats (BRCT) Protein 53BP1 in Maintaining Genomic Stability. **Journal of Biological Chemistry,** 278 (17): 14971-14977.

Morris, J.R., Boutell, C., Keppler, M., et al. (2009) The SUMO modification pathway is involved in the BRCA1 response to genotoxic stress. **Nature,** 462 (7275): 886-890.

Morris, J.R., Keep, N.H. and Solomon, E. (2002) Identification of residues required for the interaction of BARD1 with BRCA1. **Journal of Biological Chemistry,** 277 (11): 9382-9386.

Morris, J.R., Pangon, L., Boutell, C., et al. (2006) Genetic analysis of BRCA1 ubiquitin ligase activity and its relationship to breast cancer susceptibility. **Human molecular genetics,** 15 (4): 599-606.

Morris, J.R. and Solomon, E. (2004) BRCA1 : BARD1 induces the formation of conjugated ubiquitin structures, dependent on K6 of ubiquitin, in cells during DNA replication and repair. **Human molecular genetics,** 13 (8): 807-817.

Moynahan, M.E., Cui, T.Y. and Jasin, M. (2001a) Homology-directed dna repair, mitomycin-c resistance, and chromosome stability is restored with correction of a Brca1 mutation. **Cancer research,** 61 (12): 4842-4850.

Moynahan, M.E., Pierce, A.J. and Jasin, M. (2001b) BRCA2 is required for homology-directed repair of chromosomal breaks. **Molecular cell,** 7 (2): 263-272.

Muniandy, P.A., Liu, J., Majumdar, A., et al. (2010) DNA interstrand crosslink repair in mammalian cells:step by step. **Critical Review in Biochemical Molecular Biology,** 45 (1): 23-49.

Murai, J., Huang, S.Y., Das, B.B., et al. (2012) Trapping of PARP1 and PARP2 by Clinical PARP Inhibitors. **Cancer research,** 72 (21): 5588-5599.

Murai, J., Yang, K., Dejsuphong, D., et al. (2011) The USP1/UAF1 complex promotes double-strand break repair through homologous recombination. **Molecular and cellular biology,** 31 (12): 2462-2469.

Nakada, S., Yonamine, R.M. and Matsuo, K. (2012) RNF8 Regulates Assembly of RAD51 at DNA Double-Strand Breaks in the Absence of BRCA1 and 53BP1. **Cancer research,** 72 (19): 4974-4983.

Nakamura, K., Kogame, T., Oshiumi, H., et al. (2010) Collaborative action of Brca1 and CtIP in elimination of covalent modifications from double-strand breaks to facilitate subsequent break repair. **PLoS genetics,** 6 (1): e10000828.

Nakamura, K., Sakai, W., Kawamoto, T., et al. (2006) Genetic dissection of vertebrate 53BP1: a major role in non-homologous end joining of DNA double strand breaks. **DNA repair,** 5 (6): 741-749.

Nelson, A.C. and Holt, J.T. (2010) Impact of RING and BRCT domain mutations on BRCA1 protein stability, localization and recruitment to DNA damage. **Radiation research,** 174 (1): 1-13.

Neuhausen, S.L. and Marshall, C.J. (1994) Loss of heterozygosity in familial tumors from three BRCA1-linked kindreds. **Cancer Research,** 54 (23): 6069-6072.

Nieuwenhuis, B., Van Assen-Bolt, A.J., Van Waarde-Verhagen, M.A., et al. (2002) BRCA1 and BRCA2 heterozygosity and repair of X-ray-induced DNA damage. **International Journal of Radiation Biology,** 78 (4): 285-295.

Nijman, S.M., Huang, T.T., Dirac, A.M., et al. (2005) The deubiquitinating enzyme USP1 regulates the Fanconi anemia pathway. **Molecular cell,** 17 (3): 331-339.

Nimonkar, A.V., Ozsoy, A.Z., Genschel, J., et al. (2008) Human exonuclease 1 and BLM helicase interact to resect DNA and initiate DNA repair. **Proceedings of the National Academy of Sciences of the United States of America,** 105 (44): 16906-16911.

Noon, A.T., Shibata, A., Rief, N., et al. (2010) 53BP1-dependent robust localized KAP-1 phosphorylation is essential for heterochromatic DNA double-strand break repair. **Nature cell biology,** 12 (2): 177-184.

Norquist, B., Wurz, K.A., Pennil, C.C., et al. (2011) Secondary somatic mutations restoring BRCA1/2 predict chemotherapy resistance in hereditary ovarian carcinomas. **Journal of clinical oncology,** 29 (22): 3008-3015.

Oplustilova, L., Wolanin, K., Mistrik, M., et al. (2012) Evaluation of candidate biomarkers to predict cancer cell sensitivity or resistance to PARP-1 inhibitor treatment. **Cell cycle,** 11 (20): 3837-3850.

O'Regan, P., Wilson, C., Townsend, S., et al. (2001) XRCC2 is a nuclear RAD51-like protein required for damage-dependent RAD51 focus formation without the need for ATP binding. **The Journal of biological chemistry,** 276 (25): 22148-22153.

Ossareh-Nazari, B., Bachelerie, F. and Dargemont, C. (1997) Evidence for a role of CRM1 in signal-mediated nuclear protein export. **Science (New York, N.Y.),** 278 (5335): 141-144.

Ouchi, T., Lee, S.W., Ouchi, M., et al. (2000) Collaboration of signal transucer and activator of transcription 1 (STAT1) and BRCA1 in differential regulation of IFN-gamma target genes. **Proc.Natl.Acad.Sci.U.S.A.,** 97 (10): 5208-5213.

Pace, P., Mosedale, G., Hodskinson, M.R., et al. (2010) Ku70 corrupts DNA repair in the absence of the Fanconi anemia pathway. **Science,** 329 (5988): 219-223.

Painter, R.B. (1974) DNA damage and repair in eukaryotic cells. **Genetics,** 78 (1): 139-148.

Parameswaran, B., Chiang, H.C., Lu, Y., et al. (2015) Damage-induced BRCA1 phosphorylation by Chk2 contributes to the timing of end resection. **Cell Cycle,** 14 (3): 437-448.

Parvin, J.D. and Sankaran, S. (2006) The BRCA1 E3 ubiquitin ligase controls centrosome dynamics. **Cell Cycle,** 5 (17): 1946-1950.

Pascoe, J.M. and Roberts, J.J. (1974) Interactions between mammalian cell DNA and inorganic platinum compounds—I: DNA interstrand cross-linking and cytotoxic properties of platinum(II) compounds. **Biochemical pharmacology,** 23 (9): 1345-1357.

Paull, T.T., Rogakou, E.P., Yamazaki, V., et al. (2000) A critical role for histone H2AX in recruitment of repair factors to nuclear foci after DNA damage. **Current Biology,** 10 (15): 886-895.

Peng, Y., Dai, H., Wang, E., et al. (2015) TUSC4 functions as a tumor suppressor by regulating BRCA1 stability. **Cancer research,** 75 (2): 378-386.

Pickart, C.M. and Eddins, M.J. (2004) Ubiquitin: structures, functions, mechanisms. **Biochimica et Biophysica Acta (BBA) - Molecular Cell Research,** 1695 (1): 55-72.

Plans, V., Scheper, J., Soler, M., et al. (2006) The RING finger protein RNF8 recruits UBC13 for lysine 63-based self polyubiquitylation. **Journal of cellular biochemistry,** 97 (3): 572-582.

Plechanovova, A., Jaffray, E.G., Tatham, M.H., et al. (2012) Structure of a RING E3 ligase and ubiquitin-loaded E2 primed for catalysis. **Nature,** 489 (7414): 115-120.

Poccia, D.L., LeVine, D. and Wang, J.C. (1978) Activity of a DNA topoisomerase (nicking-closing enzyme) during sea urchin development and the cell cycle. **Developmental biology,** 64 (2): 273-283.

Polanowska, J., Martin, J.S., Garcia-Muse, T., et al. (2006) A conserved pathway to activte BRCA1-dependent ubiquitylation at DNA damage sites. **EMBO J.,** 25 (10): 2178-2188.

Polato, F., Callen, E., Wong, N., et al. (2014) CtIP-mediated resection is essential for viability and can operate independently of BRCA1. **Journal of Experimental Medicine,** 211 (6): 1027-1036.

Qin, Y., Xu, J., Aysola, K., et al. (2011) Ubc9 mediates nuclear localization and growth suppression of BRCA1 and BRCA1a proteins. **Journal of cellular physiology,** 226 (12): 3355-3367.

Ramadan, K. (2012) p97/VCP- and Lys48-linked polyubiquitination form a new signaling pathway in DNA damage response. **Cell cycle (Georgetown, Tex.),** 11 (6): 1062-1069.

Ramirez, A., Bravo, A., Jorcano, J.L., et al. (1994) Sequences 5' of the bovine keratin 5 gene direct tissue- and cell-type-specific expression of a lacZ gene in the adult and during development. **Differentiation; research in biological diversity,** 58 (1): 53-64.

Ramsden, D.A. (2011) Polymerases in nonhomologous end joining: building a bridge over broken chromosomes. **Antioxidants & redox signaling,** 14 (12): 2509-2519.

Ransburgh, D.J., Chiba, N., Ishioka, C., et al. (2010) Identification of breast tumor mutations in BRCA1 that abolish its function in homologous DNA recombination. **Cancer Research,** 70 (3): 988-995.

Ratajska, M., Antoszewska, E., Piskorz, A., et al. (2012) Cancer predisposing BARD1 mutations in breast-ovarian cancer families. **Breast cancer research and treatment,** 131 (1): 89-97.

Reczek, C.R., Szabolcs, M., Stark, J.M., et al. (2013) The interaction between CtIP and BRCA1 is not essential for resection-mediated DNA repair or tumor suppression. **Journal of Biological Chemistry,** 201 (5): 693-707.

Reid, L.J., Shakya, R., Modi, A.P., et al. (2008) E3 ligase activity of BRCA1 is not essential for mammalian cell viability or homology-directed repair of double-strand DNA breaks. **Proceedings of the National Academy of Sciences of the United States of America,** 105 (52): 20876-20881.

Rock, K.L., Gramm, C., Rothstein, L., et al. (1994) Inhibitors of the proteasome block the degradation of most cell proteins and the generation of peptides presented on MHC class I molecules. **Cell,** 78 (5): 761-771.

Rodriguez, J.A. and Henderson, B.R. (2000) Identification of a functional nuclear export sequence in BRCA1. **The Journal of biological chemistry,** 275 (49): 38589-38596.

Rodriguez, J.A., Au, W.W.Y. and Henderson, B.R. (2004) Cytoplasmic mislocalization of BRCA1 caused by cancer-associated mutations in the BRCT domain. **Experimental cell research,** 293 (1): 14-21.

Rodriguez, J.A., Schuchner, S., Au, W.W.Y., et al. (2003a) Nuclear-cytoplasmic shuttling of BARD1 contributes to its proapoptotic activity and is regulated by dimerization with BRCA1. **Oncogene,** 23 (10): 1809-1820.

Rodriguez, M., Yu, X., Chen, J., et al. (2003b) Phosphopeptide binding specificities of BRCA1 COOH-terminal (BRCT) domains. **Journal of Biological Chemistry,** 278 (52): 52914-52918.

Romanienko, P.J. and Camerini-Otero, R. (2000) The Mouse Spo11 Gene Is Required for Meiotic Chromosome Synapsis. **Molecular cell,** 6 (5): 975-987.

Rosen, E.M., Fan, S. and Ma, Y. (2006) BRCA1 regulation of transcription. **Cancer letters,** 236 (2): 175-185.

Rothfuss, A., Schutz, P., Bochum, S., et al. (2000) Induced micronucleus frequencies in peripheral lymphocytes as a screening test for carriers of a BRCA1 mutation in breast cancer families. **Cancer Res.,** 60 (2): 390-394.

Rottenberg, S., Jaspers, J.E., Kersbergen, A., et al. (2008) High sensitivity of BRCA1-deficient mammary tumors to the PARP inhibitor AZD2281 alone and in combination with platinum drugs. **Proceedings of the National Academy of Sciences of the United States of America,** 105 (44): 17079-17084.

Royer-Pokora, B., Gordon, L.K. and Haseltine, W.A. (1981) Use of exonuclease III to determine the site of stable lesions in defined sequences of DNA: the cyclobutane pyrimidine dimer and cis and trans dichlorodiammine platinum II examples. **Nucleic acids research,** 9 (18): 4595-4609.

Royo, H., Polikiewicz, G., Mahadevaiah, S.K., et al. (2010) Evidence that meiotic sex chromosome inactivation is essential for male fertility. **Current Biology,** 20 (23): 2117-2123.

Ruffner, H. and Verma, I.M. (1997) BRCA1 is a cell cycle-regulated nuclear phosphoprotein. **Proceedings of the National Academy of Sciences of the United States of America,** 94 (14): 7138-7143.

Ruffner, H., Joazeiro, C.A.P., Hemmati, D., et al. (2001) Cancer-predisposing mutations within the RING domain of BRCA1: Loss of ubiquitin protein ligase activity and protection from radiation hypersensitivity. **Proceedings of the National Academy of Sciences,** 98 (9): 5134-5139.

Saha, T., Rih, J.K., Roy, R., et al. (2010) Transcriptional regulation of the base excision repair pathway by BRCA1. **Journal of Biological Chemistry,** 285 (25): 19092-19105.

Saintigny, Y., Delacote, F., Vares, G., et al. (2001) Characterization of homologous recombination induced by replication inhibition in mammalian cells. **The EMBO journal,** 20 (14): 3861-3870.

Saleh-Gohari, N. and Helleday, T. (2004) Conservative homologous recombination preferentially repairs DNA double-strand breaks in the S phase of the cell cycle in human cells. **Nucleic acids research,** 32 (12): 3683-3688.

Sankaran, S., Starita, L.M., Groen, A.C., et al. (2005) Centrosomal microtubule nucleation activity is inhibited by BRCA1-dependent ubiquitination. **Molecular and cellular biology,** 25 (19): 8656-8668.

Sankaran, S., Starita, L.M., Simons, A.M., et al. (2006) Identification of domains of BRCA1 critical for the ubiquitin-dependent inhibition of centrosome function. **Cancer Research,** 66 (8): 4100-4107.

Santos, M.A., Huen, M.S., Jankovic, M., et al. (2010) Class switching and meiotic defects in mice lacking the E3 ubiquitin ligase RNF8. **Journal of Experimental Medicine,** 207 (5): 973-981.

Sartori, A.A., Lukas, C., Coates, J., et al. (2007) Human CtIP promotes DNA end resection. **Nature,** 450 (7169): 509-514.

Sasco, A.J., Lowenfels, A.B. and Pasker-De Jong, P. (1993) Epidemiology of male breast cancer. A meta-analysis of published case-control studies and discussion of selected aetiological factors. **International Journal of Cancer,** 53 (4): 538-549.

Sato, K., Sundaramoorthy, E., Rajendra, E., et al. (2012) A DNA-damage selective role for BRCA1 E3 ligase in claspin ubiquitylation, CHK1 activation, and DNA repair. **Current biology : CB,** 22 (18): 1659-1666.

Satoh, M.S. and Lindahl, T. (1992) Role of poly(ADP-ribose) formation in DNA repair. **Nature,** 356 (6367): 356-358.

Savage, K.L., Gorski, J.J., Barros, E.M., et al. (2014) Identification of a BRCA1-mRNA splicing complex required for efficient DNA repair and maintenance of genome stability. **Molecular Cell,** 54 (3): 445-459.

Sawyer, S.L., Tian, L., Kahkonen, M., et al. (2015) Biallelic mutations in BRCA1 cause a new Fanconi anemia subtype. **Cancer discovery,** 5 (2): 135-142.

Scardocci, A., Guidi, F., D'Alo', F., et al. (2006) Reduced BRCA1 expression due to promoter hypermethylation in therapy-related acute myeloid leukaemia. **British Journal of Cancer,** 95 (8): 1108-1113.

Schaetzlein, S., Chahwan, R., Avievich, E., et al. (2013) Mammalian Exo1 encodes both structural and catalytic functions that play distinct roles in essential biological processes. **Proc.Natl.Acad.Sci.U.S.A.,** 111 (27): 2470-2479.

Schlegel, B.P., Jodelka, F.M. and Nunez, R. (2006) BRCA1 promotes induction of ssDNA by ionizing radiation. **Cancer research,** 66 (10): 5181-5189.

Schneider, C.A., Rasband, W.S. and Eliceiri, K.W. (2012) NIH Image to ImageJ: 25 years of image analysis. **Nature Methods,** 9 (7): 671-675.

Schreiber, F., Patricio, M., Muffato, M., et al. (2014) TreeFam v9: a new website, more species and orthology-on-the-fly. **Nucleic acids research,** 42 (D1): D922-D925.

Schultz, L.B., Chehab, N.H., Malikzay, A., et al. (2000) p53 binding protein 1 (53bp1) is an early participant in the cellular response to DNA double-strand breaks. **The Journal of cell biology,** 151 (7): 1381-1390.

Scully, R., Chen, J., Ochs, R.L., et al. (1997a) Dynamic changes of BRCA1 subnuclear location and phosphorylation state are initiated by DNA damage. **Cell,** 90 (3): 425-435.

Scully, R., Chen, J., Plug, A., et al. (1997b) Association of BRCA1 with Rad51 in mitotic and meiotic cells. **Cell,** 88 (2): 265-275.

Scully, R., Ganesan, S., Brown, M., et al. (1996) Location of BRCA1 in human breast and ovarian cancer cells. **Science (New York, N.Y.),** 272 (5258): 123-126.

Shabbeer, S., Omer, D., Berneman, D., et al. (2013) BRCA1 targets G2/M cell cycle proteins for ubiquitination and proteasomal degradation. **Oncogene,** 32 (42): 5005-5016.

Shakya, R., Reid, L.J., Reczek, C.R., et al. (2011) BRCA1 tumor suppression depends on BRCT phosphoprotein binding, but not its E3 ligase activity. **Science (New York, N.Y.),** 334 (6055): 525-528.

Shakya, R., Szabolcs, M., McCarthy, E., et al. (2008) The basal-like mammary carcinomas induced by Brca1 or Bard1 inactivation implicate the BRCA1/BARD1 heterodimer in tumor suppression. **Proceedings of the National Academy of Sciences of the United States of America,** 105 (19): 7040-7045.

Shao, G., Patterson-Fortin, J., Messick, T.E., et al. (2009a) MERIT40 controls BRCA1-Rap80 complex integrity and recombination to DNA double-strand breaks. **Genes and Development,** 23 (6): 740-754.

Shao, G., Lilli, D.R., Patterson-Fortin, J., et al. (2009b) The Rap80-BRCC36 de-ubiquitinating enzyme complex antagonizes RNF8-Ubc13-dependent ubiquitination events at DNA double strand breaks. **Proceedings of the National Academy of Sciences,** 106 (9): 3166-3171.

Sharma, S., Hicks, J.K., Chute, C.L., et al. (2012) REV1 and polymerase zeta facilitate homologous recombination repair. **Nucleic acids research,** 40 (2): 682-691.

Shen, D., Wu, Y., Chillar, R., et al. (2000) Missense alterations of BRCA1 gene detected in diverse cancer patients. **Anticancer Research,** 20 (2B): 1129-1132.

Shen, M., Zheng, T., Lan, Q., et al. (2006) Polymorphisms in DNA repair genes and risk of non-Hodgkin lymphoma amoung women in Connecticut. **Human Genetics,** 119 (6): 659-668.

Shen, S.X., Weaver, Z., Xu, X., et al. (1998) A targeted disruption of the murine Brca1 gene causes gamma-irradiation hypersensitivity and genetic instability. **Oncogene,** 17 (24): 3115-3124.

Shibata, A., Moiani, D., Arvi, A.S., et al. (2014) DNA double-strand break repair pathway choice is directed by distinct MRE11 nuclease activities. **Molecular cell,** 53 (1): 7-18.

Shih, H.A., Nathanson, K.L., Seal, S., et al. (2000) BRCA1 and BRCA2 mutations in breast cancer families with mulitple primary cancers. **Clinical cancer Research,** 6 (11): 4259-4264.

Simhadri, S., Peterson, S., Patel, D.S., et al. (2014) Male fertility defect associated with disrupted BRCA1-PALB2 interaction in mice. **Journal of Biological Chemistry,** 289 (35): 24617-24629.

Singh, T.R., Saro, D., Ali, A.M., et al. (2010) MHF1-MHF2, a histone-fold-containing protein complex, participates in the Fanconi anemia pathway via FANCM. **Molecular cell,** 37 (6): 879-886.

Sinha, N.K. and Snustad, D.P. (1972) Mechanism of inhibition of deoxyribonucleic acid synthesis in Escherichia coli by hydroxyurea. **Journal of Bacteriology,** 112 (3): 1321-1324.

Smith, S.A., Easton, D.F., Evans, D.G., et al. (1992) Allele losses in the region 17q12-21 in familial breast and ovarian cancer involve the wild-type chromosome. **Nature Genetics,** 2 (2): 128-131.

Snouwaert, J.N., Gowen, L.C., Latour, A.M., et al. (1999) BRCA1 deficient embryonic stem cells display a decreased homologous recombination frequency and an increased frequency of non-homologous recombination that is corrected by expression of a brca1 transgene. **Oncogene,** 18 (55): 7900-7907.

Sobhian, B., Shao, G., Lilli, D.R., et al. (2007) RAP80 targets BRCA1 to specific ubiquitin structures at DNA damage sites. **Science (New York, N.Y.),** 316 (5828): 1198-1202.

Somasundaram, K., Zhang, H., Zeng, Y.X., et al. (1997) Arrest of the cell cycle by the tumour-suppressor BRCA1 requires the CDK-inhibitor p21WAF1/CiP1. **Nature,** 389 (6647): 187-190.

Sommers, J.A., Rawtani, N., Gupta, R., et al. (2009) FANCJ uses its motor ATPase to destabilize protein-DNA complexes, unwind triplexes, and inhibit RAD51 strand exchange. **The Journal of biological chemistry,** 284 (12): 7505-7517.

Somyajit, K., Mishra, A., Jameei, A., et al. (2015) Enhanced non-homologous end joining contributes toward synthetic lethality of pathological RAD51C mutants with poly (ADP-ribose) polymerase. **Carcinogenesis,** 36 (1): 13-24.

Song, M., Hakala, K., Weintraub, S.T., et al. (2011) Quantitative proteomic identificatio of the BRCA1 ubiquitination substrates. **Journal of Proteome Research,** 10 (11): 5191-5198.

Soutoglou, E., Dorn, J.F., Sengupta, K., et al. (2007) Positional stability of single double-strand breaks in mammalian cells. **Nature cell biology,** 9 (6): 675-682.

Speit, G. and Trenz, K. (2004) Chromosomal mutagen sensitivity associated with mutations in BRCA genes. **Cytogenetic and Genome Research,** 104 (1-4): 325-332.

Speit, G., Trenz, K., Schütz, P., et al. (2000) Mutagen sensitivity of human lymphoblastoid cells with a BRCA1 mutation in comparison to ataxia telangiectasia heterozygote cells. **Cytogenetic and Genome Research,** 91 (1-4): 261-266.

Starita, L.M., Horwitz, A.A., Keogh, M.C., et al. (2005) BRCA1/BARD1 ubiquitinate phosphorylated RNA polymerase II. **Journal of Biological Chemistry,** 280 (26): 24498-24505.

Starita, L.M., Machida, Y., Sankaran, S., et al. (2004) BRCA1-dependent ubiquitination of gamma-tubulin regulates centrosome number. **Molecular and cellular biology,** 24 (19): 8457-8466.

Stebbing, J., Zhang, H., Xu, Y., et al. (2015) KSR1 regulates BRCA1 degradation and inhibits breast cancer growth. **Oncogene,** 34 (16): 2103-2114.

Stewart, G.S., Panier, S., Townsend, K., et al. (2009) The RIDDLE Syndrome Protein Mediates a Ubiquitin-Dependent Signaling Cascade at Sites of DNA Damage. **Cell,** 136 (3): 420-434.

Strathdee, C.A., Gavish, H., Shannon, W.R., et al. (1992) Cloning of cDNAs for Fanconi's anaemia by functional complementation. **Nature,** 356 (6372): 763-767.

Strom, C.E., Johansson, F., Uhlen, M., et al. (2011) Poly (ADP-ribose) polymerase (PARP) is not involved in base excision repair but PARP inhibition traps a single-strand intermediate. **Nucleic acids research,** 39 (8): 3166-3175.

Suhasini, A.N., Rawtani, N.A., Wu, Y., et al. (2011) Interaction between the helicases genetically linked to Fanconi anemia group J and Bloom's syndrome. **The EMBO journal,** 30 (4): 692-705.

Sung, P. (1994) Catalysis of ATP-dependent homologous DNA pairing and strand exchange by yeast RAD51 protein. **Science,** 265 (5176): 1241-1243.

Sung, P. and Robberson, D.L. (1995) DNA strand exchange mediated by a RAD51-ssDNA nucleoprotein filament with polarity opposite to that of RecA. **Cell,** 82 (3): 453-461.

Swisher, E.M., Sakai, W., Karlan, B.Y., et al. (2008) Secondary BRCA1 mutations in BRCA1-mutated ovarian carcinomas with platinum resistance. **Cancer research,** 68 (8): 2581-2586.

Sy, S.M.H., Huen, M.S.Y. and Chen, J. (2009) PALB2 is an integral component of the BRCA complex required for homologous recombination repair. **Proceedings of the National Academy of Sciences,** 106 (17): 7155-7160.

Sylvain, V., Lafarge, S. and Bignon, Y.J. (2002) Dominant-negative activity of a Brca1 truncation mutant: effects on proliferation, tumourigenicity in vivo, and chemosentivity in a mouse ovarian cancer cell line. **International Journal of Oncology,** 20 (4): 845-853.

Tang, J., Cho, N.W., Cui, G., et al. (2013) Acetylation limits 53BP1 association with damaged chromatin to promote homologous recombination. **Nature structural & molecular biology,** 20 (3): 317-325.

Taniguchi, T., Garcia-Higuera, I., Andreassen, P.R., et al. (2002) S-phase-specific interaction of the Fanconi anemia protein, FANCD2, with BRCA1 and RAD51. **Blood,** 100 (7): 2414-2420.

Taniguchi, T., Tischkowitz, M., Ameziane, N., et al. (2003) Disruption of the Fanconi anemia-BRCA pathway in cisplatin-sensitive ovarian tumors. **Nature medicine,** 9 (5): 568-574.

Tassone, P., Di Martino, M.T., Ventura, M., et al. (2009) Loss of BRCA1 function increases the antitumor activity of cisplatin against human breast cancer xenografts in vivo. **Cancer biology & therapy,** 8 (7): 648-653.

Tassone, P., Tagliaferri, P., Perricelli, A., et al. (2003) BRCA1 expression modulates chemosensitivity of BRCA1-defective HCC1937 human breast cancer cells. **British journal of cancer,** 88 (8): 1285-1291.

Taylor, E.M., Cecillon, S.M., Bonis, A., et al. (2010) The Mre11/Rad50/Nbs1 complex functions in resection-based DNA end joining in Xenopus laevis. **Nucleic acids research,** 38 (2): 441-454.

Thakur, S., Zhang, H.B., Peng, Y., et al. (1997) Localization of BRCA1 and a splice variant identifies the nuclear localization signal. **Molecular and cellular biology,** 17 (1): 444-452.

Thompson, E.G., Fares, H. and Dixon, K. (2012) BRCA1 requirement for the fidelity of plasmid DNA double-strand break repair in cultured breast epithelial cells. **Environmental and Molecular Mutagenesis,** 53 (1): 32-43.

Thorslund, T., Ripplinger, A., Hoffmann, S., et al. (2015) Histone H1 couples initiation and amplification of ubiquitin signalling after DNA damage. **Nature,** 527 (7578): 389-393.

Tian, F., Sharma, S., Zou, J., et al. (2013) BRCA1 promotes the ubiquitination of PCNA and recruitment of translesion polymerases in response to replication blockade. **Proceedings of the National Academy of Sciences,** 110 (33): 13558-13563.

Timmers, C., Taniguchi, T., Hejna, J., et al. (2001) Positional cloning of a novel Fanconi anemia gene, FANCD2. **Molecular Cell,** 7 (2): 241-248.

Tischkowitz, M., Xia, B., Sabbaghian, N., et al. (2007) Analysis of PALB2/FANCN-associated breast cancer families. **Proc.Natl.Acad.Sci.U.S.A.,** 104 (14): 6788-6793.

Tischkowitz, M.D. and Hodgson, S.V. (2003) Fanconi anaemia. **Journal of Medical Genetics,** 40 (1): 1-10.

Trenz, K., Landgraf, J. and Speit, G. (2003a) Mutagen sensitivity of human lymphoblastoid cells with a BRCA1 mutation. **Breast Cancer Res.Treat.,** 78 (1): 69-79.

Trenz, K., Lugowski, S., Jahrsdörfer, U., et al. (2003b) Enhanced sensitivity of peripheral blood lymphocytes from women carrying a BRCA1 mutation towards the mutagenic effects of various cytostatics. **Mutation Research,** 544 (2–3): 279-288.

Trenz, K., Rothfuss, A., Schütz, P., et al. (2002) Mutagen sensitivity of peripheral blood from women carrying a BRCA1 or BRCA2 mutation. **Mutation Research,** 500 (1–2): 89-96.

Tripathi, V., Nagarjuna, T. and Sengupta, S. (2007) BLM helicase-dependent and -independent roles of 53BP1 during replication stress-mediated homologous recombination. **The Journal of cell biology,** 178 (1): 9-14.

Turner, J.M.A., Aprelikova, O., Xu, X., et al. (2004) BRCA1, Histone H2AX Phosphorylation, and Male Meiotic Sex Chromosome Inactivation. **Current Biology,** 14 (23): 2135-2142.

Turner, J.M.A., Mahadevaiah, S.K., Fernandez-Capetillo, O., et al. (2005) Silencing of unsynapsed meiotic chromosomes in the mouse. **Nature genetics,** 37 (1): 41-47.

Turner, N.C., Lord, C.J., Iorns, E., et al. (2008) A synthetic lethal siRNA screen identifying genes mediating sensitivity to a PARP inhibitor. **The EMBO journal,** 27 (9): 1368-1377.

Typas, D., Luijsterburg, M.S., Wiegant, W.W., et al. (2015) The de-ubiquitylating enzymes USP25 and USP37 regulate homologous recombination by counteracting RAP80. **Nucleic Acids Research,** 43 (14): 6919-6933.

van Nocker, S. and Vierstra, R.D. (1991) Cloning and characterization of a 20-kDa ubiquitin carrier protein from wheat that catalyzes multiubiquitin chain formation in vitro. **Proc.Natl.Acad.Sci.U.S.A.,** 88 (22): 10297-10301.

VanDemark, A.P., Hofmann, R.M., Tsui, C., et al. (2001) Molecular insights into polyubiquitin chain assembly: crystal structure of the Mms2/Ubc13 heterodimer. **Cell,** 105 (6): 711-720.

Vandenberg, C.J., Gergely, F., Ong, C.Y., et al. (2003) BRCA1-independent ubiquitination of FANCD2. **Molecular cell,** 12 (1): 247-254.

Vasanthakumar, A., Arnovitz, S., Marquez, R., et al. (2016) Brca1 deficiency causes bone marrow failure and spontaneous hematologic malignancies in mice. **Blood,** 127 (3): 310-313.

Vassar, R., Rosenberg, M., Ross, S., et al. (1989) Tissue-specific and differentiation-specific expression of a human K14 keratin gene in transgenic mice. **Proceedings of the National Academy of Sciences of the United States of America,** 86 (5): 1563-1567.

Vaughn, J.P., Davis, P.L., Jarboe, M.D., et al. (1996) BRCA1 expression is induced before DNA synthesis in both normal and tumor-derived breast cells. **Cell growth & differentiation : the molecular biology journal of the American Association for Cancer Research,** 7 (6): 711-715.

Vaz, F., Hanenberg, H., Schuster, B., et al. (2010) Mutation of the RAD51C gene in a Fanconi anemia-like disorder. **Nature genetics,** 42 (5): 406-409.

Venere, M., Snyder, A., Zgheib, O., et al. (2007) Phosphorylation of ATR-interacting protein on Ser239 mediates an interaction with breast-ovarian cancer susceptibility 1 and checkpoint function. **Cancer research,** 67 (13): 6100-6105.

Vikrant, Kumar, R., Siddiqui, Q., et al. (2015) Mislocalization of BRCA1-complex due to ABRAXAS Arg361Gln mutation. **Journal of Biomolecular Structure & Dynamics,** 33 (6): 1291-1301.

Wagner, K.U., Wall, R.J., St-Onge, L., et al. (1997) Cre-mediated gene deletion in the mammary gland. **Nucleic acids research,** 25 (21): 4323-4330.

Wang, B. and Elledge, S.J. (2007) Ubc13/Rnf8 ubiquitin ligases control foci formation of the Rap80/Abraxas/Brca1/Brcc36 complex in response to DNA damage. **Proceedings of the National Academy of Sciences,** 104 (52): 20759-20763.

Wang, B., Matsuoka, S., Ballif, B.A., et al. (2007) Abraxas and RAP80 form a BRCA1 protein complex required for the DNA damage response. **Science,** 316 (5828): 1194-1198.

Wang, H.C., Chou, W.C., Shieh, S.Y., et al. (2006) Ataxia telangiectasia mutated and checkpoint kinase 2 regulate BRCA1 to promote the fidelity of DNA end-joining. **Cancer research,** 66 (3): 1391-1400.

Wang, J., Aroumougame, A., Lobrich, M., et al. (2014a) PTIP associates with Artemis to dictate DNA repair pathway choice. **Genes and Development,** 28 (24): 2693-2698.

Wang, R.H., Yu, H. and Deng, C.X. (2004a) A requirement for breast-cancer-associated gene 1 (BRCA1) in the spindle checkpoint. **Proc.Natl.Acad.Sci.U.S.A.,** 101 (49): 17108-17113.

Wang, X., Wang, R.H., Li, W., et al. (2004b) Genetic interactions between Brca1 and Gadd45a in centrosome duplication, genetic stability, and neural tube closure. **The Journal of biological chemistry,** 279 (28): 29606-29614.

Wang, X., Lu, G., Li, L., et al. (2014b) HUWE1 interacts with BRCA1 and promotes its degradation in the ubiquitin–proteasome pathway. **Biochemical and biophysical research communications,** 444 (4): 549-554.

Wang, X. and Haber, J.E. (2004) Role of *Saccharomyces* Single-Stranded DNA-Binding Protein RPA in the Strand Invasion Step of Double-Strand Break Repair. **PLoS Biol,** 2 (1): e21.

Wang, Y., Cortez, D., Yazdi, P., et al. (2000) BASC, a super complex of BRCA1-associated proteins involved in the recognition and repair of abberant DNA structures. **Genes and Development,** 14 (8): 927-939.

Ward, I.M., Minn, K., Jorda, K.G., et al. (2003a) Accumulation of checkpoint protein 53BP1 at DNA breaks involves its binding to phosphorylated histone H2AX. **The Journal of biological chemistry,** 278 (22): 19579-19582.

Ward, I.M., Minn, K., van Deursen, J., et al. (2003b) p53 binding protein 53BP1 is required for DNA damage responses and tumor suppression in mice. **Molecular and Cellular Biology,** 23 (7): 2556-2563.

Watanabe, K., Iwabuchi, K., Sun, J., et al. (2009) RAD18 promotes DNA double-strand break repair during G1 phase through chromatin retention of 53BP1. **Nucleic Acids Research,** 37 (7): 2176-2193.

Wei, L., Lan, L., Hong, Z., et al. (2008) Rapid recruitment of BRCA1 to DNA double-strand breaks is dependent on its association with Ku80. **Molecular and cellular biology,** 28 (24): 7380-7393.

Wei, M., Grushko, T.A., Dignam, J., et al. (2005) BRCA1 promoter methylation in sporadic breast cancer is associated with reduced BRCA1 copy number and chromosome 17 aneusomy. **Cancer Research,** 65 (23): 10692-10699.

Weinfeld, M., Mani, R.S., Abdou, I., et al. (2011) Tidying up loose ends: the role of polynucleotide kinase/phosphatase in DNA strand break repair. **Trends in biochemical sciences,** 36 (5): 262-271.

Whitelaw, C.B., Harris, S., McClenaghan, M., et al. (1992) Position-independent expression of the ovine beta-lactoglobulin gene in transgenic mice. **The Biochemical journal,** 286 (Pt 1) (Pt 1): 31-39.

Williams, R.S., Chasman, D.I., Hau, D.D., et al. (2003) Detection of protein folding defects caused by BRCA1-BRCT truncation and missense mutations. **Journal of Biological Chemistry,** 278 (52): 53007-53016.

Williams, R.S., Dodson, G.E., Limbo, O., et al. (2009) Nbs1 Flexibly Tethers Ctp1 and Mre11-Rad50 to Coordinate DNA Double-Strand Break Processing and Repair. **Cell,** 139 (1): 87-99.

Williams, R.S. and Glover, J.N. (2003) Structural consequences of a cancer-causing BRCA1-BRCT missense mutation. **Journal of Biological Chemistry,** 278 (4): 2630-2635.

Williams, R.S., Green, R., Glover, J.N., et al. (2001) Crystal structure of the BRCT repeat region from the breast cancer-associated protein BRCA1. **Nature Structural Biology,** 8 (10): 838-842.

Williams, S.A., Longerich, S., Sung, P., et al. (2011) The E3 ubiquitin ligase RAD18 regulates ubiquitylation and chromatin loading of FANCD2 and FANCI. **Blood,** 117 (19): 5078-5087.

Wilson, C.A., Payton, M.N., Elliott, G.S., et al. (1997) Differential subcellular localization, expression and biological toxicity of BRCA1 and the splice variant BRCA1-delta11b. **Oncogene,** 14 (1): 1-16.

Wiltshire, T., Senft, J., Wang, Y., et al. (2007) BRCA1 contributes to cell cycle arrest ad chemoresistance in response to the anticancer agent irofulven. **Molecular Pharamocology,** 71 (4): 1051-1060.

Wolff, B., Sanglier, J.J. and Wang, Y. (1997) Leptomycin B is an inhibitor of nuclear export: inhibition of nucleo-cytoplasmic translocation of the human immunodeficiency virus type 1 (HIV-1) Rev protein and Rev-dependent mRNA. **Chemistry & biology,** 4 (2): 139-147.

Wong, A.K., Ormonde, P.A., Pero, R., et al. (1998) Charracterization of a carboxy-terminal BRCA1 interacting protein. **Oncogene,** 17 (18): 2279-2285.

Wu, L.C., Wang, Z.W., Tsan, J.T., et al. (1996) Identification of a RING protein that can interact in vivo with the BRCA1 gene product. **Nature genetics,** 14 (4): 430-440.

Wu, Q., Paul, A., Su, D., et al. (2016) Structure of BRCA1-BRCT/Abraxas complex reveals phosphorylation-dependent BRCT dimerization at DNA damage sites. **Molecular Cell,** 15 973-979.

Wu, W., Nishikawa, H., Hayami, R., et al. (2007) BRCA1 ubiquitinates RPB8 in response to DNA damage. **Cancer research,** 67 (3): 951-958.

Wu, W., Sato, K., Koike, A., et al. (2010) HERC2 is an E3 ligase that targets BRCA1 for degradation. **Cancer research,** 70 (15): 6384-6392.

Wu, Y., Shin-ya, K. and Brosh, R.M. (2008) FANCJ Helicase Defective in Fanconia Anemia and Breast Cancer Unwinds G-Quadruplex DNA To Defend Genomic Stability. **Molecular and cellular biology,** 28 (12): 4116-4128.

Wu-Baer, F., Ludwig, T. and Baer, R. (2010) The UBXN1 protein associates with autoubiquitinated forms of BRCA1 tumor suppressor and inhibits its enzymatic function. **Molecular and cellular biology,** 30 (11): 2787-2798.

Wu-Baer, F., Lagrazon, K., Yuan, W., et al. (2003) The BRCA1/BARD1 Heterodimer Assembles Polyubiquitin Chains through an Unconventional Linkage Involving Lysine Residue K6 of Ubiquitin. **Journal of Biological Chemistry,** 278 (37): 34743-34746.

Xia, B., Sheng, Q., Nakanishi, K., et al. (2006) Control of BRCA2 cellular and clinical functions by a nuclear partner, PALB2. **Molecular Cell,** 22 (6): 719-729.

Xian Ma, Y., Fan, S., Xiong, J., et al. (2003) Role of BRCA1 in heat shock response. **Oncogene,** 22 (1): 10-27.

Xie, A., Hartlerode, A., Stucki, M., et al. (2007) Distinct Roles of Chromatin-Associated Proteins MDC1 and 53BP1 in Mammalian Double-Strand Break Repair. **Molecular cell,** 28 (6): 1045-1057.

Xie, J., Peng, M., Guillemette, S., et al. (2012) FANCJ/BACH1 acetylation at lysine 1249 regulates the DNA damage response. **PLoS genetics,** 8 (7): 1002786.

Xu, B., Kim, S. and Kastan, M.B. (2001a) Involvement of Brca1 in S-phase and G(2)-phase checkpoints after ionizing irradiation. **Molecular and cellular biology,** 21 (10): 3445-3450.

Xu, X., Li, C., Garrett-Beal, L., et al. (2001b) Direct removal in the mouse of a floxed neo gene from a three-loxP conditional knockout allele by two novel approaches. **Genesis (New York, N.Y.: 2000),** 30 (1): 1-6.

Xu, X., Qiao, W., Linke, S.P., et al. (2001c) Genetic interactions between tumor suppressors Brca1 and p53 in apoptosis, cell cycle and tumorigenesis. **Nature genetics,** 28 (3): 266-271.

Xu, X., Wagner, K.U., Larson, D., et al. (1999a) Conditional mutation of Brca1 in mammary epithelial cells results in blunted ductal morphogenesis and tumour formation. **Nature genetics,** 22 (1): 37-43.

Xu, X., Weaver, Z., Linke, S.P., et al. (1999b) Centrosome amplification and a defective G2-M cell cycle checkpoint induce genetic instability in BRCA1 exon 11 isoform-deficient cells. **Molecular cell,** 3 (3): 389-395.

Xu, X., Aprelikova, O., Moens, P., et al. (2003) Impaired meiotic DNA-damage repair and lack of crossing-over during spermatogenesis in BRCA1 full-length isoform deficient mice. **Development,** 130 (9): 2001-2012.

Xu, Y., Ashley, T., Brainerd, E.E., et al. (1996) Targeted disruption of ATM leads to growth retardation, chromosomal fragmentation during meiosis, immune defects, and thymic lymphoma. **Genes & development,** 10 (19): 2411-2422.

Yamamoto, O., Fuji, I. and Ogawa, M. (1985) Difference in DNA strand break by gamma- and beta-irradiations: an in vitro study. **Biochemistry international,** 11 (2): 217-223.

Yamane, K., Katayama, E. and Tsuruo, T. (2000) The BRCT regions of tumor suppressor BRCA1 and of XRCC1 show DNA end binding activity with a multimerizing feature. **Biochemical and biophysical research communications,** 279 (2): 678-684.

Yan, Z., Delannoy, M., Ling, C., et al. (2010) A Histone-Fold Complex and FANCM Form a Conserved DNA-Remodeling Complex to Maintain Genome Stability. **Molecular cell,** 37 (6): 865-878.

Yang, Y., Swaminathan, S., Martin, B.K., et al. (2003) Aberrant splicing induced by missense mutations in BRCA1: clues from a humanized mouse model. **Human molecular genetics,** 12 (17): 2121-2131.

Yarden, R.I. and Brody, L.C. (1999) BRCA1 interacts with components of the histone deacetylase complex. **Proc.Natl.Acad.Sci.U.S.A.,** 96 (9): 4983-4988.

Yarden, R.I., Pardo-Reoyo, S., Sgagias, M., et al. (2002) BRCA1 regulates the G2/M checkpoint by activating Chk1 kinase upon DNA damage. **Nature genetics,** 30 (3): 285-289.

Ye, Q., Hu, Y., Zhong, H., et al. (2001) BRCA1-induced large-scale chromatin unfolding and allele-specific effects of cancer-predisposing mutations. **The Journal of cell biology,** 155 (6): 911-922.

Yeo, J.E., Lee, E.H., Hendrickson, E.A., et al. (2014) CtIP mediates replication fork recovery in a FANCD2-regulated manner. **Human molecular genetics,** 23 (14): 3695-3705.

Yoo, E., Kim, B.U., Lee, S.Y., et al. (2005) 53BP1 is associated with replication protein A and is required for RPA2 hyperphosphorylation following DNA damage. **Oncogene,** 24 (35): 5423-5430.

Yoo, H.Y., Kumagai, A., Shevchenko, A., et al. (2007) Ataxia-telangiectasia mutated (ATM)-dependent activation of ATR occurs through phosphorylation of TopBP1 by ATM. **Journal of Biological Chemistry,** 282 (24): 17501-17506.

Yossepowitch, O., Olvera, N., Satagopan, J.M., et al. (2003) BRCA1 and BRCA2 germline mutations in lymphoma patients. **Leukaemia and Lymphoma,** 44 (1): 127-131.

You, F., Chiba, N., Ishioka, C., et al. (2004) Expression of an amino-terminal BRCA1 deletion mutant causes a dominant growth inhibition in MCF10A cells. **Oncogene,** 23 (34): 5792-5798.

Young, C.W., Robinson, P.F. and Sacktor, B. (1963) Inhibition of the synthesis of protein in intact animals by acetoxycycloheximide and a metabolic derangement concomitant with this blockade. **Biochemical pharmacology,** 12 (8): 855-865.

Yu, X. and Chen, J. (2004) DNA damage-induced cell cycle checkpoint control requires CtIP, a phosphorylation-dependent binding partner of BRCA1 C-terminal domains. **Molecular and cellular biology,** 24 (21): 9478-9486.

Yu, X., Chini, C.C., He, M., et al. (2003) The BRCT domain is a phospho-protein binding domain. **Science (New York, N.Y.),** 302 (5645): 639-642.

Yu, X., Fu, S., Lai, M., et al. (2006) BRCA1 ubiquitinates its phosphorylation-dependent binding partner CtIP. **Genes & development,** 20 (13): 1721-1726.

Yu, X., Wu, L.C., Bowcock, A.M., et al. (1998) The C-terminal (BRCT) domains of BRCA1 interact in vivo with CtIP, a protein implicated in the CtBP pathway of transcriptional repression. **Journal of Biological Chemistry,** 273 (39): 25388-25392.

Yu, X., Jacobs, S.A., West, S.C., et al. (2001) Domain structure and dynamics in the helical filaments formed by RecA and Rad51 on DNA. **Proceedings of the National Academy of Sciences,** 98 (15): 8419-8424.

Yuan, J. and Chen, J. (2010) MRE11-RAD51-NBS1 complex dictates DNA repair independent of H2AX. **Journal of Biological Chemistry,** 285 (2): 1097-1104.

Yuan, S.S., Lee, S.Y., Chen, G., et al. (1999) BRCA2 is required for ionizing radiation-induced assembly of Rad51 complex in vivo. **Cancer research,** 59 (15): 3547-3551.

Yuan, Z.M., Huang, Y., Ishiko, T., et al. (1998) Regulation of Rad51 function by c-Abl in response to DNA damage. **The Journal of biological chemistry,** 273 (7): 3799-3802.

Yun, M.H. and Hiom, K. (2009) CtIP-BRCA1 modulates the choice of DNA double-strand-break repair pathway throughout the cell cycle. **Nature,** 459 (7245): 460-463.

Zhang, F., Fan, Q., Ren, K., et al. (2010) FANCJ/BRIP1 recruitment and regulation of FANCD2 in DNA damage responses. **Chromosoma,** 119 (6): 637-649.

Zhang, F., Ma, J., Wu, J., et al. (2009a) PALB2 links BRCA1 and BRCA2 in the DNA-damage response. **Current Biology,** 19 (6): 524-529.

Zhang, F., Fan, Q., Ren, K., et al. (2009b) PALB2 Functionally Connects the Breast Cancer Susceptibility Proteins BRCA1 and BRCA2. **Molecular Cancer Research,** 7 (7): 1110-1118.

Zhang, H., Liu, H., Chen, Y., et al. (2016) A cell cycle-dependent BRCA1-UHRF1 cascade regulates DNA double-strand break repair pathway choice. **Nature Communications,** 7 10201.

Zhang, H., Somasundaram, K., Peng, Y., et al. (1998) BRCA1 physically associates with p53 and stimulates its transcription activity. **Oncogene,** 16 (13): 1713-1721.

Zhang, X., Timmermann, B., Samadi, A.K., et al. (2012) Withaferin A induces proteasome-dependent degradation of Breast Cancer Susceptibility Gene 1 and Heat Shock Factor 1 proteins in breast cancer cells. **ISRN biochemistry,** 2012 707586.

Zheng, L., Annab, L.A., Afshari, C.A., et al. (2001) BRCA1 mediates ligand-independent transcriptional repression of the estrogen receptor. **Proc.Natl.Acad.Sci.U.S.A.,** 98 (17): 9587-9592.

Zheng, L., Pan, H., Li, S., et al. (2000) Sequence-specific transcriptional corepressor function for BRCA1 through a novel zinc finger protein ZBRK1. **Molecular cell,** 6 (4): 757-768.

Zhong, Q., Boyer, T.G., Chen, P.L., et al. (2002a) Deficient nonhomologous end-joining activity in cell-free extracts from BRca1-null fibroblasts. **Cancer research,** 62 (14): 3966-3970.

Zhong, Q., Chen, C.F., Chen, P.L., et al. (2002b) BRCA1 facilitates microhomology-mediated end joining of DNA double strand breaks. **The Journal of biological chemistry,** 277 (32): 28641-28647.

Zhong, Q., Chen, C., Li, S., et al. (1999) Association of BRCA1 with the hRad50-hMre11-p95 Complex and the DNA Damage Response. **Science,** 285 (5428): 747-750.

Zhu, C., Bogue, M.A., Lim, D.S., et al. (1996) Ku86-deficient mice exhibit severe combined immunodeficiency and defective processing of V(D)J recombination intermediates. **Cell,** 86 (3): 379-389.

Zhu, Q., Pao, G.M., Huynh, A.M., et al. (2011) BRCA1 tumour suppression occurs via heterochromatin-mediated silencing. **Nature,** 477 (7363): 179-184.

Zhuang, J., Zhang, J., Willers, H., et al. (2006) Checkpoint kinase 2-mediated phosphorylation of BRCA1 regulates the fidelity of nonhomologous end-joining. **Cancer research,** 66 (3): 1401-1408.

Zimmermann, M., Lottersberger, F., Buonomo, S.B., et al. (2013) 53BP1 regulates DSB repair using Rif1 to control 5' end resection. **Science,** 339 (6120): 700-704.

Zou, L., Cortez, D. and Elledge, S.J. (2002) Regulation of ATR substrate selection by Rad17-dependent loading of Rad9 complexes onto chromatin. **Genes & development,** 16 (2): 198-208.

Zou, L. and Elledge, S.J. (2003) Sensing DNA damage through ATRIP recognition of RPA-ssDNA complexes. **Science,** 300 (5625): 1542-1548.

Zou, L., Liu, D. and Elledge, S.J. (2003) Replication protein A-mediated recruitment and activation of Rad17 complexes. **Proceedings of the National Academy of Sciences,** 100 (24): 13827-13832.